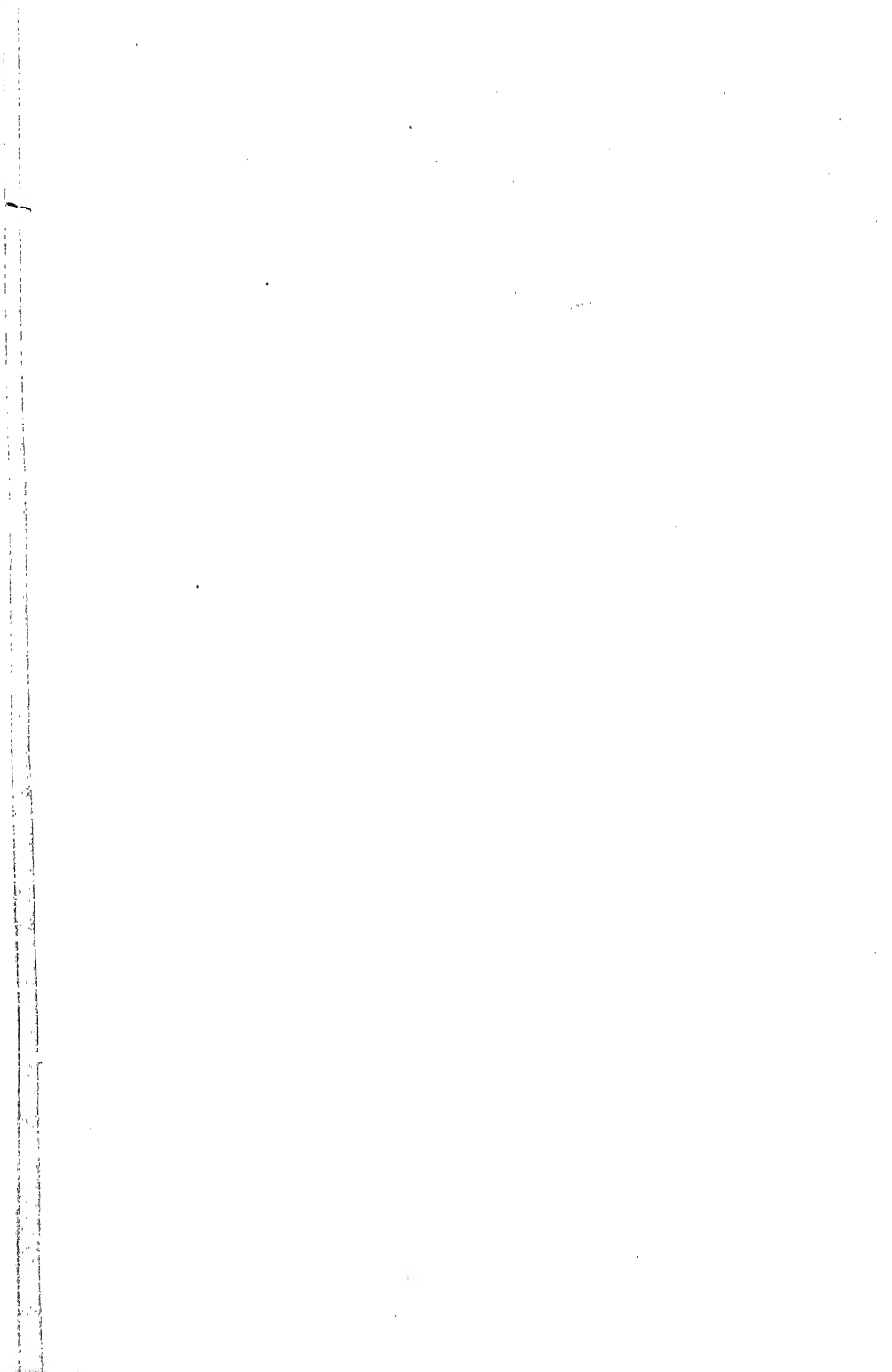


THE SPECTROSCOPY  
OF X-RAYS



# THE SPECTROSCOPY OF X-RAYS

BY

MANNE SIEGBAHN

Professor in the University of Upsala

TRANSLATED

WITH THE AUTHOR'S ADDITIONS

BY

GEORGE A. LINDSAY

Assistant Professor of Physics in the University of Michigan

OXFORD UNIVERSITY PRESS

LONDON: HUMPHREY MILFORD

1925

1125

4598



# PREFACE

## TO THE ENGLISH EDITION

IN this translation from the German Edition I have revised several chapters so as to incorporate the results of recent researches. More particularly the account of the deviations from the Bragg law, which is of fundamental importance in all X-ray measurements, has been rewritten in the light of the beautiful experiments of Bergen-Davis and his collaborators. While revising this chapter I was fortunate in being able to discuss the problem with Mr. Ivar Waller, an expert in X-ray theory, to whom I am indebted for many valuable suggestions.

A few words may be said about the wave-length tables and the accuracy of the wave-length measurements attainable with modern X-ray spectrographs. A comparison with ordinary optical spectroscopy is of interest. In his *Treatise on the Analysis of Spectra* W. M. Hicks gives the following table to show the increasing accuracy attained in the measurement of optical wave-lengths (*D* line of sodium) with the help of grating spectrographs :

	Å.U.	Δ
Frauenhofer (1821-23) -	5887.7	9.2
Ångström (1864-69) -	5895.13	0.8
Rowland-Bell (1893) -	5896.129	0.2

The values  $\Delta$  show the deviation from the wave-length 5895.932, which Michelson found by the interference method, and which may be considered as the true value, at least to the second decimal place.

Taking now some X-ray measurements, we get for the Cu-*K*- $\alpha_1$ -line (in X.U.) the following table :

	X.U.	Δ
Moseley (1913) -	1549	12
Siegbahn-Stenström (1916) -	1539	2
Siegbahn (1918) -	1537.36	0.10
Siegbahn (1922) -	1537.30	0.04
Siegbahn (1924) -	1537.26	—

The last three values are obtained with the author's precision-spectrographs. The figures under  $\Delta$  give the differences from the latest and best established wave-length.

Of the accuracy that has been attained in ordinary optics, Hicks, in the above-mentioned treatise, says : " It may be taken in general that with good lines and spectroscopic apparatus of fair resolving power, an accuracy of from 0.03 to 0.05 Å.U. is attainable, but it is easy to over-rate the accuracy obtained." I think the same might be said to-day of X-ray spectroscopic measurements, if "X.U." is substituted for "Å.U." But it must be emphasized that very few of the actual wave-lengths given in this book are measured with the latest high-precision instruments and methods now available. In the author's laboratory redeterminations have been begun, but rather a long time will be required for their completion.

In the chapters taken from the former edition without revision, I may mention the concluding section of the book dealing with the interesting researches of Millikan and his collaborators in the extreme ultra-violet. In this region the authors mentioned have lately been very successful, and have published a series of papers of the utmost interest. If I have not included an account of the main results of their researches it is for the reason given in the last sentence of that section.

The remarkable discovery by Compton of the displacement of wave-lengths on scattering has been omitted here in order to keep the subject-matter within the limits originally prescribed. This effect has no influence on the ordinary reflection from crystals, which has hitherto been the only method of studying X-ray spectra.

It is more difficult to decide whether the interesting experiments of Duane fall within the scope of this book. After some hesitation I have decided to await further developments in a field to which Duane and his collaborators are devoting themselves with such success.

Tables 37 and 38 on the energy levels have been corrected with the help of new measurements kindly put at my disposal by Mr. Nishina. To the Appendix some tables have been added, which I think will be useful for practical work in X-ray spectroscopy. One of these contains (with few exceptions) all known wave-lengths arranged in order of magnitude. With the help of this table lines found on the spectral plates can easily be identified. It must be remembered that in some instances lines in higher orders are mixed with the lines of the first order, and that it is necessary to divide the value found by 2, 3, 4 ... for the purpose of identification. The shortest possible wave-length can be found from Table II., if the maximum potential on the tube is known. I am indebted to Messrs.

Fagerberg and Thoræus for these two tables, of which the former is an extension of one published by me in 1916.

The table of the approximate absorption in substances of special interest for spectroscopic work has also been revised, and some new values in the region of longer wave-lengths have been added. These have been kindly supplied by Mr. Jönsson from an unpublished paper by him.

The bibliography has been completed to date, and in this part of the work I am indebted to Mr. Tandberg for valuable assistance.

My deep gratitude is due to Mr. Lindsay, of Ann Arbor, Mich., who has taken the greatest pains with the translation, and has drawn my attention to some inadequacies and misprints in the former edition.

MANNE SIEGBAHN.

UPSALA, PHYSICAL LABORATORY,  
*March 1925.*



# PREFACE

## TO THE GERMAN EDITION

THERE is no lack of good monographs on X-rays. I may refer especially to the well known and excellent treatment by Pohl, as well as to the textbooks of Kaye and of Bragg. Recently the works of Dauvillier and Ledoux-Lébard, of de Broglie, and of Cermak have appeared, all dealing with the latest developments in this new province of physics. A masterly exposition of a particular branch of the subject, which has initiated a new era in crystallography, has just been published by P. P. Ewald.

The present monograph concerns itself with another phase of the physics of X-rays, which during the last few years has yielded so many valuable results. It is the purpose of the author to set forth the spectroscopy of X-rays, from the purely technical rudiments to the most important results, with special reference to atomic physics. In the first-mentioned part of the work—the description of the technique and experimental methods and of the apparatus—I have sought to give sufficient detail to enable any experimenter who wishes to turn his attention to this division of the subject to make immediate headway. I hope also, by the directions given, to serve those who, for other purposes, employ the methods of röntgenography. That the description of the methods and instruments which have been developed and tested in the author's laboratory has been accorded a relatively large space should give rise to no misconception.

In the second part of the subject, namely, the significance for atomic physics of the results of X-ray research, I have discussed mainly the direct conclusions drawn from the empirical material, and have not entered into a deeper consideration of the more theoretical side of the problem. In the celebrated book of Sommerfeld, *Atomic Structure and Spectral Lines*, the reader will find a treatment of the theoretical side, as well as a consideration of the latest results of experimental investigation.

The question of limiting the material presents certain difficulties. Thus, after much hesitation, I have refrained from discussing absorption phenomena in their relation to wavelength, even though in many respects they are very closely bound up with the question in hand. Similarly I have omitted the subject of the scattering of X-rays. The surprising discovery by Duane of abnormal reflection of X-rays became known to me only after finishing the manuscript, and could not therefore be taken

into account. In general I have taken note of the literature, as far as it has been available to me, up to the beginning of this year.

In the preparation of the illustrations, some of the tables, and also of the bibliography, I have been aided by Messrs. Nils Stensson, John Tandberg, and Robert Thoræus. It is my privilege to tender my heartiest thanks to these, my co-workers.

But I am under yet greater obligation to the publishers, who have spared no pains to make the best possible reproduction of the numerous illustrations, and in other respects to give the book typographic excellence.

UPSALA, *September* 1923.

# CONTENTS

	PAGE
I. BRIEF SUMMARY OF OUR KNOWLEDGE OF X-RAYS UP TO LAUE'S DISCOVERY - - - - -	1
1. Introduction - - - - -	1
2. Characterization of X-rays by their Penetrating Power -	1
3. Secondary Rays and Characteristic Radiation of the Elements	2
4. <i>K</i> and <i>L</i> Radiation of the Elements - - - - -	4
5. Absorption and Emission of Characteristic Radiation -	6
6. Polarization of X-rays - - - - -	7
7. Distribution and Total Intensity of the Scattered Radiation	9
II. INTERFERENCE OF X-RAYS - - - - -	13
8. Laue's Discovery and the Experiments of Friedrich and Knipping - - - - -	13
9. The Investigations of W. H. and W. L. Bragg and their Explanation of Interference Phenomena - - - - -	15
10. Bragg's Experimental Arrangement and the Determination of the Atomic Distances in Rocksalt - - - - -	16
11. The Condition of Focussing given by Bragg - - - - -	20
12. The Invalidity of the Bragg Interference Equation in Measurements of Greater Precision - - - - -	21
III. TECHNIQUE OF X-RAY SPECTROSCOPY - - - - -	30
13. Excitation of X-rays - - - - -	30
14. Gas-filled Tubes - - - - -	31
15. Electron Tubes - - - - -	37
16. Spectroscopic Apparatus - - - - -	50
17. Sources of High Tension for the Operation of Tubes -	74
18. High Vacuum Technique - - - - -	80
19. Crystals used in X-ray Spectroscopy and the Values of their Lattice Constants - - - - -	83
IV. EMISSION SPECTRA - - - - -	86
20. General Survey of Emission Spectra - - - - -	86
21. Laws of Excitation of X-ray Spectra - - - - -	91
22. The <i>K</i> Series - - - - -	96
23. The <i>L</i> Series - - - - -	109
24. The <i>M</i> and the <i>N</i> Series - - - - -	125

	PAGE
V. ABSORPTION SPECTRA - - - - -	131
25. General Survey of Absorption Spectra - - - - -	131
26. The <i>K</i> Absorption - - - - -	135
27. The <i>L</i> and the <i>M</i> Absorption - - - - -	138
28. Dependence of Absorption on the Chemical Combination of the Element - - - - -	142
VI. SYSTEMATIC ARRANGEMENT AND THEORY OF X-RAY SPECTRA -	150
29. General Ideas on the Origin of X-ray Spectra. Energy Level Diagrams - - - - -	150
30. Doublets in X-ray Spectra - - - - -	156
31. Sommerfeld's Theory - - - - -	163
32. The Complete Energy Level Diagram - - - - -	171
33. X-ray Spectra of Multiply-Ionized Atoms according to Wentzel - - - - -	190
34. X-ray Spectra and Atomic Structure - - - - -	195
VII. THE CONTINUOUS X-RAY SPECTRUM - - - - -	204
35. The General Character of the Continuous Spectrum - -	204
36. Determination of the Limiting Wave-lengths of the Con- tinuous Spectrum and the Evaluation of Planck's Constant - - - - -	209
37. Total Intensity and Intensity Distribution in the Continuous Spectrum - - - - -	213
VIII. OTHER METHODS OF EVALUATING THE INNER ENERGY LEVELS OF THE ATOMS - - - - -	228
38. Electron Emission by Excitation with X-rays - - -	228
39. $\beta$ -ray Spectra - - - - -	230
40. Determination of Excitation Voltages by Means of the Photoelectric Action of the Emitted Radiation - -	236
41. Wave-length Measurements by Millikan in the Extreme Ultra-violet Region - - - - -	243
APPENDIX OF TABLES - - - - -	246
BIBLIOGRAPHY - - - - -	265
NAME INDEX - - - - -	286



# I

## BRIEF SUMMARY OF OUR KNOWLEDGE OF X-RAYS UP TO LAUE'S DISCOVERY

### 1. Introduction

IN his first publications on the discovery of the rays which have been named after him Röntgen gave an account of their most important properties, and directed further investigation into the proper channels. Thus he already knew the three very important properties of X-rays; namely, their action on the photographic plate, their power of exciting fluorescence in certain suitable substances, and their ability to render conducting the air through which they pass.

Röntgen found, further, that different bodies transmit the radiation in very different degrees, and he was able to give rough quantitative relations. He also recognised that the penetrating power of the X-rays depends much on the pressure of the air in the tube, and he introduced the terms "hard" and "soft" tubes and rays—terms which are still in use to-day.

It was also well established from the beginning that the cathode rays, on being stopped suddenly at the glass wall of the tube, or at the "anti-cathode," gave rise to X-rays. Röntgen also showed that these new rays suffered no deviation in a strong magnetic field. But it was reserved until much later to demonstrate interference phenomena with these rays, and thereby to establish their wave nature. Röntgen endeavoured to show this, but without result.

### 2. Characterization of X-rays by their Penetrating Power

Following Röntgen's original work, investigation turned to a surprising property of X-rays which gave them a place apart from all previously known types of radiation, namely, their strong power of penetration through various substances. Since this property depends not only on the kind of substance, but also, as just indicated, on the kind of

radiation, there is here the possibility of characterizing the radiation by determining its penetrating power in a given substance.

Further investigation showed that a "homogeneous" radiation is absorbed according to the law

$$I = I_0 e^{-\mu d},$$

where  $I_0$  represents the observed intensity at incidence, and  $I$  the intensity after passing through a thickness  $d$  of a given substance.  $\mu$  is a constant which depends on the absorbing material and on the kind of radiation, but is independent of  $I_0$  and  $d$ . The determination of the constant  $\mu$  may thus serve, either to trace the variation of the penetrating power of a given homogeneous radiation in different substances, or, by the use of one and the same absorbing substance, to characterize different kinds of rays. Even before the discovery of Laue, various investigators had worked on the solution of this question, and had thereby attained a relatively deep insight into the physics of X-rays.

The validity of the absorption law introduced above is limited to homogeneous X-rays. If one attempts, without further precautionary measures, to apply this equation to the radiation which is sent out from an ordinary X-ray tube and absorbed in a given substance, it is at once found that no constant value of  $\mu$  is obtained. With increasing thickness of the absorber  $\mu$  continually decreases, approaching asymptotically a limiting value. This proves to us that the radiation emitted from a tube is primarily "heterogeneous," and only after "filtering" through a sufficiently thick screen is the remaining radiation approximately homogeneous.

The method of filtering is often used for obtaining homogeneous radiation, especially in medical work, where, of course, there is no need for a high degree of homogeneity. The method was also previously made use of as a necessary expedient in physical measurements, since other means were not then available. It must be remembered, however, that the homogeneous radiation so obtained is really a mixture of rays of high, but different, penetrating powers, and their hardness continually changes, though it may be only in slight degree, with increasing depth of penetration.

### 3. Secondary Rays and Characteristic Radiation of the Elements

For a deeper view into the process of absorption we are indebted to Barkla and his co-workers. Without going particularly into the experimental methods we will give a brief account of the chief results obtained in these investigations. For this purpose consider the schematic representation of Fig. 1. A beam of primary X-rays coming from the anti-

cathode of an X-ray tube falls upon a plate of some chosen element. A part of the radiation goes on through the plate, while the remaining part is transformed into radiation of another sort, or into heat. The rays going out from the plate, which have been excited by the primary radiation, we call collectively the *secondary radiation*.

In this secondary radiation we may now distinguish four separate principal types :

- (a) Scattered X-radiation ;
- (b) Characteristic X-radiation ;
- (c) Scattered  $\beta$ -radiation ;
- (d) Characteristic  $\beta$ -radiation.

The last two are thus a corpuscular radiation, while the first two are of the same kind as the incident rays, that is, X-rays.

Attention may be called to the following characteristics of these various types of radiation. The scattered X-radiation exhibits in its general hardness quite the same properties as the incident primary beam, and is thus in character independent of the nature of the secondary radiator. On the other hand, the relative intensity—that is to say, the fraction which is sent out as scattered X-rays—depends on the secondary radiator. The scattered radiation goes out from the secondary radiator in all directions in space, but in general the radiation is stronger in the direction of the primary beam than in the opposite direction.

Since with an ordinary X-ray tube the incident X-radiation is heterogeneous, this is also the case with the scattered radiation.

On the contrary, the *characteristic* X-radiation which is emitted from a given secondary radiator is homogeneous, and always possesses exactly the same hardness, independently of the hardness of the incident radiation. *It is characteristic of the element in question.* The necessary condition that this radiation shall appear at all, is, however, that the incident radiation shall possess not less than a certain minimum hardness. Just as in the case of the scattered radiation, the characteristic radiation is sent out in all directions in space, but without any favoured direction.

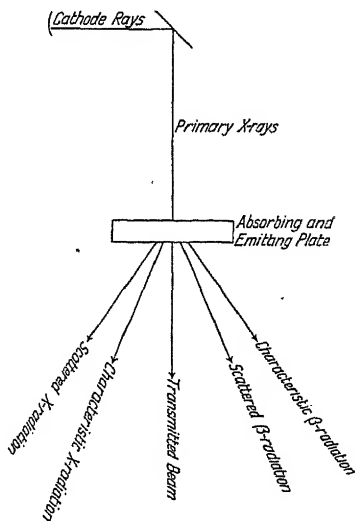


FIG. 1.

An explanation of the corpuscular radiation emitted had also been arrived at before the Laue discovery, but in important points the results were mutually contradictory. Not until recently have these contradictions been reconciled. In this introductory account of the earlier results we need not enter into a further consideration of this question. It will be enough to point out that the existence of a secondary corpuscular radiation had been demonstrated, and that certain measurements of the velocity of the emitted  $\beta$  particles had been carried out.

#### 4. *K* and *L* Radiation of the Elements.

Barkla has made detailed measurements of the hardness of the characteristic secondary radiation emitted from various elements. The hardness was determined by the aid of aluminium foil, and was given numerically by the value of  $\mu$  in equation (1) (generally divided by 2.7, the density of aluminium). Instead of expressing the absorption in terms of the thickness of the lamina of aluminium as in equation (1), we may also refer it to the unit of mass. If we represent the density of the absorbing material by  $\rho$ , and put  $\rho d$  equal to  $m$ , where  $m$  is the mass which the radiation passes through, we may write equation (1) in the following form:

$$I = I_0 e^{-\frac{\mu}{\rho} m}. \quad (2)$$

$\frac{\mu}{\rho}$  is called the mass coefficient of absorption of the given radiation in aluminium. It characterizes the radiation.

The investigations of Barkla and his co-workers showed that the elements possess in general two types of characteristic radiation which differ greatly in hardness. He called these the *K* and the *L* radiation, the *K* being the harder.

A table summarizing the values of the coefficients of absorption of the *K* and *L* series for the elements, according to the measurements of Barkla, is given below. The second column contains the atomic number of the elements listed. The fourth and the sixth contain the so-called half-value thickness for the radiation in aluminium. By this we understand the thickness of a sheet of aluminium such that the intensity of the radiation is reduced, in passing through it, to half its incident value. This number is computed from the absorption coefficient by the formula

$$d_{\frac{1}{2}} = \frac{0.2567}{\frac{\mu}{\rho}}.$$

TABLE 1

Element.	Atomic Number.	K Radiation		L Radiation	
		$\frac{\mu}{\rho}$ in Al	$d_{\frac{1}{2}}$	$\frac{\mu}{\rho}$ in Al	$d_{\frac{1}{2}}$
Ca	20	435	0.00059	—	—
Cr	24	136	0.0019	—	—
Mn	25	100	0.0026	—	—
Fe	26	88.5	0.0029	—	—
Co	27	71.6	0.0036	—	—
Ni	28	59.1	0.0043	—	—
Cu	29	47.7	0.0054	—	—
Zn	30	39.4	0.0065	—	—
As	33	22.5	0.0114	—	—
Se	34	18.5	0.0139	—	—
Br	35	16.3	0.0157	—	—
Rb	37	10.9	0.0235	—	—
Sr	38	9.4	0.027	—	—
Mo	42	4.8	0.053	—	—
Ag	47	2.5	0.103	700	0.00037
Sn	50	1.57	0.164	—	—
Sb	51	1.21	0.213	435	0.00059
I	53	0.92	0.28	300	0.00086
Ba	56	0.8	0.32	224	0.00115
Ce	58	0.6	0.43	—	—
W	74	—	—	30.0	0.0086
Pt	78	—	—	22.2	0.0116
Au	79	—	—	21.6	0.0119
Pb	82	—	—	17.4	0.0148
Bi	83	—	—	16.1	0.016
Th	90	—	—	8.0	0.032
U	92	—	—	7.5	0.034

From this table it may be seen that the hardness of the two series increases throughout with increasing atomic number of the elements. It is very important to note here that this law holds only under the assumption that the substance used for the determination of hardness possesses no characteristic radiation of its own in the region investigated. Aluminium fulfils this condition. Any element of lower atomic weight would do equally well.

In the Appendix there is a summary of absorption coefficients and half-value thicknesses for a series of substances, which is especially important for practical X-ray spectroscopy. The numbers there given are based on more recent measurements with monochromatic X-rays by Richtmyer, Hewlett, Hull and Rice, Owen, Dauvillier, and also—in the region of the longest waves—on unpublished measurements of Edv. Jönsson.

### 5. Absorption and Emission of Characteristic Radiation

For systematic investigation of the emissive and absorptive properties of the elements, a very convenient method has been attained through the use of the characteristic radiation of the elements, which (as may be seen from Table 1) give a number of well-defined rays with different degrees of hardness.

We will first consider more closely the results obtained from a study of the absorption in a given material such as iron. As incident radiation

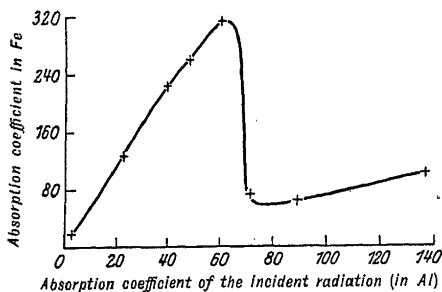


FIG. 2. Relation of the absorption to the hardness of the radiation.

we use the characteristic emission from some secondary radiator. Its hardness is determined with aluminium as an absorbing substance (see Table 1). For the investigation of the absorption in iron we employ a series of secondary radiators, arranged in order of increasing hardness, *i.e.* in order of increasing atomic

weight. If we then represent graphically the absorption coefficient in iron as a function of  $\frac{\mu}{\rho}$  in Al, we have the typical curve shown in Fig. 2.

The softest radiation thus corresponds to the point with the greatest abscissa. With increasing hardness the value of the absorption in iron diminishes. At a certain hardness, however, ( $\frac{\mu}{\rho}$  about 70), the quantity of radiation absorbed by iron suddenly increases, and then with further increasing hardness it again steadily decreases.

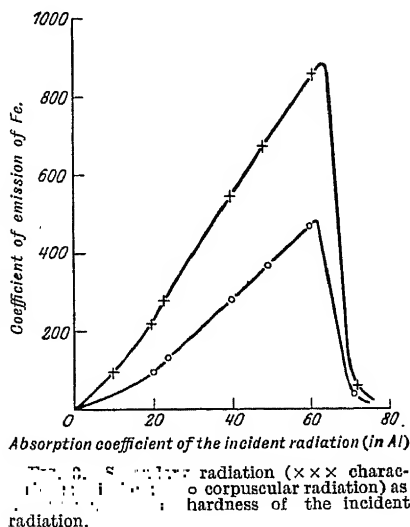
The characteristic radiation of iron and the  $\beta$ -ray emission both follow a corresponding course. The intensity of characteristic radiation excited by irradiation with rays softer than that corresponding to an absorption coefficient  $\frac{\mu}{\rho}$  of about 70, is vanishingly small, as seen from Fig. 3. But as soon as the hardness exceeds this critical value, a strong homogeneous characteristic radiation sets in. This is the characteristic  $K$  radiation of the iron. The hardness of this radiation is to be seen from Table 1. It corresponds to a value of  $\frac{\mu}{\rho} = 88.5$ .

As may be seen from the curves of Fig. 3, the  $\beta$ -ray emission behaves in much the same way. Thus the three curves, which represent in the one figure the quantity of absorbed radiation, in the other the

quantities of the characteristic radiation and of the corpuscular radiation, are quite analogous. The discontinuity lies at the same place—where  $\frac{\mu}{\rho}$  is about 70—while the characteristic radiation of iron corresponds to about 88. We may draw from this the conclusion that the characteristic radiation is excited only by those rays whose hardness exceeds that of the characteristic radiation. The emission of characteristic radiation is accompanied by an augmented absorption.

This augmented absorption is often called selective absorption, an expression which is used in ordinary optics. This appellation is not really suitable, however, and has often given rise to an erroneous conception of this phenomenon. The ordinary selective absorption is limited in wave-length to a small region, the absorption having on each side of the region a much smaller value. But in this case there appears at a certain point a strong increase in the absorption which is closely connected with the setting in of the characteristic radiation.

The excitation of the characteristic radiation is not, however, restricted on both sides to a certain region, but is dependent only on the one condition, that the exciting radiation must be harder than the characteristic radiation itself. It is thus more fitting to speak of an absorption *limit* than of a selective absorption. This does not mean that a selective absorption may not also exist within the X-ray region, for it actually has been demonstrated. We shall return to this question later.



## 6. Polarization of X-rays

We shall now very briefly call attention to a few investigations having to do with polarization phenomena in Röntgen rays. For this purpose it is necessary to consider a little more closely the mechanism of excitation of X-rays in a tube, or in a secondary radiator. Let  $K$  (Fig. 4) be the cathode of an ordinary X-ray tube, and  $A$  the anode on which the cathode rays impinge; then the sudden stopping of the cathode rays as they fall upon the anode gives rise to X-radiation. According to classical mechanics we think of it as an impulse radiation which owes its origin

to the sudden change of velocity of the electrons. The electric vector of the emitted impulse radiation lies then in the plane of the figure and perpendicular to the ray. In the secondary radiator, therefore, the electrons will be set into rapid motion, also in the plane of the figure by the force due to the electric field of the impulse radiation. This motion of the electrons leads again to the emission of secondary radiation which is of the same nature as the X-rays. If we consider the intensity of the secondary radiation in a plane perpendicular to the primary radiation, we may thus expect that it will show a maximum in the direction *perpendicular* to the plane of the paper, and a minimum *in* the plane of the

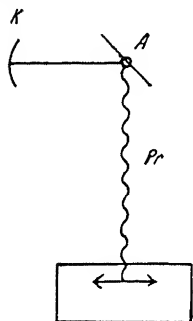


FIG. 4.

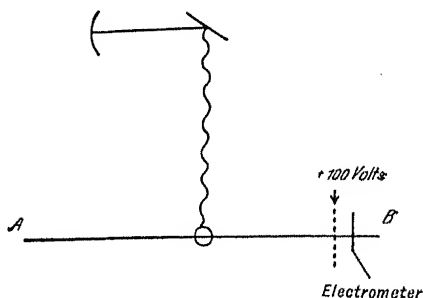


FIG. 5. Diagram of Bassler's arrangement for demonstrating the polarization of X-rays.

paper itself. That this accords with the actual facts has been demonstrated several times. Barkla, first, was able to demonstrate some, if not a very striking amount, of polarization. That the polarization cannot be complete is at once plain from the fact that the electrons, on striking the anticathode, are not brought to rest at the first collision, but are in general hurled off in another direction by the atoms they strike, and at the same time suffer a loss in speed. Only with the hardest rays, which correspond to a complete stoppage of the electrons at the first collision, could a total polarization be expected.

For very detailed researches on this question we are indebted to Bassler, who studied the intensity distribution of the secondary radiation sent out from a sphere of paraffin. The plan of his arrangement may be gathered from Fig. 5. The intensity of the secondary radiation was observed in the plane  $AB$  perpendicular to the incident primary radiation. The distribution of intensity in this plane could be determined with the aid of two ionization chambers turned at an angle of  $90^\circ$  from each other. (For example, if one chamber stood at  $B$ , the other was at right angles to the plane of the figure.) Each chamber consisted of a wire gauze placed opposite to a plate. The two gauzes were charged oppositely, the one to  $+100$  volts, the other to  $-100$  volts, while the two plates were con-



nected together and to an electroscope. With equal intensity of radiation in the two chambers the two ionization currents were compensatory. A deflection of the electroscope indicated a difference of intensity of the radiation. If, being careful to keep the position of the two chambers unchanged with respect to each other, we then rotate them about the primary beam (or, what amounts to the same thing, rotate the X-ray tube about this beam as axis), we perceive the intensity distribution as determined by the polarization. A graph of the variation of the intensity is given in Fig. 6. As may be therein seen, the secondary

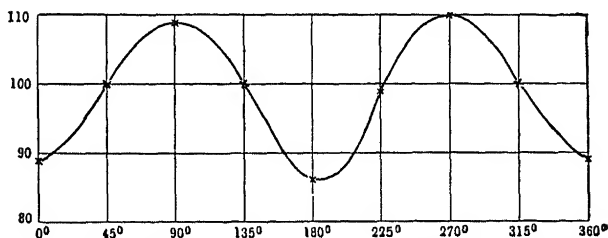


FIG. 6. Intensity distribution of secondary radiation in different directions at right angles to the primary beam.

radiation sent out has marked maxima in directions at right angles to the plane of the cathode rays and the primary X-rays, and this is entirely in accord with the ideas stated above concerning the excitation of the radiation. Vegard, Ham, and others, have also obtained similar results.

Barkla also investigated *characteristic* radiation for polarization, and found that the intensity showed no such variation with direction.

## 7. Distribution and Total Intensity of the Scattered Secondary Radiation.

As has just been stated, the intensity distribution of the secondary radiation in a plane perpendicular to the primary beam may be qualitatively explained on the old ideas of the electron theory. The question then arises as to whether the distribution of intensity in a plane containing the primary beam can be explained on the basis of the same ideas. The theory of this phenomenon was first developed by J. J. Thomson on the basis of classical electrodynamics, supported also here by the important early experimental researches of Barkla.

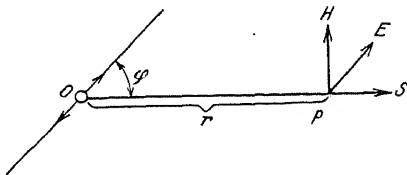


FIG. 7.

According to Thomson, one may explain the scattering of the primary Röntgen radiation in the following manner. The incident impulse radiation imparts to an electron in a secondary radiator *O* (Fig. 7) a

certain acceleration  $\frac{dv}{dt}$ . At a point  $P$  at a distance  $r$  this acceleration causes an electromagnetic disturbance, whose magnetic intensity vector  $H$  lies perpendicular to  $OP$  and to the direction of motion of the electron. Its magnitude is  $H = \frac{e}{rc} \frac{dv}{dt} \sin \phi$ , where  $e$  is the charge of the electron in E.M.U.,  $c$  the velocity of light, and  $\phi$  the angle between  $OP$  and the direction of motion of the electron.

The electric intensity  $E$ , at this point, is perpendicular to  $H$  and to  $OP$ , and is given by

$$E = \frac{e}{r} \frac{dv}{dt} \sin \phi.$$

From Poynting's theorem the energy flux at this point proves to be

$$S = \frac{E \cdot H}{4\pi} = \frac{e^2}{4\pi r^2 c} \left( \frac{dv}{dt} \right)^2 \sin^2 \phi. \quad (3)$$

With complete polarization of the incident radiation, therefore, the combined action of a great number of electrons, all suffering parallel accelerations, would result in an intensity distribution as in Fig. 8. By finding the mean value one then obtains the distribution for the case in which all directions of polarization occur in the incident beam. Thomson has shown that in this case a distribution is obtained according to the formula

$$I_\theta = I_{\frac{\pi}{2}}(1 + \cos^2 \theta). \quad (4)$$

$\theta$  denotes here the angle between the incident beam and the direction of the secondary rays. This intensity distribution is represented graphically in Fig. 9. The experimental researches of Barkla and Ayres verify

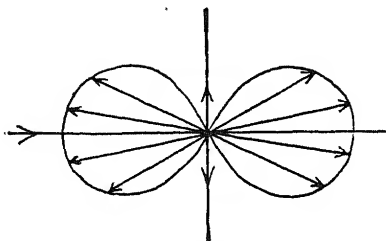


FIG. 8. Intensity distribution of secondary radiation with complete polarization of the primary radiation.

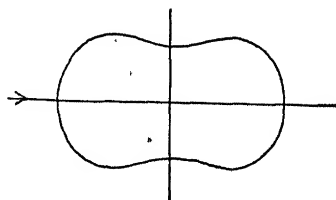


FIG. 9. Intensity distribution of the secondary radiation excited by unpolarized primary radiation.

this intensity distribution of scattered secondary radiation for moderately hard rays. In other cases, however, various investigators have shown a not insignificant departure from it. Experiments altogether show that in the direction of propagation of the primary rays the scattered radiation is appreciably stronger than in the opposite direction.

In the consideration of secondary radiation, if we direct our attention only to the intensity distribution, we see immediately that the results obtained by the classical electromagnetic theory are to a certain extent in accord with experience. This leads us to assume that to the same degree we may also expect an agreement between the calculated total secondary radiation and that experimentally determined. This is fundamentally very important, because thereupon we can base a method for finding the number of electrons in the atom.

In order to find the total scattered energy we must integrate the expression (3) over the entire sphere, whereby we obtain

$$\frac{2}{3} \frac{e^2}{c} \left( \frac{dv}{dt} \right)^2. \quad (5)$$

The acceleration is determined from the equation

$$m \frac{dv}{dt} = eE_e, \quad (6)$$

where  $m$  denotes the mass of the electron, and  $E_e$  the electric intensity vector of the primary radiation. Hence the energy  $W$  radiated per electron in the time  $dt$  is

$$W = \frac{2}{3} \frac{e^4}{m^2 c} E_e^2 dt. \quad (7)$$

If all the electrons scatter radiation quite independently of each other, and if in unit volume there are  $N$  atoms, each with  $Z$  electrons, then the energy  $W_a$  scattered by these  $NZ$  electrons in the time  $dt$  becomes

$$W_a = \frac{2}{3} \frac{e^4}{m^2 c} NZ E_e^2 dt. \quad (8)$$

The incident energy  $W_i$  in the same time  $dt$  is

$$W_i = \frac{1}{4\pi c} E_e^2 dt. \quad (9)$$

The ratio of these two quantities of energy is thus

$$\frac{W_a}{W_i} = \frac{8\pi}{3} \frac{e^4}{m^2} NZ. \quad (10)$$

In order to have a measurable quantity a coefficient of scattering  $s$  has been defined in analogy to the absorption coefficient. It is the part of the incident energy which is scattered per unit length of path along the beam according to the equation

$$\frac{dW}{dx} = -sW, \quad (11)$$

where  $W$  is the incident energy and  $dW$  the energy scattered in the

distance  $dx$ . If we integrate this equation, we obtain the following equation, which is analogous to (1) :

$$W_d = W_e e^{-sd}. \quad (12)$$

Here  $W_e$  indicates the incident radiation,  $W_d$  the intensity of radiation at the depth  $d$ . Ordinarily one refers the scattering to the unit of mass instead of to the unit of distance :

$$W_d = W_e e^{-\frac{s}{\rho} m}. \quad (13)$$

$\frac{s}{\rho}$  is thus the scattering per unit mass and  $m$  the mass producing the scattering.

Barkla and Sadler have found experimentally that within certain limits of hardness the scattering has the value

$$\frac{s}{\rho} = 0.2,$$

independently of the hardness and of the scattering material. Since equation (10) is just what we have denoted by  $s$ , and since  $\rho$  may be replaced by  $\frac{NM}{L}$  ( $M$  being the atomic weight of the scattering substance, and  $L$  the Loschmidt number per mol), we therefore obtain

$$\frac{W_d}{W_i} \frac{1}{\rho} = \frac{8\pi}{3} \frac{e^4}{m^2} L \frac{Z}{M} = \frac{s}{\rho}. \quad (14)$$

By the insertion of the known values of  $e$ ,  $m$  and  $L$ , this reduces to

$$0.4 \frac{Z}{M} = \frac{s}{\rho}. \quad (15)$$

If we now substitute the value found experimentally  $\left(\frac{s}{\rho} = 0.2\right)$ , we arrive at the important result :

$$\frac{Z}{M} = \frac{1}{2},$$

*i.e. the number of electrons per atom is about half the atomic weight.*

Strictly, this result, like that previously obtained from a consideration of the distribution of the scattered energy, has only a limited validity. Here, again, we have assumed that the laws of classical electromagnetics hold, an assumption which other experiments tell us is not permissible with the frequencies here involved, at least if we wish more than a qualitative agreement, and sometimes not even this is attained. We must, therefore, be careful in making use of this result, and not overestimate its conclusiveness.

## II

### INTERFERENCE OF X-RAYS

#### 8. Laue's Discovery and the Experiments of Friedrich and Knipping

THE above explanations of the scattered radiation, as well as the relations discussed under polarization, are based on the assumption that the Röntgen radiation is electromagnetic in nature. Especially polarization, which was demonstrated with certainty experimentally, seemed to be a sound proof of the wave nature of the radiation. Contrary to the supposition of Röntgen, we certainly are confronted, not with longitudinal, but with transverse ether vibrations. If this assumption were true we should be led to expect that other physical phenomena, which are characteristic of electromagnetic waves, would also be capable of demonstration with X-rays. At different times attempts have been made to observe such effects as refraction, reflection and interference, but only in a single case with a positive result. This was an interference phenomenon in which a thin bundle of X-rays was sent through a narrow slit. The work was carried out in 1902 by Haga and Wind with great skill and considerable care; seven years later it was repeated by Walter and Pohl, but, on account of the extraordinary smallness of the effects found, these experiments were not especially convincing.

Then, in the year 1912, the happy idea came to Laue to use the crystal edifice as a grating for the X-rays, since the atomic distances in crystals are of the right order of magnitude. In the years preceding, the quantum theory of radiation had succeeded in determining at least the order of magnitude of the wave-length of X-rays, and it had turned out to be about  $10^{-9}$  cm., while the atomic distances are of the order of  $10^{-8}$  cm. Hence, according to Laue, one might foresee that the very orderly arranged space lattice of a crystal would give rise to interference phenomena with X-rays. The experiments in this line undertaken by Friedrich and Knipping afforded a beautiful confirmation of the truth of Laue's conception.

The arrangement which for the first time showed the phenomenon of interference of X-rays through the use of crystals is shown in Fig. 10. By means of several windows a narrow beam is separated out from the entire radiation of an X-ray tube. At *K* this beam falls upon a thin

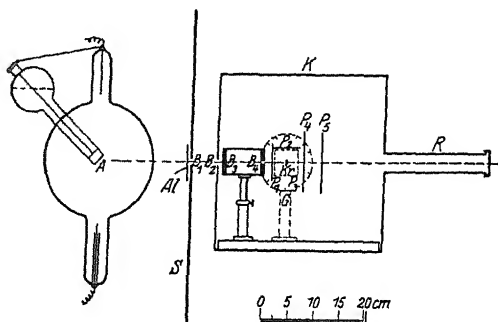


FIG. 10. Diagram of the apparatus of Laue, Friedrich and Knipping for the demonstration of interference of X-rays.

crystal plate, whose thickness may be from a few tenths of a mm. up to 2 or 3 mm. The major part of the radiation traverses the crystal without change of direction, and then falls upon the photographic plate. A part of the beam is of course scattered as secondary radiation in all direc-

tions. But, in addition to these portions, there occur in certain very definite directions comparatively strong bundles of rays, which produce black spots on the plate behind the crystal. Such a "spot diagram" is shown in Fig. 11 from a beautiful photograph by Friedrich and Knipping. The crystal used in this was a ZnS plate, 0.5 mm. thick.

The theoretical calculations of this interference phenomenon, which were carried through by Laue, predicted such a spot diagram. If, with Laue, we picture to ourselves the crystal as consisting of a number of points capable of vibration and arranged in a regular space lattice, then the incident X-radiation would set up a to-and-fro oscillation of the lattice points with the same period as that of the incident radiation.

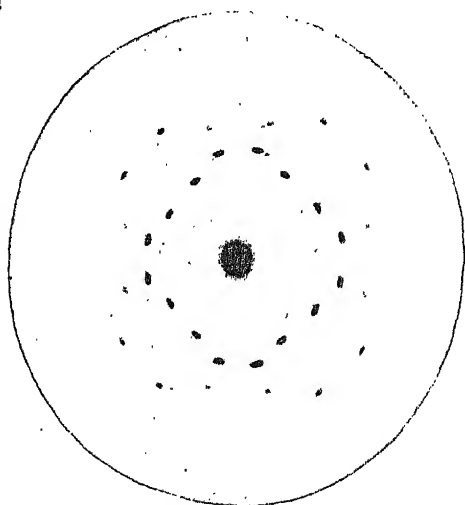


FIG. 11. X-ray interference, after Laue.

Since there exists through such a set of vibrating points a definite progression in phase, and since they all act as secondary vibration centres, the radiation sent out will be reinforced in certain directions, and extinguished in others. It is at once evident that a symmetry in the

crystal lattice must also be manifest in the emitted radiation. The mathematical theory shows that the reinforcement occurs only in *very narrow bundles of rays*. The directions in which the reinforced rays appear are determined by the structure of the space lattice, and also by the wave-length of the radiation.

## 9. The Investigations of W. H. and W. L. Bragg, and their Explanation of Interference Phenomena

After Laue, Friedrich and Knipping had succeeded in demonstrating crystal interference with X-rays, the investigation of this phenomenon was taken up by Messrs. Bragg in a somewhat modified form. The Bragg experiments showed that a natural crystal surface, for example a cleavage face, can under certain conditions reflect X-rays, and indeed, in part according to the same laws which obtain in ordinary optical reflection. Thus the incident and reflected rays lie in the same plane with the normal through the point of reflection, and the angles formed by the normal with the incident ray and the reflected ray respectively are equal.

Bragg also deduced in a simple manner the conditions for reflection which were adapted to his experimental arrangement. He arrived thus at the exceedingly important and very simple formula for the reflection of X-rays from crystal planes :

$$n\lambda = 2d \sin \phi, \quad (16)$$

which we call the *Bragg Equation*.

$\lambda$  is the wave-length of the Röntgen radiation,  $d$  is the distance (see Fig. 12) between two planes of atoms which are parallel to the reflecting plane of the crystal, and  $\phi$  is the angle between the atomic plane and the ray.  $n$  is a small integer which determines the "order" of the spectrum. This equation was proved to be identical with the general interference formula given by Laue. We will reproduce here the simple Bragg derivation.

Let the planes  $Y_1 Y_2 Y_3 Y_4$  (Fig. 12), which pass through the atoms of the crystal grating, be parallel to the external reflecting plane. Let the distance between two of these planes be  $d$ . We will represent by  $ABCD$  the incident beam, which is assumed to be monochromatic, and of wave-length  $\lambda$ . If the rays reflected from the various planes  $Y$  are to reinforce each other in a certain direction  $T$ , making the same angle with the planes as the incident beam, it is necessary that the difference in path of the several rays shall be an integral multiple of the wave-length of the radiation in question. From the figure it may be observed that the difference in path between  $AOT$  and  $BPT$ , for example, is

$$OP + PP_1.$$

But

$$OP = \frac{ON}{\sin \phi} = \frac{d}{\sin \phi},$$

and  $PP_1 = OP \cdot \cos(180 - 2\phi) = -OP \cdot \cos 2\phi = -\frac{d \cos 2\phi}{\sin \phi}.$

We thus obtain for the difference in path  $OPP_1$

$$OPP_1 = 2d \sin \phi.$$

Reinforcement thus occurs when this difference in path is equal to a whole multiple  $n$  of the wave-length, and this completes the derivation

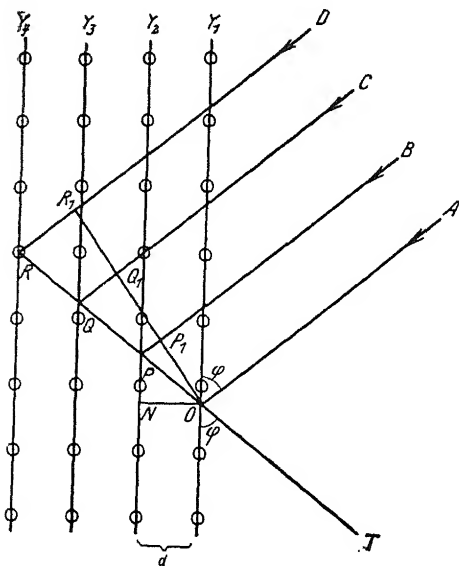


FIG. 12.

of the Bragg equation. If the difference of path be equal to *one* wave-length, we speak of a reflection or of a spectrum of the "first order." If the difference of path be two or several wave-lengths, we have correspondingly reflections or spectra of the "second" or of higher orders.

Every system of atomic planes, that can be drawn in a given crystal, has the power of reflecting the X-rays. The reflection spots shown in the experiment of Knipping and Laue were caused by the inner atomic planes of the crystal acting

as reflectors. It is important to note that each reflected ray contains only a *single definite wave-length*, together perhaps with a half, a third, etc., of this value, in the case that reflections of higher order are present.

#### 10. The Experimental Arrangement of Bragg, and the Determination of the Atomic Distances in Rocksalt

The first fundamental researches of Bragg on the structure of rock-salt, and the evaluation of  $d$  in equation (16), are of great importance for X-ray spectroscopy. The above simple derivation assumed that we are concerned with only a single system of equidistant atomic planes. This happens, however, only in exceptional cases. In general, several such systems of atomic planes are interspaced. Although all the parallel planes of a group are necessarily separated individually from each



other by the same distance  $d$ , yet separate groups of planes may be displaced with respect to each other by a certain fraction of this value.

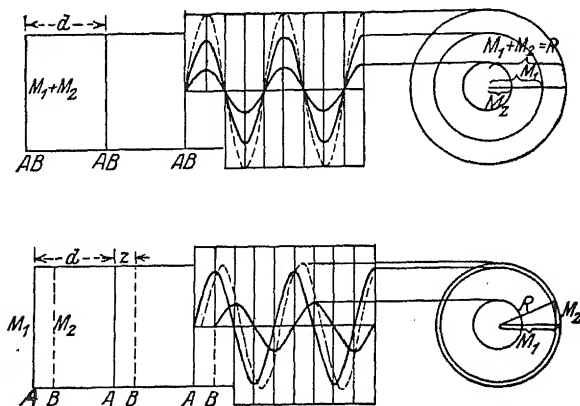


FIG. 13. Diagram of rays reflected at different groups of planes.

Since for each system we may calculate a reflected beam according to equation (16), we must consider the united action of all these partial beams in order to account for the observed beam. If, for example, half-way between the planes of one system there is a series of planes belonging to another system, then the two partial beams in the first order will evidently destroy each other if they are of equal intensity. If the partial beams are of different intensities only a partial extinction will take place.

With a given displacement of the first system with respect to the second, and different reflecting powers of the two groups of planes, one may obtain the resulting beam, according to Bragg, from a diagram like that shown in Fig. 13. Of course, in the reflection of higher orders, the wave-lengths reflected in the same direction are only half as large, or one-third as large, etc., while the relative displacement of the two wave systems (as in Fig. 13) is the same. Hence the interference of the two

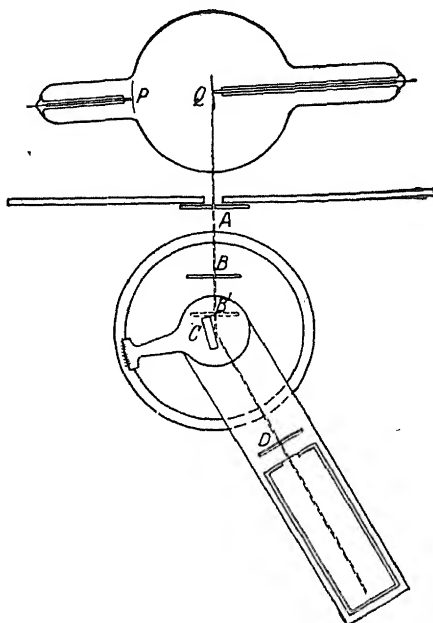


FIG. 14. Diagram of the geometry of Bragg for the diffraction of X-rays in crystals.

combining systems will turn out to be quite different for the different orders. On the other hand, with certain assumptions, it is possible, from the relative intensities of different orders, to draw conclusions concerning the arrangement of the systems of planes.

The research of the Braggs was built on this idea, and aimed at ascertaining the intensity of the reflected radiation in different orders. The experimental arrangement may be seen in Fig. 14. Since here a monochromatic radiation was necessary, they used an X-ray tube with a rhodium anticathode. This tube gave a strong monochromatic radiation corresponding to the  $K$ -radiation of rhodium found by Barkla. In order

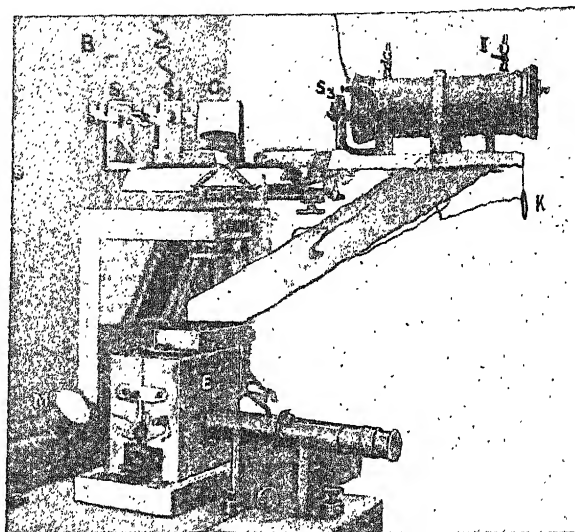


FIG. 15. Bragg's Spectrometer.

to make the best possible use of the radiation in the desired direction, the tube was placed with its anticathode so that the grazing rays were admitted through the two openings  $A$  and  $B$ . The crystal was mounted at  $C$  upon a revolving table provided with a divided circular scale. Independently of this, an arm was mounted carrying an ionization chamber, capable of turning about the same axis. With the help of this chamber the intensity of the reflected beam was measured. For this purpose, as required by the conditions of reflection, the chamber was always turned through an angle twice as large as that of the crystal. The chamber contained two electrodes, one of which was charged to a potential of one to two hundred volts, while the other was connected to an electroscope.

A photograph of the apparatus is shown in Fig. 15.

If we denote by  $\lambda_m$  the wave-length of the monochromatic beam sent out by the X-ray tube, then it is evident from equation (16) that only those positions  $\phi_1, \phi_2, \phi_3, \dots$  will give rise to a reflected beam, which fulfil the following conditions :

$$\lambda_m = 2d \sin \phi_1,$$

$$2\lambda_m = 2d \sin \phi_2,$$

$$3\lambda_m = 2d \sin \phi_3.$$

These correspond to reflections of the same wave-length in the first, second, third, etc., order. Simultaneously with these positions of the crystal, the ionization chamber must be placed respectively at the double angles  $2\phi_1, 2\phi_2, 2\phi_3$ , etc., in order that the electroscope may show any current. The strength of this current, assuming a constant intensity of the incident radiation, is a relative measure of the reflecting power of the crystal plane in question for the order under examination.

In this way Bragg and others investigated rocksalt, and especially the faces which are the most important in crystallography. Since Bragg in his book *X-Rays and Crystal Structure* has discussed in detail this method of crystal study, and has given a series of especially important results obtained by it, we will not enter farther here into this question, but will only call attention to the result that the NaCl atoms in the rocksalt space lattice occupy alternately the corners of the elementary cube.

Their distance apart  $d$  may then be calculated easily by the aid of the density and the value of Avogadro's constant. On the average, with every atom goes a volume  $d^3$ , corresponding to a mass  $\rho d^3$ , where  $\rho$ , the density, is equal to 2.17. Since, further, 1 gm. mol., that is,

$$23.05 + 35.45 \text{ gm.}$$

of rocksalt, contains  $N$  (Avogadro's number) molecules, the average mass per atom is  $\frac{58.50}{2N}$  gm. Equating these two expressions, we obtain

$$\rho d^3 = \frac{58.50}{2N},$$

and hence

$$d = 2.814 \cdot 10^{-8} \text{ cm.}$$

As may be seen, the accuracy of this value depends on the density of the substance and also on Avogadro's constant. Since the latter is known only approximately, the value of  $d$  cannot be determined as accurately as might be desired. Now the accuracy with which we can determine  $d$  is much less than that which we are to-day accustomed to reach in all X-ray spectroscopic measurements. (It would be necessary to determine  $d$  to two more decimal places in order to reach this degree

of accuracy.) For this reason it is necessary to agree provisionally upon a fundamental value for  $d$ . In the earlier work the above value was assumed to be correct in making calculations from measurements.

### 11. The Condition of Focussing given by Bragg

The fundamental equation for the reflection of X-rays at a crystal surface

$$n\lambda = 2d \sin \phi, \quad (16)$$

shows that a monochromatic radiation is reflected only when the beam falls upon the crystal at a very definite angle. Therefore, if we allow the cone of rays issuing from the slit at  $P$  (Fig. 16) to fall upon a crystal surface, by the simultaneous reflection at different parts of the surface, it is analysed into a spectrum. Beginning with the smallest angle of reflection present,  $\phi$ , which according to the above equation corresponds also to the shortest wave-length, we will have all reflection angles from  $\phi$  to  $\phi + \Delta\phi$ . A photographic plate, placed at  $R_1R_2$ , will receive a region of wave-lengths extending from the shortest waves at  $R_1$  to  $R_2$ . By changing the angle of the crystal we may in this way take the entire spectrum in sectional photographs. This method was used by Moseley in his famous spectral researches.

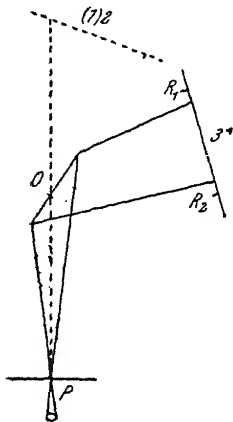


FIG. 16.

The method has certain disadvantages, however, which may easily lead to erroneous conclusions from the photographs of spectra. One is that there are often upon the anticathode several strongly luminous points, especially when the substance under investigation is rubbed in powdered form on the surface of the anticathode. The white radiation issuing from these points will appear like spectral lines on the plate. The other difficulty lies in the imperfections of the crystal. A crystal often has portions with higher reflecting power, and these may give rise to false lines.

To avoid these undesirable features a "focussing method" suggested by Bragg has been employed, and has proved very useful. Its significance for X-ray spectroscopic purposes was first clearly shown by de Broglie, who used it in his excellent early spectral researches. Fig. 17 shows the principle of "focussing."  $O$  represents the slit.  $AA$  is the crystal mounted so as to rotate about the axis  $C$ . Now if we describe a circle with  $C$  as centre, and passing through  $O$ , it is easily seen that any point  $B$  on the circumference is the point of intersection of all reflected

X-rays of a definite wave-length, independent of the angular position of the crystal.

In the position  $AA$ , only those rays will be reflected to the point  $B$  which strike the crystal at the point  $C$ . In another angular position  $A_1A_1$ , the rays reflected from the point  $P$  will reach  $B$ . That the reflection angles of the two rays indicated are the same appears at once from the geometry of the figure. Equality of angles, however, according to the law of reflection, signifies equality of wave-lengths. Thus, as the crystal is turned, the rays of the given wave-length, reflected from the various positions of the crystal, intersect in the point  $B$ , or are "focussed" at  $B$ . It may be noted, however, that this "focussing" does not in itself result in any gain in intensity at that point.

In this construction we have assumed that reflection takes place at the surface of the crystal. This reflection is really a space effect, in which a great number of atomic planes take part, but, even for rather hard rays, we seem to be justified in reckoning the depth of penetration of the reflected rays (in ideal crystal lattices) only in ten thousandths, or in thousandths of a millimetre. Since the slit width is generally of the order of tenths of a millimetre, the lack of sharpness due to the "focussing" is negligible in comparison with the width of the slit or of the lines.

However, the employment of this focussing method is limited in the case of the hardest rays. We shall return later to the precautionary measures necessary in this case.

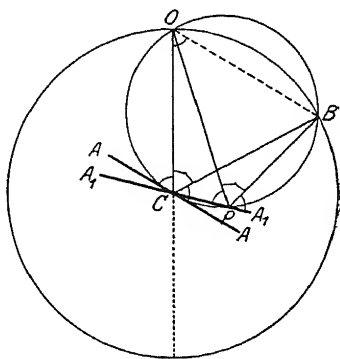


FIG. 17.

## 12. The Invalidity of the Bragg Interference Equation in Measurements of Greater Precision

The relation between the wave-length and the angle of reflection in the various orders, which was derived by Bragg in the above elementary way, was tested by him, using his ionization spectrometer, and was found to hold within the limits of accuracy attained. In particular, he was able to show that by reflection of a given wave-length in different orders, the function  $\lambda \sin \phi_n$

$$\frac{\lambda}{2d} = \frac{\sin \phi_n}{n},$$

where  $\phi_n$  represents the angle of reflection in the  $n$ th order, is a constant.

The author has endeavoured to increase as far as possible the accuracy of measurement in X-ray spectroscopy, and with this in view has con-

structed suitable types of spectrographs. After the precision of measurement had been raised to a considerable extent it was permissible to make a test to see whether or not the Bragg relation, when applied to calculate wave-lengths from angles measured experimentally, would still remain valid. The very first trials made in this direction by W. Stenström showed unequivocally, that at least with certain crystals, and especially for longer wave-lengths, the accepted relation could not be strictly true. The above function, which, when one and the same monochromatic radiation is used, was thought to be constant, showed a divergence from this simple relation; and this divergence, although small, seemed to lie outside the limits of error. However, the deviations from the constant value found by Stenström were very small, and did not permit any certain conclusions as to the manner of variation.

Since it has become possible recently to extend the accuracy of measurement still further, the author has succeeded in demonstrating the invalidity of the Bragg relation also in the case of shorter wave-lengths. With the apparatus last indicated E. Hjalmar has now investigated this question thoroughly, and has published a very good series of measurements, which suffice to make the effect quite evident. His measurements in spectra of very high orders were especially conducive to his great success. In certain cases he obtained photographs which were well capable of measurement even in the tenth order.

In the following table, taken from Hjalmar's doctor's dissertation, are assembled the values of  $\log \frac{\sin \phi_n}{n}$  for various orders  $n$  as they were obtained from the measurements. The table shows the spectral line used in each case. Only single lines without fine structure were used.

TABLE 2.

$\log \frac{\sin \phi_n}{n}$  from the spectral lines:

Order.	W $L\beta_1$ .	Cu $K\alpha_1$ .	Fe $K\beta_1$ .	Fe $K\alpha_1$ .	Va $K\alpha_1$ .	Sc $K\alpha_1$ .	Sn $L\beta_1$ .	K $K\alpha_1$ .
1	8.9269523	9.0065961	9.0635972	9.1059168	9.2174174	9.3003512	9.3482412	9.3917609
2	2986	0186	0590	3109	2169973	0059	3478718	3780
3	1675	0059561	0629822	2218	8777	2998780	7110	2741
4	1032	9043	9360	1674	7914	8130		
5	0362	8837	8975	1298	7639			
6	0009	8618		1062				
7		8400						
8		8330						
10	8.9259594							

In order that the regularity of the variation may better be seen, the values are shown graphically in Figs. 18A-18D. From these curves it may be concluded that the value of  $\log \frac{\sin \phi_n}{n}$  decreases with increasing order, and appears to approach a limiting value. That the above equation of Bragg cannot be quite correct from the theoretical point of view was first pointed out by C. G. Darwin, who gave a detailed calculation of the phenomenon of the reflection of X-rays. A more profound theory, on the same basis as that given in the treatment of the diffraction of X-rays by Laue, has been worked out by P. P. Ewald. In their main results the theories of Darwin and Ewald are identical. In both of them the extension of the simpler treatment is due to the necessity of taking the mutual action of the vibrating particles into consideration:

If this mutual action be considered, the observable angle of reflection  $\phi_n$  in the  $n$ th order has a value slightly different from that ( $\bar{\phi}_n$ ) given by the Bragg equation :

$$n\lambda_0 = 2d \sin \bar{\phi}_n, \quad (17)$$

where

$$\lambda_0 = \text{wave-length in vacuum (or air).}$$

The theory also shows that with a crystal of sufficient thickness there is total reflection for a small region  $\Delta\phi_n$  on either side of the angle  $\phi_n$ . In many cases the Bragg angle  $\bar{\phi}_n$  falls quite outside of this region  $\phi_n \pm \Delta\phi_n$ . The value

$$\bar{\phi} - \phi_n \quad (18)$$

is a measure of the deviation from the Bragg formula. The theoretical results give for this deviation the formula :

$$\bar{\phi}_n - \phi_n = \frac{2}{\Omega \sin 2\bar{\phi}_n}, \quad (19)$$

where

$$\frac{1}{\Omega} = \frac{e^2}{2\pi c^2 m} \sum_i \frac{N_i}{\nu_i^2 - \nu^2}. \quad (20)$$

[ $e$  and  $m$  are the charge and the mass of the electron respectively,  $N_i$  the number of electrons per unit volume with the natural frequency<sup>1</sup>  $\nu_i$ , and  $\nu$  is the frequency<sup>1</sup> of the incident radiation.]

By suitable transformation of the above equations, we obtain

$$\log \frac{\sin \phi_n}{n} = \text{const.} + \frac{A}{n^2}, \quad (21)$$

where

$$A = -\frac{4d^2}{\lambda_0^2 \Omega}. \quad (22)$$

The negative sign is here chosen in the expression for  $A$ , because  $\Omega$  itself is negative. If we compare the experimental value of  $\log \frac{\sin \phi_n}{n}$

<sup>1</sup>  $\nu = \frac{1}{\lambda}$ .

with the expression found for it in Ewald's theory we see that the general agreement is surprisingly good. This appears most readily from the graph of the function  $A/n^2$  in Fig. 18D, in which the form of the curve is very like those of the experimental curves in Figs. 18A, 18B and 18C.

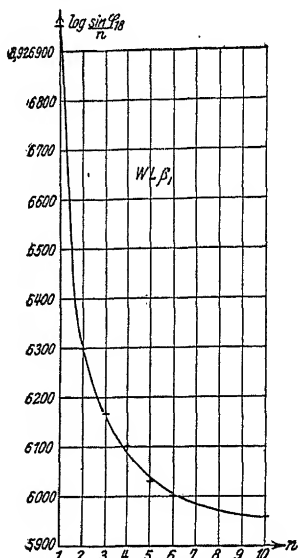


FIG. 18 A.

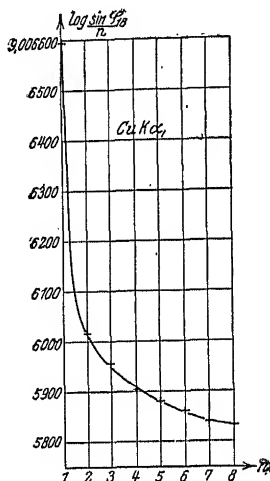


FIG. 18 B.

Equation (21) is of fundamental importance. The portion of the right-hand side denoted by "const." is, indeed, nothing else than  $\log \frac{\lambda_0}{2d}$ , and if we substitute ordinary logarithms and solve the equation for  $\lambda_0$  we obtain

$$\log \lambda_0 = \log 2d + \log \frac{\sin \phi_n}{n} - \frac{A'}{n^2}, \quad (23)$$

where

$$A' = A \log e.$$

The simple Bragg relation gave

$$\log \lambda_0 = \log 2d + \log \frac{\sin \phi_n}{n}.$$

The slight correction term  $A'/n^2$  becomes smaller and smaller as the number of the order increases, and thus for higher orders the corrected equation (23) goes over into the simple Bragg expression.

If  $\lambda_{Br}$  is the value of the wave-length which is obtained by using the simple Bragg formula when the observed angle  $\phi_n$  is introduced in it:

$$n\lambda_{Br} = 2d \cdot \sin \phi_n, \quad (24a)$$



the equations (17) and (19) give

$$\lambda_0 = \lambda_{Br} \left[ 1 + \frac{1}{\Omega \sin^2 \phi_n} \right].$$

Introducing the refractive index  $\mu$ , or better still the value  $\delta$ , for the small difference  $1 - \mu$  in the following relations :

$$\delta = 1 - \mu = -\frac{1}{\Omega} = \frac{e^2}{2\pi c^2 m} \sum_i \frac{N_i}{v^2 - v_i^2}, \quad (20b)$$

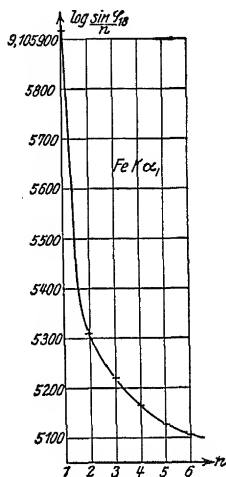


FIG. 18 c.

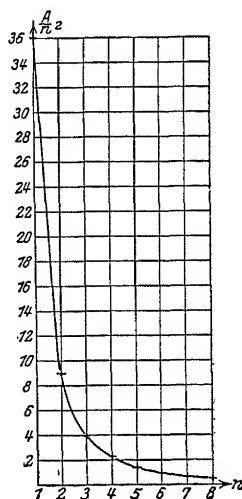


FIG. 18 d.

we obtain for the connection between the true wave-length and that calculated from the simple Bragg law :

$$\lambda_0 = \lambda_{Br} \left[ 1 - \frac{4d^2\delta}{n^2\lambda_0^2} \right]. \quad (24b)$$

This shows that—if this theory is in accordance with empirical data—we have only to multiply the calculated wave-lengths  $\lambda_{Br}$  by the factor

$$\left[ 1 - \frac{4d^2\delta}{n^2\lambda_0^2} \right],$$

to get the true wave-lengths. It is not difficult to find a good approximate value for this factor. In the expression for  $\delta$  in equation (20b), the values of  $v_i$  are negligible for most of the electrons, as compared with  $v$ . If we neglect them, and note the density  $\rho$  of the crystal, we get the approximate expression :

$$\frac{\delta}{\lambda_0^2} = 1.35\rho \cdot 10^{10}.$$

This gives the multiplying factor the following value :

$$\left[ 1 - 5.4 \frac{\rho d^2}{n^2} \cdot 10^{-6} \right],$$

where  $d$  is in Å.U.

The correction resulting from this formula is *proportional* to

- (1) *the density of the crystal,*
- (2) *the square of the lattice-constant,*

and *inversely proportional* to

- (3) *the square of the order.*

The above discussion shows that the wave-lengths  $\lambda_{Br}$ , which have been calculated by means of the ordinary form of the Bragg law, may be corrected simply by multiplying every value of  $\lambda_{Br}$  by the factor

$$\left[ 1 - 5.4 \frac{d^2 \rho}{n^2} 10^{-6} \right].$$

The process of evaluating the wave-lengths from the measured angles may be more conveniently carried out in the following way. By multiplying equation (24a) by the above correction factor, and substituting from (24b) in the left-hand member, we get

$$n\lambda_0 = 2d \left[ 1 - 5.4 \frac{d^2 \rho}{n^2} 10^{-6} \right] \sin \phi_n.$$

Hence, by using a slightly smaller lattice-constant  $d'$  given by

$$d' = d \left[ 1 - 5.4 \frac{d^2 \rho}{n^2} 10^{-6} \right],$$

instead of the true  $d$  (which represents the distance in Ångströms between the reflecting atomic planes), we get the true wave-lengths by a formula similar to the Bragg equation,

$$n\lambda_0 = 2d' \sin \phi_n. \quad (24c)$$

All wave-lengths given in the tables of this book have been calculated by means of such a formula, and if we wish to use the wave-lengths in the tables as true values, then we must consider the lattice-constant which we have employed (for calcite 3029.04) to be  $d'$ . As nearly all exact measurements have been taken in the first order, we have for the true distance  $d$  between the atomic planes parallel to the reflecting surface

$$d = d' (1 + 5.4 d^2 \rho 10^{-6}),$$

from which

$$d = 3029.45 \text{ X.U.}$$

These two values, 3029.04 and 3029.45, differ very little from each other, and both are within the limits of accuracy with which the lattice-

constant of calcite can be calculated from other data. As shown in § 19, the accuracy of this value cannot be higher than about  $\pm 2$  X.U. The last three figures are purely a matter of agreement.

If we take 3029.45 X.U. as the true value of the distance between the atomic layers of calcite, we must then use the value 3029.04 in equation (24c) for  $d'$  in the *first* order of reflection in order to calculate the *true* wave-lengths from the *observed* angles of reflection.

This discussion will serve to show that the effect in question does not seriously affect the results of the wave-length measurements, even if the theory be valid. Moreover, we have not yet sufficient experimental evidence of the exact applicability of the theory. The above measurements of Hjalmar obviously show that with gypsum there is a deviation from the Bragg law, when this equation is used to compare different orders, and also that the general nature of this deviation, as seen from the curves 18A, B, C, agrees with the theory. But these measurements are not suitable for a more detailed discussion of the exact analytical expression for this correction to the Bragg law.

A remarkable advance towards the solution of this fundamental question has been made by Bergen Davis and his collaborators, Terrill, Hatley and von Nardroff. If this effect can be treated in the same way as ordinary optical refraction, much larger deviations should be attainable by grinding the reflecting plane to a suitable angle. This is the method which Davis has used with great success. In this way he succeeded in increasing the observable deviation from 3" to 30" with calcite, and from 3".6 to 160" with iron pyrites, using Mo K-radiation. Still larger deviations were obtained by Nardroff with copper radiation reflected from ground pyrites planes; the deviations found were 210" and 218".

The refractive index  $\mu = 1 - \delta$  may be found from observations of reflection angles, as indicated in what follows. If  $\lambda$  be the wave-length in vacuo and  $\phi$  the apparent reflection angle, whereas  $\lambda'$  and  $\phi'$  are the corresponding wave-length and angle respectively within the crystal, then

$$\mu = \frac{\lambda}{\lambda'} = \frac{\cos \phi}{\cos \phi'},$$

which gives approximately

$$\frac{\sin \phi'}{\sin \phi} = \frac{1}{\mu} \left\{ 1 - \frac{1 - \mu}{\sin^2 \phi} \right\}.$$

Supposing Bragg's law to be valid for the interior of the crystal; then,

$$n\lambda' = 2d \sin \phi_n',$$

from which we derive

$$n\lambda = 2d \sin \phi_n \left\{ 1 - \frac{\delta}{\sin^2 \phi} \right\}.$$

From two reflection angles measured in different orders,  $n_1$  and  $n_2$ , this gives for  $\delta$  the value :

$$\delta = \frac{\frac{\sin \phi_1}{n_1} - \frac{\sin \phi_2}{n_2}}{\frac{1}{n_1 \sin \phi_1} - \frac{1}{n_2 \sin \phi_2}}.$$

If the beam be reflected at a plane ground to an angle  $\theta$  with the atomic planes under consideration, Nardroff gives the formula :

$$\delta = \frac{(\sin \alpha - \sin \phi')(\sin \alpha - \sin \theta)(\sin \alpha + \sin \theta)}{\sin \alpha - \sin^3 \alpha},$$

where  $2\alpha$  is the angle between the incident and the reflected beam, and  $\phi'$  is the angle for internal reflection in accordance with Bragg's law

$$\lambda' = 2d \sin \phi'.$$

As seen above, this angle is connected with the apparent angle  $\phi$  for reflection at the (*unground*) atomic plane by the formula :

$$\sin \phi' = \frac{\sin \phi}{\mu} \left\{ 1 - \frac{\delta}{\sin^2 \phi} \right\}.$$

For calcite, the value of  $\delta$  found by Davis was  $2 \times 10^{-6}$  with Mo  $K\alpha$ , whereas the dispersion-formula gives  $1.9 \times 10^{-6}$ . The most exact measurements have been carried out with iron pyrites by Nardroff, who obtained the following values :

	$\lambda \cdot 10^{11}$	$\delta$ found.	Theory.	$\frac{\delta}{\lambda^2}$
Mo $K\beta$	631.3	$2.87 \times 10^{-6}$	$2.66 \times 10^{-6}$	77
Mo $K\alpha$	710.2	3.35	3.37	66
Cu $K\beta$	1389	13.2	13.6	68
Cu $K\alpha$	1539	17.6	17.7	77
				Med. 71

From the values of  $\delta$  given by Nardroff, the function  $\frac{\delta}{\lambda^2}$  has been calculated and tabulated in the last column. As may be seen, the variation with wave-length is small and quite irregular. It would thus appear from these measurements to be permissible to utilise equation (23) for the exact calculation of wave-lengths, from the observed angles of reflection. Unfortunately, there are as yet no measurements available on crystals ordinarily used in X-ray spectroscopy, with the exception of the single value for calcite for the wave-length 710 X.U. But with this crystal the effect is rather small.

All the wave-lengths given in the following tables have been calculated with the aid of the uncorrected Bragg law.

Another consequence of the refraction theory is that there should be—for sufficiently small angles—a *total reflection* of the same kind as we observe in ordinary optics. Such total reflection should occur at angles for which

$$\cos \phi > \mu,$$

or 
$$\sin \phi < \sqrt{2\delta}.$$

This prediction has actually been confirmed by A. H. Compton for glass, silver and lacquer. His values of the limiting angles  $\cos \phi_0 = \mu$  are given in the following table :

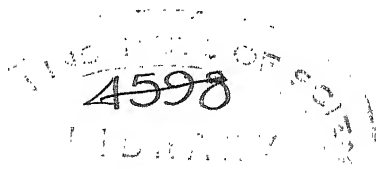
	Density.	$\lambda$ , Å.U.	$\phi_0$ .	$\delta$ found.	$\delta$ Theory.
Glass - -	2.52	1.279	10'	$4.2 \times 10^{-6}$	$5.2 \times 10^{-6}$
Glass - -	2.52	0.52	4'	0.9	0.7
Silver - -	10.5	1.279	22'.5	21.5	19.8
Lacquer - -	—	1.279	11'.0	5.1	—

Analogous results have been obtained by Lundquist and the author for much larger wave-lengths (5 Å.U.).

In this connection it may be mentioned that the so-called "Compton-effect" does not influence the angles of reflection at crystals. This has been shown by Ross, who placed two spectrometers in series, but he was unable to detect any difference in the angles of reflection.

537.5352

NS2



II Sc Lib B'lore  
537.5352 N25



4598

### III

## TECHNIQUE OF X-RAY SPECTROSCOPY

### 13. Excitation of X-rays

RÖNTGEN showed in his first work that the X-rays proceed from the place where the cathode rays strike the walls of the tube. It was soon discovered that a more powerful X-radiation could be obtained by introducing a metal plate (best of all a heavy metal) in the path of the cathode rays, so that the latter would lose their kinetic energy at impact, and this energy would be partially transformed into X-radiation. According to classical electrodynamics the sudden stoppage of a swiftly moving electric charge is accompanied by the emission of an electromagnetic pulse. This impulse radiation would thus be responsible for the major part of the energy in the emitted X-ray radiation. In part, however, the incident cathode stream gives rise to an emission from the atoms of the bombarded plate itself. This is the characteristic radiation discovered by Barkla.

The technique of the excitation of X-rays is thus faced with the problem of how to cause electrical charges or electrons to fall with sufficiently great energy upon the substance to be investigated. In the early period of development investigators were restricted to the method discovered by Röntgen, in which the cathode rays excited X-rays at the anticathode placed in a suitable evacuated tube. By regulation of the gas content and the degree of vacuum one may vary the hardness of the radiation within certain limits. Experience shows that the rays become harder with increasing tension on the tube. After it became possible to measure wave-lengths this relation was formulated more accurately, and it was found that the fundamental photoelectric equation introduced by Einstein for the relation between the kinetic energy of the electron and the wave-length or the frequency of the radiation holds here also. This equation may be written in the form

$$\frac{1}{2}mv^2 = eV = h\nu ; \quad (25)$$

$m$  and  $e$  here represent respectively the mass and the charge of an electron,  $v$  its velocity of translation,  $V$  the difference of potential through which

the electron falls,  $h$  Planck's constant, and  $\nu$  the frequency of the emitted radiation.

The left-hand member is the kinetic energy of the electron, and has been acquired by falling through the difference of potential between cathode and anticathode. If the electron gives up all its energy at once, then the emitted radiation has the frequency  $\nu$ . If we solve this equation for the frequency, or better still for the wave-length, we obtain, after introducing the known values of  $e$  and  $h$ ,

$$\lambda = \frac{12.3}{V}, \quad (26)$$

$\lambda$  being given in Ångström units and the tension in kilovolts. From this equation we may calculate the tension necessary to obtain X-radiation of a given wave-length. Since most of the electrons, however, lose their velocity in several steps, equation (26) gives only the *shortest* wave-length produced by the tension  $V$ , whilst the stoppage of the electron in several steps corresponds to the emission of greater wave-lengths.

From equation (26) we may learn within what limits of tension the X-radiation of most interest in spectroscopy will be produced. Up to the present time the wave-length measurements extend from a shortest wave-length of the order of 0.1, up to the longest of some 20 Ångström units. This corresponds to a region of voltage ranging from 130 to 0.6 kilo-volt. In present-day medical work for therapeutic purposes, considerably higher tensions, and hence shorter wave-lengths, are used.

The old-fashioned types of X-ray tube, in which the residual gas in the tube plays an important part in its operation, are often called gas-filled tubes. This kind of tube is best adapted to medium and shorter wave-lengths, while for the long, as well as for the very shortest waves, one must employ tubes with a very high vacuum. In these tubes the electrons for the bombardment of the anticathode must be produced by a special device. This type of tube is called an electron tube. A frequent name for the latter is also "gas free tube." It is true that even these tubes contain no insignificant amount of gas, but it plays no appreciable part in the working of the tube.

#### 14. Gas-filled Tubes

In the ordinary medical tubes of the gas-filled type the electrons are liberated from the cathode by positive ions, which, coming from the residual gas, are driven against the cathode. The first stage in the discharge is thus the splitting up of gas molecules in the tube through the medium of the applied voltage. The positive ions are then hurled against the negative electrode by the electric field, there freeing electrons which constitute the real cathode rays. The cathode is made concave in

order to collect the cathode rays into a small focal spot. For since the electric field near the cathode surface is nearly perpendicular to the surface, the electrons, following the lines of the field in the first part of their course, will also leave the surface almost normally. Practice has shown that the radius of the hollow cathode must, in general, be made smaller than the distance from cathode to anticathode.

Aluminium is chosen as the material for the cathode in order to reduce to the smallest possible amount the sputtering which accompanies the liberation of cathode particles. As may be seen from Fig. 19, which represents a typical gas-filled tube, the anticathode is brought into the middle of the bulb, while the cathode is placed in a special extension tube.

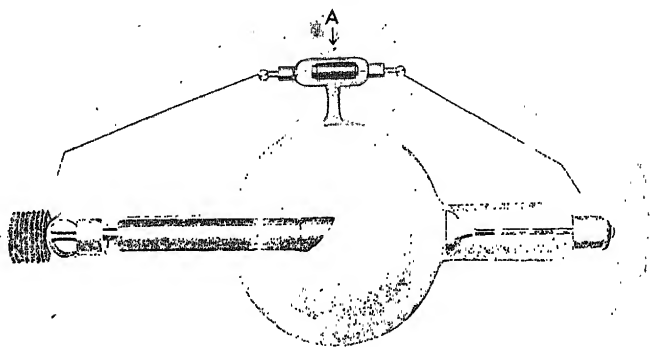


Fig. 19. Constant therapy tube TK with Gundelach Regeneration.

This location of the cathode is of very great significance for the action of the tube, because electric charges attach themselves to the glass wall around the cathode, and they greatly influence the operation of the tube. By adjusting the hollow cathode to a greater or less depth in the side tube it is possible to vary the hardness in a convenient manner. Besides the anticathode itself, which is provided with a cooling arrangement in order to sustain heavy or long continued operation, there is usually a separate anode. Its function seems to be mainly to decrease the discharge in the reverse direction. It is generally placed behind the anticathode, with which it is metallically connected.

Since the hardness, as has been already mentioned, depends on the degree of vacuum in the tube, and further, since in the operation of the tube the amount of contained gas diminishes, some mechanism must be provided for the addition of fresh gas. Many types of apparatus are provided with such "regenerative" attachments. Fig. 19 shows one in



which the current passes through *A* when the tube becomes too hard. The small quantity of gas liberated by heating or by spark discharge in the substance enclosed in this side tube is sufficient to restore the pressure to the proper value.

These brief remarks on the operation of an ordinary medical gas-filled tube will perhaps suffice to enable one to understand the further development of special tubes which are constructed to meet the various needs of X-ray spectroscopy.

In order to meet such demands of X-ray spectroscopic work, the firm of Emil Gundelach in Gehlberg, from specifications of the author, has constructed tubes embodying a slight modification of the above type (see

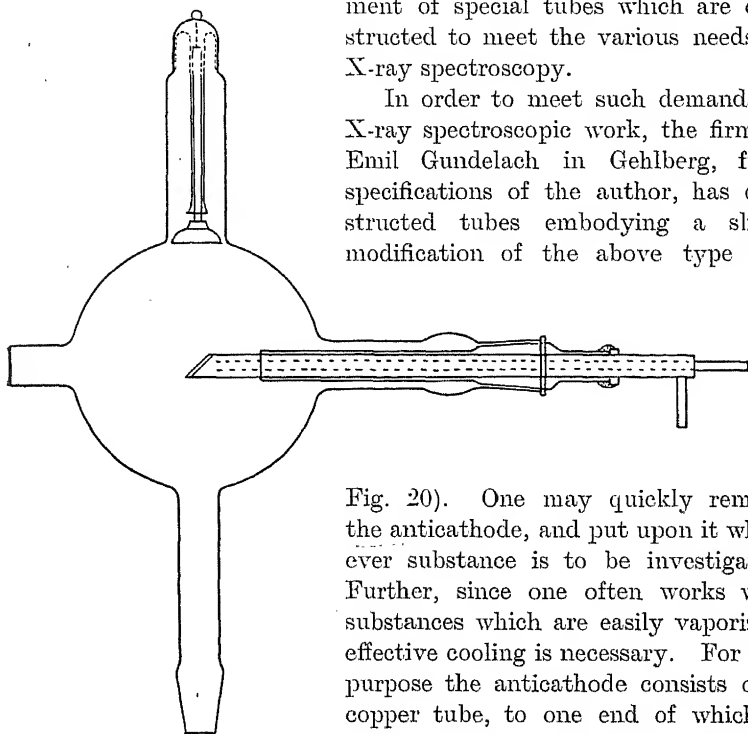


FIG. 20. Gas-filled X-ray tube with window and changeable anticathode for spectroscopic purposes.

Fig. 20). One may quickly remove the anticathode, and put upon it whatever substance is to be investigated. Further, since one often works with substances which are easily vaporized, effective cooling is necessary. For this purpose the anticathode consists of a copper tube, to one end of which is soldered obliquely a plate of copper or silver 1 to 2 mm. thick, while the other end is provided with two tubes for water

cooling. Opposite the anticathode is a side tube, over the end of which is sealed a thin sheet of aluminium, so that even the softer radiation may pass through. Pizein serves very well for the cement, and for the ground joints Ramsay grease prepared according to the directions in Kohlrausch's *Lehrbuch*.

For the operation of the tube a rapid pump is attached, and the vacuum thus regulated to obtain suitable currents. This demands a little practice, because so many variable factors are present. In addition to the rate of pumping the external electrical conditions are also variable, and these modify the pressure in the tube, even with a constant rate of

pumping. In the discussion of the medical tubes we mentioned the fact that the discharge used up the enclosed gas. But with freshly evacuated tubes, in which water vapour is adsorbed on the walls, the discharge may have the reverse effect, and even liberate enormous quantities of gas, especially when a volatile substance has been placed on the anticathode. At the beginning of operations this is the normal condition of affairs, and as a consequence one cannot run the tube continuously at the beginning. On this account it is very important, in using the tube with an induction coil, to connect in the high tension circuit a suitable rectifier, such as a valve spark gap or some other of the commercial types.

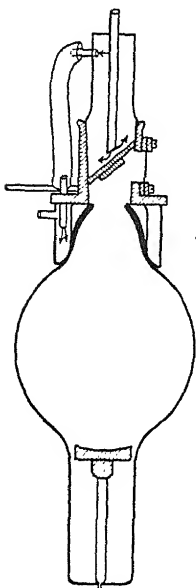


FIG. 21A. Glass-metal X-ray tube of Rausch von Traubenberg, constructed especially for crystal study by the powder method.

In order that these tubes may function well—and this is also true of all other types of tubes—it is absolutely necessary to maintain the most painstaking cleanliness. For example, a tiny speck of grease on the anticathode is continually bombarded by scattered cathode rays, even when it is far away from the focal spot, and thus the vacuum is destroyed, or at least the discharge becomes unruly. Also, when the anticathode is put in place, one should see to it that only the outer two-thirds of the ground joint are greased, the rest remaining clean. This permits only a slow inward diffusion of the vapour of the grease.

The tubes just described are very stable in their operation, because of their great volume, but they have the disadvantage that the anticathode is necessarily at a considerable distance from the analyzing apparatus. With large spectrographs, where the distances are considerable in any case, this is not of so much consequence; but in certain investigations, for example, in the study of crystals by the powder method, where with a small apparatus an intense radiation is desired, the large distance to the focus is very disadvantageous. To avoid this difficulty Rausch von Traubenberg constructed the tube shown in Fig. 21A.

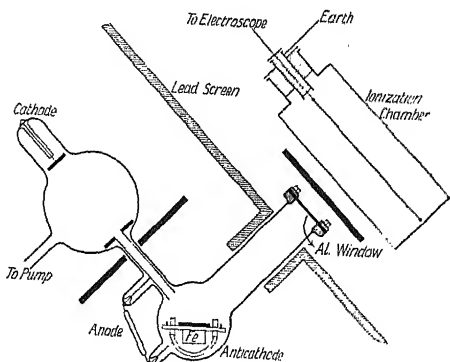


FIG. 21B. Kaye's X-ray tube with changeable anticathode.

The anticathode is here sealed in a side tube, and, like the one in the previous tube, is removable and water-cooled, the cooling being good in the neighbourhood of the seal. In this tube also the rays escape through an aluminium window.

Kaye used a gas-filled tube which permitted quick change of the material of the anticathode. His arrangement also allowed soft radiation to escape from the tube, and is shown in Fig. 21B. The change

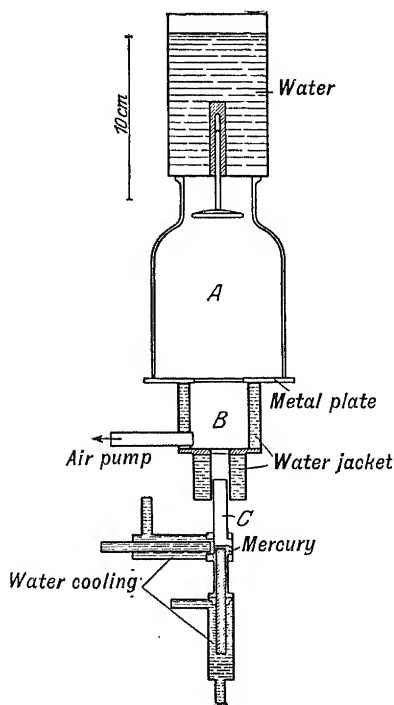


FIG. 21C. Gas-filled tube for the X-ray.

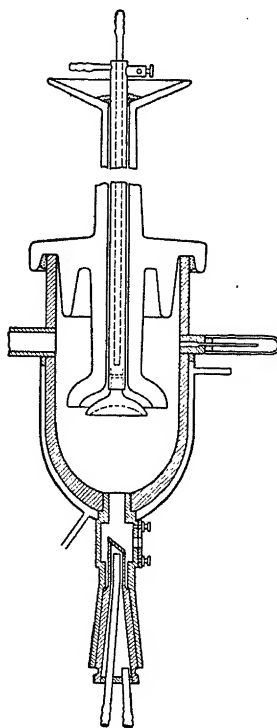


FIG. 22. Porcelain-metal X-ray tube of Radding for crystallographic purposes.

from one anticathode to another was made by means of a magnet. The tube was provided with aluminium windows. It was a tube of this kind that Moseley used in his famous researches.

A very interesting form of tube is that devised by A. Müller for exciting the spectrum of mercury vapour. It was only a provisional arrangement, but the results show that the tube works very successfully. The construction and manner of operation may be understood from Fig. 21c without further explanation.

A metallic X-ray tube, which serves the same purpose as that of Traubenberg described above, was constructed by the author and tested

by A. Hadding for crystallographic and mineralogical investigations (Fig. 22). In comparison with the glass tubes it has the advantage of being practically indestructible, and will carry a much heavier load without any danger to the tube. The cathode passes through a specially constructed porcelain insulator, and is water-cooled. It is, however, in general, hardly necessary to cool the cathode; it is sufficient, even with moderately heavy loads, to send a little water through occasionally. On the other hand, the cathode of a tube, such as that shown in Fig. 20, when carrying so heavy a load becomes red-hot in a short time, as Hadding was able to prove by comparative tests. The metal casing is surrounded by a cooling jacket, and during the operation of the tube it, as well as the anticathode, must be cooled by running water. The anticathode fits in a cone-shaped opening, and is sealed only with Ramsay grease. Round about the anticathode, and level with the focal spot, are several windows (three has proved to be a suitable number), and across these windows aluminium foil 0.007 to 0.015 mm. in thickness is stretched and fastened, the joint being sealed with a little Ramsay grease.

The tube is intended to be permanently connected to a vacuum pump. The most convenient thing for this connection is a metallic tube such as that furnished by the *Waffen-und Munitionsfabrik* at Karlsruhe (the so-called flexible tombac tubing). One end of this metallic tubing is then soldered to the X-ray tube, and the other end is attached to the outer portion of a ground metal joint if a molecular pump is to be used. If we connect to the tube a parallel spark gap, adjusted for the proper tension on the tube, and a device for the evolution of gas, on the principle of that shown on the tube of Fig. 19, then the tube will run automatically for hours with no further attention.

A tube of the dimensions most frequently used by the author operates best with a tension of from 30 to 40 kilovolts. With a current of 10 to 20 milliamperes the monochromatic radiation from a copper or an iron anticathode is powerful enough to give a good photograph by the powder method from most crystalline powders in from 15 to 30 minutes. Three photographs may be taken at once if desired. In this method, where purely monochromatic radiation is to be desired, the use of gas-filled tubes rather than electron tubes is distinctly recommended. With electron tubes, the cathode very quickly (even after a few minutes, as the author has found in his spectroscopic work) deposits upon the anticathode a thin layer of tungsten from the hot tungsten wire, and thus a rather strong tungsten radiation is mingled with the radiation from the material of the anticathode. Further, since the tungsten spectrum in this region is very complicated, having more than 20 lines,—the interpretation of the diagram is made much more difficult. For spectroscopic purposes this tube is adapted to wave-lengths ranging from about 0.5

to 2 or 3 Å.U. when the substance to be investigated is rubbed on the anticathode.

### 15. Electron Tubes

In the electron, or "gas-free" tubes, the vacuum is so high that when the high tension is applied to the electrodes no current passes through the tube. In order to have a current flow through the evacuated space, electrons must be present at the cathode. One might think that any of the known means for producing electrons could be used, but in practice only the following have been successful :

1. The production of electrons by the hot wire cathode, the wire being usually of tungsten ;
2. Production of electrons at the cathode by hot oxide ;
3. Production of photoelectrons at the cathode by illumination with ultra-violet light ;
4. Autoelectron emission by Lilienfeld's method.

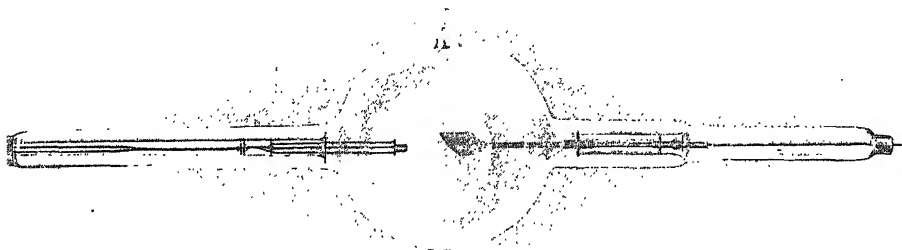


FIG. 23. The Coolidge commercial electron X-ray tube.

The first method is the one of greatest importance, if not the only practical one. Fig. 23 represents a commercial Coolidge tube constructed on this principle. The cathode is in the form of a small cylinder, within which is placed a flat spiral of tungsten wire. Two wire conductors lead in from outside the tube to the ends of this spiral, of which one is in direct metallic connection with the cylinder of the cathode. The spiral is heated to a high temperature by a separate source of current, such as a storage battery or a step-down transformer. At white heat the tungsten wire begins to emit electrons, and if now the high tension is applied to the terminals of the tube the electrons are driven at high speed against the anticathode, where they generate X-rays. By adjusting the spiral at a greater or less depth in the cylinder, one may cause the cathode rays

to be concentrated into a focus of greater or less area on the anticathode. A spherical cap on the cathode often serves the same purpose.

For medical work these tubes have recently been constructed to be run at very high tensions, the whole tube then being immersed in oil. Such tubes are rated at several milliamperes with 270 kv.

The great advantage of this type of tube is that it is possible to control the output. The applied voltage, and hence the hardness, may be varied independently of the current through the tube. The tube current depends on the number of electrons furnished by the hot filament, and since this number depends on the temperature of the filament it may be controlled by the filament current. By varying the tension these tubes are capable of producing X-rays of any hardness whatever, from the very soft rays at a few hundred volts up to those just mentioned at 270 kv.

The commercial tubes having tungsten or molybdenum anticathodes have found extensive application in X-ray spectroscopy; first to study the line spectrum of both these elements, and secondly to obtain with tungsten a strong "white" radiation, or with molybdenum (or rhodium, or palladium) a good monochromatic radiation. One important use for the white radiation is to excite characteristic, secondary radiation, as already indicated in connection with Barkla's experiments. If the intensity of the primary rays be sufficiently great the new spectroscopic methods may also be applied to such secondary rays, and there is this advantage, that the material to be investigated need not be brought inside the tube, and hence pumps and other accessories for exhausting the tube may be dispensed with. De Broglie, in particular, has studied, by this method of excitation, an extended series of emission and absorption spectra. Of course, it is self-evident that the gas-filled tubes may also be used in this way, provided they give sufficient intensity.

These tubes have found a second very important sphere of usefulness in the study of crystal structure. For photographs from powdered crystals many investigators have used hot cathode tubes provided with molybdenum or rhodium anticathodes. In the latter type of investigations, however, incomparably more is obtained by the use of the gas-filled tubes, especially the metallic ones.

The electron tubes must be modified somewhat for purposes of X-ray spectroscopy, so as to embody the following necessary features. (a) There must be a convenient way of applying the substance to be investigated to the anticathode. (b) The tube must be provided with a transparent window. (c) It must be cooled so that even with rather volatile substances a large output from the tube is possible. (d) The hot wire must be easily replaceable, for it is frequently destroyed by the vapours given off by the substance under investigation. (e) Finally, the dimensions of the tube must be as small as possible, in order that the

anticathode may approach as near as possible to the spectroscopic apparatus. A most important point to bear in mind when designing a tube is to have as few joints and wax or cement seals as possible. Every waxed joint or seal is a potential source of trouble in apparatus designed for high vacua.

The author has made thorough tests of various designs in glass, quartz and metal, in the attempt to fulfil the above conditions. The metal tubes built on the plan of Fig. 24 have given the most satisfaction.

The tube proper is a cubical piece of wrought brass, into which holes are bored from three sides. Three side tubes are soldered into these three openings, one tube being cylindrical and leading through a metal connection to the vacuum pump. The other two carry on conical joints the cathode and the anticathode respectively. These last two tubes, carrying the anode and the cathode, are cooled by water running through the passages in the cubical box, as shown in the figure. Through the side of

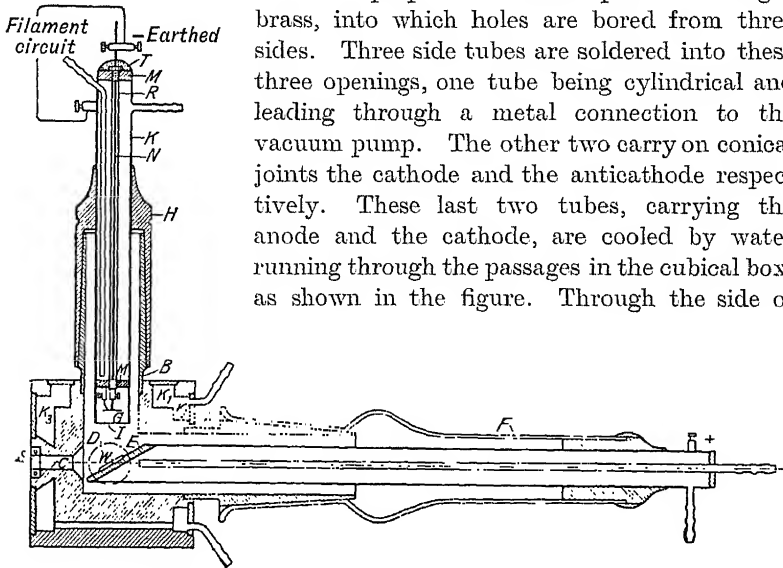


FIG. 24. Metal tube with hot cathode for spectroscopic use.

the cube facing the anode, and in the direction of the anode, a small hole is bored, 5 mm. in diameter. The outer part of this opening is enlarged to a width of 10 mm. The slit is inserted here so that its outer edge is in the plane of that face of the cube. A canal for cooling is also hollowed out round about this opening and connected with the rest of the cooling system.

In this design of tube the distance of the slit from the focus on the anode is about 25 mm., while one edge of the cube measures 55 mm. On account of the effective cooling arrangement, which is brought near to all seals and joints, this tube will operate undisturbed for hours, even under a very heavy load.

The anticathode is constructed just like that of the gas-filled tube described earlier, in which a copper plate was fastened in the focal plane with hard solder. The anticathode within the glass tube is fastened with

pizein, so that it is possible to centre the copper rod within the metal cone, even when the axis of the ground conical part does not coincide with the axis of the rest of the glass tube. A standard type of ground glass-joint was used, so that if one were broken it could easily be replaced. It is very important for the life of the glass insulator that it be kept very clean, and especially free from the grease of the ground joint. To this end a small groove is cut around the metal cone at about one-fourth of its length from the outer end. In applying the grease, and during the operation of the tube, one should see to it that no grease gets beyond this groove. In this connection attention may be called to a minor point, which is nevertheless important for the good performance of the tube; if the metal cone be shorter than the ground glass surface, so that the ground glass extends beyond the metal, and is in contact with it, then when the high tension is applied there is a strong electric field at the common boundary of glass and metal, and sparks are likely to occur along the glass. These sparks heat the tube strongly and are liable to crack it. Hence it is necessary that the metal part shall extend beyond the ground glass into the blown part of the tube; there will then be no field at the circle of contact. For similar reasons one must take care that in sealing in the anode the pizein is not exposed inside the tube so that it may serve as a starting-point for a discharge along the glass wall.

The piece which carries the hot cathode is in metallic contact with the cubical box. This cathode holder has direct electrical connection with one end of the tungsten spiral, while the circuit is made to the other end by an iron rod 2 mm. in diameter, which passes lengthwise through the middle of the holder and is insulated from it. This insulation is secured by two small pieces of quartz tubing placed at either end. At the inner end this rod bears a small nickel cylinder with a screw for attaching the tungsten wire. The entrance of the iron rod is sealed off by a little pizein at the outer end of the cathode holder. In order to focus the cathode rays a thin-walled iron cylinder surrounds the tungsten spiral. By screwing this cylinder on more or less the focus may readily be varied from a circular spot of about one mm. diameter up to one of six or eight mm.

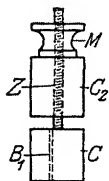


FIG. 25. Simple device for making tungsten spirals for use as hot filaments.

The production of tungsten spirals of four or five turns, from wire of 0.2 or 0.3 mm. diameter, is easily accomplished by the contrivance shown in Fig. 25. After the spiral has been wound and the top screwed on, the whole is heated a moment to a faint red glow.

Finally, the slit consists of two equal parts, one of which is shown in Fig. 26. They are of steel, and are held together by two small steel screws. The faces of the slit are polished to a plane surface with an oil-stone. Leaves of aluminium or



mica are inserted between the two sections to give the slit the required width. The slit is made fast by a little pizein in the cavity bored for it in the tube. The real vacuum seal is obtained by a foil of aluminium, or by a piece of gold-beater's skin  $15 \times 15$  mm. in size, which is laid over the slit.

This tube is suitable for tensions up to some 30 kv. In general, a current of 30 to 50 milliamperes may be used for studying infusible substances which cannot be soldered to the anode in sheet form, but which are rubbed on as powder in the ordinary way. With a larger current the material will be scattered from its place too rapidly. With a tungsten anti-cathode, which is used, for example, in photographing absorption spectra, the current may be pushed much higher. The author has even tested the tube with 200 milliamperes at 20 kv. But even the tungsten target bears up under such a load only with difficulty, and ordinarily the current should not exceed 100 milliamperes. With heavy currents there is also the danger that, as a result of the liberation of a bubble of gas, or from some other cause, a sudden lowering of the vacuum will permit a much too powerful ionic current to traverse the tube.

Since these tubes are, of course, opaque on all sides, one cannot see what is going on inside; therefore one must judge how the tube is working from the indications of the ammeter connected in the high tension circuit, and from some type of high tension voltmeter. It is also very desirable to have an ammeter in the filament circuit, so that one may know the condition of the hot spiral. It is best to heat the filament by a storage battery so that the spiral may be maintained at a constant temperature. In general, for greater convenience, we may earth the cathode, thus avoiding the necessity of insulating the rheostat in the filament circuit.

To test the tube we may simply proceed as follows: first, without turning on the filament current, see if the tube will sustain the high tension without allowing any discharge whatever to pass, even when the voltage is raised above that which it is intended to use. It is advisable at first to admit air to the tube several times at a pressure corresponding to that of the backing pump, in order that the gases adsorbed on the walls may be removed more quickly. When the vacuum has reached the stage at which no discharge occurs, then the temperature of the filament may be raised by increasing the current slowly, meanwhile keeping a moderately large voltage applied to the tube. If the vacuum is good the high tension current increases continuously with increasing filament current. Since the current in the tube depends on the number of electrons liberated from the cathode, we might expect the current to be exactly proportional

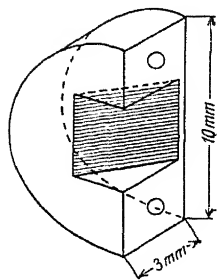


FIG. 26.

to the number of electrons. This is true at first, and is approximately so when higher tensions are applied to the tube, as in the case of ordinary medical practice, but in X-ray spectroscopy moderate tensions are often used, and then there is a disturbing effect on this proportionality. The hot wire begins to emit electrons in appreciable quantities at a temperature of about  $1800^{\circ}\text{K}$ . Above that temperature their number increases very rapidly, as indicated by the full line curve of Fig. 27. According to Richardson, the quantitative relation between the number of electrons

ejected and the temperature is given by the equation

$$N = CT^2 e^{-\frac{d}{T}}, \quad (26)$$

in which  $C$  and  $d$  are constants depending on the material of the wire, and  $T$  is its absolute temperature.

When the difference of potential between the anode and cathode is small the electric field is unable to remove the electrons from the cathode as fast as they are produced. Hence, with constant voltage and increasing temperature, the tube current increases more slowly than the number of electrons, and even approaches a limiting maximum value, so

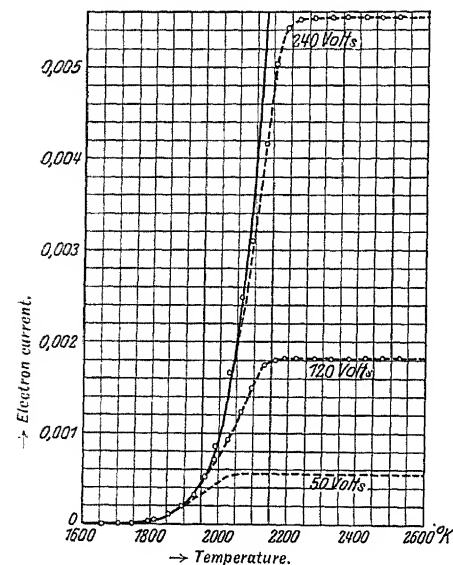


FIG. 27.

that a further rise of temperature with the consequent increase in number of electrons causes no greater current. This maximum value depends on the difference of potential between the two electrodes and increases with this difference, as may be seen from the dotted curves of Fig. 27, which are taken from Langmuir's work.

Langmuir has given a more comprehensive explanation of this phenomenon, which plays an important rôle in the use of X-ray tubes for spectroscopic purposes. We will follow his treatment in a simple case, the conditions of which are in effect very similar to those concerned in X-ray tubes. Let there be a difference of potential of  $V_0$  volts between the plane parallel plates  $A$  and  $B$  (Fig. 28). If there are no charges in the space between the plates, then the potential will evidently rise uniformly from  $A$  to  $B$  according to the line  $PQV_0$ . But if a certain number of electrons per second are given off by the plate  $A$ , the potential distribution is thereby changed. The curve showing the value of  $V$  takes

the general form of  $PSV_0$ . The more electrons given off by  $A$  the more the potential curve sinks, until at the point  $P$  it is perpendicular to the plate. This means that  $\frac{dV}{dx}$ , the intensity of the electric field, is zero in that region, and hence the electrons liberated are not carried away; a saturation current is reached. From Poisson's equation,

$$\frac{d^2V}{dx^2} = 4\pi\rho, \quad (27)$$

$\rho$  being the density of the negative electricity in the plane  $x$ . When an electron of charge  $e$  leaves the plate  $A$  and travels along the plane  $x$  through a difference of potential  $V$ , its kinetic energy is increased by

$$\frac{1}{2}mv^2 = eV, \quad (28)$$

where  $m$  is the mass of the electron and  $v$  its velocity. The current in the plane  $x$ , per unit cross-section perpendicular to the plane, is

$$i = vp. \quad (29)$$

By elimination we obtain from these three equations

$$\frac{d^2V}{dx^2} = 2\pi i \sqrt{\frac{2m}{Ve}}. \quad (30)$$

If we integrate this equation subject to the boundary conditions of the saturation current, that is, if we put

$$V = 0; \quad \frac{dV}{dx} = 0, \quad \text{when } x = 0, \quad (31)$$

we obtain

$$i_{\max} = \frac{\sqrt{2}}{9\pi} \sqrt{\frac{e}{m}} \frac{V^{\frac{3}{2}}}{x^2}. \quad (32)$$

Hence the maximum current possible is inversely proportional to the square of the distance between the two plates, and it increases as  $V^{\frac{3}{2}}$ . Langmuir was able to show, by consideration of dimensions, that the maximum current is always proportional to  $V^{\frac{3}{2}}$ . Concerning the effect of the geometrical configuration of the electrodes, it is in general true that the current may be increased by bringing the electrodes nearer to each other. The actual conditions in X-ray tubes of this kind under consideration are, moreover, very much like those in the special case of the two plates just described, and the dependence of the maximum current on  $\frac{1}{x^2}$ , expressed by (32), should, therefore, be approximately true here.

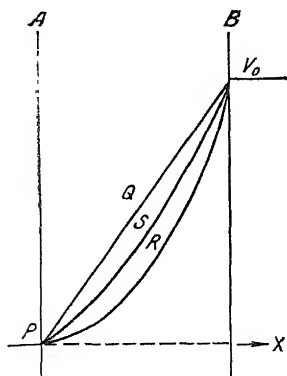


Fig. 28.

In order to obtain some idea of the order of magnitude of this maximum current the author has made a few measurements with a tube of the type of Fig. 30A. These are simply rough measurements carried out with a pulsating direct current. The following table shows the dependence of the maximum current, measured in milliamperes, on the difference in potential between the electrodes.

Tension. Volts.	Maximum Current. Millamps.	Tension. Volts.	Maximum Current. Millamps.
7,000	14	14,000	90
9,000	32	16,000	130
12,500	70	18,000	200

If unidirectional and *constant* voltage be used the maximum currents are substantially greater. With the smaller voltages the saturation value of the current is quickly reached, thus setting a very low limit to the capacity of the tube. The remedy for this difficulty is evident, however, from what has been said above; it is merely necessary to decrease the distance from cathode to anode. Fig. 29 illustrates a construction of cathode and anode which was used by Hjalmar, and found quite satisfactory for lower voltages. The distance may here be made as small as desired.

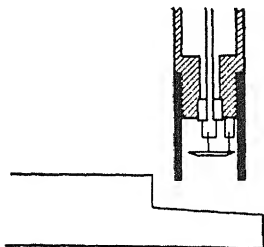


FIG. 29.

We now return to the question of the operation of the tube. If the vacuum in the tube is high enough for it to operate as an electron tube the action is as follows: with a given voltage applied to the tube, when the filament circuit is closed and the heating current raised to a certain value (6 to 8 amp. for a filament of diameter 0.25 mm.), the high tension current begins, and rises rapidly according to the curve in Fig. 27. At moderate voltages the maximum current is soon reached, and a further increase of the filament current causes no corresponding rise in the tube current, but may easily result in burning out the filament, which was at a very high temperature even when the saturation current was reached. A rise in the voltage applied to the tube immediately makes an increase in the tube current possible.

The electron discharge at first liberates absorbed gases and vapours, and thereby lowers the vacuum. The ionic current which ensues may readily endanger the glass joint. It is therefore highly advisable that the current and voltage be raised carefully at first.

When the tube is in use it must be cooled by running water. For this purpose the high tension electrode may be connected directly to the

water tap through several metres of glass or rubber tubing. With a voltage as high as 30 kv. the current through the stream of water, which is in parallel with the tube current, does not exceed a few milliamperes, and hence does no great harm. Its magnitude may be found by disconnecting the filament current.

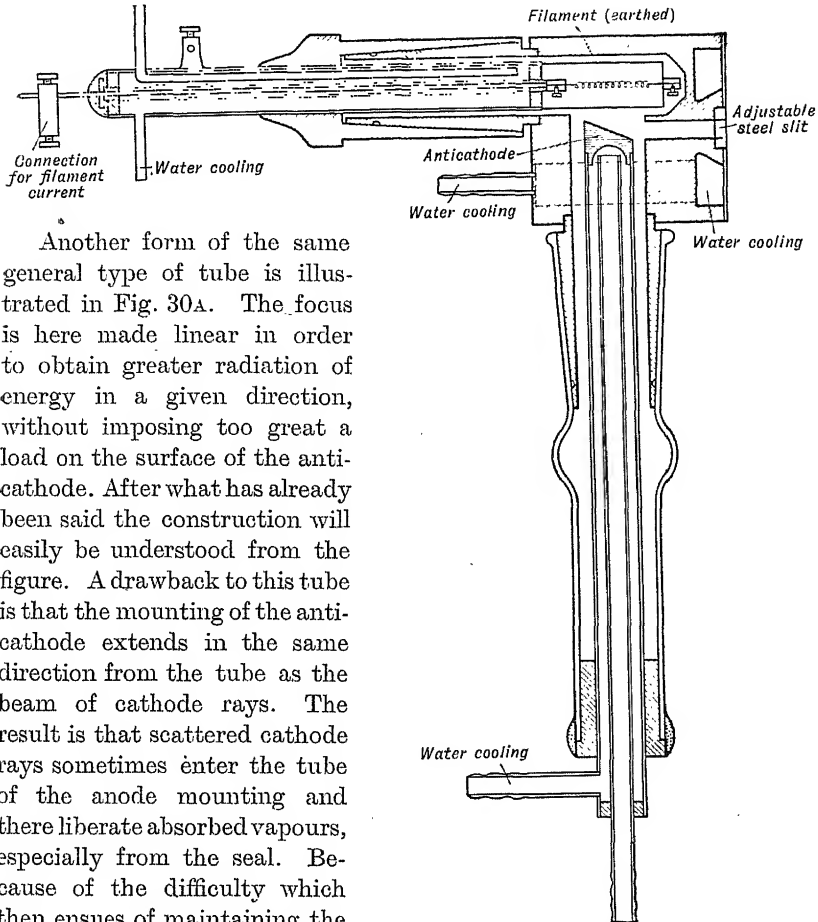


FIG. 30A. Metal hot cathode tube with linear focus.

Another form of the same general type of tube is illustrated in Fig. 30A. The focus is here made linear in order to obtain greater radiation of energy in a given direction, without imposing too great a load on the surface of the anticathode. After what has already been said the construction will easily be understood from the figure. A drawback to this tube is that the mounting of the anticathode extends in the same direction from the tube as the beam of cathode rays. The result is that scattered cathode rays sometimes enter the tube of the anode mounting and there liberate absorbed vapours, especially from the seal. Because of the difficulty which then ensues of maintaining the proper high vacuum, such large currents pass through the tube that the glass joint is liable to be cracked by local heating. This form of tube therefore demands more careful operation than the preceding one, but with this provision it works equally well.

Finally, we may mention a cylindrical tube of the same type, so constructed that it is possible to approach nearer to the anticathode than

with either of the two tubes discussed above. This tube, shown in Fig 30B, shares with the preceding one the disadvantage that the anode seal is exposed to bombardment

from the scattered cathode rays. For certain special purposes the tube has amply demonstrated its usefulness.

In his investigations of the fainter lines in the *L* series of the heaviest elements A. Dauvillier has employed tubes made entirely of quartz. Such a tube is shown in the right side of Fig. 31.

Three-electrode tubes also essentially belong to the electron type here described. Lilienfeld's tube is probably so far the one of greatest practical importance among these. Compared with the electron tubes heretofore described, the Lilienfeld tube has the essentially different feature that the cathode is not heated, and that the electrons which give rise to the X-rays are not the primary electrons from the filament. Instead, the electrons which proceed from the cathode and fall upon the anticathode are liberated from an opening in the middle of the cold cathode by primary thermoelectrons from the filament *G* (Fig. 32A). These electrons are driven by a field of several hundred volts into the opening of the cathode, and there, striking the walls, they liberate new electrons in greater numbers. Two separate voltages are thus necessary for the operation of this tube; in addition to the regular high tension between cathode and anode there is an exciting voltage *Z* to accelerate

FIG. 30B. Cylindrical metallic hot cathode tube with very short distance between focus and slit.

the electrons from the filament *G* in the direction of the cathode. A few hundred volts suffice for the latter purpose, as stated above.

No matter how many electrons are given off by the filament this tube will not emit radiation except when the exciting voltage is applied. The

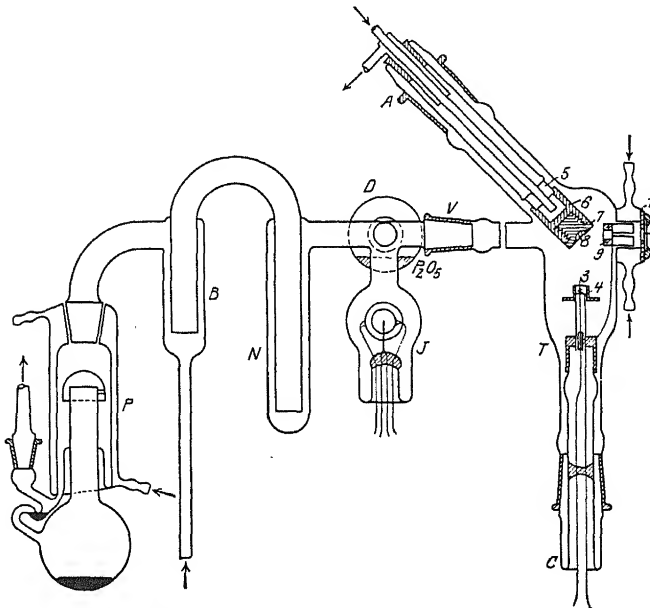


FIG. 31. Quartz tube, after Dauvillier, having hot filament, and changeable cathode and anode; evacuated by a Langmuir pump of quartz.

strength of the high voltage current can thus be controlled by means of the exciting voltage. The two voltages necessary for this tube may be supplied by the arrangement shown in Fig. 32A, in which two separate transformers are connected to the same primary alternating current circuit, while a third step-down transformer furnishes the current for the filament. Each of the two transformers is separately controlled.

Another system of connections is shown in Fig. 32B; here the tube is attached to an induction coil. A high resistance  $a$  of special construction and a "balancing" resistance  $b$  divide the available voltage in the proper ratio between the two circuits. In addition, the tube has an auxiliary electrode  $S$  with its accompanying "probing" resistance  $d$ , which provides further regulation. In both arrangements the filament is

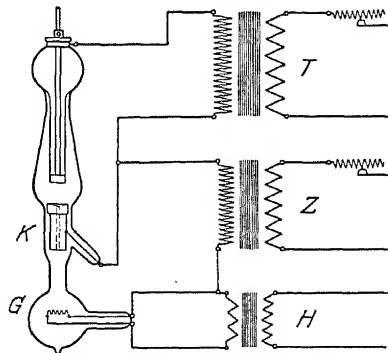


FIG. 32A. Lillienfeld tube with transformer connections.

supplied with enough current to produce an excess of electrons in the chamber *G*.

With tubes of this construction spectra have been obtained of certain elements which are suitable material for the anticathodes of commercial tubes. As far as is known to the author they are not used for purposes of general X-ray spectroscopy, because the three electrodes, in addition to the requisite exciting voltage, represent undesirable complications.

For crystallographic work, especially in photographing Laue diagrams, they have given excellent service, as is testified by the fine work in this

and other directions from the Rinne Institute in Leipzig.

Later we shall return to the construction of electron tubes which are applicable to the spectral region extending from long wave-length X-rays to the shortest light waves. Before leaving the subject of electron tubes, however, we will mention two arrangements of tubes which have been used for special purposes. In order to compare the total radiation from a series of elements, Brainin soldered sheets of the substances in question to the sides of a hexagonal prism. This prism which

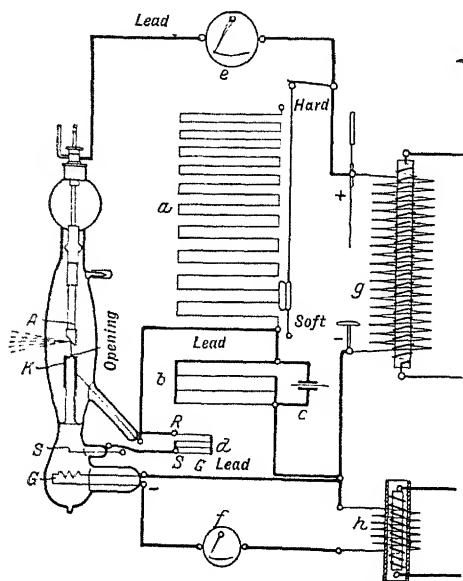


FIG. 32B. Lilliefeld tube driven by induction coil.

formed the anticathode could be rotated about its axis, while the cathode was of the ordinary Coolidge type (see Fig. 33).

C. D. Miller, using a Coolidge tube at very low voltage, investigated the absorption of long wave-length residual rays in various substances. His apparatus is represented in Fig. 34. The special side tube is covered with thin foil. Directly in front of the foil is a filter for the rays, which allows only the hardest of them to pass through. The hardness of the residual rays was varied by changing the voltage. Of course the method does not afford radiation of the homogeneity of spectral lines, but rather a spectral region of considerable width; nevertheless, if perfect homogeneity is not essential the method has the advantage of great intensity.

Concerning the methods of producing electrons mentioned at the beginning, namely, by cathodes of hot oxides, and by illumination with



ultra-violet light, we may mention that they have actually been used for special investigations; for example, to produce very soft rays. Compared with the methods previously discussed, however, which are more convenient and which yield better results, they have lost their importance for most purposes, and it does not seem necessary to enter into a further consideration of them.

This is probably not so with the last-mentioned autoelectron method of Lilienfeld. This method of producing X-rays is both simple and effective, and is full of promise.

But it was only recently invented, and the publications concerning it are yet too meagre to permit of closer study. Only the most important points may be mentioned here. With a vacuum as high as that in the ordinary electron tube, it is generally impossible, even with the highest voltage applied to the electrodes, to

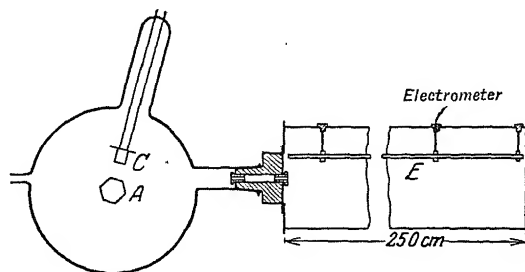


FIG. 33. Brainin's arrangement for changing the material of the anticathode in a Coolidge tube.

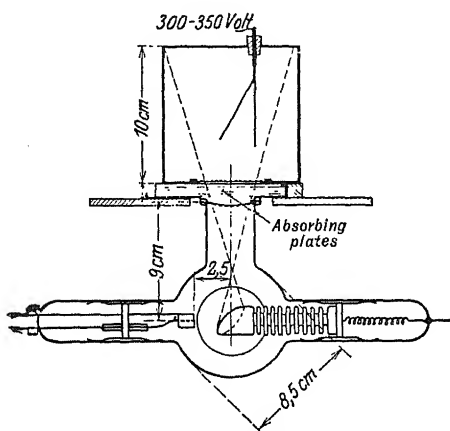


FIG. 34. C. D. Miller's apparatus for very soft rays.

cause a current to flow through the tube without first heating the cathode. Lilienfeld has found, however, that a discharge is possible when the cathode is pointed and placed within a few millimetres of the anticathode. The intense field set up around the point of the cathode can, so to speak, draw electrons out from it. Just what the mechanism of the discharge is does not yet seem to be entirely clear, but it may be noted that X-rays are emitted not only from the

anode but also from the cathode, although from the latter in much smaller quantity. Spectroscopic study of the radiation has not yet been made; nor has the suitability of the tube for spectroscopic work been investigated.

It remains to be mentioned that J. J. Thomson has performed the experiment of exciting X-rays by bombardment with positive ions. In the work of Thomson the method did not seem capable of very great

efficiency, and, so far as is known to the author, no other attempts in this direction have been made.

## 16. Spectroscopic Apparatus

### *A. Spectrographs for the photographic method.*

From the beginnings of X-ray spectroscopy use has been made of the photographic action of the rays as well as of their ionizing properties. In a few cases their property of producing optical fluorescence has also been employed to demonstrate very intense spectra. Since the last method is not a sensitive one we shall omit a discussion of it here, and devote our attention only to the first two. The photographic method has had the wider application, and we will therefore begin by describing it.

According to the fundamental equation of X-ray spectroscopy, it is necessary for the production of a spectrum to have a very definite angle

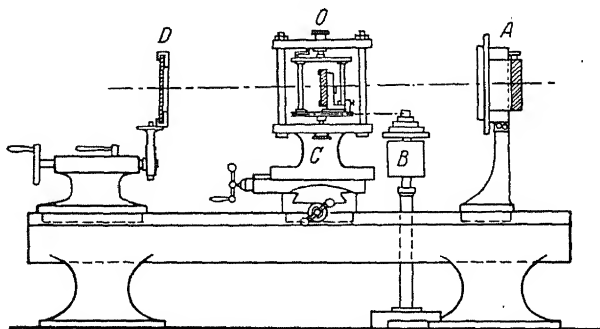


FIG. 35. Spectroscope with rotating crystal, after de Broglie.

of reflection  $\phi$  for every wave-length  $\lambda$  of the radiation to be examined. It is the problem of spectrometry to determine experimentally the angle  $\phi$  concerned, in order to compute therefrom the wave-length by the relation referred to above.

The method employed by Moseley in his experiments is portrayed in the diagram of Fig. 16. The slit at  $P$  is placed as near as possible to the focus of the X-ray tube, so as to allow the passage of a beam of rays of as large an angular width as possible. The crystal is set up at  $O$ , while the photographic plate is held by an arm capable of rotating about an axis through  $O$ . When the plate is in the position **3** it receives rays which are reflected from the crystal at various angles, the smallest angle corresponding to  $R_1$ , the largest to  $R_2$ . Thus a considerable range of wave-lengths is photographed, corresponding to the various angles of reflection. In this way, by taking a number of photographs with different angles of crystal and plate, the entire spectrum may be photographed.

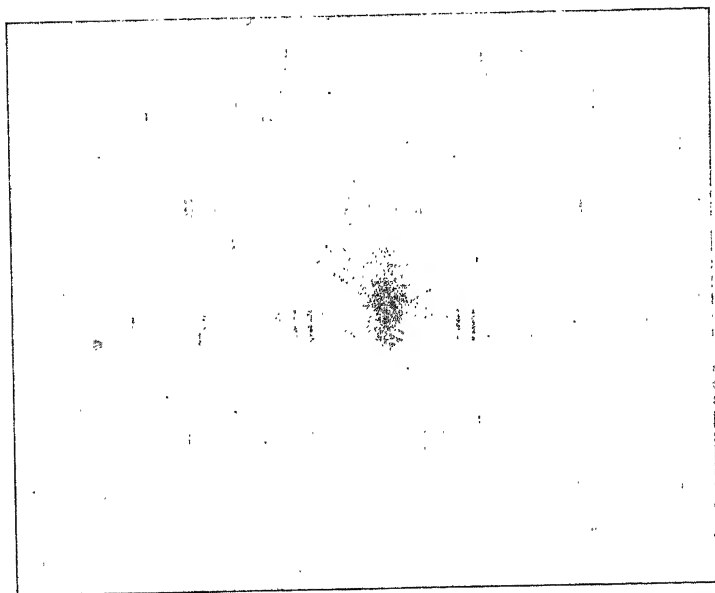


FIG. 36. Photograph of X-ray spectrum by de Broglie, taken with a rotating crystal.

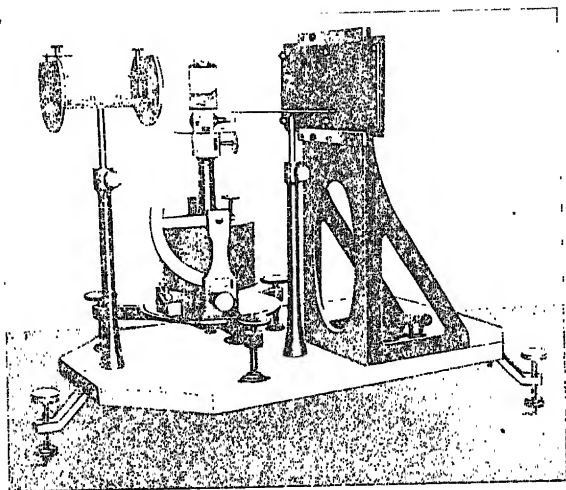


FIG. 37. Apparatus used by [illegible] for the method [illegible]

In order to determine the angles of reflection corresponding to the spectrum lines Moseley photographed two reference lines, by replacing the crystal by a slit and turning the plate through a known angle sufficient to cause the reference line to fall upon the plate. By taking a short exposure the direction of the line  $PO$  is indicated on the plate.

Directly transmitted beam

$\beta_2 \beta_1 \alpha_1 \alpha_2$   
 $\vee \quad \vee$

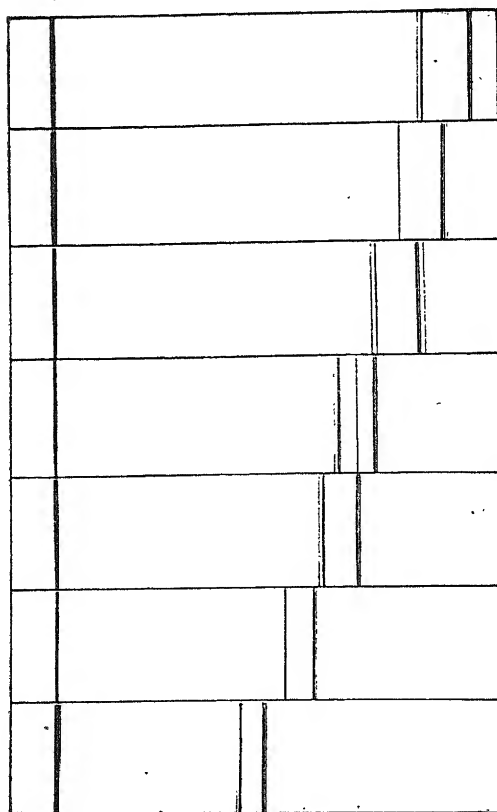


FIG. 35. Taken with the author.

By this method it is possible at each exposure to photograph only a relatively small range of wave-lengths, especially when the angle of reflection is small. But if the arrangement is such that the plate and the slit are equidistant from the axis of rotation of the crystal, then, as explained earlier, a "focussing" effect is attained. This has the advantage that with the plate (or, more accurately, with a film bent in the arc of a circle) fixed in position, one and the same wave-length is always reflected to the same point on the plate, independently of the angular position of the crystal. In this way it is possible, by slowly turning the crystal, to photograph in one

exposure a much larger region of the spectrum.

This rotating crystal method was first employed in X-ray spectroscopy by de Broglie. He caused the crystal to be turned continuously by clockwork, and, since the region under investigation was comprised between the limits of about  $0^\circ$  and  $15^\circ$ , he was able to obtain the entire spectrum on a flat plate. Fig. 35 is a reproduction of a later arrangement in which the very large distance from slit to photographic plate results in

greater dispersion. Here de Broglie mounted the entire spectrographic apparatus upon a lathe bed adapted for the purpose; the slit is at *A*, the crystal is mounted upon the rotating support, and the plate is held at *D*. The clockwork may be seen at *B*.

One of the first beautiful photographs by de Broglie is reproduced in Fig. 36. It shows those portions of the spectrum of platinum which are able to penetrate the glass wall of the tube. In addition to the principal spectrum, which lies in the horizontal plane through the directly transmitted beam, a series of subordinate spectra may be seen. These spectra are caused by reflection from crystal planes inclined to the axis of rotation.

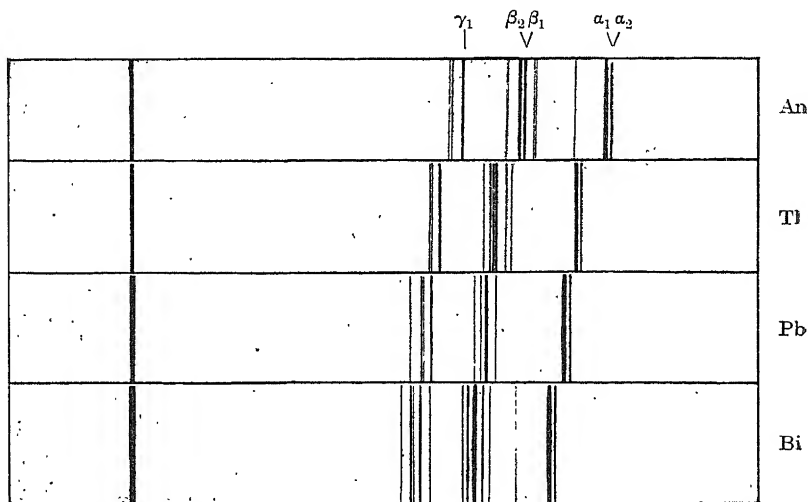


FIG. 39. The *L* series of four elements. Taken by Friman and the author with the spectrograph of Fig. 37.

The spectrographic apparatus of Fig. 37, built on the same principles as de Broglie's, was used by E. Friman and the author for the measurement of a number of spectra in the *K* and *L* series. The crystal was carried on clockwork which consisted of a demounted mirror heliostat. In addition to the adjustable slit, a second slit is placed between the X-ray tube and the crystal, and as near as possible to the latter. The direct beam through the axis of rotation of the crystal may be photographed by means of this latter slit. In order to do this the two slits are made as narrow as possible, and the crystal table is slightly displaced to one side. After this direct beam is photographed the second slit is opened to a width of two or three mm. and serves as a screen. The region of the plate upon which the direct beam would fall is protected from further radiation by a strip of lead placed just in front of the plate. Figs. 38 and 39 are reproductions of photographs of spectra taken with

this apparatus; the former belong to the  $K$  series, the latter to the  $L$  series.

Seeman has given an account of a somewhat different procedure in which, by using a rotation method, he could photograph a larger region of the spectrum.

In this arrangement a straight edge (Fig. 40A) is placed close to and parallel to the face of a good crystal. The rays from the anticathode are reflected by the crystal, and pass through the opening between the edge and the crystal. If the anticathode be continuously displaced so that the incident rays fall upon the crystal at different angles, a spectrum is thrown upon the film. The same result is attained if the entire spectrograph is rotated with respect to the X-ray tube. It is plain that the straight edge and its image in the crystal correspond in this case to the slit. Since the X-rays are not reflected exactly at the optical surface,

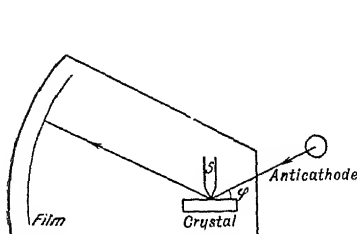


FIG. 40A. Scheme of the "edge" spectrograph of Seeman.

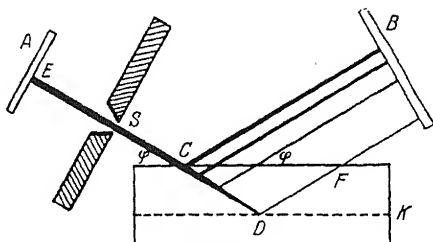


FIG. 40B.

but penetrate more or less into the crystal, the width of the slit is rather indefinite. With radiation of shorter wave-length, the depth of penetration is greater, and the apparent width of the slit increases without any change in the position of the straight edge. This is, of course, more or less the case also in the X-ray spectrographs described earlier; only there one may choose a more suitable material for the slit.

In a modification of his edge spectrograph (Schneidenspektrograph) Seeman placed the slit close *behind* the crystal, that is, the rays passed through the slit *after* reflection. The advantage of this arrangement appears from Fig. 40B. Let  $A$  be the source of the X-rays and  $K$  the crystal; then the rays reflected at various depths in the crystal give rise to a broad line on the plate, corresponding to the depth of penetration. The intensity of the line, as indicated in the diagram, will gradually fall off on the side towards the crystal, for the rays on this side of the line have travelled a greater distance in the crystal, and consequently are more strongly absorbed. But if the direction of the rays is reversed, that is, if the source is at  $B$  and the plate at  $A$ , then the rays reflected at various depths in the crystal are united in a single narrow bundle.

The justification of this last proposal rests on the imperfection of crystals. For the theory shows that if the space-lattice were perfect, the entire reflection would occur in a layer a few thousandths of a mm. in thickness, independently of the wave-length (provided equation (16) be fulfilled). As a matter of fact the crystal is composed of a multitude of micro-crystals of nearly but not quite common orientation, and hence it

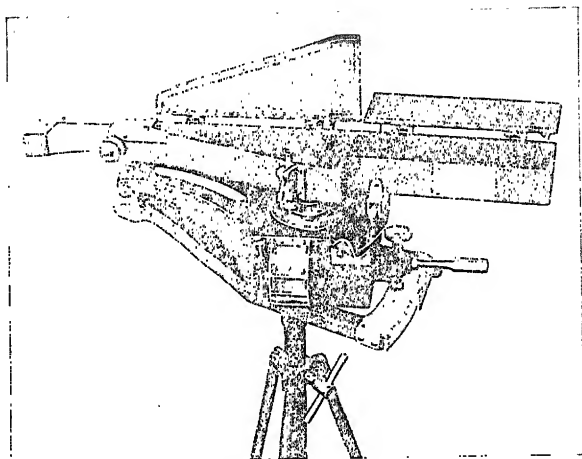


FIG. 41. Spectrograph of Seeman.

is possible that with hard radiation portions of the beam may be reflected only from planes lying deeper in the crystal, while they are only slightly absorbed by the surface layers according to the ordinary laws. The beam leaving the crystal will, of course, suffer the broadening which is due to irregular orientation of the microcrystals, but with the slit placed as in Fig. 40B the reflection at different depths in the crystal produces no such effect. Experience shows that under certain conditions the sharpness of the lines may be increased in this manner.

Seeman has constructed spectrographs of several different designs according to the above principles; they are very carefully worked out, and are especially adapted to shorter wave-lengths. In particular, they have found large application in medical X-ray practice. With the permission of Mr. Seeman one of his latest spectrographs of this type is reproduced in Fig. 41.

Earlier than Seeman's work, Rutherford, in his investigations of  $\gamma$ -rays from radioactive materials, had used an arrangement in which the

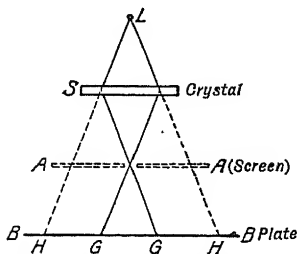


FIG. 42. Diagram of Rutherford's transmission method.

slit was placed behind the crystal. The principle may be seen from Fig. 42.  $L$  is a linear source of radiation. The rays reflected from the crystal  $S$  all meet at the point  $O$  and pass through a slit which is placed there. Behind this slit is the photographic plate  $B$ .

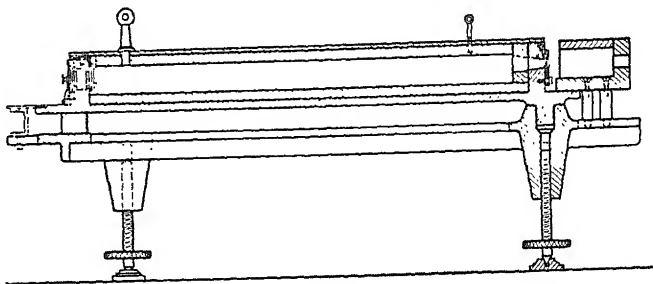


FIG. 43A.

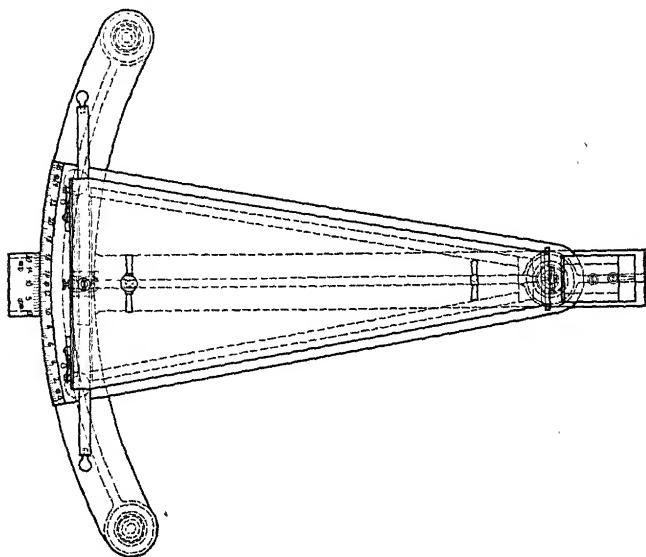


FIG. 43B.

FIGS. 43A, B, C. Spectrograph for the determination of very short wave-lengths (up to  $0.5 \text{ \AA.U.}$ ).

In order to obtain spectrograms capable of accurate measurement, the author has carried out two spectrograph designs suitable to the same region of wave-lengths as the Seeman type, namely, up to about  $1.2 \text{ \AA.U.}$ , and has made a series of measurements with them. It is readily seen on studying the question that one and the same spectrograph can hardly be used for the entire region if the highest precision is desired. The spectrograph shown in the two figures, 43A and 43B, is designed for the



shortest wave-lengths. The action of the spectrograph and the method of measurement may be understood most easily from Fig. 43D.

The X-ray beam under investigation passes through the opening *Bl.* and is deviated from its original direction through an angle  $2\phi$  on reflection at an inner system of atomic planes in the crystal *Cr.* Immediately behind the crystal is a gold slit, which transmits a narrow beam of the

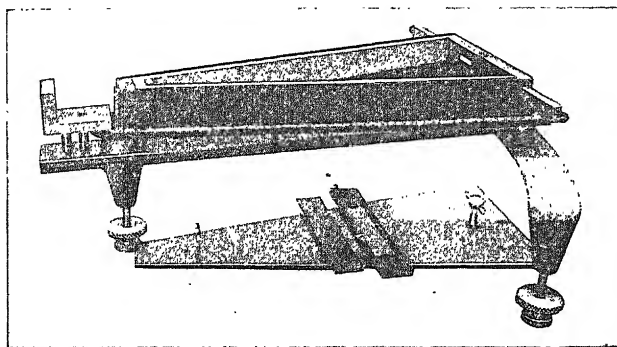


FIG. 43C.

reflected rays. At the back of the spectroscope this beam falls upon the photographic plate. Crystal, slit and plate are rigidly connected together, and may be rotated about a common axis passing through the slit. After the spectral line has been photographed in the position indicated, the system is rotated about its axis far enough so that the symmetrically located beam is reflected on the other side. In each case the part of the

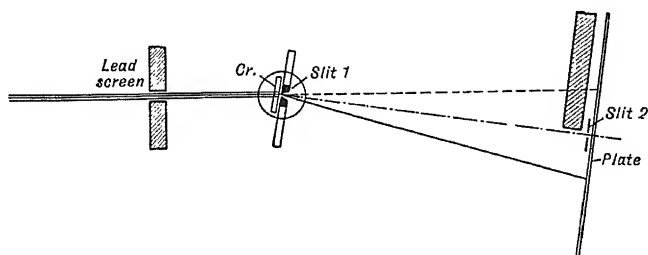


FIG. 43D.

plate not receiving the reflected beam is protected from blackening by a movable lead screen. In addition to the two lines symmetrically located with respect to the middle point, the middle of the plate, or the foot of the perpendicular from the slit upon the plate, is marked by allowing the X-rays to pass for a moment through a slit, *Sp. 2*, adjusted at this middle point.

In the construction of this instrument care is taken to shield the interior of the spectrograph from the very hard radiation used. Very thick lead screens and coatings over the walls exclude entirely all stray radiation. In order to facilitate adjustments the box which contains

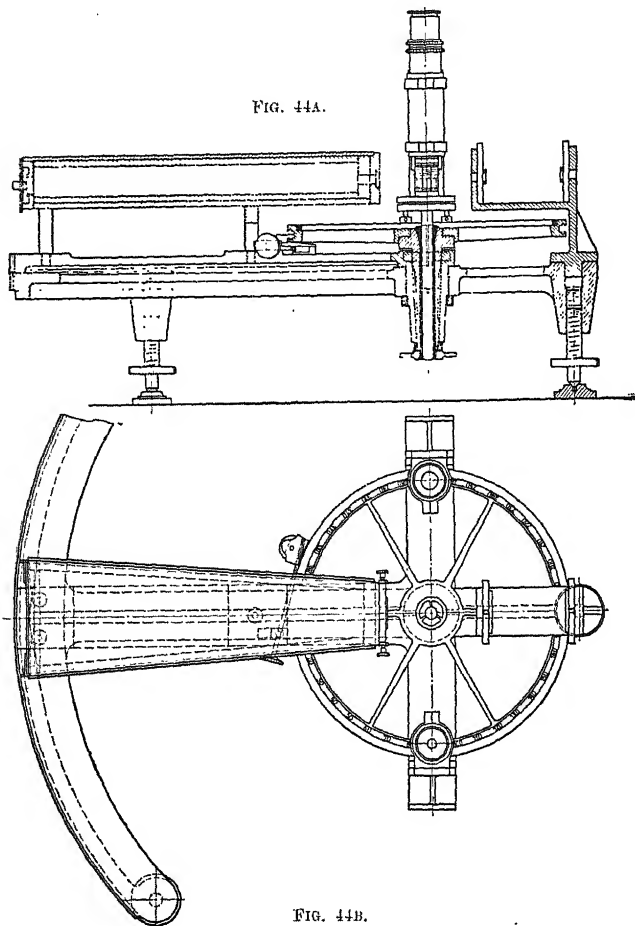


FIG. 44B.

FIGS. 44A, B, C. Spectrograph for the accurate determination of medium wave-lengths (0.5 to 2  $\text{\AA}$ .U.).

the real spectrograph is mounted upon a tripod in such a manner that the axis of rotation fits directly under the slit into a depression in one of the legs of the support below. The rear part of the instrument carries a circular scale on which the position of the spectrograph box can be read.

The crystal, which is of calcite, is so cut that the cleavage planes, at which reflection occurs, can be adjusted parallel to the normal to the

photographic plate. The thickness of the crystal should be from two to four mm., according to the penetrating power of the radiation under investigation. Slit 2 is adjusted first. The plate is replaced by a mirror, a beam of light is sent through the first slit, and the second one so placed that the beam of light passes through it also, is reflected at the mirror and returned to the first slit. The proper position of the crystal may be determined by a trial photograph of the tungsten *K* lines, for example. When the crystal is properly adjusted the two symmetrical images must be approximately equidistant from the central line. The angle of reflection is then calculated from measurements of the distance between the two lines and the distance between slit and plate, which latter need be measured but once. The photograph may be taken on only one side, and the distance between the line and the slit 2 measured, provided the slight displacement of the middle line from its true position has been determined from a previous photograph taken on both sides.

This method is suitable for the determination of very small angles where the distance out to the spectral lines is not very large. In case this distance is too large, and the surface of the plate is uneven, the result may be considerably in error, and it is then better to change the

method so that the distances to be measured on the plate are small. This necessitates a corresponding rotation of the plate holder, and this rotation must be determined by an accurate circular scale. The construction is then that represented in Figs. 44A, B, C. As the diagram of Fig. 44D shows, the slit and the photographic plate form the two opposite ends of a pyramid-shaped box. The crystal is fastened, separate from the slit, on a rotating mechanism with a precision scale attached. The reading on the scale always gives the amount the crystal is turned with respect to the line joining slit and plate. First the crystal is placed in position 1, so that the wave-length to be measured is reflected through the slit. Then the crystal is turned far enough to reflect rays of the same wave-length into the box in the position 2. The angle of rotation of the crystal which is necessary for this purpose is read from the circular scale. If the rotation of the crystal with respect to the line from slit to plate

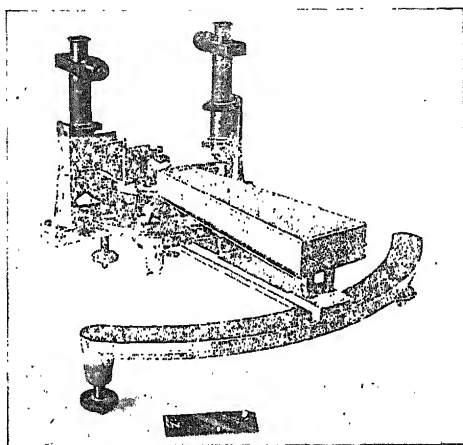


FIG. 44c.

is exactly  $2\phi$ , then the two lines will be superposed. But if we make the angle a little larger or a little smaller than  $2\phi$  we obtain two lines lying near to each other, and their angular separation may be calculated with sufficient accuracy by measuring their linear separation and the distance from slit to plate. This small angle is then applied as a correction to the angle read off from the circular scale.

Figs. 44A, B, C represent the construction of the spectrograph necessary to accord with the diagrammatic representation given above. The under part consists of a tripod, to which the real spectrograph is attached so as to be capable of rotation. A plate of cast iron carries the slit and plate holder, as well as two microscopes for reading the precision scale.

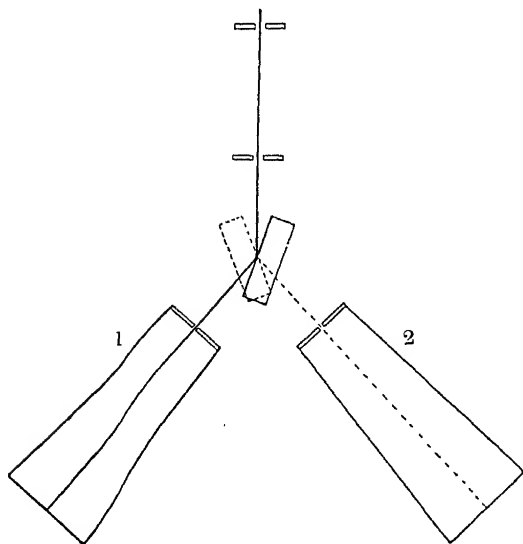


FIG. 44D.

The crystal holder, on the contrary, is fixed to the circular scale, and turns in a conical hole bored in the cast-iron plate.

This spectrograph is best suited for measurements of wave-lengths in the region from about 0.5 to 2 Å.U. Measurements by this spectrograph and by the previous one of the same wave-length in the region where their spectral fields meet have shown a satisfactory agreement.

Uhler and Cooksey have built, on another principle, a spectrograph which serves to make measurements in the same region of wave-lengths. The plan of the apparatus is represented in Fig. 45. Two successive slits,  $S$  and  $S'$ , separate out a very narrow beam, which after reflection by the crystal at  $O$ , falls upon the photographic plate. The latter is mounted on the carriage of a dividing engine, so that it can be moved parallel to

itself an accurately measurable distance. By measuring the distances between the symmetrically placed spectrum line the angle of reflection is easily computed.

All the spectrographs previously described were designed for comparatively short wave-lengths, so that the absorption in the walls of the tube and in the air path is of no significance. But we must not forget that much the greatest part of the X-ray spectrum falls in a region where these factors cannot be neglected. Even for a wave-length of about  $1 \text{ \AA.U.}$  the absorption in the walls of an ordinary commercial tube becomes very considerable,

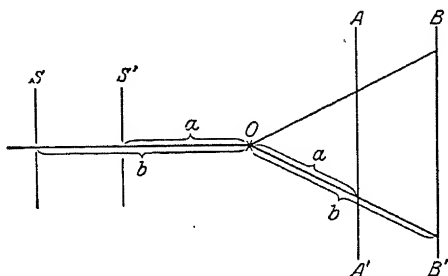


FIG. 45. Diagram showing the method of Uhler and Cooksey.

and at  $2.3 \text{ \AA.U.}$  the absorption in the air becomes strongly evident. As a glance at the table of wave-lengths shows, a part of the *K* series, most of the *L* series, and all of the *M* and *N* series fall in the region of greater wave-lengths. From this it is evident that the X-ray spectrograph needs above all else some provision for carrying out photography in a vacuum.

The first spectrograph for the investigation of the region of long wave-lengths was the vacuum spectrograph of Moseley, constructed as indicated in Fig. 46. As previously stated, Moseley worked with a fixed crystal, and without the "focussing" arrangement, hence the slit was located outside the spectrograph proper, and very close to the anticathode. Moseley thereby attained the large angular width of beam which his method postulated. The crystal upon the table *B* had during each exposure a definite position angle, and hence reflected each time a very definite region of the spectrum upon the plate *P*. As a source of radiation Moseley used a gas-filled tube of the Kaye type. The spectrograph was evacuated to a pressure of a few millimetres of mercury, and was separated from the higher vacuum in the tube by a diaphragm of gold-beaters' skin at *W*.

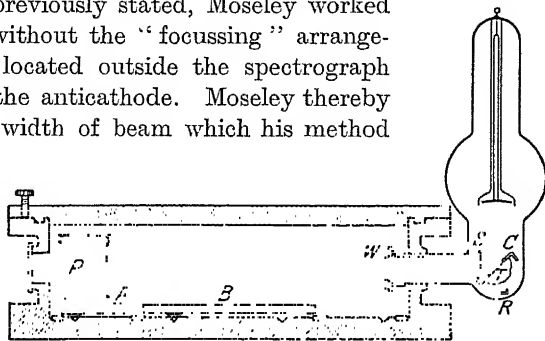


FIG. 46. Vacuum spectrograph of Moseley.

Moseley's method of measuring the spectral lines has already been given. It consisted in removing the crystal from its table, then turning

the plate holder from its original position through a known angle and photographing upon it two reference lines.

The author has built a spectrograph adapted to the rotating crystal method, in which, accordingly, the slit and the plate are equidistant from the axis of rotation of the crystal, and in which the crystal may be turned during the exposure. The earliest form of this apparatus is shown in Fig. 47A. In the centre of the large vessel was a conical bearing with a holder for the crystal. This cone could be turned from the outside by means of an arm which also gave readings on a graduated scale. The plate holder, however, in this apparatus was capable of only a few definite positions. The values of the angle corresponding to these possible positions were known from previous measurements. The source

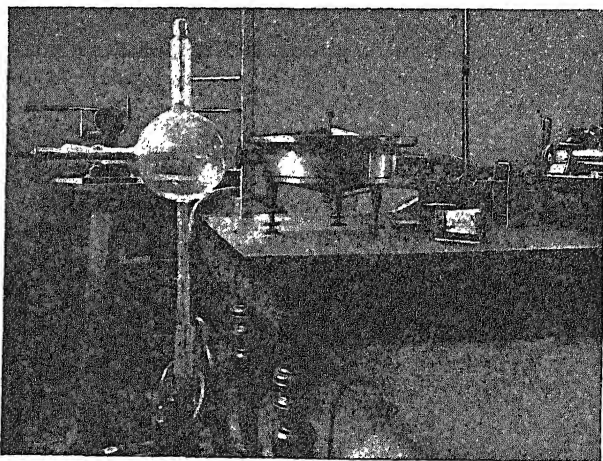


FIG. 47A. The author's first vacuum spectrograph with large glass X-ray tube.

of radiation was a large gas-filled tube with removable anticathode, such as has already been described. That this tube was capable of affording good spectrograms is evident from Fig. 47B, which represents the *L* series of ytterbium taken with this apparatus. (The *K* line of copper may also be seen upon the plate, since the material was rubbed on the copper plate of the anticathode.)

In the endeavour to attain greater accuracy of measurement than was possible with the apparatus just described, and, in addition, to make available greater intensity in the region of long wave-lengths, the author has made various changes in this vacuum spectrograph. We may first explain the principle of measurement on which these changes are based, since that is the determining factor in the construction.

The method of measurement is represented diagrammatically in Fig. 48. The crystal is mounted for the method of rotation, which means

that the crystal is at the same distance from slit and from plate. If the crystal is in the position 1, and the photographic plate at  $AA'$ , then a certain part of the spectrum appears on the plate. If now, keeping the plate fixed, we rotate the crystal, the position of the various spectral lines on the plate is not thereby changed, but the only result is that other parts of the crystal and of the focal spot take part in the reflection. When a given desired line has been photographed in this position, the plate is brought into the symmetrically opposite position  $BB'$  by turning through

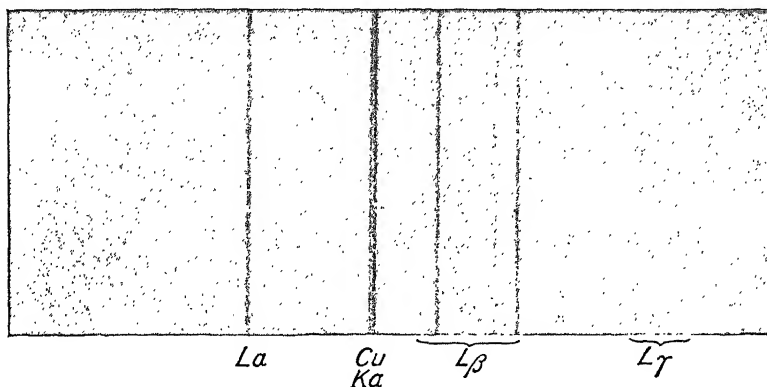


FIG. 47B. Spectrum of the  $L$  series of ytterbium taken with the spectrograph of Fig. 47 A.

an angle which can be read from a circular precision scale. Now if we bring the crystal into the position 2, the same spectral region is again obtained. On developing the plate we have two impressions of this spectral region which are related to each other on the plate as object and image in a mirror. The spectrum line under consideration thus appears twice on the plate, and the distance between its two positions may be made very small by a proper setting of the plate holder. If the rotation were exactly four times the angle of reflection for the wave-length concerned, then the lines would be precisely superposed. The plate holder should, however, be turned a little more or less, so that the lines are separated by two or three millimetres, a distance which can be measured accurately. By knowing the distance between the plate and the axis of rotation we are able to calculate the small angle corresponding to the distance between the two lines. We then obtain the true angle of reflec-

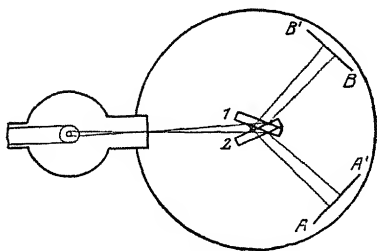


FIG. 48.

tion for the line concerned by adding (or subtracting) the small angle thus calculated to the angle of rotation.

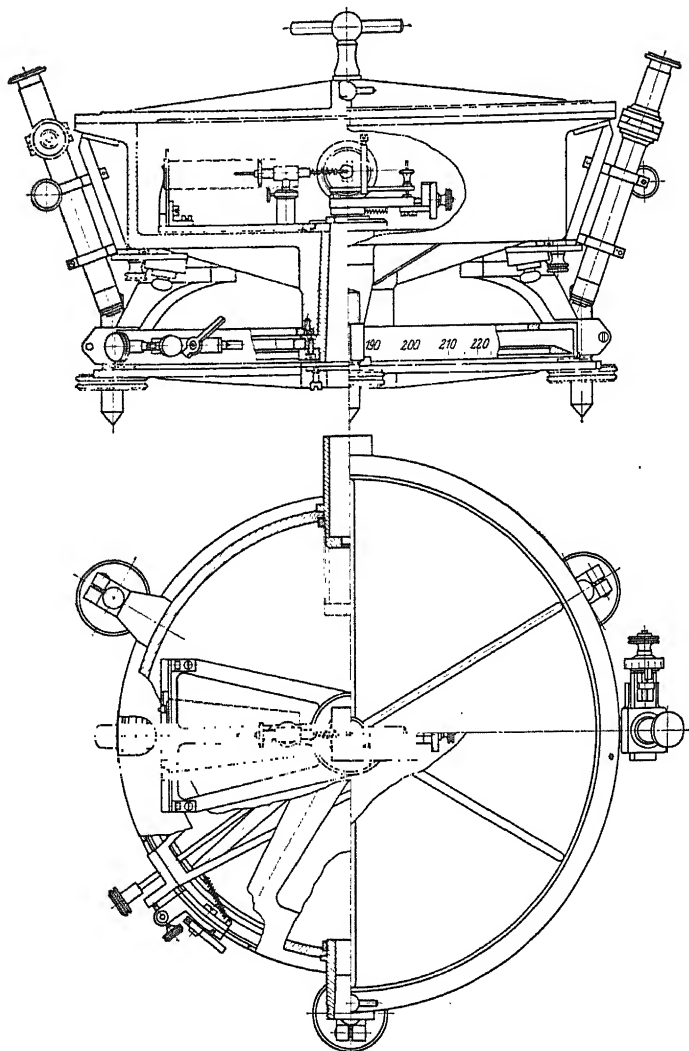


FIG. 49. Vacuum spectrograph of the author for accurate wave-length measurements. Plate holder and crystal are turned from without.

From this account of the method of measurement it is evident that the angle of rotation of the plate holder must be capable of accurate determination, while, for the crystal, a rough setting in angular position will suffice.



The way in which these requirements are fulfilled may be seen from Fig. 49. Through the bottom of the vacuum chamber two cones pass, having a common axis; the inner cone carries the crystal table, the outer the plate holder. Four horizontal arms at right angles are attached to the bottom of the inner cone. Each arm carries near the outer extremity a vernier which moves along a simple scale. This scale is marked on a guard ring, which serves as a protection for the precision scale. The latter is mounted rigidly on the outer cone, and the amount of rotation is read off by means of two microscopes provided with micrometer eyepieces. On the most recent spectrographs the smallest scale division is

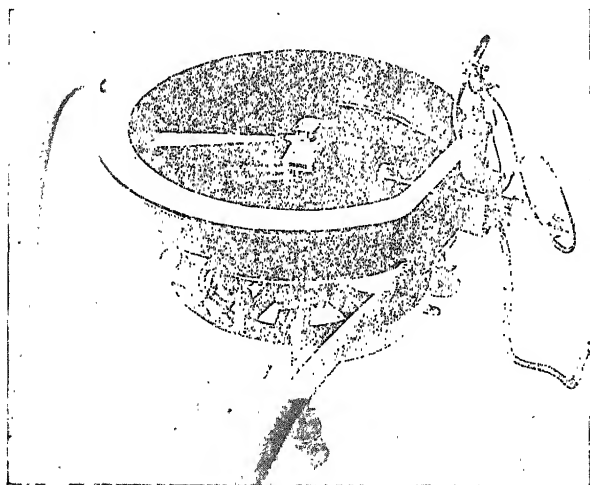


FIG. 50. View of a vacuum spectrograph according to the latest model.

5', and readings are accurate to 1 or 2 sec. of arc. A tangent screw to the outer cone allows the plate holder to be set accurately at the prescribed angle.

To conform to the conditions for focussing it must be possible to adjust the crystal so that the reflecting plane is parallel to, and coincides with, the axis of rotation. To permit these adjustments the crystal table first may be rotated about a horizontal axis, and second, it may be displaced by a micrometer in a horizontal plane perpendicular to the horizontal axis. Further, the plate holder may be moved in the direction towards the crystal, so that the plate may be set at a distance from the axis of rotation of the crystal equal to the distance between that axis and the slit. Great precision in this adjustment of the plate is unnecessary, but the distance from the axis of rotation to the middle of the plate must be determined to about 0.01 mm., in order to permit the

calculation of the angle corresponding to the small distance between lines on the plate to the desired degree of accuracy.

A more recent model<sup>1</sup> of the same spectrograph is shown in Fig. 50. In order to bring the tube and the anticathode nearer to the slit, the vacuum chamber is flattened on the side next the tube. The source of the radiation, the cubical electron tube which has been described before, is attached to the spectrograph by four screws. The entire equipment is depicted in Fig. 51. A capsule pump is used to evacuate the spectro-

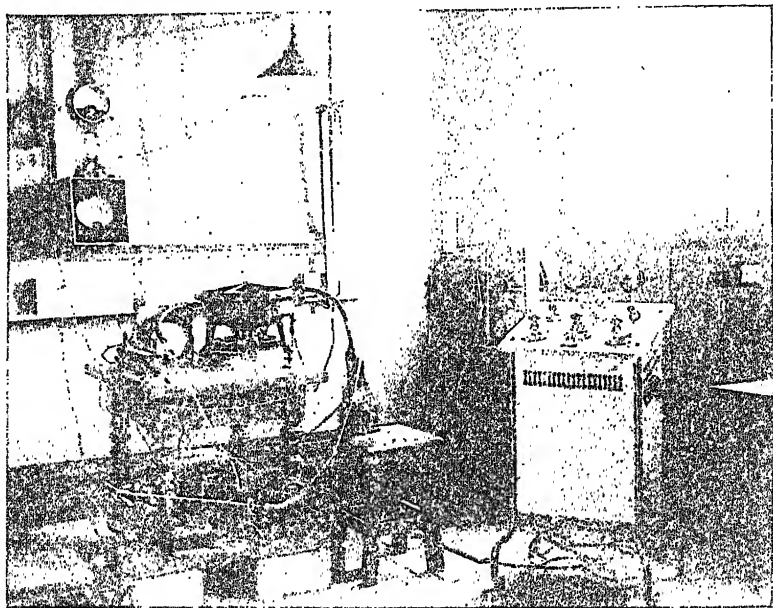


FIG. 51. Complete view of the vacuum spectrograph and accessories.

graph, and it serves at the same time as backing pump for the molecular pump. The latter is connected to the electron tube by a metal pipe.

A few words may be said on the adjustment of this spectrograph. The principal difficulty lies in getting the reflecting plane of the crystal actually to coincide with the axis, while it is comparatively easy to make them parallel to a sufficient degree of approximation. The latter adjustment is carried out by the help of a telescope and scale and by means of a plane parallel strip of glass, which is pressed against the face of the crystal and fastened there. Since the glass strip in general is not perfectly plane, and the observations are made from the upper half of it, the mean value is taken of two observations, for the second of which the glass strip is turned with the other side facing the crystal (see Fig. 52).

<sup>1</sup> Built by the Carl Leiss firm, Berlin-Steglitz, Stubenrauchplatz 1.

These two adjustments, namely, making the reflecting plane parallel to the axis of rotation, and causing this axis to fall in the plane of reflection, are of especial importance, and should be performed with care. The crystal is placed in the horizontal plane containing the focus of the anticathode and the part of the plate on which measurements are to be carried out. A slight error in adjusting the crystal surface parallel to the axis is then of less consequence. To adjust so that the axis falls in the crystal plane, a small auxiliary apparatus is temporarily attached to the arm of the plate holder (Fig. 52). This instrument is provided with a screw by means of which, when the plate holder is rotated, an ivory point may be adjusted, with the help of a microscope, until it is as nearly as possible in the axis of rotation. After this is done, the crystal, which was previously moved back somewhat, is now brought slowly towards the ivory point until they come in contact. The contact may be closely observed, for the point and its image in the crystal may both be seen in the microscope, and hence the instant when they touch is easily determined. This method makes it possible to adjust the crystal surface to coincidence with the axis of rotation with an accuracy of about 0.001 mm.

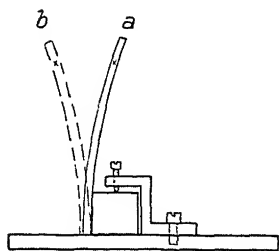


FIG. 52.

It is of no advantage to diminish the width of the slit to less than 0.02 or 0.03 mm., for in general the imperfections of the crystal are of such an order that a narrower slit does not increase the sharpness of the lines. For the same reason an increase in dimensions of the spectrograph gives no greater resolution, as experiments of the author have shown. In the neighbourhood of the copper *K* lines, whose wave-length is 1537 X.U. ( $1 \text{ X.U.} = \frac{1}{1000} \text{ \AA.U.}$ ), the author's larger spectrograph, with a slit width of 0.025 mm., gives a dispersion such that two lines which differ in wave-length by 0.4 X.U. are just resolved in the first order. The last investigation with this apparatus carried out by Hjalmar on the validity of the Bragg equation shows that it is possible to obtain spectrograms which may be satisfactorily measured even in the tenth order. Theoretically the dispersion should increase as the order increases, but for various reasons the lines lose in sharpness, so that the actual increase in resolving power is not very great.

With large angles of reflection the spectral lines on the plate appear curved. The following simple explanation shows how this curvature arises. According to the law of reflection a given wave-length is reflected at a definite angle of incidence. Let us now think of a given point source in the slit, and imagine the reflecting plane extending to infinity in all directions. All rays whose reflection is possible at a given angle

form a cone whose apex is at the point source, and whose axis is perpendicular to the reflecting surface. The reflected rays also form a cone whose apex is the image of the point source, and which cuts the reflecting surface in the same circle as the first cone. Since the photographic plate

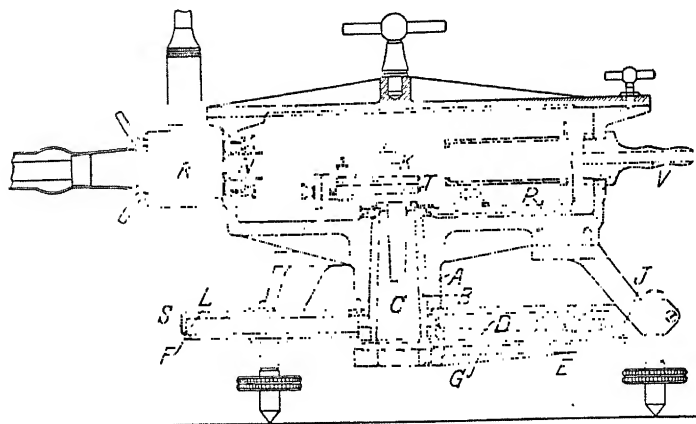


FIG. 53A.

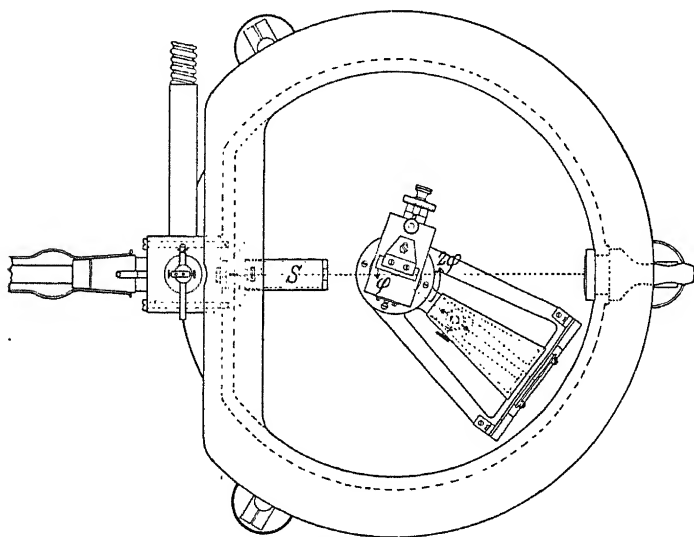


FIG. 53B.

is perpendicular to the reflected ray, the spectral line becomes the curve of intersection between a cone and a plane perpendicular to its generatrix. From this it is evident that when the angle of reflection is less than  $45^\circ$  the line on the plate is part of an hyperbola, at  $45^\circ$  it becomes a parabola,

and with more than  $45^\circ$  it goes over into a portion of an ellipse. Since the focus does not lie in the slit, however, the actual line is composed of a number of such portions of curves superposed one upon another.

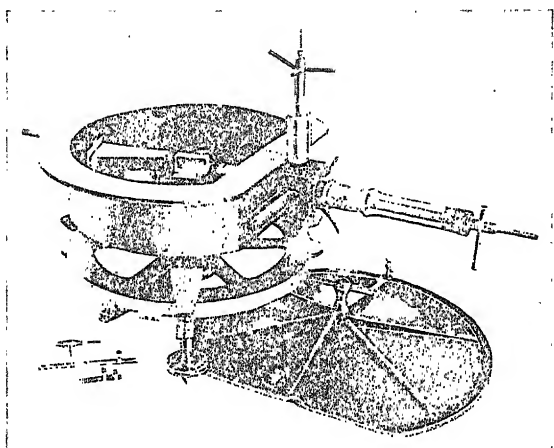


FIG. 53c.

FIGS. 53A, B, C. Vacuum spectrograph designed by the author for relative measurements of wave-length.

Since we now possess fairly complete, and rather accurate data on X-ray spectra, and besides are able to find comparison lines in all parts of the spectrum, it is desirable for many purposes of spectroscopy to make relative measurements. This is,

indeed, the ordinary method in optical spectroscopy. In this case we may use a far simpler apparatus than that heretofore described. In the author's laboratory during the last few years a model has been used for such purposes, which has about the same dispersion as the types just discussed. Its appearance and construction may be seen in Figs. 53A, B, C. The precision circle is here dispensed with, and one circular scale serves for both crystal and plate holder. This scale is graduated in  $20'$  intervals, and the plate holder bears a vernier reading to  $1'$ . The plate holder may be clamped from without in any desired position. Close in front of the plate is a cross of fine platinum or tungsten wire, the shadow of which serves as a starting point for

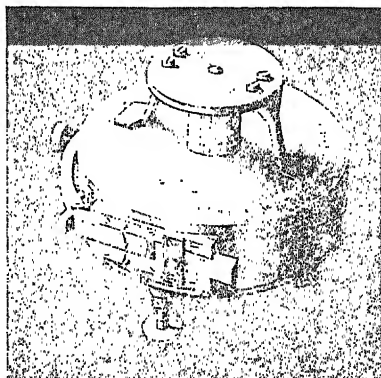


FIG. 54. Small spectrograph with rotating crystal for less accurate photographic work, especially for analysis.

measurements. The tube of Fig. 24, fastened to the spectrograph with screws, serves as the source of radiation. The adjustments and operation are exactly like those of the vacuum spectrograph just described.

If one wishes to obtain quickly a general idea of the X-ray spectrum of a given material, as for purposes of analysis, it is of advantage to have a spectrograph with smaller dispersion requiring a correspondingly shorter time of exposure. We shall here describe a spectrograph used by Hadding for such purposes. The type shown in Fig. 54 is not intended for vacuum work. A cylindrical vessel with a cover attached by soldering has in the wall an adjustable slit. In the middle of the cover is the crystal table, capable of being turned by means of a cone. Attached to the cone on the outside is a knob bearing a pointer, by which one may read off the angle on a simple circular scale.

The film used for photographing the spectrum is inserted along the inner wall of the cylindrical box so that the focussing condition is fulfilled. In taking a photograph it is only necessary to turn the crystal slowly backwards and forwards over the desired range of angle. The adjustment of the spectrograph is very simple. After the reflecting surface of the crystal has been adjusted parallel to the axis of rotation, and then moved parallel to itself until the axis lies in the surface itself, a position of the box must be found such that when the crystal is turned through  $180^\circ$  the X-rays pass through the spectrograph equally well on both sides of the crystal. A slit about 1 cm. wide is cut in the cylindrical wall of the box diametrically opposite the slit. This hole is covered with black paper, and by holding a fluorescent screen behind this opening one may easily observe the distribution of radiation as required above.

The X-ray tube used is that of Fig. 22, on the copper anode of which the material to be investigated is rubbed in powdered form. In order to keep sufficient material on the anode it is well to roughen the copper plate by scratching it with a knife, so that it is furrowed somewhat like a file. The copper lines are taken at the same time, and they afford the necessary reference lines upon the film.

This little spectrograph is very useful and convenient in making rough observations quickly, and in certain cases it probably also gives all the information desired. One must be expressly warned, however, against drawing definite conclusions from these photographs, such as, for example, concerning the presence of a certain element, when one or two of the observed lines agree satisfactorily with the known wave-lengths of that element. In this region, and with the small dispersion, lines of the first and higher orders fall so near together, and are mingled also perhaps with lines not yet identified, that definite conclusions can seldom be drawn. This is especially true if the tube is driven at high voltage, *e.g.* with more than 40 kv. maximum tension, for then lines in higher

orders are multiplied greatly. It is therefore strongly recommended that in all doubtful cases the observation be checked by taking and measuring a photograph with an apparatus of greater dispersion. The higher resolving power will then often at once give the desired information through the very characteristic appearance of the strongest lines of the different series. The X-ray spectroscopic method is undeniably very valuable in furnishing information about the elements, especially in the rare earth group, but it is greatly to be deplored when uncritical and superficial experimental results, obtained in this way, fail to stand the test, and thus partially deprive this method of the well-earned confidence placed in it. Unfortunately, the literature is not entirely free from such tendencies.

Quite a different type of spectrograph is that described by Karcher, and used by him in an investigation of the *M* series of several elements. Fig. 55 shows two sections of this apparatus. Source and spectrograph are here in the same evacuated space. The actual spectrograph was built on the rotating crystal method. The spectrum was photographed on flat plates, which could be introduced in certain positions. This did not afford the best focussing, a fact which perhaps explains the rather large error in the wave-length determinations. The source was a gas-filled tube, the cooled anticathode of which projected out through the floor of the vacuum chamber. The plates were wrapped in carbon paper to protect them against ordinary light.

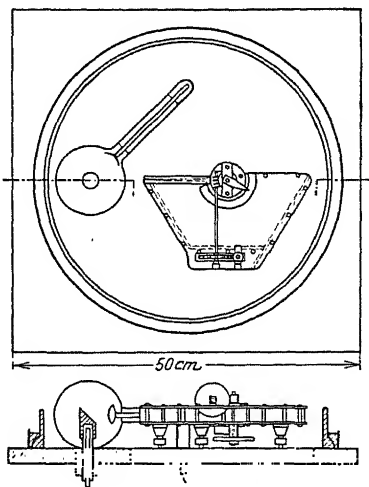


FIG. 55. Spectrograph and tube entirely enclosed in a high vacuum, after Karcher.

### *B. Spectrographs with Ionizing Chambers.*

The great advantage of the spectrographs with ionizing chambers lies, of course, in the fact that with them it is possible to measure at the same time the intensity of the spectral lines. Nevertheless, it is probably not possible to measure wave-lengths, especially of the weak lines, with the same accuracy attained in the photographic method. Up to the present spectrographs with ionizing chambers have been built only for relatively short wave-lengths; for easily absorbed rays they become altogether too complicated.

We need say but little concerning the construction of ionization spectrometers, since they are similarly designed to the Bragg spectrometer already described. As a typical example we may mention the self-recording spectrometer of Compton, reproduced in Fig. 56. Crystal and ionization chamber are automatically turned, the chamber at double the rate of the crystal. The turning mechanism also rotates a drum

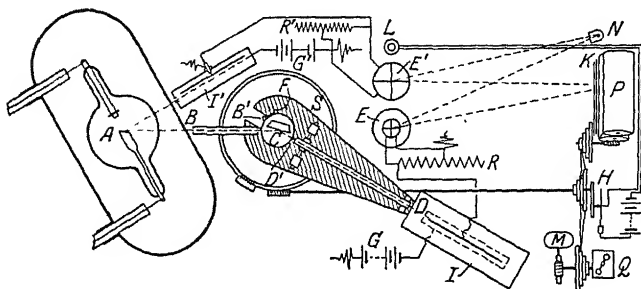


FIG. 56. Compton's recording ionization spectrometer.

covered with photographic paper, upon which the deflection of the electrometer is recorded. In order that these deflections may always be proportional to the conductivity of the ionization chamber, the free electrode of the chamber, in addition to being connected to the quadrant pair, is also connected through a high resistance to earth. Further, in order to prevent any confusion among the spectral lines due to fluctua-

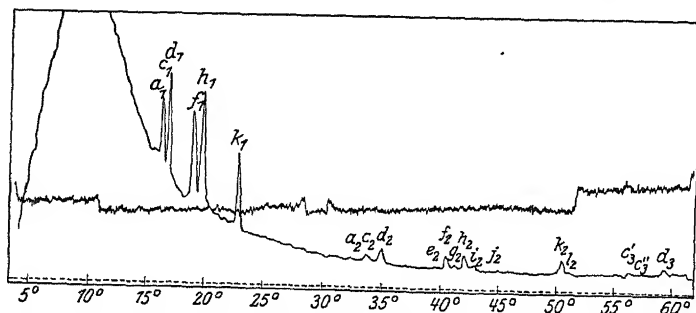


FIG. 57. Spectrum from a Coolidge tube recorded by the spectrograph of Fig. 56.

tions in the intensity of radiation from the tube, the total intensity of the radiation is recorded along with the reflected beam by a similar electrometer arrangement.

The electrometer constructed and used by Compton possesses a very high sensitivity. He states that it works well even at a sensitivity of 25,000 mm. deflection per volt. The success of the apparatus is shown by Fig. 57, which is a record of the spectrum of the tungsten anticathode in a commercial Coolidge tube.



This process of compensating for the fluctuations of the tube current and voltage by simultaneous registration of the total intensity is for the most part unsatisfactory, because a given change in total intensity does not cause the same relative change at different wave-lengths. In particular, a change in voltage produces very unequal effects on different wave-lengths. If the X-ray generator, as is often the case, is connected to the municipal power supply there will be in many localities very considerable fluctuations, making any quantitative measurements impossible unless special precautions are taken.

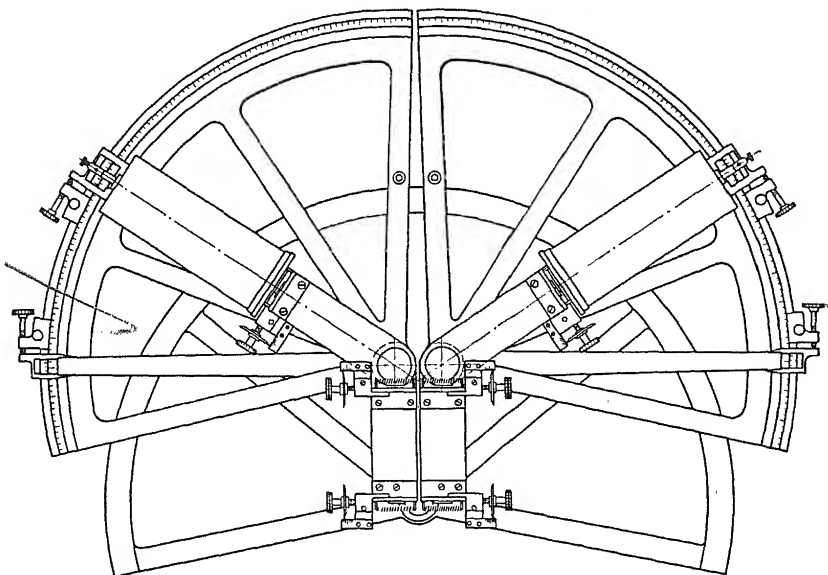


FIG. 58. Double spectrograph of Windg rdh and the author, used for absorption measurements.

Windg rdh and the author have employed a device in connection with an ionization spectrometer for absorption measurements, in which radiation of a given wave-length from the same bundle of rays is reflected from two separate crystals into two separate ionization chambers. Otherwise the apparatus (Fig. 58) was built on the principle of the Bragg spectrometer, that is, it consisted of two Bragg spectrometers placed very close together, with half of each circular scale removed. The two half spectrometers were then so adjusted that the line from the axis of rotation of the crystal to the slit for each spectrometer was directed toward the same point in the focal spot of the anticathode. The two ionization chambers were connected in opposition; one was charged to +200 volts, the other to -200, while the free electrodes of the two chambers were joined and connected to the electrometer. Thus, when equal ionization

currents were passing through the two chambers the electrometer needle showed no deflection. In the absorption measurements referred to, various substances to be investigated were introduced into the path of one of the reflected beams, while an interposed sector disc diminished the intensity of the other beam in a known ratio until the ionization currents were equal.

Williams used a similar arrangement for absorption and other like purposes. In his apparatus one ionization chamber was placed above the other.

In general, in all spectrometers of this class, an ionization chamber is filled with some gas which will give ionization currents as large as possible. Among the gases most often used we may mention  $\text{CH}_3\text{I}$ ,  $\text{CH}_3\text{Br}$  and  $\text{SO}_2$ . The first two give especially large currents for wave-lengths which are shorter than the characteristic wave-lengths of the  $K$  series of I (for  $\text{CH}_3\text{I}$ ) and of Br (for  $\text{CH}_3\text{Br}$ ), for in these regions the absorption increases suddenly. The characteristic radiation of the other components of the gases lies far outside the region of investigation. The choice of insulators presents some difficulty. Ebonite and amber are attacked by the gases, and quickly rendered conducting. Quartz is probably best, and sulphur may

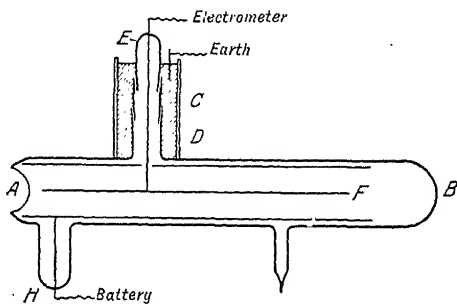


FIG. 59. Air-tight ionization chamber of Duane and Blake.

be used in many cases. A device which solves this difficulty very nicely is that described by Duane and Blake. The chamber, shown in Fig. 59, consists of a sealed glass vessel, in which the insulated electrode is held by a quartz joint.  $C$  is a metallic shield, earthed and inserted to prevent electricity from reaching the insulated electrode. Since the chamber is so well sealed the gas content remains constant for a considerable time, so that results obtained at different times may safely be compared.

### 17. Sources of High Tension for the Operation of Tubes

The following sources of high tension are the ones principally used for the operation of X-ray tubes :

1. Induction coils ;
2. Alternating current high tension transformers ;
3. High voltage batteries ;
4. High voltage direct current generators ;
5. Static machines.

The first two are of the greatest practical importance, while the last three find application only in exceptional cases. A high voltage battery is, indeed, an ideal source when a constant direct current for quantitative measurements is needed. But in the first place, on account of the high voltage necessary for such use, these batteries are very expensive; and in the second place they require constant and wearisome attention, so that for the most part, at the present time, when it is possible to attain the same end in other ways, the use of the high voltage battery as a source of power is avoided. Such sources have been used, however, by some American experimenters in investigating the validity of the Einstein equation in the domain of X-rays. E. Wagner also, in his researches on this question, as well as on the subject of the continuous X-ray spectrum, used such a source of high voltage.

High tension direct current machines are of importance only for voltages below some 10 kv. They are used sometimes singly, sometimes several machines of 1 to 2 kv. each are joined in series. But they also are losing their importance as laboratory apparatus. The static machines have the disadvantage that they are built for only a very moderate power output, which is quite insufficient for most of the needs of X-ray spectroscopy.

Induction coils represent the earliest source of high voltage for X-ray tubes. In general they are driven by direct current, with some sort of interrupter to produce the necessary sudden variations in current strength. To vary the voltage of the induction coil, the primary winding is generally subdivided and provided with means of reversing the current through part of it. The weak point of the induction coil lies in the interrupter, which is in most cases not yet developed for intensive working. Still it must be admitted that the more recent gas-filled rotating interrupters, which several firms now manufacture, are able to satisfy the demands of rather heavy loads. The electrolytic interrupters of Wehnelt and Simon also give very good satisfaction for many purposes.

The induction coil finds its greatest application with medium to high voltages, and especially with gas-filled tubes. It is then very important, however, to have an effective valve in the high tension circuit, in order to cut off the reverse current from the tube. The simplest of such devices consists of an unsymmetrical spark gap which requires a much higher sparking potential in one direction than in the other. An adjustable point-plate spark gap with the plate connected to the negative pole of the induction coil also serves well as a rectifier.<sup>1</sup> The distance between the electrodes is adjusted by hand during the operation of the tube, and so accommodated to the vacuum that the tube works as well as possible.

<sup>1</sup> Even when the gas-filled tubes are operated with rectified high tension current the insertion of an adjustable spark gap in series with the tube is not amiss.

Such spark gaps in closed gas-filled bulbs are placed on the market by various firms dealing in X-ray apparatus. Anyone may build for himself very good spark gap rectifiers by connecting some ten point-plate spark gaps in series; any desired number of them may then be short circuited when in use. Spark gaps in which the points are replaced by short bevelled cylinders (Fig. 60) are an improvement over those with points.

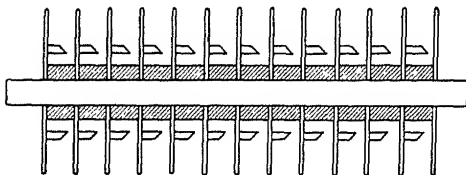


FIG. 60. Valve spark gaps in series.

Other high tension rectifiers which have found wide application consist of evacuated glass bulbs in which one electrode is closely confined, preventing the formation of the cathode space necessary for the passage of the current. The other free electrode, when acting as cathode, offers very little resistance to the current (Fig. 61).

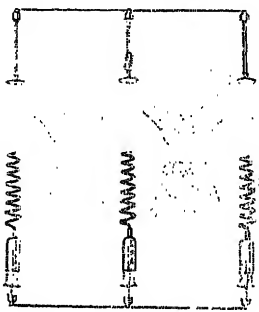


FIG. 61. Valve tube rectifier.

For continued use the most satisfactory source is the high tension transformer in conjunction with a mechanical rectifier, which either suppresses alternate impulses (which are in the wrong direction) or reverses their direction. Fig. 62 shows an arrangement of this sort which makes available both halves of the wave in the high tension alternating current. The machine is driven by direct current. On the other end of the rotor are two brushes from which the low tension alternating current is taken, and led through an adjustable rheostat to the primary of the transformer. The primary winding is generally provided with several terminals, so that different values of the transformation ratio may be used. There are several types of rectifier, some like that of Fig. 62, some with cross arms made of non-conducting material. In order not to waste energy, systematic attempts have been made, in the construction of recent types of rectifier, to eliminate points and sharp corners. This is of especially great importance when working with the highest voltages. The newer commercial apparatus is controlled by resistance as well as by autotransformers,

which is of importance if one sometimes wishes to use gas-filled tubes and sometimes electron tubes.

The commercial X-ray outfits are built for voltages of from 30 to 40 kv. upwards. For most purposes of X-ray spectroscopy, however, a maximum voltage of 30 kv. is sufficient. This voltage corresponds, according to the Einstein relation, to a minimum wave-length of about  $0.5 \text{ \AA.U.}$ , and, as the table of wave-lengths shows, this includes most of the spectrum lines. Hence, for spectroscopic purposes it is best to modify the apparatus somewhat. If no transformer with the proper transformation ratio is available, an ordinary induction coil may be used and driven with alternating current instead of direct current and interrupter. A mechanical rectifier is not at all necessary with electron tubes, but one may easily be improvised by fixing a disc on the axis of the

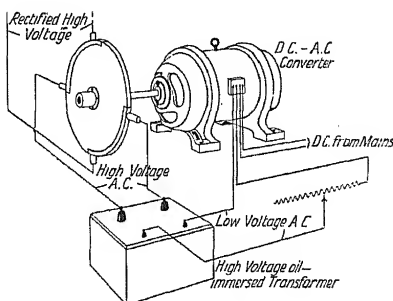


FIG. 62. Mechanical rectifier on the axis of the converter.

alternating current generator, or by means of a synchronous motor. At these low voltages it is advisable to substitute for the spark gap—which does not interfere with the current at high voltages—some easily replaceable brushes, thereby making a continuous conducting connection between the different parts of the circuit.

A complete outfit for the operation of electron tubes for X-ray spectroscopic work with maxima of 30 kv. and 200 milliamp. which was made from specifications of the author by the firm of Järnh in Stockholm, is shown in Figs. 63 and 51. The direct current at 240 volts is changed over in the converter to alternating current, which, by controlling resistances and autotransformer, is supplied to the high tension transformer. A disc on the motor axis acts as rectifier for the high voltage current. In the set there is also a transformer for supplying low voltage current to the filament. This transformer also receives its power from the same A.C. circuit, and is regulated by resistance and autotransformer. On the switchboard may be seen, in addition to the main switch (upper right), the three knobs for controlling the high voltage (two resistances and one autotransformer), and at the upper left the control for the

filament current. Three measuring instruments are also available, one for indicating the current in the main circuit, the second is a voltmeter which gives the voltage on the primary side of the high voltage transformer, while the third, an ammeter, indicates the current in the filament circuit.

We have described this complete outfit in detail, but, as already mentioned, one may manage very well with much simpler equipment. If alternating current is available, it may be connected through some regulating device, for simplicity a rheostat, to the primary of the induc-

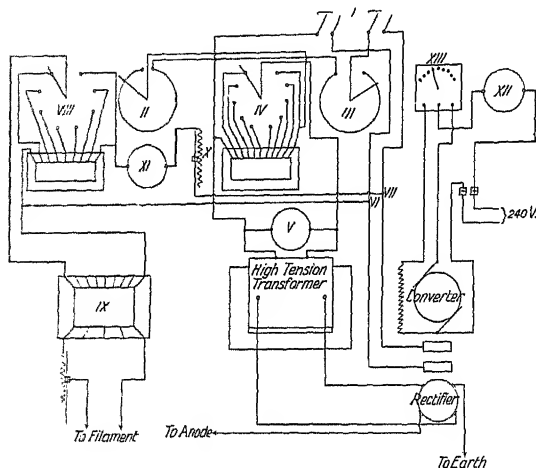


FIG. 63. Diagram of connections for the operation of a tube with hot cathode.

- I. Switch for primary alternating current.
- II. and III. Fine and rough control rheostat in the primary A.C. circuit.
- IV. Autotransformer in the same circuit.
- V. Voltmeter on the primary side of the high tension transformer.
- VI. and VII. Branch circuit from the A.C. line for the filament transformer.
- VIII. Autotransformer for control of the filament transformer.
- IX. Filament transformer.
- X. Sliding resistance for regulating the filament current.
- XI. Ammeter for the filament transformer.
- XII. Ammeter in the D.C. circuit leading to the rotary converter.
- XIII. Starting rheostat for the converter.

tion coil, while the secondary winding may be attached directly to the electron tube. If the cathode is connected to earth, any source of direct current may be used to heat the filament.

If direct current is necessary for the experimental work in hand, it is best to employ a high tension equipment, such as that first described and used for X-ray spectroscopic work by Hull. Here, also, the high voltage current is furnished by a transformer, but as rectifiers we have two or four high vacuum tubes with hot cathodes, like the tubes which are now built for use in wireless telegraphy.

With the kenotrons alone such an arrangement delivers a pulsating high tension direct current. But if sufficiently large condensers and inductances are connected in the secondary circuit, the pulsations may be smoothed out to whatever degree desired. Since this smoothing out process is easier the more frequent the impulses, it is preferable to use alternating current having a frequency above the ordinary, *e.g.* 500 or as high as 1000. The connections of such a system are shown in Fig. 64.

A voltmeter connected to the primary coil of the transformer serves to indicate the voltage of the secondary, if the transformation ratio between primary and secondary is known. This method, however, gives only an approximation to the true value of the voltage. From the standpoint of X-ray spectroscopy it is generally more important to know the peak value than the effective value. This point may be made plainer by

a consideration of Fig. 65, which represents the course of the high tension when a mechanical rectifier is used. The rectifier reverses every second-half of the wave, and the intermittent contacts apply only the uppermost part of these waves to the tube. The result is that the tube is driven by pulses of voltage, nearly uniform while they last and of approximately the same value as the peak voltage. In between these pulses are intervals of rest. A parallel spark gap is a convenient means for measuring this maximum



FIG. 65.

voltage. The following table is a collection of data for the determination of potential difference from the measurement of spark gap. The values for the sphere of 2 cm. diameter are given by Heydweiller, the others by the American Institute of Electrical Engineers.

Greater accuracy in the measurement of voltage presupposes, of course, also a more definite and more nearly constant source of potential than those mentioned above. If a source with approximately constant voltage is used, then the ordinary movable coil voltmeters are suitable, although for the higher voltages they must, of course, be in series with very high resistances. The use of these high resistances may be avoided by employing electrostatic voltmeters, which are placed on the market by various firms, such as Hartmann & Braun, Siemens & Halske, and others. Dauvillier, whose tube is driven by an outfit built

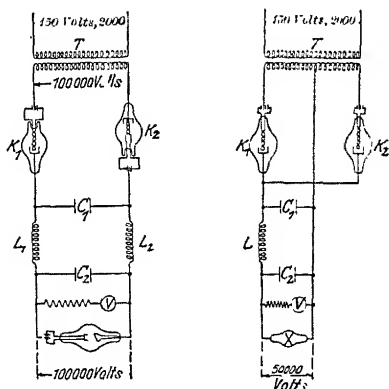


FIG. 64. Kenotron rectifier with condensers and inductances for smoothing out pulsations in the current, used by Hull.

on the Hull principle, uses an Abraham-Villard high tension electrostatic voltmeter.

TABLE 3.

Spark gap ( $s$ ) in mm. Voltage in kilovolts.

Diam. of sphere.	20 mm.	62.5 mm.		125 mm.	
$s$ in mm.		One sphere earthed.	Both spheres insulated.	One sphere earthed.	Both spheres insulated.
1	4.7	—	—	—	—
2	8.1	—	—	—	—
3	11.4	—	—	—	—
4	14.4	13.5	—	—	—
5	17.4	17.0	—	—	—
6	20.4	20.3	—	—	—
7	23.1	23.5	—	—	—
8	26.1	26.6	—	—	—
9	28.8	29.5	—	—	—
10	31.2	32.3	—	—	—
11	33.3	34.9	—	—	—
12	35.4	37.4	—	—	—
13	37.2	39.8	—	—	—
14	38.7	42.1	—	—	—
15	40.2	44	44	44	—
20	—	59	59	59	—
25	—	70	71	72	—
30	—	79	81	85	—
35	—	86	91	97	—
40	—	92	100	109	—
45	—	98	108	119	—
50	—	103	115	129	129
55	—	108	121	140	141
60	—	112	126	147	151
70	—	—	—	159	168
80	—	—	—	170	186
90	—	—	—	181	201
100	—	—	—	191	214
110	—	—	—	199	226
120	—	—	—	—	237
130	—	—	—	—	247
140	—	—	—	—	258

### 18. High Vacuum Technique

An especially important part of the technical equipment in spectroscopic X-ray apparatus, unless commercial tubes are used, is the vacuum outfit. Thanks to the eminent contributions of Gaede and Langmuir, the methods of production of high vacua have advanced with enormous



strides during recent years. Which of the two types of pump is to be chosen, the rotating molecular pump, or the condensation pump, depends probably on particular conditions. The molecular pumps have the advantage that they work very neatly, and require no cooling. For an experimental physicist who is accustomed to handle delicate instruments the operation of the molecular pump offers no difficulty. However, if molecular pumps are to be used for long intervals, it is certainly advisable to modify the Leybold type slightly. Oil cups must be placed inside the pump to collect the oil which slowly works in, so that it does not reach the revolving drum. Provision should be made for emptying these cups occasionally. If this is done these pumps may be kept in operation several hours a day for years without any difficulty.

According to published accounts of the Holweck pump, which is built on the same principle, it should be still better. Here the rotating drum is cylindrical, and the spaces are spiral furrows cut in the outer casing itself. A three phase motor is mounted directly on the axis, so that the armature itself is in the auxiliary vacuum. This pump has the advantage compared with the previous one that it requires only a relatively low preliminary vacuum. A point of very great importance is whether the pump can be cleaned readily or not, for in working with various materials on the anticathode it is not easy to prevent small particles from occasionally entering the pump. In this respect the Leybold pump is very convenient.

For the connection of glass tubes to the molecular pumps, standard glass joints are used, ground to fit the metal cone on the pump. We may again call attention to the very important point that only the outer two-thirds of the joint should be greased, and that there should be no superfluous grease left inside the joint. On first evacuating the tube it is advisable, for the rapid removal of adhering gases and vapours, to admit air several times from the auxiliary vacuum, and meanwhile to send heavy discharges through the tube.

The following table shows the pressures necessary in gas-filled tubes for three different degrees of hardness of X-rays.

Pressure in 0.001 mm. of Hg.

Hardness.	Air.	Hydrogen.	Helium.	Oxygen.	Carbon dioxide.	Argon.
Soft - -	11.6	20.7	38.0	6.6	7.4	11.6
Medium - -	6.2	11.2	22.5	4.8	5.0	6.6
Hard - -	4.2	6.8	11.0	3.4	3.6	4.0

The table shows that if the tube is to work well the pressure must be kept within rather narrow limits. One method of regulating the pressure

is to attach a fine capillary tube to the X-ray tube, and to adjust the speed of the molecular pump until a stationary state is reached in which the pressure is of about the magnitude desired. A fine adjustable valve inserted in the connecting tube between the two pumps serves the same purpose, and in this case the speed of the molecular pump may also be varied. With a little practice, moreover, especially when using metal X-ray tubes, one may quite easily hold the vacuum to the proper degree by means of the high tension current itself (the speed of the pump being varied as required). When the tube begins to harden, simply release some absorbed gas from the walls of the tube by a sudden and powerful discharge until the desired degree of vacuum is reached. A very convenient automatic arrangement for maintaining a constant hardness is that often employed in commercial tubes, namely, of sending a parallel discharge through the side tube provided with an auxiliary electrode and some material which gives off gas on the passage of a discharge. As soon as the tube becomes too hard the parallel discharge takes place, and then is extinguished again as soon as sufficient gas is liberated. This entire process is very little noticed, because it takes place constantly more or less by a silent discharge.

Electron tubes demand a much higher vacuum, but on the other hand the pumps are quite capable of satisfying this requirement, and the higher the vacuum the better the tube performs. A metal tube soldered to a metal casing joint is best for connecting the pump to the metal X-ray tube. The author has found the so-called flexible tombac tubing manufactured by the Arms and Munitions Factory at Karlsruhe to be very satisfactory. Before beginning to use the tube it is necessary to see that it is carefully freed from all traces of soldering materials, etc. For this purpose it is well to send a current of steam through the tube, but afterwards it must be dried thoroughly. Warming the metal connecting tube while it is being pumped out the first time also expedites matters considerably. It is absolutely necessary that all soldered joints should be quite tight, and that there be no pores through the metal parts. Much time and labour can be saved by first testing with compressed air, the individual parts being immersed in water. In such a trial, however, the part to be tested must remain under water some time, at least half an hour, to allow time for the air to pass through a very small leak.

With waxed seals we must obey the old rule and see that the parts to be sealed, especially the metal parts, are hot enough to cause the wax to run on them. It is best to warm the parts first and "paint" them with the wax. The seal is then finished off with a minute flame.

The Langmuir condensation pumps are now obtainable in various forms, made of metal, quartz or glass. The initial cost is less than that of the molecular pumps, but when freezing traps are required the cost of

operation is probably higher. In many cases, of course, traps are not necessary with certain constructions of tubes or if the mercury vapour does not disturb the spectrographic work. Fig. 31 represents an apparatus in which a quartz condensation pump is used to evacuate a tube of the same material.

### 19. Crystals used in X-ray Spectroscopy and the Values of their Lattice Constants

The principal crystal lattices used up to the present are those of rocksalt, calcite, gypsum, mica, sugar, quartz, and occasionally potassium ferrocyanide and carborundum. Of these Bragg has ascertained the structure of rocksalt, and has determined the distance between its atoms. We are here most interested in the distance between planes which are parallel to a cleavage surface, since these are the surfaces always used in spectroscopy. The most accurate of the early determinations of these grating constants dates from Moseley, who found the value  $2.814 \times 10^{-8}$  cm. for rocksalt.

According to Bragg's measurements, the approximate relative intensities of the reflected beams in the first, second, third, fourth and fifth orders have the values 100, 20, 7, 3, and 1. Hence the first order reflection is the one generally used. The increase in resolution which should be obtained from photographs taken in higher orders is largely illusory in rocksalt, because the crystal imperfections, which are generally large in this substance, prevent sharpness of the lines. This characteristic of rocksalt, and the difficulty of determining the density accurately, are reasons why this crystal, formerly much employed in spectroscopy, is now no longer used in measurements requiring a high degree of accuracy.

Calcite possesses about the same dispersive power as rock salt, and good samples of the crystal are much more easily obtained. In order to reach the best possible agreement in wave-length measurements made with rocksalt on the one hand and with calcite on the other, the author has carried out an accurate measurement of the grating space of calcite on the basis of that of rocksalt. Three different wave-lengths from the spectra of the elements indicated in the table were used, and the reflection angles compared for the two crystals. The results of this determination are as follows :

Element.	$\lambda$ in X.U.	$\log 2d$ .	$d$ in X.U.
Cu - -	1537	0.7823339	3029.03
Fe - -	1932	0.7823386	3029.07
Sn - -	3593	0.7823327	3029.02

In calculating  $2d$  the value of  $d$  for rocksalt was taken as 2.81400 and  $\log 2d = 0.7503541$ . Thus the mean value of  $2d$  above is found to be

$$\log 2d = 0.7823347,$$

$$d = 3029.04 \times 10^{-11} \text{ cm.}$$

On the other hand, we might calculate the grating constant of calcite directly from primary measurements as Bragg did in the case of rocksalt. This has been done by several writers. Uhler and Cooksey, who made a very accurate measurement of the  $K$  spectrum of gallium, using both rocksalt and calcite, calculated their wave-lengths on the basis of the value

$$d = 3030.7 \text{ X.U.}$$

for calcite.

To calculate the grating constant we have the formula

$$d = \left( \frac{10MeE}{2\rho VSc} \right)^{\frac{1}{3}}.$$

$M$ = molecular weight of $\text{CaCO}_3$	-	-	-	100.075
$\rho$ = density of calcite	-	-	-	$2.7125 \pm 0.0015$
$E$ = electrochemical equivalent of silver	-	-	-	0.00111827
$V$ = volume of a rhombohedron of calcite having the distance unity between cleavage faces	-	-	-	$1.0963 \pm 0.0007$
$e$ = charge of an electron	-	-	-	$(4.774 \pm 0.005) \times 10^{-10}$
$S$ = atomic weight of silver	-	-	-	107.88
$c$ = velocity of light	-	-	-	$2.9986 \times 10^{10}$

Calculating from the above fundamental values, we obtain

$$d = 3028.3 \pm 2.2 \text{ X.U.,}$$

which agrees within the rather large limits of error with the previous value obtained by comparison with rocksalt. It is to be noted, however, that with the most recent spectrographs the accuracy of the measurement of the angle of reflection is greater than that attainable in the calculation of  $d$ . Therefore, unless we wish to renounce this greater accuracy, we must fix on a value of the grating constant within the above limits of error, and use this value as a basis for the calculation of wave-lengths. Since the great majority of wave-lengths have been calculated, using the value  $\log 2d = 0.7823347$ , this value will be accepted in this book unless otherwise stated. We have already given a full discussion of a serious difficulty, which until quite recently was disregarded, namely, the discrepancy in the fundamental Bragg equation.

From measurements of the  $Pd$   $K$ -radiation, Bragg found the following values for the intensities of the beams reflected from a cleavage surface of calcite in the first four orders : 100, 20, 20, 9.

Even though the thermal coefficient of expansion of calcite is quite small, it must be taken into account in the most accurate measurements. The coefficient of expansion at right angles to the cleavage plane is 0.0000104. If we accept the above value of  $d$  as correct at 18° C., at other temperatures we have to use the values of  $\log 2d$  from the following table :

## GRATING CONSTANT OF CALCITE.

$$d_{18^\circ} = 3029.04; \log 2d_{18^\circ} = 0.7823347$$

	$d$	$\log 2d$		$d$	$\log 2d$
17°	3029.01	0.7823305	19°	3029.07	0.7823389
16°	3028.98	0.7823263	20°	3029.10	0.7823431
15°	3028.95	0.7823221	21°	3029.13	0.7823473
14°	3028.92	0.7823179	22°	3029.16	0.7823515

The two crystal lattices, rocksalt and calcite, with their relatively small grating constants, are suitable for the shorter waves. With an angle of reflection of 60°, which is, as a rule, practically as large an angle as may be used, we would be able to reach, as the greatest wave-length possible with these crystals :

for rocksalt 4.87 Å,

for calcite 5.25 Å.

For greater wave-lengths crystals with greater atomic distances must be used. The following crystals offer a good gradation of constants : quartz (prism face), gypsum (cleavage face), and sugar (100 face). The values of the grating constants for these three crystals as well as for several others used in spectroscopy are contained in the following table :

Crystal.	Surface.	$d$ in Å.	$\log 2d$ .	Author.
Quartz -	Prism face	4.247	0.92908	Siegbahn and Dolejšek
Gypsum -	Cleavage face	7.578	1.18056	Hjalmar
Sugar -	(100)	10.57	1.32512	Stenström
K <sub>4</sub> FeCN <sub>6</sub> -	(100)	8.454	1.22809	Moseley
K <sub>4</sub> FeCN <sub>6</sub> -	(100)	8.408	1.22572	Siegbahn
Carborundum	(111)	2.49	0.6975	Owen
Mica -	Cleavage face	9.93	1.29823	A. Larsson

## IV

### EMISSION SPECTRA

#### 20. General Survey of Emission Spectra

WE have already discussed the discoveries of Barkla, and stated that he was able to demonstrate that when substances are exposed to X-rays they send out a secondary radiation which is characteristic of the element concerned. Barkla found two types of such radiation, which he named the *K* and *L* radiations, and which he found to differ greatly in their hardness for any given element, the *K* series being the harder. Each of these series seemed to be homogeneous when tested by its absorption coefficient, which was the method in use at that time.

Kaye showed that the characteristic radiation is preserved when the element in question is made the anticathode in the X-ray tube, and, since a much greater intensity may be obtained in this way, the method is used almost exclusively for the production of characteristic radiation. Barkla's method, that of secondary radiation, may, however, be used in spectrographic work, as demonstrated by the beautiful experiments of de Broglie.

After the interference method had been proved to be applicable to analysis and wave-length determinations, a closer study of these characteristic radiations was at once undertaken. Using his ionization spectrometer, Bragg thus investigated the characteristic radiations from Pt, Os, Ir, Pd and Rh, and found that they are not so simple as might be supposed from Barkla's absorption measurements, but that they are separated into a number of sharp spectral lines. Moseley first systematically investigated a series of successive elements in the periodic system, the elements from Ca to Zn. He employed the photographic method, and used potassium ferro-cyanide as the crystal. He photographed the spectrum in the second and third orders, and found for each element two spectral lines which he called  $\alpha$  and  $\beta$ ; together they correspond to the *K* series of Barkla. The wave-lengths found by Moseley, and calculated

from the value  $8.454 \times 10^{-8}$  cm. for  $2d$ , are recorded in the accompanying table.

TABLE 4.

Element.	Line.	$\lambda, 10^8$ cm. from 2. Order.	$\lambda, 10^8$ cm. from 3. Order.	$\sqrt{\frac{\nu}{\frac{1}{3} \nu_0}}$	$N$
Ca	$\alpha$	3.357	3.368	19.00	20
	$\beta$	3.085	3.094		
Sc	—	—	—	—	21
Ti	$\alpha$	2.766	2.758	20.99	22
	$\beta$	2.528	2.524		
Va	$\alpha$	2.521	2.519	21.96	23
	$\beta$	2.302	2.297		
Cr	$\alpha$	2.295	2.301	22.98	24
	$\beta$	2.088	2.093		
Mn	$\alpha$	2.117	2.111	23.99	25
	$\beta$	1.923	1.918		
Fe	$\alpha$	1.945	1.946	24.99	26
	$\beta$	1.765	1.765		
Co	$\alpha$	1.794	1.798	26.00	27
	$\beta$	1.635	1.629		
Ni	$\alpha$	1.664	1.662	27.04	28
	$\beta$	1.504	1.506		
Cu	$\alpha$	1.548	1.549	28.01	29
	$\beta$	1.403	1.402		
Zn	$\alpha$	1.446	1.445	29.01	30
	$\beta$	—	1.306		

Moseley's spectrum photographs are shown in Fig. 66. The most important result of this investigation is the remarkable fact that the spectra shift uniformly according to a very simple law when we pass from one element to the next in the periodic system. This may be seen from column five of the table which contains the square root of the frequency divided by a constant. In the last column the elements are numbered according to their order in the Mendelejeff table, by calling H number 1, He 2, Li 3, and so on. The number proportional to the square root of the frequency is seen to be surprisingly close to the atomic number less one.

In the same year (1913) came de Broglie's experiments on the elements Pt, W, Cu, etc., by the rotating crystal method and photographic registration.

Development along this line then proceeded rapidly. Moseley extended his earlier systematic study of the  $K$  series to the  $L$  series also, and found that all the elements from Zr to Au were subject to relations

such as he had previously found for a portion of the *K* series. We shall return later to these laws. Malmer investigated the *K* series of the heavier elements, from Zr to Nd, and showed that the *K* spectrum consists of four lines. Friman and the author analysed the *L* series of the heaviest elements from gold to uranium, and showed that the *L* series for these elements has a very complicated line structure. Wagner obtained corresponding results with Pt, W, and Ta. In the case of the lightest elements new lines appear in the *K* series, as shown by the author in conjunction with Stenström.

In January 1916 the author demonstrated the existence of a group of lines in the spectrum of the heaviest elements, which are still softer

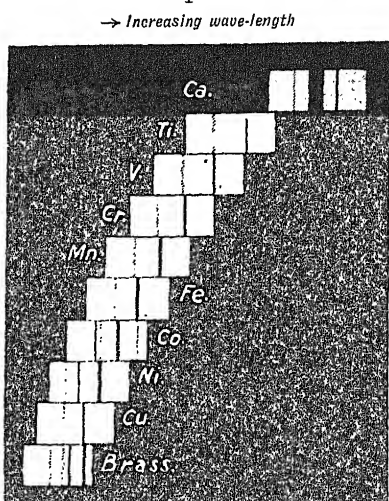


FIG. 66. *K* series of a succession of elements, from the first photographs of Moseley.

than the *L* series. In accordance with Barkla's notation these lines were called the *M* series; it is of the same general character as the series previously known. Very recently certain lines have been discovered by Hjalmar, which may safely be ascribed to a still softer series, the *N* series. The results of an earlier investigation by Dolejšek have not been entirely confirmed. (On this question see Hjalmar's thesis for the doctorate.)

From measurements of absorption and of secondary rays Barkla, in 1916, believed he had found evidence of a harder series of lines than the *K* series, which from analogy with the others he denoted by *J*. This series, to which it is difficult to assign a place theoretically, has not been confirmed, in spite of the fact that methods much more sensitive than that of Barkla have been utilised in the search. Neither in emission nor in absorption has any further evidence of this series been observed. Among the negative results published concerning the *J* series we may mention that of Duane and Shimizu, who found no trace of it in the spectrum of aluminium. Hewlett and Richtmyer, by analysis of the spectrum, sought for an absorption discontinuity in this region, but with no positive result. The author and Windgårdh also found no indication of an absorption discontinuity for magnesium in this region. Neither has the author been able to find the least trace of an emission spectrum in the wave-length region where, according to Barkla, the *J* radiation should be. The discontinuities in the absorption measurements found by



certain observers for a few elements are not very concordant in respect of wave-length, and are probably due to some other cause than the supposed *J* series. Since the *J* series would be expected chiefly in the case of the very light elements, it seems quite likely that these observed irregularities were due to small impurities of heavier elements, which would cause a relatively strong absorption.

Recapitulating, we may say that the X-ray spectra of the elements in the wave-length region from about  $0.1 \text{ \AA.}$  to  $13 \text{ \AA.}$  may be divided

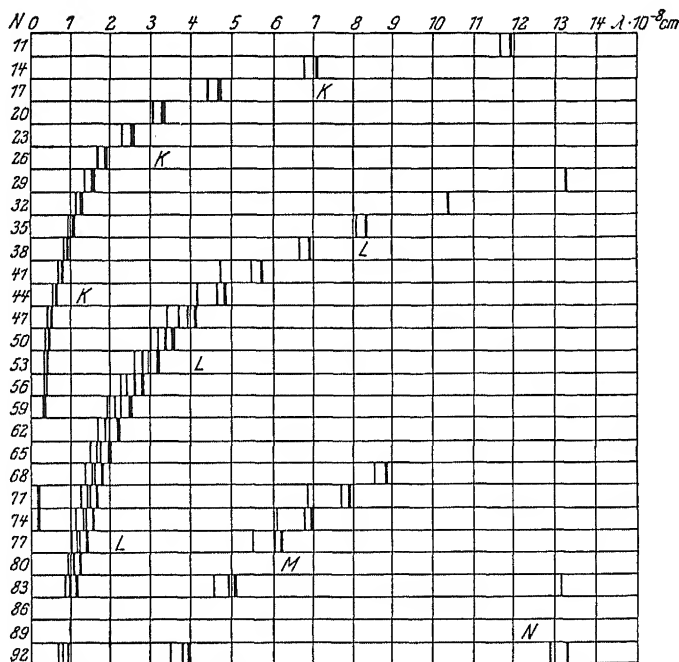


FIG. 67. The strongest lines of the several X-ray series for every third element from No. 11 to No. 92.

into four groups, which we call the *K*, *L*, *M*, and *N* series. Each group is divided into a number of more or less sharp spectral lines. Between these groups lie regions which, so far as examinations up to the present show, are quite devoid of lines. Further, photographs of the spectra of adjacent elements show that each group retains its general appearance with only small changes from element to element. A given line is merely displaced towards shorter wave-lengths when we pass from a lighter to a heavier element.

Fig. 67 shows a general view of the strongest lines of the several series for a number of elements. Quantitatively, we may call attention to tungsten; for this element three series have been measured, the *K*,

the *L*, and the *M* series. The wave-lengths of the *N* series of *W* are far too long to permit of their study with the crystals available at present. The wave-lengths of the *K* series of tungsten lie between the limits 178 and 214 X.U.; then up to 1025 X.U. there are no lines. There the *L* series begins and extends to 1675 X.U., after which there is another region free from lines. The first known *M* line of tungsten lies at 6066 X.U., and the one of longest wave-length is situated at 6973 X.U.

In addition to the line spectra which we have discussed, every substance emits independently a *continuous*, or "white" radiation, whether it is excited to the emission of X-rays by cathode ray impacts, or whether it is caused to give off its characteristic radiation by exposure to primary X-rays as in Barkla's method. The reproduction of Compton's photograph in Fig. 57, taken with a Bragg spectrometer, shows how these two radiations stand to each other in intensity. It is at once evident that the principal part of the energy belongs to the continuous spectrum, and that the line spectrum is superposed upon it. Even when the intensity of certain lines is very great, the total intensity of this narrowly localized energy beam is still very small in comparison with the total energy, a fact which is often overlooked in using secondary radiators as monochromatic sources. We shall return later to a more detailed description of the properties of the white radiation.

It is readily seen that X-ray line spectra provide a very valuable implement for qualitative chemical analysis. The great simplicity of X-ray spectra in comparison with ordinary optical spectra, and the fact that they are quite uninfluenced by the chemical state of the atom emitting them, are essential points for this purpose. It may be recalled that X-ray analysis has already been successfully applied to prove the existence of a new chemical element, hafnium, the presence of which in zirconium minerals Bohr predicted from his theory of the atom. In such a case, an analytical test with the aid of X-ray spectroscopy may be carried out in an hour or two, whereas ordinary chemical methods would involve a long and laborious investigation.

For chemical purposes, it should be of great interest to develop the analytical X-ray method into a quantitative process. As this question is very often raised, a few words may be said about it.

If we use the most effective method of generating X-rays from the substance to be investigated, *i.e.* by bombardment with cathode rays in a vacuum, we can at once say that *in general* a quantitative analysis is not possible. Suppose we had some mercury, together with other elements which are not readily volatilized, then we should require very little experience in X-ray spectroscopy to know that the mercury-lines never possess an intensity proportional to the amount of mercury present. Thus it is clear that a quantitative analysis by means of the spectro-

grams is only possible if the different elements in the substance under examination are about equally volatilized under the action of cathode-ray bombardment. Moreover, the more purely chemical effects of the cathode-rays on the anticathode material must be taken into consideration in this connection.

But there are also other important points to be considered. The potential on the tube has an important influence on the emission of the characteristic X-ray spectra, as shown in detail in the next section. A variation of the potential of ten produces a differential action on and strongly affects the relative intensities of the spectral lines emitted from the different elements on the anticathode. Only when the elements have about the same atomic number in the periodic table, and the potential is considerably higher than the minimum potential necessary to excite the characteristic rays of the elements, is quantitative estimation possible by comparison of the intensities of the spectral lines.

In short, we conclude that, in general, a quantitative analysis is only possible for elements which withstand the cathode-ray bombardment in the same degree, and the atomic numbers of which differ but slightly.

An interesting quantitative analysis in accordance with these general principles is afforded by the investigations of Coster and Hevesy on the hafnium-content of zirconium-minerals. These authors compared the spectra emitted by Ta (73) and Hf (72) mixed together on the anticathode, and determined the unknown percentage of Hf from the known percentage of Ta.

## 21. Laws of Excitation of X-ray Spectra

At quite an early date Barkla pointed out that to excite the characteristic radiation of an element by exposure to primary rays, the latter must be harder than the radiation to be excited. In accordance with this result, Kaye, in 1909, made a first attempt with the apparatus shown in Fig. 68 to show the dependence of the excitation on the velocity of the impinging cathode rays. A magnetic field deflected the cathode rays to a greater or lesser extent according to their velocity. By a proper choice of the strength of the magnetic field only electrons of a very definite velocity were allowed to strike the anticathode. The X-rays thus excited passed through a thin aluminium window and entered an ionization chamber.

Whiddington settled this point definitely by the very skilful use of the apparatus

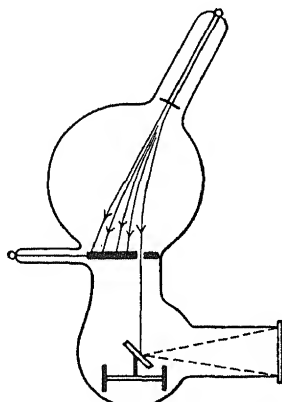


FIG. 68. Apparatus of Kaye for bombarding the anticathode with cathode rays of definite velocity.

represented in Fig. 69, which may be seen to embody the same principle. He was able by this arrangement to show that a certain minimum velocity of the electrons striking on the anticathode was necessary before the primary X-rays thus produced were able to excite characteristic radiation in the secondary radiator. Further, it was proved by Beatty that the same law holds for the direct excitation of characteristic radiation by primary cathode rays. The quantitative relations involved, however, are capable of much more definite expression in the light of more recent experimental results, so that we may hereforego a further discussion of these experiments.

The evidence essential for a better answer to these questions was afforded by X-ray spectrographs and Röntgen tubes with hot cathodes.

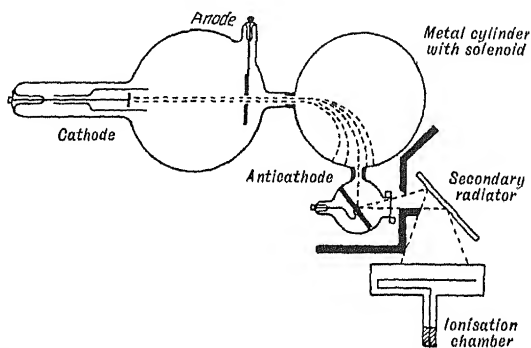


FIG. 69. Whiddington's apparatus for the production of X-rays by means of cathode rays of known velocity.

These instruments were used by Webster in an experiment which very greatly clarified the problem. A Coolidge tube with a rhodium target was used to furnish characteristic radiation, and the voltage was obtained from a storage battery of 20,160 cells. By connecting up a larger or smaller number of cells, the electrons could be given any desired velocity according to the equation

$$\frac{1}{2}mv^2 = eV,$$

where  $m$  is the mass of an electron,  $e$  its charge, and  $v$  its velocity after falling through a difference of potential  $V$ .

Webster's spectrographic apparatus was an ionization spectrometer like that of Bragg. He placed the ionization chamber in the position corresponding to the strongest line of the  $K$  series of rhodium, the  $K\alpha_1$  line, and ran the tube at constant voltage. He determined the ionization current for various tube voltages, and thus found a relation between the intensity of the radiation of the selected wave-length and the applied voltage, with the result shown in Fig. 70A. The significance of this curve is self-evident. At voltages below 23.2 kv. the ionization

chamber receives only the white radiation which falls in the neighbourhood of this wave-length. At 23.2 kv. the characteristic radiation of rhodium suddenly begins and adds itself to the white radiation. By producing the straight portion of the curve which corresponds to the general radiation the characteristic radiation may easily be separated out on the graph. This is done in Fig. 70B for the two lines  $\alpha$  and  $\beta$  of the K series. From this figure we may draw the very important conclusion that both lines of the K series appear at a certain critical value of

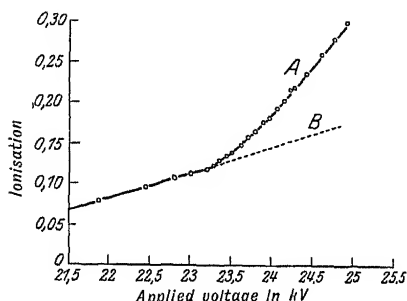


FIG. 70A.

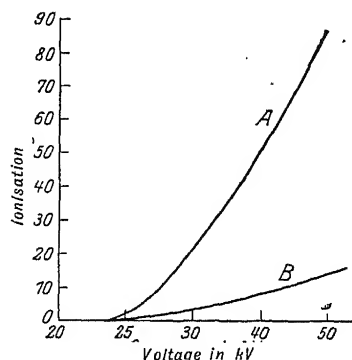


FIG. 70B.

the voltage, and that this critical value is the same for both lines. A further investigation in this same direction leads to the following conclusion :

*The K group is excited in its entirety when a certain critical value of the voltage is exceeded.*

A second conclusion from these experiments is that this value  $V$  of the voltage corresponds, according to the Einstein equation

$$eV = h\nu,$$

to a frequency  $\nu$  which, within the limits of error, coincides with the frequency of the line of shortest wave-length in the K series.

A better view of these relations may be obtained from the curves of total intensity for different voltages shown in Fig. 70c. The curves correspond to three constant voltages, namely, 23.2, 31.8, and 40.0 kv. With the lowest voltage only the general radiation is seen with no indication of the superposed line spectrum. But with the two higher voltages the lines of the K group of rhodium all appear together (and also as an impurity of the anode, the lines of ruthenium).

A third result of these measurements is, according to Webster, that the ratio of the intensities of the two lines  $\alpha$  and  $\beta$  is constant, that is, independent of the voltage. In measuring the intensity of each component  $\alpha_1$  and  $\alpha_2$  are taken together, and in the same way  $\beta_1$  and  $\beta_2$  are reckoned together as  $\beta$ .

Finally, as a fourth result of the measurements, Webster and Clark stated that the intensity  $I$  of the lines may be expressed as a function of the voltage  $V$  as follows :

$$I = K(V - V_0)^{\frac{3}{2}},$$

where  $V_0$  is the critical voltage of the group to which the line belongs.

Results similar to these were found by Wooten, using Mo and Pd as anticathodes. Wooten found for the critical voltage of the  $K$  series of

Mo 19.2 kv. and of Pd 24.0 kv. We may compare with these the voltages calculated from the Einstein equation

$$eV = h\nu$$

by substituting the values of  $e$  and  $h$ . Solving for  $V$ , we have

$$V = \frac{12.345}{\lambda} \text{ kv.},$$

where  $\lambda$  is the wavelength in Å. If we substitute 0.6194 for  $\lambda$  in the case of Mo, and 0.5102 in the case of Pd, these being the shortest wavelengths of the  $K$  series for these elements, we obtain as the calculated voltages 19.5 and 23.7 kv., values which agree well with the experimental ones given above.

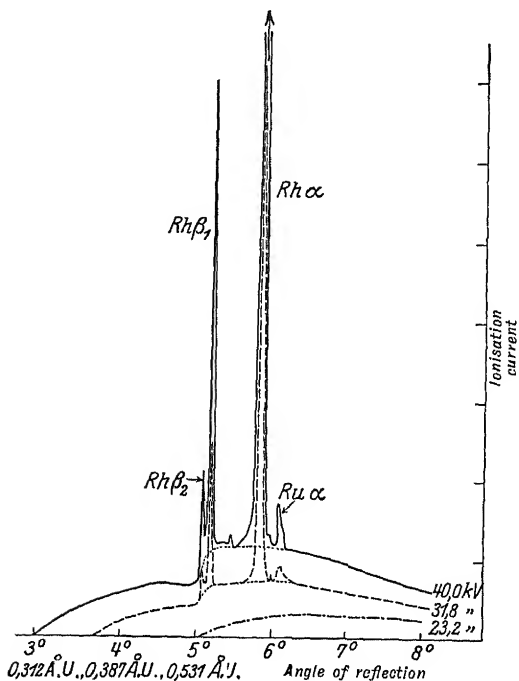


FIG. 70c.

Wooten also investigated the intensity of the lines as a function of the voltage applied to the tube. If the intensity be plotted against the square of the potential on the tube, both the  $\alpha$  and the  $\beta$  curves are straight lines except in the vicinity of the minimum voltage necessary to produce the lines, where they are slightly bent. The intensity curve was studied for voltages ranging from the minimum potential (19.2 kv. for Mo and 24.0 kv. for Pd) up to 50 kv. Within this interval, with the exception of a small fraction of the curve at the beginning, the following equation holds :

$$I = c(V^2 - V_0^2).$$

While  $V_0$  is a tension a little higher than the minimum potential, the value of  $V_0$  is the same for both the  $\alpha$  and the  $\beta$  lines of the same element.

Some recent measurements on this question have been performed by Kettmann, who used a photographic method for registering the intensity of the  $K$  series lines of the elements Cr, Cu, Ag and some  $L$  series lines belonging to La and Pb. In particular, Kettmann endeavoured to follow the intensity curve up to potentials many times greater than the minimum potential. The aforementioned measurements by Webster and by Wooten embraced an interval only up to *twice* the minimum potential. Kettmann in some cases determined the intensity up to 6 or 7 times the value of this potential. The first part of the curves—from  $V_0$  to  $2V_0$ —shows the same feature as those of Webster and of Wooten. But on further raising the potential the increase of the intensity is retarded, and at the highest potentials (about seven times the minimum potential) the intensity seems to approach asymptotically a limiting value. This fact is due to the absorption of the X-rays in the anticathode, from which the rays were emitted at nearly glancing angles. If the absorption in the anticathode is negligible the intensity is proportional to the square of the potential.

Both Wooten and Kettmann compare their results with the theory of Bergen Davis, and find quite satisfactory agreement.

The same results were found by Unnewehr, who investigated the characteristic radiation from Cr, Cu, Rh and Ag at tensions ranging from the minimum potential up to about 45 kv. The curves for Rh and Ag show good agreement with the formula of Davis, which has been given the form :

$$I = C \left[ \frac{1}{K^2} \left( 1 - e^{-K^2(V^2 - V_0^2)} - \left( 2 \frac{V_0}{K} \right) e^{-K^2 V^2} \int_{KV_0}^{KV} x^2 dx \right) \right],$$

where 
$$C = \frac{1}{b} \cdot E_a h \nu_a \cdot B \cdot N,$$

$$K^2 = \frac{\mu c}{b}.$$

$E_a$  = the fraction of the excited atoms emitting the  $\alpha$ -line.

$B$  = number of collisions between electrons and atoms per unit path of the electron.

$N$  = number of electrons striking the anticathode per sec.

$b$  is the constant of the Thomson-Whiddington law :

$$V_x^2 = V^2 - bx.$$

For Cu and Cr the experiments show small deviations from the formula. Unnewehr suggests that this may be due to absorption and re-emission of some parts of the continuous spectrum as characteristic radiation. Such an effect is not considered in the theory of Davis, but it may be of importance with lighter elements.

The results obtained for the characteristic radiation of certain elements in the *K* series are also valid in the *L* series, as appears from Webster and Clark's measurements, as well as from those of Hoyt for platinum. Experiments show, however, that in the *L* region the lines fall into three sub-groups, to each one of which the four propositions stated above apply.

By reasons of analogy, the fundamental aspects of which will be discussed in detail under the systematic classification of Röntgen spectra, it may be concluded that the number of sub-groups in the *M* series is five, and in the *N* series in all probability seven.

For reasons to be discussed later we must assume that the frequencies, which in the Einstein equation correspond to the exciting voltages of the various groups, are each actually a little greater than the frequency of the line of shortest wave-length in the group.

For practical X-ray spectroscopy it is of interest to know for each element and each series of spectra the critical voltage necessary for excitation. Even though only a few of the smaller values of the critical voltage have been experimentally determined, it is nevertheless possible, from the above relation between voltage and line spectra, to calculate in advance the voltages concerned, by making use of spectral measurements. In the appendix is a table containing values of the minimum voltage for the sub-group of shortest wave-length in each of the series, the computations having been made from line spectra in the manner just described.

## 22. The *K* Series

In Figs. 38 and 66 on pages 52 and 88 we have reproduced a series of spectrograms from which the general character of this spectral series may be seen. The *K* series consists almost throughout of four components, which we shall call  $\alpha_1$ ,  $\alpha_2$ ,  $\beta_1$  and  $\beta_2$  (the last was called  $\gamma$  by Moseley, Sommerfeld and others), whereby the lines are given in the order of decreasing intensity. The first two lie very near together, and hence are scarcely separated from each other in the diagrams. The difference in wave-length of the  $\alpha$  components is nearly constant for all elements and is about 4 X.U.

The ratio of the intensity of the  $\alpha$  group to that of the  $\beta$  group was determined by Wooten to be 5.55 for Mo and 6.25 for Pd, while Owen found 1.90 for the latter element. Unnewehr has also measured the intensity ratios,  $\frac{K\alpha}{K\beta}$ , of these two groups for four elements, and found the following corrected values :

24 Cr	-	-	-	-	-	7.36
29 Cu	-	-	-	-	-	6.53
45 Rh	-	-	-	-	-	4.75
47 Ag	-	-	-	-	-	4.65



Duane and Stenström made a closer study of the relative intensities of the lines of the *K* series of tungsten by the same method, using a Bragg spectrometer. In the case of tungsten these investigators also discovered a fifth component in the *K* series, which they called  $\alpha_3$ . Indicating the intensity of the strongest line by 100, these authors found the following relative values :

Line	-	-	-	$\alpha_3$	$\alpha_2$	$\alpha_1$	$\beta_1$	$\beta_2$
Intensity	-	-	-	4	50	100	35	15

In the same way Duane and Patterson arrived at the following relative intensities for Mo :

$$\frac{\alpha_1}{\alpha_2} = 1.93 \text{ in the 2nd order,}$$

$$\frac{\beta_1}{\beta_2} = 6.3 \text{ in the 1st order,}$$

$$\frac{\beta_1}{\beta_2} = 5.5 \text{ in the 2nd order.}$$

Záček and the author, in an investigation by the photographic method, and using a photometric method of comparison, obtained similar results for the relatively long wave-lengths of the *K* series of Cu, Zn, and Fe. The intensities are given in the following table, and are expressed in terms of  $\alpha_1 = 100$ . The intensities of  $\alpha_2$  and  $\beta_1$  in this table were obtained from different spectrograms, and by two photometric methods of comparison.

Cu		Zn		Fe
$\alpha_2$	$\beta_1$	$\alpha_2$	$\beta_1$	$\alpha_2$
48	24	59	29	51
48	24	53		47
50	28	51		52
55		47		50
56		46		51
49		47		49
51		50		49
51		47		
52				
52				
Mean	51.2	50.0	29	49.9

From these results it appears that the ratio of the intensities of the two  $\alpha$  components for elements so far apart in the periodic system as W, Mo, and Cu, Zn, and Fe remains constant and has the approximate value of 2 to 1. It is certain that the  $\beta_2$  line is relatively much

weaker in the case of the last three elements. It would also appear, so far as can be judged from the above scanty data, that the  $\beta_1$  line is slightly reduced in intensity.

Whilst in the case of elements whose atomic number is higher than that of Zn (30), the  $K$  series has the line structure shown in Fig. 71A, a study of the long wave-length region, such as has been made in the author's laboratory, reveals quite a different appearance in this series. Fig. 71B is a diagram prepared by Hjalmar, which represents the spectrum for the lightest elements. Wentzel offers very convincing arguments indicating that these additional lines are due to multiple ionization of the atom, and thus are related to the ordinary lines as

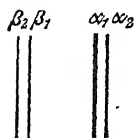
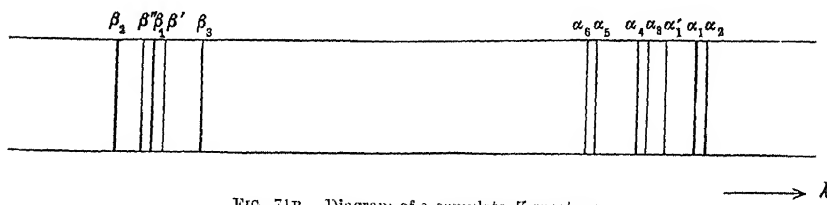


FIG. 71A.

the spark lines are to the arc lines in optical spectra. These lines are hence sometimes referred to as "spark lines." Corresponding lines have been revealed more recently in the other series, and these will be discussed later.

In the case of the heavier elements isolated lines have also been found which fall outside the simple scheme of lines in Fig. 71A; as an example,

FIG. 71B. Diagram of a complete  $K$  spectrum.

we may mention the  $\alpha_3$  line of tungsten discovered by Duane and Stenström. Furthermore, de Broglie was able to show that the  $\beta_1$  line of tungsten and rhodium is resolved by greater dispersion into two components. He found a wave-length difference between the two components of 0.7 X.U. for W and 0.6 X.U. for Rh. The intensity of the component  $\beta_3$  on the long wave-length side is considerably less than that of the other. Duane and Patterson measured the  $\beta_3$  line for Mo and found its separation from the  $\beta_1$  line to be 0.9 X.U. These lines are probably not to be considered as spark lines. At least for the first one, another explanation seems more probable if we assume a violation of the generally valid selection rule, and it also agrees well in its quantitative aspects, as Duane has shown. Crofutt, who has made a careful examination of the tungsten spectrum, gives for the separation  $\beta_3 - \beta_1$  0.89 X.U. He did not succeed in finding the line  $\alpha_3$ . In the classification of spectra we shall return to this point.

Concerning the appearance of the spectrum lines it may be stated that with the heavier elements the lines are everywhere sharp, and as a rule do not exceed in breadth what is to be expected from the width of

slit used. As we pass to the lighter elements, however, we observe a broadening of the lines which indicates a fine structure. The photometric curves published by Hjalmar give an idea of this structure for a number of the lighter elements.

Until recently no influence of the state of chemical combination of the atom upon the emission lines in X-ray spectra had been found, in spite of many attempts to detect such an influence. But recently Lindh and Lundquist have given evidence of such an effect, and precisely for those elements with which the absorption-spectra show a dependence on the

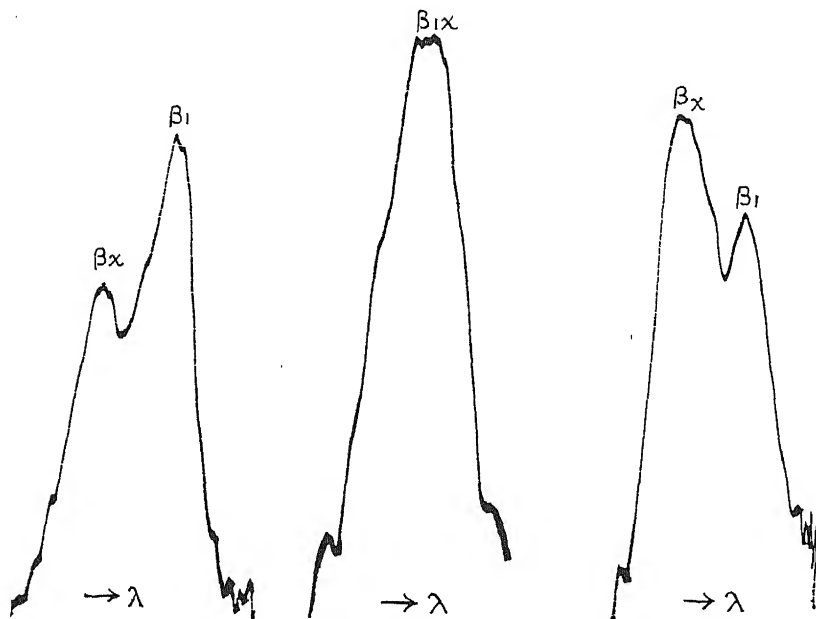


FIG. 71C. The  $\beta$ -lines,  $K$ -series, of Sulphur from  $Ag_2S$  on different anticathodes.

chemical state, namely, for the elements P, S and Cl. It is the lines belonging to the  $K$ - $\beta$ -group which show the effect. Lindh and Lundquist have studied many different salts containing atoms of these three elements, using different materials for the anticathode.

The difficulty in such investigations is to know which substance is really emitting the spectrum, as the cathode ray bombardment and the consequent heating effects may cause a transformation of the salt placed on the anticathode. It is known that the cathode rays in many cases have a strong reducing action on the salts bombarded.

But, in every case, the investigations of Lindh and Lundquist seem to show definitely that slightly different spectra are obtained with variation of the state of chemical combination.

The general characteristics of the phenomenon are as follows: with some salts two different lines are found, and these we may denote by  $\beta_1$  and  $\beta_x$ , of which  $\beta_1$  has the greater wave-length. With very few exceptions this is the more intense line. With other salts these two lines apparently coalesce and give a diffuse and somewhat broader line, denoted by  $\beta_{1x}$ .

In exceptional cases the intensity-relation is modified so that  $\beta_x$  has a greater intensity than  $\beta_1$  (the line of longer wave-length). This is the case with  $\text{Ag}_2\text{S}$  on different anticathodes, as shown in Fig. 71c.

In some cases small variations in the wave-lengths of the lines have also been detected, but for the majority of the salts the wave-lengths remain the same.

In cases where the lines do not appear to differ from each other by more than the error of measurement, the mean values of the wave-lengths (in X.U.) are given in the following tables.

#### Sulphur $\beta$ -Lines.

---

---

Substance on an anticathode of Cu.

---

$$\left. \begin{array}{l} \beta_1 = 5021.1 \\ \beta_x = 5012.8 \end{array} \right\} \begin{array}{l} \text{S (rhomb.), CuS; SnS}_2, \text{P}_4\text{S}_3; \\ \text{CuSO}_4, \text{ZnSO}_4, \text{SnSO}_4, \text{Fe}_2(\text{SO}_4)_3; \text{PbSO}_4, \text{Ag}_2\text{SO}_4. \end{array}$$

$$\beta_{1x} = 5017.8 \quad - \quad \text{Cr}_2\text{S}_3, \text{ZnS, PbS, CdS, FeS, CdSO}_4.$$


---

---

---

Substance on an anticathode of Al.

---

$$\left. \begin{array}{l} \beta_1 = 5021.1 \\ \beta_x = 5012.8 \end{array} \right\} \text{CuS, CuSO}_4.$$

$$\beta_{1x} = 5017.8 \quad \left\{ \begin{array}{l} \text{S (rhomb.), ZnS, FeS, SnS}_2, \text{CdS, Al}_2\text{S}_3, \text{ZnSO}_4, \\ \text{Fe}_2(\text{SO}_4)_3, \text{SnSO}_4, \text{CdSO}_4. \end{array} \right.$$


---

---

---

Substance on an anticathode of Fe.

---

$$\left. \begin{array}{l} \beta_1 = 5021.1 \\ \beta_x = 5012.8 \end{array} \right\} \text{CuS, CuSO}_4.$$

$$\beta_{1x} = 5017.8 \quad \left\{ \begin{array}{l} \text{S (rhomb.), Ag}_2\text{S, ZnS, FeS, SnS}_2, \text{CdS, Ag}_2\text{SO}_4 \\ \text{ZnSO}_4, \text{Fe}_2(\text{SO}_4)_3, \text{CdSO}_4. \end{array} \right.$$


---

Sulphur  $\beta$ -Lines.

Substance.	Line.	Anticathode.		
		Cu.	Fe.	Al.
$\text{Ag}_2\text{S}$	$\beta_1$	5021.0 $\dot{i}$ *		5023.6
	$\beta_{1x}$		5017.8	
	$\beta_x$	5013.4		5015.0 $\dot{i}$ *
$\text{Ag}_2\text{SO}_4$	$\beta_1$	5020.9		
	$\beta_{1x}$		5018.1	5015.1
	$\beta_x$	5012.7		

Phosphorus  $\beta$ -Lines.

Anticathode Cu.									
						$\beta_1$	$\beta_x$		
Red Phosphorus	-	-	-	-	-	5789.0	5779.5		
Cu phosphide	-	-	-	-	-	5790.9	5778.7		
							$\beta_{1x}$		
Phosphates of Ca, Mg, Cu, Zn, Fe (ferrous and ferrie)						-	-	5787.1	

Chlorine  $\beta$ -Lines.

Anticathode Cu.	
$\beta_1=4394.2$	} NaCl, NaClO <sub>3</sub> , KCl, SrCl <sub>2</sub> , CaCl <sub>2</sub> , BaCl <sub>2</sub> , Ba(ClO <sub>3</sub> ) <sub>2</sub> .
$\beta_x=4390.6$	
$\beta_1=4394.75$	} CuCl <sub>2</sub> .
$\beta_x=4388.4$	
$\beta_{1x}=4393.2$	{ LiCl, FeCl <sub>2</sub> , ZnCl <sub>2</sub> , CdCl <sub>2</sub> , SnCl <sub>2</sub> , PbCl <sub>2</sub> .

\* The letter  $\dot{i}$  following the wave-length indicates the more intense of the two lines.

In the law of Moseley already referred to we have a sure means of identifying associated lines in the spectra of different elements. For the four principal lines of the  $K$  series the similarity is so pronounced that no doubt can arise as to their identification, but for the fainter lines the law is quite useful, while in the other more complicated series its application becomes simply indispensable. According to our present conception of the structure of the atom, the essence of the law of Moseley is that the atomic number represents the positive nuclear charge of

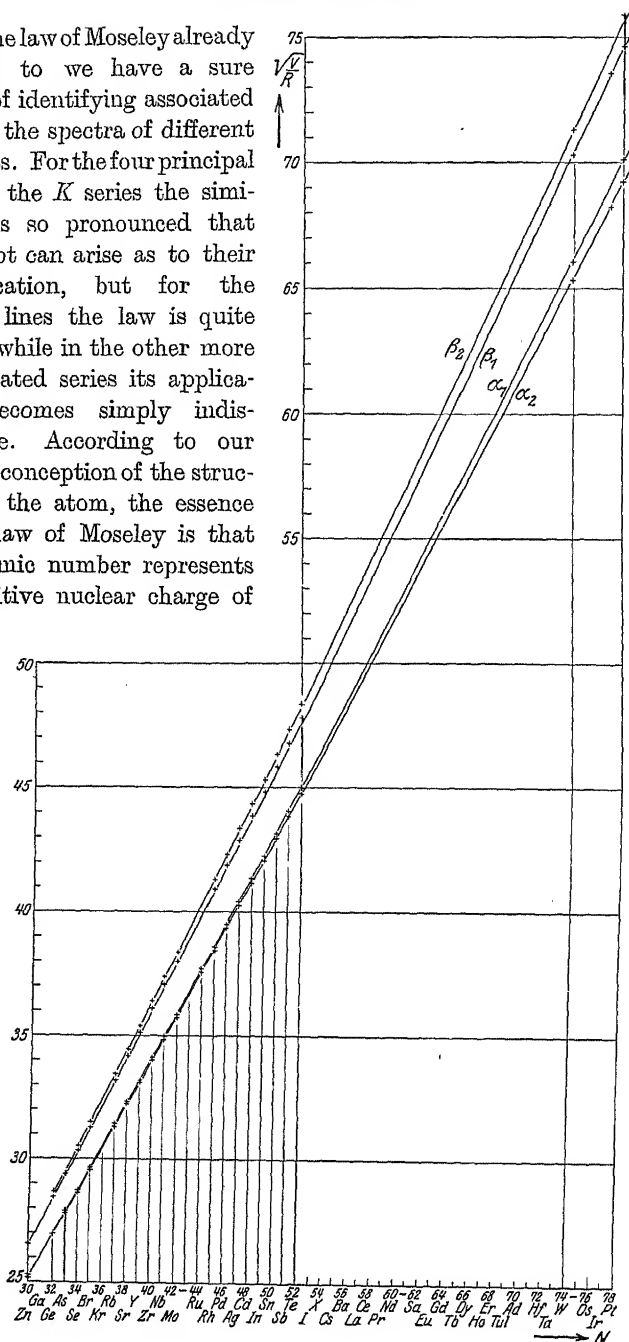


FIG. 72.  $\sqrt{\frac{\nu}{R}}$  for the  $K$  lines as a function of the atomic number of the elements.

the atom, and as such it is the primary factor in determining the frequency of the X-ray spectra.

In the table of Moseley's original measurements on the  $K$  series which will be found on page 87, it was shown that, for a number of elements, the expression  $\sqrt{\frac{\nu}{\frac{3}{4}\nu_0}}$ , in which  $\nu$  is the frequency determined experimentally, and  $\nu_0$  is a constant, is surprisingly near to the atomic number, less 1. An extension of this law to other related lines asserts that to a very close degree of approximation *the square root of the frequency is a linear function of the atomic number*.

How well this law is fulfilled appears from Fig. 72, which is plotted from data taken in the author's laboratory. The curves are very slightly concave upward. With the help of this law we are able to arrange all the lines in series, as has been done in the following tables.

On account of their great historical interest let us first repeat here the wave-lengths in the  $K$  series as determined by Moseley. In order to judge them in their proper light, it must be stated that in his calculation of wave-lengths Moseley used a value for the lattice constant of his potassium ferrocyanide crystal which is not in good agreement with the accepted value of the constant for rocksalt, but is some 0.54 per cent. too large. Further, the spectrograms did not permit of a resolution of the two  $\alpha$  components, so that the tabulated values represent an average of these two lines. On the contrary, we may assume that the  $\beta$  values are not affected by the  $\beta_2$  component, which is faint and farther away.

TABLE 5.

Moseley's measurements of wave-lengths (in X.U.) of the  
 $K$  series (1913).

	$K\alpha.$	$K\beta.$		$K\alpha.$	$K\beta.$
13 Al	8364	7912	28 Ni	1662	1506
14 Si	7142	6729	29 Cu	1549	1402
17 Cl	4750	—	30 Zn	1445	1306
19 K	3759	3463	39 Y	838	—
20 Ca	3368	3094	40 Zr	794	—
22 Ti	2758	2524	41 Nb	750	—
23 Va	2519	2297	42 Mo	721	—
24 Cr	2301	2093	44 Ru	638	—
25 Mn	2111	1918	46 Pd	584	—
26 Fe	1946	1765	47 Ag	560	—
27 Co	1798	1629			

In Table 6 are tabulated measurements of the  $K$  series of several elements, particularly W and Pt, which are used as material for anti-cathodes in commercial tubes; a single measurement for gallium by Uhler and Cooksey is also included. In the work on this last element the authors used the lattice constants  $3.0307 \times 10^{-8}$  cm. for calcite, and  $2.814 \times 10^{-8}$  for rocksalt, taking photographs with both crystals. In the remainder of the calculations the same value was used for rocksalt, but for calcite the slightly different value  $3.02904 \times 10^{-8}$  cm.

TABLE 6.

Element.	$a_0$	$a_2$	$a_1$	$\beta_1$	$\beta_2$	Measured by
31 Ga		1341.61	1337.85	1205.91		Uhler-Cooksey
42 Mo		712.35	708.06	631.31	619.9	Duane et al.
42 Mo		713.1	708.1	632.4	621.4	Overn
44 Ru		645.4	641.0	570.5	559.3	Auger and Dauvillier
45 Rh		616.56	612.30	545.45	534.4	Overn
74 W		203		177		de Broglie (1916)
74 W		218	214	192		Hull and Rice
74 W		212.8	205.3	182.6	176.8	Le. and Dau.
74 W		212.4	207.6	183.4	178.4	Dershem
74 W		213.52	208.85	184.36	179.40	Siegbahn
74 W	215	213.48	208.67	184.26	179.07	Du.-St.
77 Ir		195.8		168.4		Li.-Se
78 Pt			185.3		159.3	Li.-Se.
78 Pt		186	180	158	154	Le.-Dau.
78 Pt		189.8	185.0	163.4	157.4	de Broglie
78 Pt		190.10	185.28	163.4	158.2	Tandberg
78 Pt		189.5	185.1	164.4	159.6	Rogers
92 U		154		104		Dessauer and Back

*Abbreviations:* Le. and Dau.=Ledoux-Lebard and Dauvillier; Du.-St.=Duane and Stenström; Li.-Se.=Lilienfeld and Seeman.

Finally, in Table 7 we have as complete a list as possible of wave-lengths in the  $K$  series from the most recent measurements in the author's laboratory. The measurements are mostly the work of Hjalmar, Leide, Stenström, Stensson, Malmer, Friman, and Dolejšek. The wave-lengths are followed also by tables of the values of  $\frac{\nu}{R}$  and of  $\sqrt{\frac{\nu}{R}}$ . ( $R=109,737$ , the Rydberg constant.)



TABLE 7.

Wave-lengths of the K series. Emission.

	$\alpha_2$	$\alpha_1$	$\beta_1$	$\beta_2$
11 Na	11883.6		11591	—
12 Mg	9867.75		9534.5	—
13 Al	8319.40		7940.5	—
14 Si	7109.17		6739.3	—
15 P	6141.71		5789.0	—
16 S	5363.75	5360.90	5021.3	—
17 Cl	4721.36	4718.21	4394.6	—
19 K	3737.06	3733.68	3446.80	—
20 Ca	3354.95	3351.69	3083.43	—
21 Sc	3028.40	3025.03	2773.94	—
22 Ti	2746.81	2743.17	2508.98	2493.7
23 Va	2502.13	2498.35	2279.72	2264.6
24 Cr	2288.95	2284.84	2080.45	2067.0
25 Mn	—	2097.32	1905.91	1893.2
26 Fe	1936.51	1932.30	1752.72	1740.6
27 Co	1789.56	1785.28	1617.13	1605.4
28 Ni.	1658.54	1654.61	1497.03	1485.4
29 Cu	1541.16	1537.30	1389.33	1378.0
30 Zn	1435.87	1432.06	1292.71	1281.11
31 Ga	—	—	—	—
32 Ge	1255.21	1251.30	1126.46	1114.41
33 As	1177.41	1173.44	1055.11	—
34 Se	1106.42	1102.41	990.00	977.44
35 Br	1041.72	1037.68	930.73	918.22
37 Rb	927.73	923.61	826.73	814.62
38 Sr	877.45	873.28	781.06	768.74
39 Y	831.21	827.03	739.02	726.77
40 Zr	788.27	784.06	699.98	688.08
41 Nb	748.79	744.54	663.98	652.37
42 Mo	711.87	707.59	630.75	619.27
44 Ru	645.88	641.54	—	—
45 Rh	616.37	612.01	544.67	534.37
46 Pd	588.60	584.21	519.48	508.94
47 Ag	562.59	558.16	495.85	485.42
48 Cd	538.32	533.89	474.09	463.96
49 In	515.48	511.05	453.63	443.98
50 Sn	493.88	489.41	434.25	424.72
51 Sb	473.84	469.29	416.16	406.81
52 Te	454.91	450.37	398.92	389.88
74 W	213.52	208.85	184.36	179.40
77 Ir	195.8	—	168.4	—
78 Pt	190.10	185.28	163.4	158.2

TABLE 8.

Values of  $\lambda$  in the K series; fainter emission lines by Dolejšek  
and by Dolejšek and Siegbahn.

	$\alpha''$	$\alpha'$	$\alpha_3$	$\alpha_4$	$\beta_3$	$\beta'$
15 P	—	—	—	—	5820.2	—
16 S	—	—	—	—	5044.7	—
17 Cl	4712	4702.5	4688	4684	4406.0	—
19 K	3730	—	3711.0	3708.8	—	—
20 Ca	3349	—	3332.3	3330.0	—	3091.1
21 Sc	3023	—	3006	—	—	2799.2
22 Ti	—	—	2726.9	—	—	—
23 Va	—	—	2484.6	—	—	—
24 Cr	—	—	2273.3	—	—	2085.7
25 Mn	—	—	2087.9	—	—	1910.5
26 Fe	—	—	1923.3	—	—	1756.0
27 Co	—	—	1777.4	—	—	1619.7
28 Ni	—	—	1647.6	—	—	1499.0
29 Cu	—	—	1530.7	—	—	—
30 Zn	—	—	1428.8	—	—	—

TABLE 9.

Values of  $\lambda$  in the K series; fainter emission lines by Hjalmar.

	$\alpha'$	$\alpha_3$	$\alpha_4$	$\alpha_5$	$\alpha_6$	$\beta_3$	$\beta'$	$\beta_2(?)$	$\beta''$
11 Na	11835	11802	11781	—	×	—	—	—	—
12 Mg	9826.5	9799.4	9786.2	9730.2	9711.8	9647	×	—	—
13 Al	8285.6	8264.6	8253.0	8205.8	8189.2	8025	×	—	—
14 Si	7083	7063.8	7053.7	7014	7003	6793.3	6744.2	—	—
15 P	×	6102.2	6095.0	—	—	5820.4	×	—	—
16 S	5340.6	5329.37	5323.25	5262.6	—	5047	5045.0	5012.7	—
17 Cl	—	—	—	—	—	—	—	—	4390.8
19 K	3718.7	3708.83	—	—	—	—	—	3434.6	3442.5
20 Ca	—	—	—	—	—	—	—	3067.4	3079.6
21 Sc	—	—	—	—	—	—	—	2755.5	—
22 Ti	—	—	—	—	—	—	2515.1	2493.7	—
23 Va	—	—	—	—	—	—	2285.3	2265.4	—

TABLE 10.

Values of  $\frac{\nu}{R}$ , K series. Emission.

	$\alpha_2$	$\alpha_1$	$\beta_1$	$\beta_2$
11 Na		76.68	78.62	—
12 Mg		92.34	95.57	—
13 Al		109.53	114.76	—
14 Si		128.18	135.21	—
15 P		148.37	157.41	—
16 S	169.89	169.98	181.48	—
17 Cl	193.01	193.14	207.36	—
19 K	243.84	244.07	264.38	—
20 Ca	271.61	271.88	295.51	—
21 Sc	300.90	301.24	328.51	—
22 Ti	331.75	332.20	363.20	365.42
23 Va	364.19	364.75	399.72	402.40
24 Cr	398.11	398.83	438.00	440.86
25 Mn	—	434.49	478.13	481.34
26 Fe	470.56	471.60	519.90	523.54
27 Co	509.20	510.44	563.51	567.63
28 Ni	549.42	550.75	608.72	613.48
29 Cu	591.27	592.75	655.91	661.30
30 Zn	634.63	636.34	704.93	711.31
32 Ge	726.55	728.24	808.94	819.68
33 As	773.94	776.56	863.65	—
34 Se	823.60	826.59	920.45	932.28
35 Br	874.75	878.15	979.07	992.40
37 Rb	982.23	986.61	1102.2	1118.6
38 Sr	1038.5	1043.5	1166.7	1185.4
39 Y	1096.3	1101.8	1233.1	1253.8
40 Zr	1156.0	1162.2	1301.7	1324.4
41 Nb	1216.9	1223.9	1372.4	1396.8
42 Mo	1280.1	1287.8	1444.7	1471.5
44 Ru	1410.9	1420.4	—	—
45 Rh	1478.4	1488.9	1673.0	1705.3
46 Pd	1548.2	1559.8	1754.2	1790.3
47 Ag	1619.7	1632.6	1837.7	1877.2
48 Cd	1692.7	1706.8	1922.1	1964.1
49 In	1767.8	1783.1	2008.8	2052.4
50 Sn	1845.0	1861.9	2098.5	2145.5
51 Sb	1923.7	1941.7	2189.7	2240.0
52 Te	2003.1	2023.3	2284.3	2337.2
74 W	4267.8	4363.3	4942.9	5079.5
77 Ir	4654	—	5411	—
78 Pt	4793	4918	5577	5760

TABLE 11.

Values of  $\sqrt{\frac{\nu}{R}}$ ,  $K$  series. Emission.

	$\alpha_2$	$\alpha_1$	$\beta_1$	$\beta_2$
11 Na		8.757	8.867	—
12 Mg		9.609	9.776	—
13 Al		10.465	10.712	—
14 Si		11.321	11.627	—
15 P		12.176	12.546	—
16 S	13.034	13.037	13.470	—
17 Cl	13.893	13.897	14.400	—
19 K	15.616	15.623	16.259	—
20 Ca	16.481	16.488	17.191	—
21 Sc	17.346	17.356	18.126	—
22 Ti	18.214	18.226	19.057	—
23 Va	19.084	19.097	19.993	20.06
24 Cr	19.953	19.970	20.929	21.00
25 Mn	—	20.844	21.866	21.94
26 Fe	21.692	21.716	22.801	22.88
27 Co	22.566	22.593	23.738	23.82
28 Ni	23.440	23.467	24.672	24.77
29 Cu	24.316	24.347	25.610	25.72
30 Zn	25.192	25.225	26.55	26.671
32 Ge	26.955	26.986	28.442	28.628
33 As	27.820	27.867	29.388	—
34 Se	28.698	28.750	30.339	30.533
35 Br	29.576	29.633	31.291	31.502
37 Rb	31.340	31.410	33.200	33.446
38 Sr	32.226	32.303	34.156	34.429
39 Y	33.110	33.193	35.115	35.409
40 Zr	34.000	34.091	36.079	36.392
41 Nb	34.885	34.984	37.046	37.375
42 Mo	35.778	35.886	38.009	38.360
44 Ru	37.561	37.688	—	—
45 Rh	38.450	38.587	40.902	41.295
46 Pd	39.347	39.494	41.883	42.311
47 Ag	40.246	40.405	42.869	43.322
48 Cd	41.142	41.314	43.841	44.318
49 In	42.045	42.227	44.819	45.304
50 Sn	42.954	43.149	45.809	46.320
51 Sb	43.852	44.065	46.794	47.328
52 Te	44.756	44.982	47.794	48.345
74 W	66.074	65.327	70.304	71.270
77 Ir	—	68.21	73.561	—
78 Pt	70.13	69.23	74.68	75.89

23. The  $L$  Series

The general structure of the  $L$  series may be seen from Fig. 39, page 53. For the heavier elements three groups of lines may be distinguished, and the author has chosen the notation so that these groups are denoted by  $\alpha$ ,  $\beta$ , and  $\gamma$ ;  $\alpha$  denotes the group of longest wave-length,  $\beta$  the intermediate group, and  $\gamma$  the group of shortest wave-length. Within each group the lines are numbered with the subscripts 1, 2, 3, etc., in their order of intensity. Then later a line of considerably lower frequency was found, and received the designation  $l$ . It may be stated here that this division into the  $\alpha$ ,  $\beta$ , and  $\gamma$  groups is not identical with that previously mentioned, in which three sub-groups were formed on the basis of the different voltages necessary to excite them. The three groups  $\alpha$ ,  $\beta$ , and  $\gamma$  may be ascribed to a pure chance in the order of the lines in the spectrum. But in the classification of new experimental results this notation has the advantage that new lines, which are generally weaker than those already known, may be included in the series of subscripts, and it also enables one to form some idea of the intensity of the various lines. Until a rigid and theoretically founded nomenclature can be adopted, the one just indicated is in my opinion the most advantageous. Another system of notation is in use. It was proposed by Moseley, and Sommerfeld has further extended it from theoretical considerations on the relationships between the lines. Later on we shall discuss a rational system of notation. The correspondence between the Moseley-Sommerfeld notation and ours may be seen from the following parallel arrangement. Moseley discovered and named the lines  $\alpha$ ,  $\beta$ ,  $\gamma$ ,  $\phi$ , while Sommerfeld introduced the other symbols.

Siegbahn	-	-	$\alpha_2$	$\alpha_1$	$\beta_1$	$\beta_2$	$\beta_3$	$\beta_4$	$\beta_5$	$\beta_6$	$\gamma_1$	$\gamma_2$	$\gamma_3$	$\gamma_4$	$\gamma_5$	$l$	$\eta$
Moseley-Sommerfeld			$\alpha'$	$\alpha$	$\beta$	$\gamma$	$\phi$	$\phi'$	$\zeta$	$\iota$	$\delta$	$\theta$	$\chi$	$\psi$	$\kappa$	$\epsilon$	$\eta$

The diagram of Fig. 73 gives a better and more detailed picture of the  $L$  series than do the spectrograms in Fig. 39. The lines here are in their proper relative positions on a scale of wave-lengths, and are so placed that the strongest line lies in the same position for all elements. Lines associated by the Moseley law are connected from element to element.

We have already mentioned that the  $L$  series is divided into three groups, of which each shows the same character as the  $K$  series, *i.e.* all the lines of one of these sub-groups appear simultaneously when a certain minimum voltage is reached, and on further increase in the voltage they all increase in intensity in the same ratio. Webster and Clark, and also Hoyt, assigned the lines to groups as follows :

First sub-group	-	$l$	$\alpha_2$	$\alpha_1$	$\beta_2$	$\beta_5$	$\beta_7$
Second sub-group	-		$\eta$	$\beta_1$	$\gamma_1$		
Third sub-group	-		$\beta_3$	$\beta_4$	$\gamma_4$		

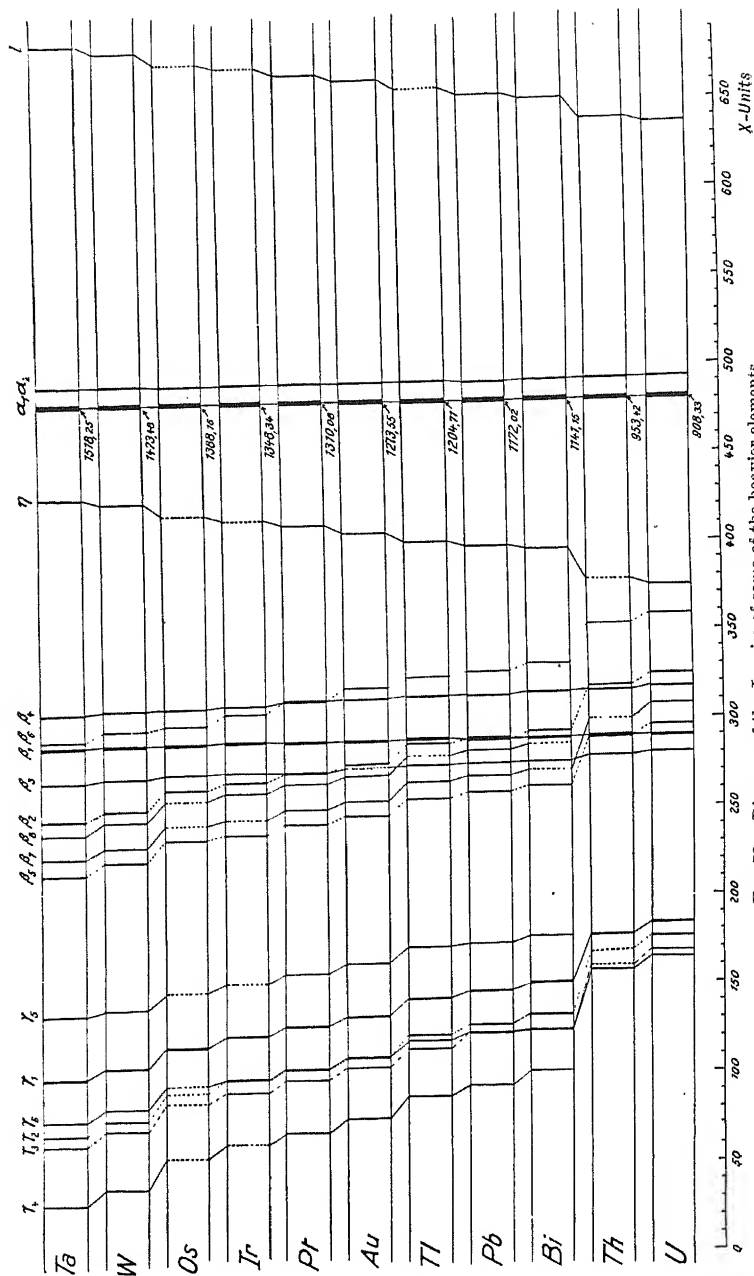


FIG. 73. Diagram of the L series of some of the heavier elements.

For platinum Hoyt gives as the critical voltages of these three groups 10.2, 11.6 and 12.0 kv.

Really precise measurements of the intensities of the lines of each group are not very numerous. Duane and Patterson made a few observations with tungsten; they could not compare different lines of the same

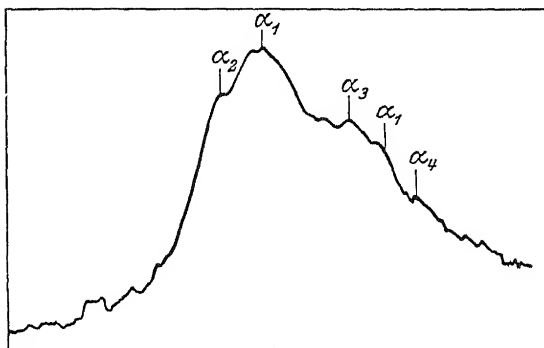


FIG. 74A. Photometric registration of the intensity distribution of the line  $La_1$  of Rh and its satellites (calcite crystal).

sub-group, but only neighbouring lines. On account of differences in ionizing action, in reflecting power, etc., lines differing greatly in wavelength are difficult to compare. From amongst the results of Duane and Patterson the following may be mentioned. The two  $\alpha$  lines have the ratio 10 to 1;  $\beta_2$  and  $\beta_3$  at most 116 to 1; for  $\beta_1, \beta_2, \beta_3, \beta_4$  the relative

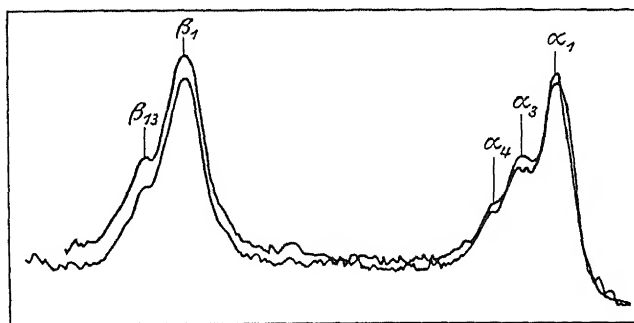


FIG. 74B. Intensity distribution of the lines  $La_1$  and  $L\beta_1$  of Zr and their satellites (gypsum crystal).

intensities are as 100, 55, 15, 9 (voltage on the tube, 24.8 kv.) ; while, finally, the lines  $\gamma_1, \gamma_2, \gamma_3, \gamma_4$  have the relative intensities 100, 14, 18, 6, with a tube voltage of 22.75 kv.

The *L* series exhibits its greatest abundance of lines among the heavier elements. In the case of uranium no fewer than 22 lines have been

established. In passing to the lighter elements some lines of the series disappear, since the outer electron shells of the atom, in which, according to Bohr's theory, the process giving rise to the lines is initiated, are no longer present. The lightest element for which the  $L$  series has been measured is copper, and in this case only a single line was obtained with a wave-length of 13,309 X.U. This was, a short time ago, the longest known X-ray wave-length.

Just as in the  $K$  series, many of the lines of the  $L$  series become broader with decreasing atomic weight, that is, with increasing wave-length. Such a broadening of the strongest lines becomes noticeable first on the short wave-length side. A distinct structure

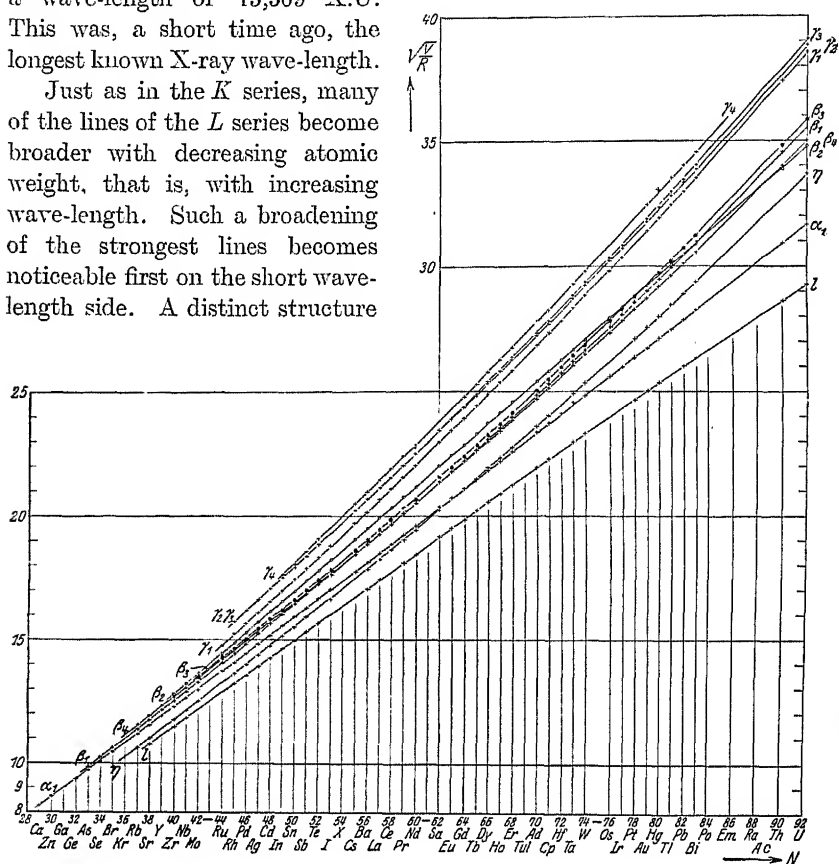


FIG. 75.  $\sqrt{\frac{1}{\lambda}}$  for the  $L$  lines as a function of the atomic numbers of the elements.

is also evident within the line. Details in this respect may be found in the doctorate thesis of Coster, where photometric curves of intensity of the lines are shown. Two typical examples of these diagrams are here reproduced (Figs. 74A and 74B).

The first is a photogram of the strongest line of rhodium from a photograph taken with a calcite crystal. In the diffuse broadening towards short wave-lengths a number of lines  $\alpha_3$ ,  $\alpha'_1$  and  $\alpha_4$  may be seen. The



other photograph is from a spectrogram of the  $L_\alpha$  and  $L_\beta$  lines of zirconium taken with smaller dispersion (gypsum crystal). Both lines are accompanied by satellites on the short wave-length side,  $\alpha_3$  and  $\alpha_4$  in the one case and  $\beta_{13}$  in the other.

Fig. 75 is a Moseley diagram of the  $L$  series. As in the  $K$  series, points representing the same lines for different elements lie upon curves which are almost straight lines, but the curves of the  $L$  series differ from those of the  $K$  series in that here certain curves intersect each other. This is explained by the circumstance mentioned above, that the  $L$  series consists of three groups, and a curve belonging to one group may intersect one of another group.

Of the wave-length measurements in the  $L$  series we shall give first (Table 12) those of Moseley, who investigated a large number of elements. A few spectra had previously been partially measured, as we have stated, by Bragg and de Broglie.

TABLE 12.

Measurements of wave-lengths in the  $L$  series (Moseley, 1914).

Element.	$\alpha (\alpha_1)$	$\beta (\beta_1)$	$\phi (\beta_2)$	$\gamma (\beta_2)$
40 Zr	6091			
41 Nb	5749	5507		
42 Mo	5423	5187		
44 Ru	4861	4660		
45 Rh	4622			
46 Pd	4385	4168		3928
47 Ag	4170			
50 Sn	3619			
51 Sb	3458	3245		
57 La	2676	2471	2424	2313
58 Ce	2567	2360	2315	2200
59 Pr	2471	2265		
60 Nd	2382	2175		
62 Sm	2208	2008	1972	1893
63 Eu	2130	1925	1888	1814
64 Gd	2057	1853	1818	
66 Ho	1914	1711		
68 Er	1790	1591	1563	
73 Ta	1525	1330		1287
74 W	1486			
76 Os	1397	1201		1172
77 Ir	1354	1155		1138
78 Pt	1316	1121		1104
79 Au	1287	1092		1078

The spectrum of tungsten (Table 13) has been investigated frequently, for the obvious reason that this element is the one most used as the material for the anticathode.

Croftutt has found some additional lines in the wave-length region of the tungsten  $L$  series, which he also ascribes to the spectrum of that element. The reason is that these lines fit in well between energy-levels known for tungsten. The corresponding transitions for two of them,  $\gamma_{11}$  and  $\gamma_{12}$  are ruled out by the selection principle just as in the case of the formerly known  $\beta_9$  and  $\beta_{10}$ .  $\gamma_{11}$  has been observed also by Dershem and by Overn. The wave-lengths and transitions of these lines are :

$$\beta_{15} - 1243.2 (L_1 N_4),$$

$$\beta_{16} - 1216.6 (L_1 O_2),$$

$$\gamma_{12} - 1074.8 (L_3 N_7),$$

$$\gamma_{11} - 1044.4 (L_3 N_4).$$

TABLE 13.

$L$  series of tungsten from various observers.

	Dershem.	Overn.	Compton.	Siegbahn and Coster.	Duane and Patterson.	Croftutt.	Rogers.
$l$				1675.05	1676.1		
$a_2$	1482.8	1483.9	1484.6	1484.52	1484.4	1484.4	1484.3
$a_1$	1472.2	1473.1	1473.6	1473.48	1473.5	1473.3	[1473.27]
$\eta$	1416.3			1417.7	1418.1	1418	1417.3
—			1336.0 ?				
$\beta_4$	1297.7	1298.4	1298.7	1298.74	1298.9	1298.8	1298.7
$\beta_6$	1286.8	1287.2		1287.1		1287.5	1287.6
$\beta_1$	1278.4	1279.3	1279.2	1279.17	1279.3	1279.3	[1279.05]
$\beta_3$	1258.6	1259.8	1260.2	1260.00	1260.5	1260.2	1260.1
$\beta_2$	1241.6	1243.4	1242.1	1241.91	1242.3	1242.1	[1241.92]
$\beta_8$		1235.5		1235.4		1236.4	1235.5
$\beta_7$	1220.2	1221.2	1218.7	1220.8		1221.7	1220.6
$\beta_5$		1213.2		1212.5		1213.3	1212.6
$\beta_{10}$	1209.8	1209.7		1209.4		1209.9	
$\beta_9$	1177.3 ?	1202.1		1202.1	1204.4	1202.7	1202.1
$\gamma_5$	1129.2	1130.2		1129.2		1129.9	1129.2
$\gamma_1$	1095.3	1096.7	1096.5	1095.53	1096.4	1096.4	[1095.53]
—		1079.4				1078.6	1078.0
$\gamma_6$	1070.5	1072.4		1072.0		1072.3	1071.5
$\gamma_2$	1064.8	1065.9	1065.3	1065.84	1065.9	1065.9	1065.0
$\gamma_3$	1058.7	1059.6	1058.4	1059.65	1060.0	1059.9	1059.0
—	1042.1	1044.6				1044.4	1043.3
$\gamma_4$	1025.3	1026.3	1025.1	1026.47	1026.5	1026.6	1025.6

Rogers, whose values are tabulated in the last column of Table 13, also gives lines having the following wave-lengths:

1450.3	1230.0
1373.5	1113.8
1321.2	1086.2
1248.7	

It is doubtful whether these lines really belong to the tungsten spectrum. None of the new lines given by Crofutt were found by Rogers. Moreover, the  $\beta_{10}$  line obtained by other observers is missing in the table of Rogers.

In some quite recent researches performed with a view to extending the methods of X-ray spectroscopy in the direction of longer wave-lengths, the author and Mr. Thoraens have obtained as a preliminary result the strongest lines in the *L* series of the elements Zn to Fe. In these investigations only a very thin coloured foil of gelatine separated the X-ray tube from the spectrograph. The spectrograms were taken on Schumann plates, and an organic crystal (palmitic and stearic acid) with large lattice constant was used as a grating. The preliminary results are collected together in Table 13A.

TABLE 13A.

Element.	Older values and extrapolated values [ ], in Å.		New preliminary wave-lengths in Å.	
	$\alpha$	$\beta$	$\alpha$	$\beta$
Zn	12.22	11.95	12.25	11.99
Cu	13.31	—	13.39	13.10
Ni	[14.55]	—	14.65	14.33
Co	[15.97]	—	16.07	15.80
Fe	[17.6]	—	17.66	17.33

In the following tables (pp. 116-124), the measurements of the *L* series made in the laboratory of the author are tabulated. The stronger and more accurately measurable lines have been redetermined by Hjalmar. The weaker lines have been contributed by Coster, who also discovered a large number of new lines in the *L* series; these are included here in the general scheme. The elements from Os (76) upwards have all been measured anew by Coster, and their spectra enlarged by the addition of lines previously unknown. The spectrum of Hafnium, discovered in the Bohr Institute with the help of X-ray spectroscopy, has been measured there by Coster. Also Thulium (69) has been measured by the same observer.

Wave-lengths of the L series. Emission.

	92 U.	90 TH.	83 BI.	82 Pb.	81 TL.	80 HG.	79 AU.	78 Pt.	77 Ir.	76 Os.	74 W.	73 TH.	72 HF.	71 Cp.	70 Ad.	69 Tm.	68 Er.
$\lambda$	1064.77	1112.41	1312.95	1346.62		1418.3	1456.54	1497.23			1675.05	1724.2	1777.4	1831.8	1890.0	1951.1	2015.1
$\alpha_2$	920.14	965.24	1153.3	1183.52	1216.03	1249.7	1284.89	1321.21	1359.39	1398.2	1484.52	1529.4	1577.04	1626.36	1678.9	1733.9	1781.40
$\alpha_1$	908.33	953.42	1141.15	1172.02	1204.71	1238.5	1273.55	1310.08	1348.34	1388.16	1473.48	1518.25	1566.07	1615.51	1667.79	1722.8	1780.40
$\eta$	802.9		1057.—	1090.2	1125.—	1161.9	1199.5	1240.1			1417.7	1465.5	1519.7	1573.8	1631.0	1692.3	1754.8
$\beta_4$	745.4	789.—	975.4	1004.69	1037.1	1068.6	1104.4	1139.8	1176.4	1215.0	1298.74	1342.2	1389.3	1437.2	1488.2	1541.2	1596.4
$\beta_6$	786.6	826.2	991.6	1018.8	1048.0	1077.4	1110.6	1139.8	1171.7	1204.8	1287.1	1326.7	1371.1	1414.3	1462.7	1511.5	1563.6
$\beta_1$	718.07	762.59	949.30	979.90	1012.66	1045.8	1080.93	1117.22	1154.95	1194.59	1279.17	1323.54	1371.1	1420.7	1472.5	1526.8	1583.44
$\beta_{13}$																	1575.6
$\beta_3$	708.4	752.1	935.7	966.02	997.8	1030.1		1099.50	1137.9	1177.2	1260.00	1303.3	1349.7	1398.2	1449.4	1502.3	1557.9
$\beta_{14}$																	1512.—
$\beta_2$	752.68	791.08	952.93	979.90	1007.86		1067.75	1099.50	1132.87	1168.38	1241.91	1281.0	1323.5	1367.2	1412.8	1460.2	1510.6
$\beta_{11}$											1235.4	—		1359.—	—		1501.4
$\beta_{12}$																	
$\beta_{10}$																	
$\beta_9$			893.8	922.3	959.0		1025.7	1057.0			1209.4	1250.6		1339.8			1482.3
$\beta_8$				973.5	995.0		1018.8	1051.9	1126.7		1202.1	1242.9		1333.0			
$\beta_7$	736.—	762.59	922.3	949.52	978.3	1007.8	1046.5	1078.5	1103.0	1140.—	1220.8	1260.0	1303.5	1345.9			1489.2
$\beta_5$	724.13						1038.2	1070.1			1212.5	1250.6					
$\gamma_5$			837.8	863.9	894.2	914.4	954.2	985.5			1129.2	1170.0	1212.1	1256.—	1303.0	1352.3	1403.—
$\gamma_9$																	
$\gamma_1$	612.83	651.03	810.65	837.08	865.29	898.5	924.37	955.45	988.41	1022.47	1095.53	1134.71	1176.5	1220.3	1264.8	1312.7	1362.3
$\gamma_6$	592.6	630.1	787.4	813.70	841.7		901.25	931.7	963.6		1072.0	1110.0					
$\gamma_7$											1079.—	—					
$\gamma_8$																	
$\gamma_{10}$																	
$\gamma_2$	604.4		792.9	818.2	844.7	869.5	901.25	931.7	963.6		1065.84	1102.0	1141.3	1183.2	1225.6	1271.2	1318.4
$\gamma_3$	597.0		787.4	813.70	837.9	869.5	895.68	925.6	956.6		1059.65	1096.2	1135.6	1177.5	1219.8	1265.3	1311.8
$\gamma_4$			761.—	783.6	810.0	834.8	866.3	895.0			1026.47	1062.4	1100.1	1141.1	1182.0	1226.4	1273.2

Wave-lengths of the *L* series. Emission.

	67 H $\alpha$ .	66 D $\gamma$ .	65 T $\beta$ .	64 G $\delta$ .	63 E $\epsilon$ .	62 S $\eta$ .	60 N $\delta$ .	59 P $\zeta$ .	58 C $\epsilon$ .	57 L $\alpha$ .	56 B $\alpha$ .	55 C $\delta$ .	53 I.	52 T $\epsilon$ .	51 S $\beta$ .	50 S $\eta$ .	49 H $\gamma$ .
$\iota$	2082.1	2154.0	2229.0	2307.1	2390.3	2477.0	2670.3	2778.1	3000.—	3128.7	3380.3	3710.1	3880.3	4063.3	4259.3	4499.3	4752.4
$\alpha_2$	1852.06	1915.64	1982.31	2052.62	2127.33	2205.68	2375.63	2467.63	2565.11	2668.93	2779.02	2895.60	3150.87	3291.00	3440.75	3601.08	3772.42
$\alpha_1$	1840.98	1904.60	1971.49	2041.93	2116.33	2195.01	2365.31	2457.70	2556.00	2659.68	2769.64	2886.10	3141.66	3281.99	3431.77	3592.18	3763.67
$\alpha_3$	1822.0	1892.2				2214.—	2404.2	2507.—	2614.7	2734.—	2857.1	2983.3			3599.6	3781.8	3976.1
$\gamma$																	
$\beta_4$	1655.3	1716.7	1781.4	1849.3	1922.1	1996.4	2162.2	2250.1	2344.2	2443.8	2549.8	2660.5	2906	3040.0	3184.3	3336.3	3499.0
$\beta_6$	1618.8	1677.7	1737.5	1803.1	1870.5	1942.2	2099.3	2185.9	2276.9	2373.9	2477.2	2587.5		2964.4	3107.8	3262.2	3428.0
$\beta_1$	1643.52	1706.58	1772.68	1842.46	1916.31	1993.57	2162.21	2253.90	2351.00	2453.30	2562.24	2677.84	2930.33	3069.97	3218.36	3377.92	3547.83
$\beta_{13}$	1635.5	1699.2	1765.5	1835.5	1909.2	1987.1											
$\beta_3$	1616.0	1677.7	1742.5	1810.9	1882.7	1958.0	2122.2	2212.4	2305.9	2405.3	2511.0	2622.93	2867	3001.3	3145.14	3298.9	3461.9
$\beta_{14}$	1567.—	1625.1	1685.1	1748.1	1781.4	1855.1	2038.8	2122.0	2212.1								
$\beta_2$	1563.7	1619.8	1679.0	1741.9	1808.2	1878.1	2031.4	2114.8	2204.1	2298.0	2399.3	2506.4	2746.08	2876.1	3016.6	3167.9	3331.2
$\beta_{11}$																	
$\beta_{12}$																	
$\beta_{10}$			1664.—	1728.1	1796.—	1865.7	2019.3	2102.5	2191.6	2285.—					2993.4	3142.6	3304.0
$\beta_9$				1788.—	1788.—	1858.1	2011.7	2095.8	2184.0	2277.—					2985.8	3134.7	3295.9
$\beta_8$															2972.5	3114.4	3265.8
$\beta_7$		1595.7	1655.8	1719.6	1784.—	1852.3	2004.3	2087.4	2176.3	2270.—	2375.6	2480.—			2965.8	3108.1	3259.8
$\beta_5$																3149.—	3317.—
$\gamma_5$	1459.—	1515.2	1574.2	1637.6	1705.—	1775.1	1931.3	2016.1	2105.6	2200.8	2302.3	2411.1		2783.1	2925.6	3077.4	3241.8
$\gamma_9$	1416.—		1531.4	1593.6	1659.3	1728.5	1880.4	1962.2	2051.—								
$\gamma_1$	1414.2	1469.7	1526.6	1558.63	1654.3	1723.09	1873.83	1956.81	2044.33	2137.20	2236.60	2342.52	2577.48	2706.47	2845.07	2994.93	3155.29
$\gamma_6$																	
$\gamma_7$				1644.—	1644.—	1644.—	1859.—	1942.2	2029.—	2218.—	2218.—					2968.5	3125.—
$\gamma_8$				1629.—	1629.—	1629.—		1932.2	2019.—	2218.—							
$\gamma_{10}$							1881.1	1962.3	2048.1	2140.2	2236.9						
$\gamma_2$	1367.7	1420.3	1473.8	1531.0	1593.9	1655.9	1797.4	1875.0	1955.9	2041.6	2134.0	2232.2	} 2564.9			2688.9	2827.3
$\gamma_3$	1361.3	1413.9	1468.3	1525.9	1587.7	1651.7	1792.5	1869.9	1950.9	2036.5	2129.5	2227.0					2973.6
$\gamma_4$	1319.7	1371.4	1423.9	1481.8		1603.3	1740.8	1815.3	1895.2	1978.7	2071.5	2169.1		2505.7	2633.6	2771.3	2919.1

Wave-lengths of the *L* series. Emission.

[illegible]

	92 U.	90 Th.	83 Bi.	82 Pb.	81 Tl.	80 Hg.	79 Au.	78 Pt.	77 Ir.	76 Os.	74 W.	73 Ta.	72 Hf.	71 Cp.	70 Ad.	69 Tm.	68 Er.
$l$	855.84	819.19	694.07	676.70		642.50	625.63	608.64			544.03	528.50	512.70	497.47	482.15	467.05	452.22
$a_2$	990.37	944.08	790.20	769.96	749.39	729.19	709.22	689.73	670.35	651.75	613.85	595.83	577.84	560.31	542.78	525.57	508.69
$a_1$	1003.23	955.78	798.54	777.51	756.42	735.79	715.53	695.58	675.84	656.45	618.45	600.20	581.89	564.08	546.39	528.93	511.83
$a_3$																	
$\eta$	1134.9		862.3	835.90	810.3	784.29	759.97	734.82			642.78	621.83	599.66	579.01	558.72	538.49	519.30
$\beta_4$	1222.5	1155.0	934.22	907.01	878.64	852.77	825.15	799.52	774.62	748.25	701.66	678.93	655.91	634.06	612.33	591.26	570.83
$\beta_6$	1158.7	1102.7	918.97	894.50	869.49	845.80	820.51	799.52	777.75	756.33	708.00	686.87	664.60	644.33	623.01	602.90	582.80
$\beta_1$	1269.08	1194.94	959.93	929.98	899.88	871.36	843.02	815.65	788.99	762.83	712.39	688.51	664.60	641.42	618.86	596.84	575.50
$\beta_{13}$																	578.36
$\beta_3$	1286.2	1211.6	973.8	943.3	913.2	884.6		823.80	800.82	774.08	723.23	699.23	675.20	651.75	628.72	606.60	584.93
$\beta_{14}$																	602.6
$\beta_2$	1210.70	1151.93	956.28	929.98	904.16		853.46	823.80	804.39	780.58	733.76	711.40	688.51	666.52	645.01	624.10	603.25
$\beta_{11}$											737.63			670.5			606.95
$\beta_{12}$																	
$\beta_{10}$								861.63			753.49	723.65		680.15			614.77
$\beta_9$			1019.6	987.82			894.44	866.28			758.07	733.22		683.62			
$\beta_8$				936.0			858.94	833.90	808.82		737.63	715.60					
$\beta_7$	1238.1			950.2	922.61		870.77	844.93			746.45	723.30	699.08	677.07			611.92
$\beta_5$	1258.43	1194.94	987.98	959.72	931.41		877.70	851.57	826.18	799.6	751.56	728.65					
$\gamma_5$			1087.7	1054.8	1019.1	996.5	955.0	924.71			807.00	778.86	751.80	725.5	699.3	673.88	649.5
$\gamma_9$																	
$\gamma_1$	1486.98	1399.74	1124.10	1088.37	1053.12	1019.89	985.83	953.77	921.96	891.25	831.81	803.04	774.55	746.76	720.49	694.23	668.92
$\gamma_6$	1537.7	1446.2	1157.5	1119.97	1082.6		1011.12	978.07	945.6		850.07	820.98					
$\gamma_7$																	
$\gamma_8$											844.5						
$\gamma_{10}$																	
$\gamma_2$	1507.8		1149.2	1113.8	1078.8	1048.0	1011.12	978.07	945.6		854.98	826.90	798.46	770.17	743.53	716.83	691.19
$\gamma_3$	1526.4		1157.5	1119.9	1087.5	—	1017.41	984.52	952.6		859.97	831.28	802.48	773.90	747.07	720.22	694.67
$\gamma_4$			1106.8	1162.8	1125.0	1091.6	1051.8	1018.17			887.77	857.74	827.68	798.59	770.96	743.03	715.73

$\frac{\nu}{R}$  for the  $L$  series. Emission.

	67 Ho.	66 Dy.	65 Tb.	64 Gd.	63 Eu.	62 Sm.	60 Nd.	50 Pr.	58 Co.	57 La.	56 Ba.	55 Cs.	53 I.	52 Te.	51 Sb.	50 Sn.	40 In.
$l$	437.67	423.06	408.82	394.99	381.24	367.89	341.26	328.02	303.7	291.26				245.62	234.85	224.27	213.95
$\alpha_2$	492.03	475.70	459.70	443.05	428.36	413.15	383.59	369.29	355.26	341.44	327.91	314.71	289.21	276.83	264.85	253.05	241.56
$\alpha_1$	494.99	478.46	462.22	446.28	430.59	415.16	385.26	370.78	356.52	342.62	329.02	315.74	290.05	277.66	265.54	253.68	242.12
$\alpha_3$																	243.01
$\eta$	500.15	481.59				411.5	379.03	363.4	348.52	333.3	318.95	305.46			253.16	240.96	229.19
$\beta_4$	550.52	530.83	511.55	492.76	474.10	456.46	421.44	404.99	388.73	372.89	357.39	342.52	313.5	299.76	286.18	273.14	260.44
$\beta_6$	562.93	543.17	524.47	505.39	487.18	469.19	434.08	416.89	400.22	383.87	367.86	352.18		307.40	293.22	279.34	265.83
$\beta_1$	554.46	533.94	514.06	494.59	475.53	457.10	421.45	404.31	387.31	371.45	355.65	340.30	310.91	296.83	283.15	269.77	256.85
$\beta_{13}$	557.18	536.29	516.15	496.47	477.30	458.59											
$\beta_3$	563.90	543.17	522.97	503.21	484.02	465.41	429.40	411.89	395.19	378.86	362.91	347.42	317.8	303.63	289.74	276.23	263.22
$\beta_{14}$	581.5	560.75	540.78	521.29	511.55	483.41	446.96	429.44	411.95								
$\beta_2$	582.77	562.58	542.75	523.15	503.97	485.21	448.59	430.90	413.44	396.55	379.81	363.58					
$\beta_{11}$																	
$\beta_{12}$																	
$\beta_{10}$			547.6	527.32	507.3	488.43	451.28	433.42	415.80	398.8		367.0		316.84	302.09	287.66	273.56
$\beta_9$					509.6	490.43	452.99	434.81	417.25	400.2	384.31	368.4			304.43	289.97	275.81
$\beta_8$															305.20	290.70	276.49
$\beta_7$		571.08	550.35	529.93	510.8	491.97	454.66	436.56	418.72	401.4	383.60	367.4			306.57	292.60	279.03
$\beta_5$															307.26	283.19	279.55
																289.3	274.7
$\gamma_5$	624.5	601.42	578.88	556.47	534.4	513.36	471.84	452.00	432.78	414.06	395.81	377.95		327.43	311.48	296.12	281.10
$\gamma_9$	643.5		595.06	571.83	549.19	527.20	484.61	464.41	444.3								
$\gamma_1$	644.37	620.04	596.93	573.62	550.85	528.86	486.31	465.69	445.75	426.38	407.44	389.01	363.55	336.70	320.30	304.27	288.81
$\gamma_6$							490.1	469.19	449.1		410.8					306.98	291.61
$\gamma_7$					554.3			471.62	451.3		410.8						
$\gamma_8$					559.4			484.43	464.39	444.93	425.79	407.38					
$\gamma_{10}$								486.01	465.91	446.35	427.02	408.24		355.26	338.90	322.31	306.45
$\gamma_2$	666.28	641.60	618.31	595.21	571.72	550.32	506.99	486.01	465.91	446.35	427.02	408.24					
$\gamma_3$	669.41	644.51	620.63	597.20	573.96	551.72	508.38	487.34	467.10	447.45	427.93	409.19					
$\gamma_4$	690.5	664.48	639.98	614.98		568.37	523.48	501.99	480.83	460.54	439.91	420.11		363.68	346.02	328.82	312.17



$$\nu \frac{1}{R}$$
 for the  $L$  series. Emission.[illegible]

$$\sqrt{\frac{\nu}{R}}$$
 for the  $L$  series. Emission.

	92 U.	90 Th.	83 Bi.	82 Pb.	81 Tl.	80 Hg.	70 At.	78 Pt.	77 Ir.	76 Os.	74 W.	73 Ta.	72 Hf.	71 La.	70 Yb.	69 Tm.	68 Er.
$L$	29-254	28-621	26-345	26-013		25-348	25-012	24-671			23-325	22-989	22-643	22-304	21-957	21-611	21-265
$\alpha_2$	31-470	30-726	28-111	27-748	27-375	27-004	26-631	26-263	25-891	25-529	24-776	24-410	24-038	23-671	23-297	22-926	22-554
$\alpha_1$	31-074	30-916	28-259	27-884	27-503	27-125	26-749	26-374	25-997	25-621	24-869	24-499	24-125	23-751	23-375	22-998	22-623
$\alpha_3$																	
$\eta$	33-68		29-36	28-902	28-46	28-005	27-568	27-108			25-353	24-937	24-488	24-062	23-637	23-212	22-789
$\beta_4$	34-96	33-98	30-565	30-116	29-642	29-202	28-726	28-276	27-832	27-355	26-489	26-057	25-611	25-180	24-746	24-316	23-892
$\beta_6$	34-04	33-20	30-314	29-909	29-487	29-083	28-645	28-276	27-888	27-501	26-608	26-208	25-780	25-384	24-960	24-554	24-141
$\beta_1$	35-624	34-568	30-983	30-496	29-998	29-519	29-034	28-560	28-089	27-619	26-690	26-240	25-780	25-326	24-877	24-431	23-990
$\beta_{13}$																	24-049
$\beta_3$	35-86	34-80	31-20	30-71	30-22	29-74		28-789	28-299	27-822	26-893	26-443	25-985	25-529	25-074	24-629	24-186
$\beta_{14}$																	24-55
$\beta_2$	34-795	33-940	30-924	30-496	30-070		29-214	28-789	28-362	27-938	27-088	26-672	26-238	25-817	25-397	24-982	24-561
$\beta_{11}$											27-159			25-89			24-636
$\beta_{12}$																	
$\beta_{10}$							29-81	29-35			27-450	27-00		26-080			24-794
$\beta_9$				31-43			29-90	29-43			27-533	27-08		26-146			
$\beta_8$				30-59			29-308	28-877	28-440		27-159	26-750					
$\beta_7$	35-18			30-82	30-37	30-071	29-509	29-068			27-321	26-894	26-440	26-020			24-737
$\beta_5$	35-474	34-568	31-432	30-980	30-52		29-626	29-182	28-743	28-27	27-415	26-993					
$\gamma_5$			32-98	32-48	31-92	31-56	30-90	30-409			28-408	27-908	27-419	26-93	26-446	25-959	25-48
$\gamma_9$																	
$\gamma_1$	38-562	37-413	33-528	32-991	32-452	31-935	31-398	30-883	30-363	29-854	28-841	28-338	27-831	27-327	26-842	26-348	25-863
$\gamma_6$	39-21	38-02	34-02	33-466	32-90		31-799	31-274	30-75		29-854	28-653					
$\gamma_7$											29-06						
$\gamma_8$																	
$\gamma_{10}$																	
$\gamma_2$	38-83		33-89	33-37	32-84		31-799	31-274	30-75		29-240	28-756	28-257	27-752	27-268	26-291	26-291
$\gamma_3$	39-07		34-02	33-46	32-97	32-37	31-897	31-377	30-86		29-325	28-832	28-328	27-819	27-332	26-837	26-337
$\gamma_4$			34-59	34-10	33-54	33-03	32-43	31-909			29-795	29-288	28-769	28-260	27-766	27-259	26-753

$$\sqrt{\nu} \text{ for the } L \text{ series.} \quad \text{Emission.}$$

	67 Ho.	66 Dy.	65 Tb.	64 Gd.	63 Eu.	62 Sm.	60 Nd.	59 Pr.	58 Ce.	57 La.	56 Ba.	55 Cs.	53 I.	52 Te.	51 Sb.	50 Sn.	49 In.
$\lambda$	20-921	20-568	20-219	19-875	19-525	19-180	18-473	18-112		17-42	17-067			15-672	15-325	14-976	14-627
$\alpha_2$	22-182	21-810	21-441	21-070	20-697	20-326	19-586	19-217	18-848	18-478	18-108	17-740	17-006	16-638	16-274	15-939	15-542
$\alpha_1$	22-249	21-874	21-490	21-125	20-751	20-376	19-628	19-255	18-882	18-510	18-139	17-769	17-030	16-663	16-296	15-927	15-560
$\alpha_3$																	
$\eta$	22-364	21-945				20-28	19-469	19-06	18-669	18-25	17-860	17-477			15-911	15-523	15-139
$\beta_4$	23-463	23-039	22-617	22-198	21-774	21-365	20-523	20-125	19-716	19-310	18-905	18-507	17-70	17-314	16-917	16-527	16-138
$\beta_6$	23-727	23-306	22-901	22-481	22-072	21-660	20-835	20-418	20-006	19-593	19-179	18-767	17-633	17-533	17-123	16-713	16-305
$\beta_1$	23-547	23-107	22-673	22-238	21-806	21-380	20-529	20-108	19-688	19-273	18-859	18-447		17-229	16-827	16-425	16-026
$\beta_{13}$	23-605	23-158	22-719	22-281	21-847	21-415											
$\beta_3$	23-747	23-306	22-868	22-433	22-001	21-573	20-698	20-295	19-880	19-464	19-051	18-639	17-82	17-425	17-021	16-620	16-224
$\beta_{14}$	24-11	23-680	23-254	22-831	22-617	21-986	21-141	20-723	20-297								
$\beta_2$	24-140	23-719	23-297	22-872	22-449	22-028	21-180	20-759	20-333	19-914	19-480	19-068	18-217	17-800	17-381	16-961	16-540
$\beta_{11}$																	
$\beta_{12}$																	
$\beta_{10}$			23-40	22-963	22-52	22-101	21-243	20-819	20-391	19-97							
$\beta_9$					22-57	22-146	21-284	20-852	20-427	20-02	19-560	19-15			17-470	17-050	16-628
$\beta_8$															17-509	17-105	16-704
$\beta_7$															17-529	17-123	16-719
$\beta_5$		23-808	23-459	23-021	22-60	22-180	21-323	20-894	20-462	20-03	19-586	19-16				17-01	16-57
$\gamma_5$	24-99	24-524	24-060	23-590	23-11	22-658	21-722	21-260	20-804	20-349	19-895	19-441		18-995	17-649	17-209	16-766
$\gamma_9$	25-36		24-394	23-913	23-435	22-960	22-014	21-527	21-07								
$\gamma_1$	25-384	24-901	24-433	23-950	23-470	22-997	22-052	21-580	21-113	20-649	20-185	19-723	18-803	18-350	17-897	17-444	16-995
$\gamma_6$					23-54		22-14	22-660	21-19		20-26					17-520	17-077
$\gamma_7$					23-65			21-717	21-24		20-26						
$\gamma_8$								22-010	21-550	21-093	20-635	20-181					
$\gamma_{10}$								22-045	21-585	21-127	20-665	20-211		18-848	18-409	17-953	17-506
$\gamma_2$	25-812	25-330	24-866	24-397	23-911	23-459	22-516	22-076	21-612	21-152	20-686	20-229					
$\gamma_3$	25-873	25-387	24-913	24-438	23-957	23-419	22-547	22-076	21-612	21-152	20-686	20-229					
$\gamma_4$	26-278	25-778	25-298	24-799			22-880	22-405	21-928	21-460	20-974	20-496		19-071	18-602	18-133	17-669



24. The *M* and the *N* Series.

Besides the two series which have been known since Barkla's experiments two softer characteristic radiations have been discovered by the aid of vacuum spectroscopy, and have been named the *M* and the *N* series. The *M* series was discovered by the author in 1916 for uranium and gold, and later measured more accurately by Stenström as far as dysprosium. The principal lines are not sharp even with the heaviest elements, and they become very broad with decreasing atomic number. In the dissertation of Stenström there are a number of photometric records of the lines which reveal their structure. The crystals used by him were calcite, gypsum and sugar. He was thus able to find and measure three lines  $\alpha$ ,  $\beta$  and  $\gamma$  for a number of elements, and also for U and Th two fainter additional lines  $\delta$  and  $\epsilon$ . The results of Stenström's measurements are collected in Table 14.

TABLE 14.

Measurements of the *M* series by W. Stenström, using different crystals.  $\lambda$  in X.U.

Element.	$\alpha$			$\beta$			$\gamma$		
	Gyps.	Calcite.	Sugar.	Gyps.	Calcite.	Sugar.	Gyps.	Calcite.	Sugar.
92 U	3901	3901.4	3906.6	3703	3708.3	3712.8	3470	3471.4	
90 Th	4119	4129.15		3920	3933.3		3654	3656.5	
83 Bi	5100	5107.2		4893	4899.3		4515	4523.8	
82 Pb	5276	5275.1		5063.5	5064.8		4653	4663.7	
81 Tl	5445	5449.9		5223	5238.4		4802		
79 Au	5819			5601			5115		
78 Pt	6028		6043.0	1812		5824.5	5311		5279.9
77 Ir	6245	Sugar 2nd Order.		6029	Sugar $\alpha_1$ Ref.				
76 Os	6477			6250					
74 W	6973	6974.6	6979.5	6745	6752.7	6750.6			60.905
73 Ta	7237			7011.5					
71 Lu	7818		7835.5	7587	7598.2				
70 Yb	8123		8136	7895	7902				
68 Er	8770			8561					
67 Ho	9123			8930					
66 Dy	9509			9313					

Later, Karcher investigated the *M* series for the elements Pt to Bi (Table 15), and reported three other lines which he designated as  $\beta_n$ ,

TABLE 15.

Karcher's Measurements in the *M* series.  $\lambda$  in X.U.

Element.	$\alpha_1$	$\beta_1$	$\beta_2$	$\gamma_1$	$\gamma_2$	$\gamma_3$
78 Pt	6049	5831	5649	5329	4733	4623
79 Au	5848	5632	5446	5154	4530	4439
80 Hg	5649	5439	—	—	—	—
81 Tl	5468	5254	—	—	—	—
82 Pb	5290	5078	—	4675	4073	—
83 Bi	5124	4915	4604	4534	3932	3840

$\gamma_2$  and  $\gamma_3$ . His measurements are not in good agreement with Stenström's nor with the subsequent ones of Hjalmar.

After the technique of vacuum spectroscopy had been improved to a considerable degree by the construction of more powerful X-ray tubes and by more efficient vacuum spectrographs, the study of the  $M$  series was taken up again. This work was carried out by Hjalmar, and extended our knowledge of this series more than had been anticipated. (See the tables on pp. 127-129). For example, in the case of uranium, no fewer than 23 lines were shown to exist. We shall return below to the notation adopted by Hjalmar. He observed that the maxima of blackening in bands of emission (corresponding to the broadening of lines observed by Stenström) occurred only on the short wave-length side of the strong lines. These maxima were denoted by  $\alpha$ ,  $\beta$ ,  $\gamma$  and with dashes.

Using the methods developed for the longer waves already described, Thoraues has been able to photograph a much more complete  $M$ -spectrum for the lower elements than was formerly possible. The following Table, 15B, gives the results so far obtained for tungsten, using a mica crystal as grating. With this crystal the lines are very sharp, and permit a rather exact measurement. Unfortunately, the deviation from the Bragg law is large. All wave-lengths are calculated provisionally from the Bragg law and assuming  $\log 2d = 1.29823$ .

TABLE 15B.

Transition.	Calculated.		Found.		Intensity.
	$\frac{\nu}{R}$	$\lambda$ in Å.	Hjalmar.	Thoraues.	
$M_5O_{3,4}$	204.7	4.452	—	4.433	1
$M_4O_5$	183.7	4.961	—	—	—
$M_5N_5$	177.0	5.149	—	5.157	1
$M_5N_6$	172.0	5.298	—	—	—
$M_4N_4$	170.2	5.354	—	5.365	2
$M_3O_5$	162.2	5.618	—	5.607	1
$M_3N_3(\gamma)$	149.6	6.091	6.085	6.083	3
$M_3N_4$	148.7	6.128	—	6.123	1
$M_4N_7$	145.3	6.272	—	6.271	1
$M_2N_{1,2}(\beta)$	135.3	6.735	6.745	6.733	5
$M_1O_{3,4}$	134.9	6.755	—	6.750	1
$M_1N_{1,2}(\alpha)$	130.7	6.972	6.973	6.963	5
$M_1O_3$	130.3	6.994	—	—	—
$M_3N_7$	123.8	7.361	—	7.349	2
$M_2N_5$	107.2	8.501	—	8.549	1
$M_1N_5$	102.6	8.882	—	—	—
$M_2N_6$	102.2	8.917	—	8.948	2

For the new element 72, Hafnium, two  $M$  lines,  $\alpha$  and  $\beta$ , have been measured by Coster, who gives the values  $\alpha = 7521$  and  $\beta = 7286$  X.U.

Wave-lengths of the M series.

	U 92.	Th 90.	Bi 83.	Pb 82.	Tl 81.	Au 79.	Pt 78.	Ir 77.	Os 76.	W 74.	Ta 73.	Lu 71.	Yb 70.	Pr 68.	Ho 67.	Dy 66.
$M_5P_1$	2248															
$M_5O_3$	2299	2437														
$M_4O_2$	2439	2612														
$M_2N_5$	2750	2917	3672	3789	3932	4230	4407	4548	4779							
$M_4N_4$	2815	2999	3816	3945	4095	×	×	4768	4949							
$M_5N_6$	2909	3127	3884													
$M_3O_1$	2927	3109														
$M_3O_5$	3107	3276														
$M_4N_7$	3321	3530	×	4646					5802?							
$\gamma'$	3459	3645	4497	—	4798				5652	6066						
$M_2N_3(\gamma)$	3466								5672	6085	6301	6780				
$M_1P_1$	3472	3657	4513	4666	4806	5131	5303	5484								
$M_2O_4$	3514	3753		4994	5185											
$\beta'$	3570	3792	4815													
$\beta''$	3684	3921		5042	5210	—	5797	6011	6233	6726	—	7560	7852?	—	8919	—
$\beta'''$	3696	3925	4875										7870	—		
$M_2N_3(\beta)$	3700															
$\alpha'$	3709	3931	4894	5065	5233	5619	5820	6030	6256	6745	7001	7582	7891	8573	8943	9323
$\alpha''$	—	4097	5078	5242												
$M_1N_1(\alpha_1)$	3885			5250	5427	5812	6026	6223	6459	6952	—	7787	8090			
$M_1N_2(\alpha_2)$	3901	4129	5107	5273	5443	5831	6041	6250	6481	6973	7238	7803	8011			
$M_2N_7$	3913	4138	5117										8125	8783	9150	—
$M_2N_7$	4326	4569	5525	5687	5879	6264	—	6663	6882	×						
$N_1M_5$	4929	5245	6498	6727	—	×	—	8012								

$\nu$   
 $\frac{\nu}{R}$  for the  $M$  series. Emission.

	U 92.	Th 90.	Ei 83.	Pb 82.	Ti 81.	Au 70.	Pt 78.	Ir 77.	Os 76.	W 74.	Ta 73.	La 71.	Yb 70.	Er 68.	Ho 67.	Dy 66.
$M_5P_1$	406.5															
$M_5O_3$	396.5	374.0														
$M_4O_2$	373.5	348.9														
$M_3N_6$	331.4	312.4	248.2	240.5	231.8	215.4	206.8	200.4	190.7							
$M_4N_4$	324.1	303.8	238.8	231.0	222.5			191.1	184.1							
$M_2N_6$	313.3	291.4	234.6													
$M_3O_1$	311.2	293.1														
$M_3O_5$	293.3	278.2														
$M_4N_7$	274.3	258.1		196.1					157.1							
$\gamma'$	263.4	250.0	202.7		190.8				161.2	150.2						
$M_3N_3(\gamma)$	262.5	249.2	201.9	195.3	189.6	177.6	171.8	166.2	160.7	149.8	144.6	134.4				
$M_4P_1$	259.3	242.8														
$M_3O_4$	255.8	240.4	189.2	182.5	175.7											
$\beta'$	247.3	232.4														
$\beta''$	246.5	232.1	186.9	180.7	174.9			151.6	146.2	135.5			116.1			
$\beta'''$	246.3												115.8			
$M_2N_2(\beta)$	245.7	231.8	186.1	179.9	174.1	162.2	156.6	151.2	145.7	135.1	130.2	120.5			102.2	
$\alpha'$		222.3	179.5	173.8												
$\alpha''$	234.6															
$M_1N_1(a_1)$	233.6	220.9	178.4	172.8	167.9	156.8	151.2	146.4	141.1	131.1	117.0	115.5	115.5	106.3	101.9	97.74
$M_1N_2(a_2)$	232.9	220.4	176.1	172.8	167.4	156.3	150.8	145.8	140.6	130.7	125.9	116.8	112.3	103.7	99.58	
$M_3N_7$	210.6	199.4	164.9	160.2	155.0	145.5		136.8	132.4			116.5	112.2			
$M_1N_5$	184.9	173.7	140.2	135.6				113.7								



$$\sqrt{\frac{\nu}{R}}$$
 for the M series. Emission.

	U 92.	Th 90.	Bi 83.	Pb 82.	Tl 81.	Au 79.	Pt 78.	Ir 77.	Os 76.	W 74.	Ta 73.	La 71.	Yb 70.	Er 68.	Ho 67.	Dy 66.
$M_5P_1$	20.16															
$M_5O_3$	19.91	19.36														
$M_4O_2$	19.33	18.68														
$M_5N_5$	18.20	17.67	15.75	15.51	15.22	14.68	14.38	14.15	13.81							
$M_4N_4$	18.00	17.43	15.45	15.20	14.92			13.82	13.57							
$M_5N_6$	17.70	17.07	15.32													
$M_3O_1$	17.64	17.12														
$M_3O_5$	17.11	16.68														
$M_4N_7$	16.56	16.07		14.00					12.53							
$\gamma'$	16.23	15.81	14.24		13.81				12.70	12.26						
$M_3N_3(\gamma)$	16.21															
$M_1P_1$	16.20	15.79	14.21	13.97	13.77	13.33	13.11	12.89	12.68	12.24	12.03	11.59				
$M_2O_4$	16.10	15.58														
$\beta'$	15.98	15.50	13.75	13.51	13.26								10.77			
$\beta''$	15.73	15.24											10.76		10.11	
$\beta'''$	15.70	15.24	13.66	13.44	13.22		12.54	12.32	12.09	11.64		10.98				
$M_5N_2(\beta)$	15.69															
$\alpha'$	15.68	15.22	13.65	13.41	13.20	12.73	12.51	12.30	12.07	11.62	11.41	10.96	10.75	10.31	10.09	9.89
$\alpha''$				13.18												
$M_1N_1(\alpha_1)$	15.31	14.92	13.40	13.17	12.96	12.52	12.30	12.10	11.88	11.45		10.82	10.61			
$M_1N_2(\alpha_2)$	15.28	14.86	13.36	13.15	12.94	12.50	12.28	12.07	11.86	11.43	11.29	10.80	10.60	10.19	9.98	
$M_3N_7$	15.26	14.84	13.34													
$M_1N_5$	14.50	14.12	12.84	12.66	12.45	12.06		11.69	11.51							
	13.60	13.18	11.84	11.64				10.66								

With the same spectrographic apparatus that he used in measurements of the *M* series Hjalmar also succeeded in finding and measuring several lines which without doubt belong to the *N* series. (On the significance of lines which had been assigned by Dolejšek to this series see the dissertation of Hjalmar.) All the lines are very indistinct, so that it seems quite possible that one line or another was wrongly interpreted. So far it has been possible to detect the *N* series only for the three elements U, Th, and Bi. The following table contains the measurements of Hjalmar. The line of thorium at 13,805 X.U. represents the longest wave-length yet measured in Röntgen spectroscopy.

TABLE 16.  
*N* series. From Hjalmar's measurements.

Element.	Line.	$\lambda$	$\frac{\nu}{R}$	$\sqrt{\frac{\nu}{R}}$
Uranium	$N_7P_1$	8,691	104.8	10.24
"	$N_7O_3$	9,619	94.75	9.72
"	$N_6O_2$	10,385	87.72	9.36
"	$N_5P_3$	12,250	74.43	8.63
"	$N_5O_1$	12,874	70.78	8.41
Thorium	$N_7P_1$	9,397	96.97	9.82
"	$N_7O_3$	10,030	90.86	9.53
"	$N_6O_2$	11,046	82.49	9.08
"	$N_5P_3$	13,149	69.3	8.32
"	$N_5O_1$	13,805	66.01	
Bismuth	$N_7P_1$	13,208	68.99	8.31

# V

## ABSORPTION SPECTRA

### 25. General Survey of Absorption Spectra

In his first photographs of X-ray spectra by the rotating crystal method de Broglie noticed a sudden and surprising change in the blackening of the plate in two places. Fig. 76A is a reproduction of one of de Broglie's

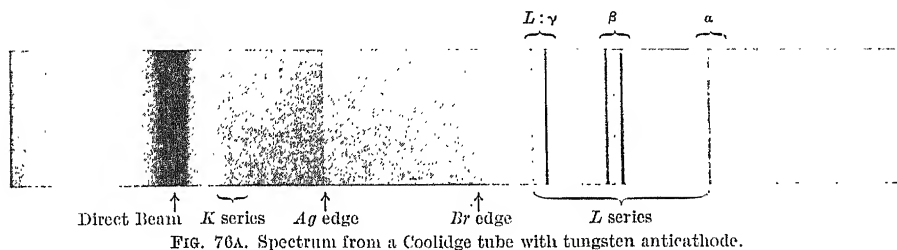


FIG. 76A. Spectrum from a Coolidge tube with tungsten anticathode.

photographs, in which this change in the blackening at the points *Ag* and *Br* shows very plainly. De Broglie at first interpreted this as a band spectrum within the region of the Röntgen spectrum. But a further study of the phenomenon proved the explanation proposed by Bragg and the author to be the right one; namely, that the sudden change of blackening is due to the sudden and large increase in the absorptive power of the *Ag* and *Br* in the emulsion of the plate, when the incident wave-length becomes small enough to excite the characteristic radiation of those two elements. This interpretation was nothing more than a simple application of the explanation of the facts discovered by Barkla in his investigations of the general absorption in a given element of X-rays of varying degrees of hardness.

The striking feature on these plates was the extraordinary sharpness of the absorption edges.

The proof that this explanation of the phenomenon is the true one lies in the fact that these discontinuities in the blackening of the plate always appear regardless of the material of the anticathode, and in the further fact that the wave-lengths of these two limits coincide with those of the lines of highest frequency in the *K* series of *Ag* and *Br* respectively. It is often possible to detect the edges in the second order also. The

extraordinary sharpness of the edges permits an accurate determination of the wave-length. Thus de Broglie found 0.482 and 0.916 Å for the

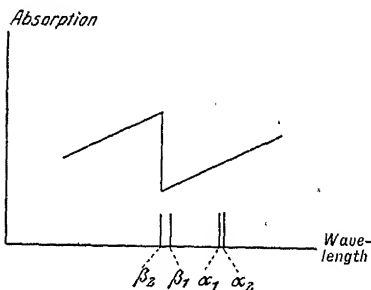


FIG. 76B. Diagram of the variation of absorption and the relative position of the *K* lines.

wave-lengths of the limits for Ag and Br. In comparison with these, the wave-lengths of  $\beta_2$ , the shortest *K* line of the same two elements, are 0.485 and 0.918 Å. The relation between the absorption curve and the line spectrum is shown in Fig. 76B. When we approach the absorption limit from the long wave-length side the absorption in the silver bromide film becomes steadily less with decreasing wave-length until the line of shortest wave-length is reached. Then the absorption suddenly increases, at the same time the *K* series radiation is excited, and an increased blackening of the plate accompanies this excitation. In the continuation of these investigations, which were simultaneously undertaken by E. Wagner, de Broglie showed that it is not at all necessary, in producing these discontinuities on the plate, that the absorbing substance should be in the photographic film. If an absorbing screen is placed anywhere in the path of the beam between anticathode and photographic plate (except that it must not be placed so near the plate that the latter is blackened by the characteristic radiation excited in the screen) a discontinuity in the blackening is produced at a wave-length practically the same as that of the highest frequency line in the spectrum of the absorbing substance. The heavier blackening of the plate in this case, however, lies on the *long wave-length* side of the discontinuity, since the shorter wave-lengths are arrested in the screen more than the longer wave-lengths.

The very interesting photograph taken by Wagner, and shown in Fig. 77, illustrates this phenomenon very nicely. In this experiment three absorbing screens were simultaneously placed in the path of the beam. Between these screens bands of direct radiation were allowed to pass unabsorbed. In the lowest of these bands is the silver edge caused

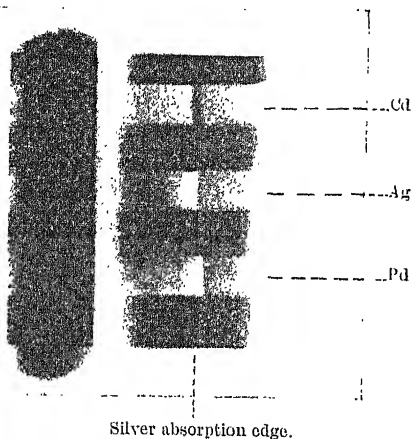


FIG. 77. Comparative limits of Cd, Ag and Pd absorption edges.

by the intensified absorption in the film of the photographic plate. If the radiation passing through the screens is of sufficient intensity to show well upon the plate, then the unabsorbed strips are necessarily overexposed. For this reason, the contrast between the blackening produced by the direct and by the absorbed beams is naturally rendered less distinct. In the middle strip, behind the silver screen, the blackening is on the whole much less, yet we can see that the discontinuity is in the same place as in the lowest spectrum, but that the regions of greater and lesser blackening have changed places. The characteristic absorption in the photographic emulsion is more than compensated for by the greater absorption of the shorter wave-length radiation in the interposed screen. The light upper strip is due to absorption in Cd.

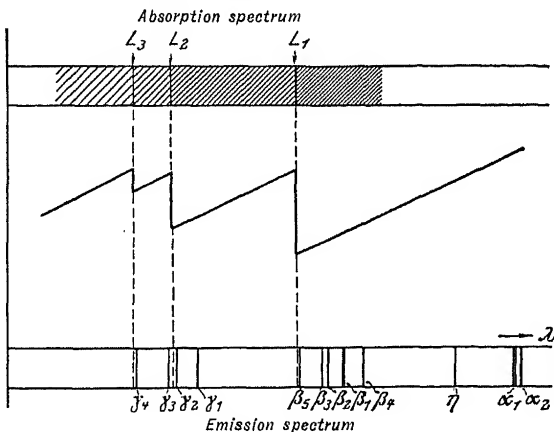


FIG. 78. Diagram of the absorption and the emission spectrum, showing the relative positions of discontinuities and lines.

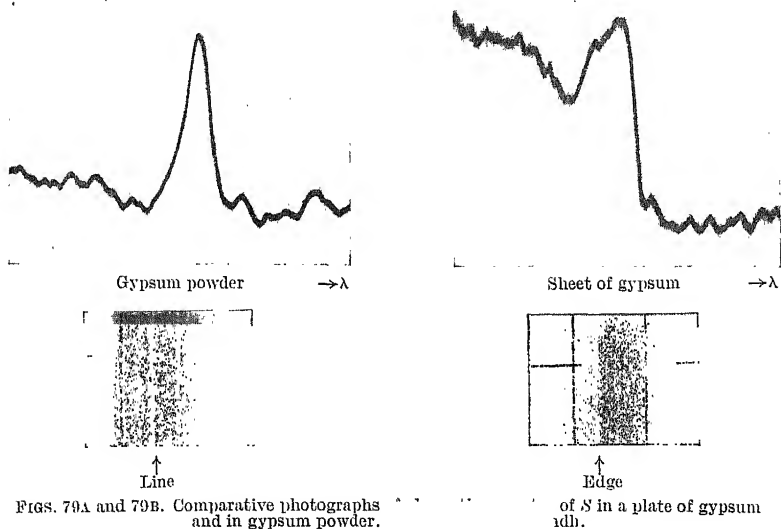
In addition to the general diminution of blackening, we observe here also a sudden marked change in intensity about 1 mm. to the left of the silver limit, which is due to stronger absorption of the radiation of shorter wave-length than that of the characteristic radiation of Cd. The same is true for the Pd screen, except that here the absorption limit is displaced to the other side of the silver edge.

Up to this point we have discussed only those absorption discontinuities associated with the  $K$  characteristic radiation of the absorbing substance.

If we examine in the same way the region of the  $L$  radiation, as was done first by de Broglie and Wagner, we find three stages in the blackening. These are due to the fact that the lines of the  $L$  series, as we have already stated, are divided into three groups requiring different voltages for their excitation. A diagram showing the connection between the emission spectrum and the absorption spectrum of the  $L$  series is presented in Fig. 78. The three  $L$  limits, which are generally as sharp as lines, are here denoted by  $L_1$ ,  $L_2$  and  $L_3$ .

In the  $M$  spectral region Stenström and Coster have also located absorption limits, which are denoted in the order of decreasing wave-lengths by  $M_1$ ,  $M_2$ ,  $M_3$ ,  $M_4$  and  $M_5$ . The first three were detected by Stenström for U, Th and Bi, the last two by Coster for U and Th.

The typical appearance of an absorption spectrum as pictured in Figs. 76B and 78, with a sharp limit separating two regions of more or less homogeneous blackening, is generally observed in the *K* series, and for the heavier elements also in the *L* series. But complicated conditions make their appearance in the absorption edges of many elements in the *L* and *M* series, as well as for the very lightest elements in the *K* series. A pure *line absorption* is also often observed. A very beautiful example of this is shown in Fig. 79A, for which I am indebted to Mr. Lindh. This



plate, representing the *K* absorption of sulphur, shows, instead of an absorption edge, a white line on a dark background. The course of the blackening may be judged better from the photometric record. Very little difference is to be observed in the blackening on the two sides of the limit. This means that precisely those wave-lengths which are just sufficient to excite the characteristic radiation of sulphur are absorbed to an extraordinary degree. We have here to do with a distinctly selective absorption, such as we are familiar with in ordinary optics. For comparison we have in Fig. 79B a photograph showing the normal appearance of the edge, obtained with the same absorbing substance, except that in the latter case a much thicker and more homogeneous screen was used. Very typical lines of this sort were first noticed by Stenström in the *M* series, several of them being shown in his dissertation. The  $M_3$  edge especially appears as a rather sharp line, while the  $M_1$  and the  $M_2$  edges are broader. The sharpness of the absorption lines seems, moreover, to be closely connected with the sharpness of the emission lines of the same

element in the same series. Hence it may be understood why this phenomenon has not been observed in the short wave-length regions of the *K* and the *L* series, where the emission lines are much narrower than the slit width, but only in regions of greater wave-length, where the lines are broader.

In his investigation of the lightest elements of the *K* series, Fricke found not only fine absorption lines of this kind, but also a complicated structure in the neighbourhood of the absorption limit. Hertz found similar appearance in the long wave-length absorption edges of the *L* series. This phenomenon must be surveyed in the light of the interesting discovery of Lindh that the form of chemical combination has a marked influence on the position and on the appearance of the absorption edge. Somewhat earlier, Bergengren, in an investigation of the *K* ab-

sorption spectrum of various modifications of phosphorus, had for the first time found an exception to the rule in Röntgen spectroscopy, according to which X-ray spectra are purely an atomic property. Bergengren supposed that the differences which he found in the position of the absorption limits were directly dependent on the modification of phosphorus present, an inference which may easily be understood from the limited scope of his data. Further investigation has shown, however, that the principal factor is the chemical valency. This was demonstrated for chlorine and sulphur by Lindh, to whose very important research on this point we shall return later.

## 26. The *K* Absorption

For the first investigations in the *K* series we are indebted to de Broglie and E. Wagner, who both worked by photography and by the rotating crystal method.

The results of their work are given in Table 17 below, along with the later measurements of other authors. Fig. 80 is a reproduction of a

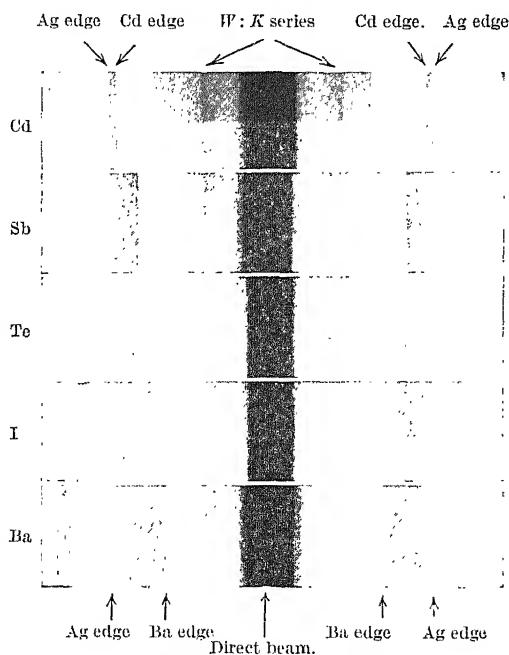


FIG. 80. Absorption spectra of the *K* series of several elements, by de Broglie.

TABLE 17.

Wave-lengths of the *K* absorption limits.  $\lambda$  in X.U.

Element.	de Broglie.	Wagner.	Fricke.	Duane, Blake, Hu, Stenström, Fricke and Shimizu.	Lindh
12 Mg	—	—	9511.2	—	—
13 Al	—	—	7947.0	—	—
15 P	—	—	5758.0	—	5767.4
16 S	—	—	5012.3	—	5008.8
17 Cl	—	—	4384.4	—	—
18 A	—	—	3865.7	—	—
19 K	—	—	3434.5	—	3431.0
20 Ca	—	—	3063.3	—	3064.3
21 Sc	—	—	2751.7	—	—
22 Ti	—	—	2493.7	—	—
23 Va	—	—	2265.3	—	—
24 Cr	—	—	2067.5	2062.3	—
25 Mn	—	—	—	1889.3	—
26 Fe	—	1740	—	1737.7	Walter.
27 Co	—	—	—	1601.8	—
28 Ni	—	1485	—	1489.0	1484.5
29 Cu	1388	1375	—	1378.5	—
30 Zn	—	—	—	1296.3	1280
31 Ga	—	—	—	1190.2	—
32 Ge	—	—	—	1114.6	—
33 As	—	—	—	1043.5	—
34 Se	1003	—	—	979.0	—
35 Br	916	917	—	917.9	—
37 Rb	812	—	—	814.3	—
38 Sr	767	—	—	769.6	—
39 Y	—	—	—	725.5	—
40 Zr	684	—	—	687.2	—
41 Nb	648	—	—	650.3	—
42 Mo	614	—	—	618.42	—
44 Ru	—	—	—	558.4	—
45 Rh	—	—	—	533.0	—
46 Pd	505	513	Siegbahn and Jönsson.	507.5	—
47 Ag	482	484	—	485.0	—
48 Cd	460	462	462.9	463.2	—
49 In	—	—	—	443.4	—
50 Sn	421	422	423.1	424.2	—
51 Sb	401	405	—	406.5	—
52 Te	385	383	387.7	389.6	Cabrera.
53 I	369	369	371.5	373.7	—
55 Cs	340	—	343.6	344.4	—
56 Ba	327	331	330.6	330.7	—
57 La	313	—	318.6	318.8	318.6
58 Ce	300	298	306.4	306.8	306.5
59 Pr	—	—	294.6	—	295.1
60 Nd	—	282	283.5	286.1	284.6
62 Sa	—	—	263.6	—	264.4



Element.	de Broglie.	Wagner.	Seigbahn and Jönsson.	Duane, Blake, Hu, Stenström, Fricke and Shimizu.	Cabrera.
63 Eu	—	—	254·3	—	254·8
64 Gd	—	—	245·6	—	246·2
65 Tb	—	—	—	239·8	237·6
66 Dy	—	—	229·4	230·8	230·1
67 Ho	—	—	221·4	—	221·8
69 Tu	208	—	—	—	208·5
70 Yb	201·5	—	—	—	201·6
71 Lu	195	—	—	—	195·1
72 Hf	—	Crofttt.	—	—	190·1
73 Ta	—	—	—	—	183·6
74 W	—	178·02	—	178·06	—
76 Os	—	—	—	168·3	—
78 Pt	152	—	157·8	158·1	—
79 Au	149	—	152·4	153·4	—
80 Hg	146	—	147·9	149·0	—
81 Tl	142	—	142·7	144·9	—
82 Pb	138	—	138·5	141·0	—
83 Bi	133	—	134·6	137·1	—
90 Th	—	—	112·7	112·9	—
92 U	—	—	—	107·5	—

TABLE 18.

 $\frac{\nu}{R}$  and  $\sqrt{\frac{\nu}{R}}$  for the K absorption limits

Element.	$\frac{\nu}{R}$	$\sqrt{\frac{\nu}{R}}$	Element.	$\frac{\nu}{R}$	$\sqrt{\frac{\nu}{R}}$	Element.	$\frac{\nu}{R}$	$\sqrt{\frac{\nu}{R}}$
12 Mg	95·81	9·79	35 Br	992·78	31·51	60 Nd	3213	56·68
13 Al	114·67	10·70	37 Rb	1119·1	33·45	62 Sa	3448	58·72
15 P	158·26	12·58	38 Sr	1184·1	34·41	63 Eu	3578	59·82
16 S	181·81	13·48	39 Y	1256·1	35·44	64 Gd	3700	60·83
17 Cl	207·84	14·42	40 Zr	1326·1	36·41	65 Tb	3834	61·92
18 A	235·73	15·35	41 Nb	1401·3	37·43	66 Dy	3960	62·93
19 K	265·33	16·29	42 Mo	1474·5	38·40	67 Ho	4108	64·09
20 Ca	297·48	17·25	44 Ru	1631·9	40·40	69 Tu	4370	66·11
21 Sc	331·17	18·20	45 Rh	1709·7	41·35	70 Yb	4520	67·23
22 Ti	365·43	19·11	46 Pd	1795·6	42·37	71 Lu	4670	68·34
23 Va	402·27	20·06	47 Ag	1878·9	43·35	72 Hf	4793	69·23
24 Cr	441·14	21·00	48 Cd	1967·3	44·35	73 Ta	4963	70·45
25 Mn	482·36	21·96	49 In	2055·2	45·33	74 W	5117	71·54
26 Fe	524·34	22·91	50 Sn	2148·2	46·35	76 Os	5414	73·58
27 Co	568·90	23·85	51 Sb	2241·7	47·35	78 Pt	5764	75·92
28 Ni	612·00	24·74	52 Te	2339·0	48·36	79 Au	5941	77·08
29 Cu	661·06	25·71	53 I	2438·5	49·38	80 Hg	6112	78·18
30 Zn	702·98	26·51	55 Cs	2646·0	51·44	81 Tl	6293	79·33
31 Ga	765·64	27·67	56 Ba	2755·6	52·49	82 Pb	6463	80·39
32 Ge	817·57	28·59	57 La	2860	53·48	83 Bi	6642	81·50
33 As	873·28	29·55	58 Ce	2973	54·53	90 Th	8057	89·76
34 Se	930·82	30·51	59 Pr	3093	55·61	92 U	8477	92·07

series of absorption edges kindly furnished me by M. de Broglie, and it shows how well defined the absorption limits are. All of these photographs show a heavy blackening in the middle due to the direct beam. Next to this on both sides may be seen the *K* series of tungsten, which comes from the anticathode of the Coolidge tube. The short wave-length boundary of the dark band lying further out is the absorption edge of the substance under investigation, while the long wave-length edge is again the absorption limit of the silver in the photographic film.

Using another photographic method already described on p. 56 ff. the author in conjunction with Jönsson investigated the short wave-length absorption spectra up to uranium, inclusive. Duane and his associates worked through the whole region from chromium upwards by the ionization method. Very recently Cabrera has added some measurements carried out in the laboratory of de Broglie. In the table measurements are also included in the long wave-length region from Mg to Cr, as obtained by Fricke in the author's laboratory with the spectrograph on p. 64 ff. As already stated, the absorption limits in this region are not so simple as those of short wave-length. The values in the table are those of the principal edge. Details are given in the article by Fricke. In the case of three of these elements, Cl, S, and P, of course, the new experiments of Lindh present a new point of view.

We may make a remark here on the significance of the material of the anticathode itself in connection with the *K* absorption. The spectrometer is often placed so that the beam entering it leaves the surface of the anticathode in a direction almost grazing the surface, so that we should expect an absorption discontinuity in the ionization curve, due to absorption in the anticathode itself. Of course, it makes no difference whether the absorbing layer is in the anticathode itself or external to it. If Rh, Pd, Mo or Ag be used as anticathode, this absorption discontinuity lies right in the middle of the main spectral region, 618 to 485 X.U., and appears just on the short wave-length side of the characteristic radiation. In the intensity curve of Rh shown on p. 94 this depression due to the absorption in the rhodium is plainly visible. Owen noticed the same thing when using a Pd anticathode (*Proc. Roy. Soc., A*, 94, 341, 1918), but in the author's opinion he interpreted it erroneously as the *J* series of silicon, produced by the carborundum crystal used as grating.

## 27. The *L* and the *M* Absorption

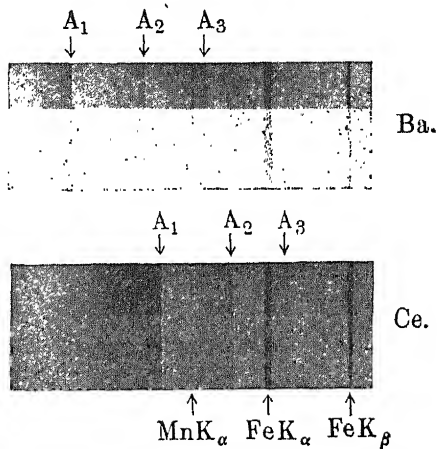
Absorption in the *L* series of the heaviest elements has been studied by de Broglie and by Wagner, using the rotating crystal method. While Wagner was not able to demonstrate the third very weak absorption edge with certainty, de Broglie succeeded in measuring all three limits for U, Th, Au and Bi. We are indebted to Duane and Patterson for a series of

very excellent measurements of the absorption limits of the elements from tungsten upwards. They used the ionization method, and Coster has pointed out that in order to obtain agreement with the values determined by photographic measurements made at the Institute at Lund on the emission spectra, as demanded by the energy level classification, it is necessary to diminish the values of the wave-lengths given by the absorption measurements of Duane and Patterson by about 1 per cent. One-third of this discrepancy is explained by the difference in the value used for the grating constant.

A very important and fundamental investigation in the *L* series of absorption spectra is that of G. Hertz, involving the elements from Cs to Nd inclusive. Here we find ourselves in a wave-length region where the absorption edges begin to show a structure. The pure line absorption also, which we have mentioned in connection with the *K* series of the lightest elements, was observed by Hertz for these elements. We shall consider later the double nature of the *L* absorption edges which Hertz discovered in his work. Two of the Hertz spectrograms are shown in Figs. 81A and 81B.

A step farther in the direction of longer wave-lengths was taken by Lindsay, who measured all three edges for the elements Ba to Sb inclusive.

The *M* absorption spectra have as yet been little investigated. Only for U and Th have 5 limits been measured and for Bi 3. At least the two faintest edges are very difficult to obtain, and demand especially favourable conditions. Stenström was obliged to make exposures of twelve hours' duration with currents of 40 to 80 milliamps. through the tube. (The voltage must, of course, always be kept so low in these photographs that the second order does not become strong enough to obscure the detail in the first.) With the newer tubes and spectrographs these spectra were obtained with the same dispersion in one or two hours. Besides the principal edge, Stenström also measured a second fainter one near by. Several of these photograms are given in his doctorate thesis, and they throw additional light on the structure of the absorption limits. Fig. 81C is a reproduction of a very beautiful photograph by Coster of the two strongest absorption edges  $M_1$  and  $M_2$  for uranium.



FIGS. 81A, B. Absorption spectra of the *L* series by Hertz.

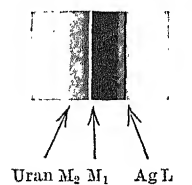


FIG. 81C. Absorption limits of the *M* series of uranium. From a photograph by Coster.

TABLE 19.

Wave-lengths of the *L* absorption limits.

Designations: C.=Coster; L.=Lindsay; H.=Hertz; D. and P.=Duane and Patterson; Br.=de Broglie; W.=Wagner; C.N.W.=Coster, Nishina, and Werner; Ck.=Cork; Cr.=Croft; L.D.=Lepape and Dauvillier.

	<i>L</i> <sub>1</sub>	<i>L</i> <sub>2</sub>	<i>L</i> <sub>3</sub>	Author.
47 Ag	3684.4	3504.7	3260.5	C.
51 Sb	2994.5	2831.0	2632.7	L.
52 Te	2847.0	2683.7	2502.6	L.
53 I	2712.4	2548.3	2381.9	L.
54 Xe	2587.5	2425.3	2272.4	L.D.
55 Cs	2467.8	2307.3	2160.5	L.
55 Cs	2459	2299	2157	H.
55 Cs	2466	—	—	C.
56 Ba	2357.7	2199.5	2060.2	L.
56 Ba	2348	2194	2063	H.
56 Ba	2356.7	2198	—	C.
57 La	2253.7	2098.9	1968.9	C.N.W.
57 La	2250	2098	1971	H.
58 Ce	2159.7	2006.7	1885.6	C.N.W.
58 Ce	2158	2007	1887	H.
59 Pr	2072.7	1919.7	—	C.
59 Pr	2071	1922	1808	H.
60 Nd	1990.3	1837.6	—	C.
60 Nd	1992	1842	1736	H.
62 Sm	1840.9	—	—	C.
62 Sm	—	1701	1608	Ck.
63 Eu	1773	—	—	C.
64 Gd	1706.2	1558.7	—	C.N.W.
64 Gd	1699	1550	1470	Ck.
66 Dy	1587.0	1441.4	1364.8	C.N.W.
66 Dy	1576	1435	1362	Ck.
68 Er	1479.6	1334.9	1266.0	C.N.W.
68 Er	1478	1336	1265	Ck.
69 Tm	1429.9	1284.9	1219.6	C.N.W.
70 Yb	1382.4	—	1176.5	C.N.W.
70 Yb	1386	1242	1171	Ck.
71 Lu	1337.7	1194.5	1136.2	C.N.W.
72 Hf	1293.0	1151.5	1097	C.N.W.
73 Ta	1253	1111.8	1058	Ck.
74 W	1213.6	1072.6	1024	D. and P.
74 W	1211.2	1071.8	1023	Ck.
74 W	1212.2	1071.6	1021.7	Cr.
47 W	1215	1083	—	Br.
76 Os	1138	998.5	951.5	Ck.
77 Ir	1103.6	965	919.5	Ck.
78 Pt	1070.4	932.1	892.1	D. and P.
78 Pt	1069	930	—	Br.
78 Pt	1072	934	—	W.
79 Au	1038.3	901.1	861.3	D. and P.
79 Au	1038	898	858	Br.
79 Au	1036	914	—	W.

	$L_1$	$L_2$	$L_3$	Author.
80 Hg	1006.7	870.0	833.5	D. and P.
80 Hg	1006	—	—	Br.
81 Tl	977.6	841.5	805.5	D. and P.
81 Tl	974	840	—	Br.
82 Pb	949.7	813.3	780.3	D. and P.
82 Pb	945	811	—	Br.
83 Bi	921.6	787.4	756.5	D. and P.
83 Bi	921	786	—	Br.
88 Ra	802	668	—	Br.
90 Th	759.6	628.6	604.4	D. and P.
90 Th	757	624	604	Br.
92 U	721.4	591.8	568.5	D. and P.
92 U	718	588	564	Br.

TABLE 20.

	$\nu$ for the <i>L</i> absorption limits.			$\sqrt{\frac{\nu}{R}}$ for the <i>L</i> absorption limits.			$\Delta \sqrt{\frac{\nu}{R}}$
	$L_1$	$L_2$	$L_3$	$L_1$	$L_2$	$L_3$	
47 Ag	247.33	260.01	279.48	15.72	16.13	16.72	0.59
51 Sb	304.32	321.89	346.14	17.44	17.94	18.60	0.66
52 Te	320.08	339.56	364.13	17.89	18.43	19.08	0.65
53 I	335.96	357.60	392.58	18.33	18.91	19.56	0.65
54 Xe	352.18	375.74	401.02	18.77	19.38	20.03	0.65
55 Cs	369.50	396.4	422.5	19.22	19.91	20.56	0.65
56 Ba	386.67	414.67	441.7	19.66	20.36	21.02	0.66
57 La	405.0	434.4	462.3	20.12	20.84	21.50	0.66
58 Ce	421.94	454.44	482.9	20.54	21.32	21.97	0.66
59 Pr	439.44	474.68	504.0	20.96	21.79	22.45	0.68
60 Nd	457.86	495.90	524.9	21.40	22.27	22.91	0.67
62 Sm	495.02	535.7	566.7	22.25	23.14	23.80	0.66
63 Eu	514.07	—	—	22.67	—	—	—
64 Gd	534.10	584.66	619.9	23.11	24.18	24.89	0.71
66 Dy	574.21	632.22	667.68	23.96	25.14	25.84	0.70
68 Er	615.85	682.62	719.78	24.82	26.13	26.83	0.70
69 Tm	637.31	709.23	747.19	25.24	26.63	27.33	0.70
70 Yb	659.20	733.7	774.55	25.67	27.09	27.83	0.74
71 Lu	681.24	762.87	802.05	26.10	27.62	28.32	0.70
72 Hf	704.77	791.37	830.70	26.55	28.13	28.82	0.69
73 Ta	727.3	819.6	861.3	26.98	28.63	29.35	0.72
74 W	750.88	849.59	889.9	27.40	29.15	29.83	0.68
76 Os	800.7	912.6	957.7	28.30	30.21	30.94	0.73
77 Ir	825.7	944.3	991.0	28.74	30.73	31.47	0.74
78 Pt	851.26	977.6	1022	29.18	31.27	32.02	0.75
79 Au	877.65	1011.3	1058	29.63	31.83	32.54	0.71
80 Hg	905.20	1047.4	1093	30.09	32.36	33.06	0.70
81 Tl	932.15	1082.9	1131	30.53	32.91	33.64	0.73
82 Pb	959.53	1120.5	1168	30.98	33.47	34.17	0.70
83 Bi	988.79	1157.5	1205	31.44	34.02	34.78	0.76
90 Th	1199.7	1449.7	1508	34.64	38.07	38.83	0.76
92 U	1263.2	1539.8	1603	35.54	39.24	40.04	0.80

TABLE 21.  
M absorption limits.

		$M_1$	$M_2$	$M_3$	$M_4$	$M_5$	Author.	
$\lambda$	83 Bi	4762	4569	3894	—	—	Coster	
	90 Th	3721	3552	3058	—	—	Stenström	
	90 Th	—	—	—	2571	2388	Coster	
	92 U	3491	3326	2873	—	—	Stenström	
	92 U	—	—	—	2385	2228	Coster	
$\frac{\nu}{R}$	83 Bi	191.36	199.44	233.9	—	—		
	90 Th	244.90	256.55	297.99	354.4	381.6		
	92 U	261.03	273.99	317.18	382.1	408.9	$M_3-M_2$	$M_5-M_4$
$\sqrt{\frac{\nu}{R}}$	83 Bi	13.84	14.13	15.30	—	—	1.17	—
	90 Th	15.65	16.02	17.26	18.83	19.53	1.24	0.70
	92 U	16.16	16.55	17.81	19.54	20.22	1.26	0.68

## 28. Dependence of Absorption on the Chemical Combination of the Element

One of the most striking distinctions between ordinary optical spectra and Röntgen spectra is the almost complete independence of the latter on the chemical nature, as well as on the chemical combination of the emitting element. While the optical spectra of chemically related elements, which are situated in the same vertical column of the periodic system, show a marked analogy in their appearance, there is no such periodicity in the Röntgen spectra. On the contrary, the structure of the Röntgen spectra changes slowly and regularly from one element to the next in the periodic system. No periodicity in this change had been observed until quite recently.

Nor had anyone, until recently, succeeded in demonstrating any influence on X-ray spectra of the chemical combination of the atom. As stated above, however, Bergengren discovered the first indications of such an influence, in an investigation of the absorption spectrum of various modifications of phosphorus. Nevertheless, the interpretation of his results is not as Bergengren concluded from his limited investigation, namely, that the basis of this difference lies in the allotropic modification of the element. Lindh, who continued the study of this phenomenon, made the very important discovery that the X-ray absorption spectrum of an element often varies greatly according to its chemical state in the compound investigated. Chlorine, sulphur and phosphorus, the elements included in this first investigation, all showed this peculiarity. Hence, in the study of absorption spectra in the region of long wave-lengths we must certainly consider that such spectra represent no purely atomic property, but that they depend on the form of chemical combination in which the element may happen to be.

We shall give an account of the results obtained by Lindh in his interesting experiments, beginning with the case of chlorine. Generally, the absorption spectrum obtained for an element in a homogeneous chemical compound shows, in addition to the absorption discontinuity, certain brighter and darker lines on the short wave-length side. In some cases this "fine structure" is more strongly developed than in others. The most complicated structure for chlorine was found in compounds where this element entered with a valency of seven. Fig. 82 is a general graphical representation of the fine structure. The points to be measured here are the two discontinuities  $K_1$  and  $K_2$ , the first of which represents the location of the principal limit, while the other one is a secondary edge.

In order to give a somewhat quantitative expression to the fine structure, Lindh also measured the intervals  $\Delta L_1$  and  $\Delta L_2$ . Their significance may be understood from the figure. On the whole, the following tables of results show that the absorption spectra of all compounds, in which the valency of chlorine is the same, are identical within the limits of experimental error. HCl apparently

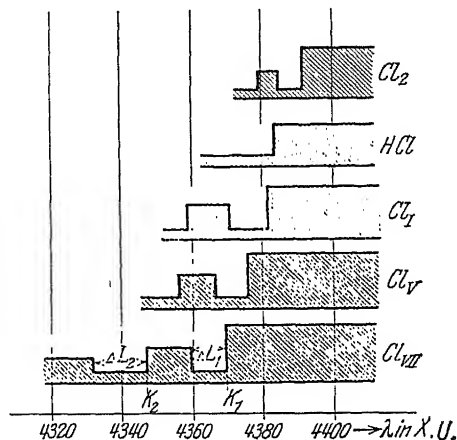


FIG. 82.  
structure of  
various chem

relative positions and the  
spectra of chlorine for  
of that element.

forms an exception, the absorption wave-length being unmistakably greater than for other monovalent compounds. Free chlorine occupies an entirely separate position with considerably greater wave-length of the absorption edge. It therefore seems justifiable to take the mean value within each of the valency groups of the chlorine compounds, since the small variations from the mean probably do not exceed the error of measurement. The mean values thus obtained are listed in Table 23, and from these the curves of Fig. 82 are constructed. In these tables of mean values may also be found the corresponding energy differences, expressed in volts.

Lindh also made a very extended investigation of sulphur. Besides crystalline sulphur in monoclinic and rhombic form, a whole series of divalent, tetravalent and hexavalent compounds were studied, organic as well as inorganic. The two allotropic modifications showed no appreciable difference in their absorption spectra. The sulphides, however, exhibit differences in the position of the principal absorption edge, which surely lie outside the limits of error. ZnS has the shortest

TABLE 22.  
Absorption for Chlorine.

		$K_1: \lambda$ .	$K_2: \lambda$ .	$L_1: \Delta \lambda$ .	$L_2: \Delta \lambda$ .
	Cl	4393.8	4381.6	7.5	—
	HCl	4385.3	—	—	—
Monovalent chlorine compounds.	H <sub>4</sub> NC1	4382.1	4360.1	10.8	—
	LiCl	4382.9	4359.6	12.4	—
	NaCl	4383.3	4359.2	10.8	—
	KCl	4382.9	—	10.8	—
	CaCl <sub>2</sub>	4382.1	—	11.3	—
	CuCl <sub>2</sub> (+ 2 H <sub>2</sub> O)	4383.3	—	11.3	—
	SrCl <sub>2</sub> (+ 6 H <sub>2</sub> O)	4383.3	—	11.3	—
	CdCl <sub>2</sub> (+ 2 H <sub>2</sub> O)	4383.7	4360.9	—	—
	CsCl	4382.9	—	—	—
	BaCl <sub>2</sub> (+ 2 H <sub>2</sub> O)	4382.9	—	10.8	—
	ThCl <sub>4</sub>	4382.9	—	12.4	—
Pentavalent.	NaClO <sub>3</sub>	4376.5	—	9.6	—
	Mg(ClO <sub>3</sub> ) <sub>2</sub>	4376.9	4358.4	10.2	—
	KClO <sub>3</sub>	4376.1	4356.3	9.1	—
	Cu(ClO <sub>3</sub> ) <sub>2</sub>	4377.8	—	—	—
	Sr(ClO <sub>3</sub> ) <sub>2</sub>	4377.8	—	—	—
	Ba(ClO <sub>3</sub> ) <sub>2</sub>	4376.1	—	—	—
Hepta-valent.	NaClO <sub>4</sub>	4369.4	4347.8	9.1	15.3
	KClO <sub>4</sub>	4370.2	4347.8	10.2	16.4

TABLE 23.  
Summary of mean values of absorption measurements for Cl.

	$K_1$ .	$K_2$ .	$L_1: \Delta \lambda$ .	$L_2: \Delta \lambda$ .	Separation in volts from the corresponding edge for Cl <sub>2</sub> .		Diff. $K_1-K_2$ in volts.
					$K_1$ .	$K_2$ .	
Cl <sub>2</sub>	4393.8	4381.6	7.5	—	0	0	7.8
HCl	4385.3	—	—	—	5.4	—	—
Cl: Monov.	4382.9	4360.0	11.3	—	7.0	13.8	14.6
Cl: Pentav.	4376.9	4357.4	9.6	—	10.8	15.5	12.5
Cl: Heptav.	4369.8	4347.8	9.7	15.9	15.3	21.6	14.1

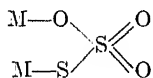
wave-length, 5005.3 X.U., while Cr<sub>2</sub>S<sub>3</sub> has the longest, 5011.7 X.U. The secondary edge shows a still greater variation in wave-length, the values here ranging from 4999.4 X.U. for H<sub>2</sub>S to 4987.2 for CuS. On the



contrary, in the group of tetravalent compounds, with the exception of  $\text{SO}_2$ , the values agree very well for both the principal edge and the secondary. Furthermore, it will be noticed that the position of these secondary limits in the tetravalent group (and also in the sulphide group) very nearly coincides with the position of the principal limit in the hexavalent group. The average values are respectively 4988.1 and 4987.9. In view of the ready oxidation of the tetravalent compounds, Lindh questions the real existence of the secondary limit for this group.

In the hexavalent group of sulphur compounds Lindh studied a long series of sulphates with various metal atoms ranging from Li to U. With these no variation was found in the principal limit. Secondary limits were measured only for Li, Na and K, but in the case of these three there was a pronounced and rather regular increase of wave-length of the secondary limit with the atomic number of the metallic atom.

Two sulphur compounds were also investigated, in which, according to the usual representation, two sulphur atoms with different valencies are present in the same molecule, as represented by the formula :



For these two compounds Lindh found three edges and also three brighter lines, which are recorded in order of decreasing wave-length in the following table :

TABLE 24.  
Absorption spectra of thiosulphates.

Compound.	Limits.			Width of lines.		
$\text{Na}_2\text{S}_2\text{O}_3(+5 \text{ H}_2\text{O})$	5009.7	5000.8	4992.1	3.8	3.2	6.0
$\text{BaS}_2\text{O}_3(+\text{H}_2\text{O})$	5008.0	5000.1	4991.6	2.6	3.4	6.0

The first of these three edges is seen to agree very well with the corresponding principal edge in the divalent sulphur group (see the table of average values below), while the third edge comes out to be about 4 X.U. greater than the principal edge of hexavalent sulphur.

By comparing the tables of averages for the inorganic and for the organic compounds we observe that in the latter the absorption edges for tetravalent and hexavalent sulphur lie about 6 X.U. farther towards greater wave-lengths.

A point of great significance for the entire absorption process and its dependence on the state of chemical combination of the element is the fact revealed by Lindh's results, that the absorption spectra of divalent sulphur are in general of the simple edge type, while in the tetravalent

and hexavalent groups distinct absorption lines are found. Even though the results before us might be utilized in drawing general conclusions, it seems better to await further experimental developments which are in progress along certain directions.

TABLE 25.  
*Absorption of Sulphur.*  
Organic Compounds.

		$K_1: \lambda$	$K_2: \lambda$	$L_1: \Delta\lambda$	$L_2: \Delta\lambda$
Divalent sulphur compounds.	Phenylthioglycollic acid	5005.8	—	5.2	—
	Thiodiglycollic acid	5006.4	—	—	—
	Ammonium thiocyanate	5007.5	—	—	—
	Sodium thiocyanate	5008.0	—	—	—
	Calcium thiocyanate	5007.4	—	—	—
	Cuprous thiocyanate	5005.8	—	—	—
	Silver thiocyanate	5005.0	4988.3*	—	4.8
	Barium thiocyanate	5007.6	—	—	—
	Mercuric thiocyanate	5007.6	4987.9*	—	—
	Lead thiocyanate	5007.0	4988.3*	—	—
Tetravalent.	Phenylsulphoxyacetic acid	5001.6	4987.9*	5.6	4.4
	Dimethylthetindicarboxylic acid	5002.2	4987.2*	4.8	—
	Diphenylsulphoxide	5001.9	—	6.0	—
Hexavalent.	Phenylsulphoneacetic acid ethyl ester	4994.1	—	6.0	—
	Sulphonediactic acid	4994.2	—	5.8	—
	Diphenylsulphone	4993.4	—	5.4	—

Summary of mean values of measurements of organic sulphur compounds.

	$K_1$	$L_2: \Delta\lambda$	$\Delta V$ . Difference in volts between $K_1$ and the same edge for crystalline S.
$S_{II}$	(5006.8)	—	—
$S_{IV}$	5001.9	5.5	3.4
$S_{VI}$	4993.9	5.7	7.3

Summary of mean values of measurements of inorganic sulphur compounds.

	$K_1$	$K_2$	$L_1: \Delta\lambda$	$L_2: \Delta\lambda$	$\Delta V$ . Difference in volts between $K_1$ and the same edge for crystalline S.
S (cryst.)	5008.8	4994.1	8.1	7.9	—
$S_{II}$	(5009.3)	—	—	—	—
$S_{IV}$ (except $SO_2$ )	4996.0	4988.1	4.3	4.2	6.3
$S_{VI}$	4987.9	—	5.2	—	10.3

\* Probably due to sulphate impurities.

TABLE 26.

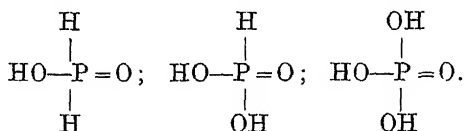
*Absorption for Sulphur. Inorganic Compounds.*

		$K_1: \lambda$	$K_2: \lambda$	$K_3: \lambda$	$L_1: \Delta \lambda$	$L_2: \Delta \lambda$	$L_3: \Delta \lambda$
Divalent Sulphur compounds.	S Monoclinic	5009.0	4994.6	—	8.5	8	—
	S Rhombic	5008.6	4993.8	—	7.7	7.7	—
	H <sub>2</sub> S	5007.1	4999.4	—	5.1	—	—
	CS <sub>2</sub>	5011.4	—	—	—	—	—
	Na <sub>2</sub> S	5009.6	—	—	—	—	—
	MgS	5005.6	—	—	—	—	—
	CaS	5006.6	4996	—	—	—	—
	Cr <sub>2</sub> S <sub>3</sub>	5011.7	4996.9	—	—	—	—
	FeS	5011.4	4988.8	—	—	—	—
	CoS	5010.9	4988.3	—	—	—	—
	CuS	5011.3	4987.2	—	—	—	—
	ZnS	5005.3	4987.8	—	—	—	—
	MoS <sub>2</sub>	5009.9	4988.4	—	—	—	—
	Ag <sub>2</sub> S	5010.1	—	—	—	—	—
	CdS	5007.5	4987.7	—	—	—	—
	SnS <sub>2</sub>	5011.3	4987.9	—	—	—	—
	Sb <sub>2</sub> S <sub>3</sub>	5009.9	—	—	—	—	—
	Sb <sub>2</sub> S <sub>5</sub>	5010.8	—	—	—	—	—
	BaS	5007.5	4987.7	—	—	—	—
	Bi <sub>2</sub> S <sub>3</sub>	5010.3	—	—	—	—	—
Tetravalent.	SO <sub>2</sub>	5004.5	4996.4	—	4.0	—	—
	Na <sub>2</sub> SO <sub>3</sub> (+ 7H <sub>2</sub> O)	4995.6	4987.7	—	4.6	4.2	—
	CaSO <sub>3</sub> (+ 2H <sub>2</sub> O)	4995.8	—	—	4.0	—	—
	CuSO <sub>3</sub>	4995.6	4998.4	—	4.4	4.0	—
	ZnSO <sub>3</sub>	4996.3	4987.7	—	4.0	4.2	—
	Ag <sub>2</sub> SO <sub>3</sub>	4995.8	—	—	—	—	—
	CdSO <sub>3</sub>	4996.4	4988.4	—	4.4	4.4	—
	BaSO <sub>3</sub>	4996.4	4988.8	—	4.2	4.4	—
	PbSO <sub>3</sub>	4996.3	4987.8	—	4.2	4.0	—
Hexavalent.	(H <sub>4</sub> N) <sub>2</sub> SO <sub>4</sub>	4987.9	—	—	5.4	—	—
	Li <sub>2</sub> SO <sub>4</sub> (+ H <sub>2</sub> O)	4987.8	4962	4937	5.8	16	10
	Na <sub>2</sub> SO <sub>4</sub> (+ 10H <sub>2</sub> O)	4987.8	4972	4960	5.6	—	—
	MgSO <sub>4</sub> (+ 7H <sub>2</sub> O)	4987.3	—	—	4.8	—	—
	Al <sub>2</sub> (SO <sub>4</sub> ) <sub>3</sub> (+ 18H <sub>2</sub> O)	4988.3	—	—	5.0	—	—
	K <sub>2</sub> SO <sub>4</sub>	4988.4	4978.3	4965.9	5.4	6.8	—
	CaSO <sub>4</sub> (+ 2H <sub>2</sub> O)	4987.7	—	—	5.2	—	—
	Fe <sub>2</sub> (SO <sub>4</sub> ) <sub>3</sub>	4987.7	—	—	5.0	—	—
	FeSO <sub>4</sub> (+ 7H <sub>2</sub> O)	4988.3	—	—	5.2	—	—
	CoSO <sub>4</sub> (+ 7H <sub>2</sub> O)	4987.9	—	—	5.6	—	—
	NiSO <sub>4</sub> (+ 7H <sub>2</sub> O)	4987.7	—	—	5.4	—	—
	CuSO <sub>4</sub> (+ 5H <sub>2</sub> O)	4988.3	—	—	5.2	—	—
	ZnSO <sub>4</sub> (+ 7H <sub>2</sub> O)	4987.8	—	—	5.0	—	—
	Rb <sub>2</sub> SO <sub>4</sub>	4987.8	—	—	4.8	—	—
	SrSO <sub>4</sub>	4987.3	—	—	5.6	—	—
	Ag <sub>2</sub> SO <sub>4</sub>	4988.3	—	—	4.8	—	—
	3CdSO <sub>4</sub> (+ 8H <sub>2</sub> O)	4988.3	—	—	5.2	—	—
	SnSO <sub>4</sub>	4987.9	—	—	5.0	—	—
	Cs <sub>2</sub> SO <sub>4</sub>	4988.3	—	—	4.8	—	—
	BaSO <sub>4</sub>	4987.9	—	—	5.0	—	—
	Hg <sub>2</sub> SO <sub>4</sub>	4987.7	—	—	6.0	—	—
	Bi <sub>2</sub> (SO <sub>4</sub> ) <sub>3</sub>	4987.8	—	—	5.4	—	—
	Th(SO <sub>4</sub> ) <sub>2</sub> (+ 9H <sub>2</sub> O)	4987.8	—	—	5.0	—	—
	(UO <sub>2</sub> )SO <sub>4</sub> (+ 3H <sub>2</sub> O)	4987.8	—	—	5.6	—	—

As mentioned above, Lindh has also studied phosphorus, and obtained results which clarify the earlier work of Bergengren. A more extensive study of the absorption spectra of this element has recently been carried out by P. Stelling, who investigated about thirty different salts. All his measurements of wave-lengths were made relatively to the  $K\beta_1$  line of phosphorus, the wave-length of which was taken as 5785.1 X.U. The following table gives a brief summary of his results. The second column gives the distance ( $a$ ) from the  $K\beta_1$ -line to the edge, the fourth column gives the wave-length differences from the edge for white phosphorus, and the fifth column expresses these differences in volts.

Substance	$a$	$\lambda$	$\Delta\lambda$	$\Delta V$
Phosphorus (white) - -	0.51	5776.9	—	—
Phosphorus (violet, black) - -	0.84	5771.5	5.4	2.0
Hypophosphite - - -	1.70	5757.5	19.4	7.2
Phosphite - - -	1.91	5754.1	22.8	8.4
Phosphate - - -	2.12	5750.7	26.2	9.7

Stelling remarks that the last three values are in arithmetical progression, which fact may be understood from the constitutional formulae :



In some recent investigations Lindh has continued his work also for higher elements, and found the same effect here. With potassium he determined the absorption edge for the pure metal and for a number of salts. For the latter the values differed from that for the pure element by amounts which, expressed in volts, varied from 1.8 to 4.9 volts. His results are collected in the following table :

Absorption edge for different salts of Potassium.

Substance.	$\lambda$ X.U.	$\frac{\nu}{R}$	$\Delta V$ in volts.
K	3431.0	265.59	—
KCN	3429.3	265.73	1.8
KSCN	3428.7	265.77	2.4
KI	3428.3	265.80	2.8
KCl	3428.0	265.82	3.1
$\text{K}_2\text{S}_2\text{O}_8$	3427.3	265.86	3.9
$\text{K}_2\text{SO}_4$	3426.7	265.93	4.5
$\text{KClO}_4$	3426.3	265.95	4.9

Calcium was also subjected to a preliminary investigation, and the following two values were found :

	$\lambda X.U.$	$\frac{\nu}{R}$	$\Delta V$ in volts.
Ca	3064.3	297.38	—
CaCO <sub>3</sub>	3060.5	297.74	5.0

All these researches have been carried out with the *K* series of the lower elements.

Some measurements in the *L* series have been made by J. Tandberg, who investigated the absorption edges *L*<sub>1</sub>, *L*<sub>2</sub> and *L*<sub>3</sub> of iodine. His results are given in the following table :

	Substance.	$\lambda X.U.$	$\frac{\nu}{R}$	$\Delta\lambda$	$\Delta V$ in volts.
<i>L</i> <sub>1</sub>	I	2711	336.1	0	0
	NaI	2708	336.5	-3	5
	NaIO <sub>3</sub>	2709	336.4	-2	4
	NaIO <sub>4</sub>	2703	337.1	-8	13
<i>L</i> <sub>2</sub>	I	2548	357.6	0	0
	NaI	2542	358.4	-6	12
	NaIO <sub>3</sub>	2544	358.3	-5	9
	NaIO <sub>4</sub>	2541	358.6	-7	14
<i>L</i> <sub>3</sub>	I	2402	379.4	0	0
	NaI	2397	380.2	-5	11
	NaIO <sub>3</sub>	2398	380.1	-4	9
	NaIO <sub>4</sub>	2397	380.2	-5	11

## VI

### SYSTEMATIC ARRANGEMENT AND THEORY OF X-RAY SPECTRA

#### 29. General Ideas on the Origin of X-ray Spectra. Energy Level Diagrams

ALTHOUGH we are still far from having reached a complete and satisfactory theory of Röntgen spectra, yet, thanks to the Bohr theory of radiation, it has become possible to unify the entire mass of empirical material in such a way as to throw considerable light on those atomic processes from which Röntgen spectra arise. From these same spectra we are now also able to draw important conclusions concerning the structure of the system of electrons surrounding the nucleus of the atom. There are also certainly many more contributions of this nature to be derived from the quantity of experimental material already available.

One of the well-known fundamental postulates of Bohr's theory is the following: When an alteration occurs in the electron system of an atom, resulting in a change in the total atomic energy from  $W_1$  to  $W_2$ , the atom emits a quantity of energy  $W_1 - W_2$  as monochromatic electromagnetic radiation of frequency  $\nu$ , which is determined by the equation

$$\nu = \frac{W_1 - W_2}{h},$$

where  $h$  represents Planck's constant.

For many reasons, of which we shall here mention two, we must assume that the changes which give rise to X-ray spectra take place in the *inner region* of the envelope of electrons. The first of these two reasons is: The X-ray spectrum is an atomic property, which in general is quite independent of the chemical nature of the element. The second is that the frequencies involved in X-ray spectra are very great in comparison to those of optical spectra, and are therefore associated, according to the above equation, with correspondingly large energy changes, which necessarily involve electron orbits of high energy content.

From the striking characteristic that Röntgen spectra differ only very slightly as we pass from element to element through the whole

atomic system, we may at once infer that the inner portions of the atoms are built up on very much the same plan. The regular increase of all frequencies with increasing nuclear charge is an evident consequence of the increase of the intensity of the electric field within the atom.

The second important feature of X-ray spectra, namely, *the wide separation of the various groups of spectrum lines*, points to a correspondingly large energy difference even between certain inner electron groups and those still nearer the nucleus.

The excitation of the characteristic radiation is always accompanied by the ejection of an electron from the atom. This idea is the foundation of Kossel's explanation of the mechanism of emission of X-rays. Let us suppose with Kossel, as the first step in emission, that an *electron from an inner electron group is thrown entirely out of the atom* by the impact of a cathode particle, or by the absorption of energy from primary Röntgen radiation. If this electron is taken from the innermost group we speak of a *K* excitation, if from the second group, of an *L* excitation, etc. The electron groups involved are thus called the *K* group, the *L* group, etc.

The second step in the emission process consists in the return of electrons to fill these vacancies, an event which may take place in several different ways. If an electron is missing in the *K* group, its place will most probably be filled by an electron from the adjacent *L* group. The energy change in the atom in this case is manifested as a *K* radiation, and the most probable transition corresponds to the strongest line of the *K* series, the *K $\alpha$*  line; if the electron comes not from the *L* but from the *M* group, the result is the radiation of the *K $\beta$ <sub>1</sub>* line. Thus, through the falling back of electrons from the outer groups into the innermost one, we obtain a series of spectral lines which, taken together, constitute the *K* series.

We may think of the *L* series as arising in a similar way; first an electron is ejected from the *L* group, and then this vacancy is filled by an electron falling from the *M*, the *N*, the *O*, or the *P* group.

There is considerable support for this conception of the mechanism of radiation, as Kossel showed by the following considerations. We may say, for example, that the vacancy in the *K* group may be filled in two ways; either an electron falls from the *M* group directly into the *K* group, giving rise to the *K $\beta$*  line, or an electron falls from the *L* group into the *K* group, emitting the *K $\alpha$*  line, while the position thus made vacant in the *L* group is filled by an electron from the *M* group, and simultaneously the *L $\alpha$*  line is emitted. Since, according to the Bohr frequency condition, the three frequencies are given by differences formed from the three values of the atomic energy, we have the relation

$$K_{\beta} = L_{\alpha} + K_{\alpha}, \quad (34)$$

where  $K_\alpha$ ,  $K_\beta$ , and  $L_\alpha$  are the *frequencies* of the three lines. Or in terms of atomic energies, if  $W_K$  represents the energy of an atom lacking an electron in the  $K$  group,  $W_L$  the energy of an atom lacking an electron in the  $L$  group, and  $W_M$  the energy of an atom lacking an electron in the  $M$  group, then before the emission of the  $K_\alpha$  line, the atom contains the energy  $W_K$ , afterwards the energy  $W_L$ . Hence the Bohr frequency equation in this case is

$$hK_\alpha = W_K - W_L. \quad (35)$$

Likewise, for the other two frequencies we have

$$hK_\beta = W_K - W_M, \quad (36)$$

$$hL_\alpha = W_L - W_M. \quad (37)$$

By adding (35) and (37) and substituting in (36) we obtain the above equation (34).

The measurements available even at the time Kossel enunciated his principle very strongly supported his conclusions. The principle is really nothing more than the Ritz combination principle carried over to the realm of Röntgen spectra.

We shall forthwith restate these relations in a graphical form which has already proved its value as a clear and practical method of representation. By means of horizontal lines we mark off on a vertical axis, as in Fig. 83A, the energy values of the atom. Instead of  $W_K$ ,  $W_L$  and  $W_M$ , we employ preferably these values divided by  $h$  and denote them by

$$K = \frac{1}{h} W_K, \quad (38)$$

$$L = \frac{1}{h} W_L, \quad (39)$$

$$M = \frac{1}{h} W_M. \quad (40)$$

We are thus enabled to read the frequencies of the lines according to the Bohr frequency condition directly from the graph of these "energy levels," since, of course,

$$K_\alpha = \frac{1}{h} W_K - \frac{1}{h} W_L, \text{ etc.} \quad (41)$$

Let us again call attention to the fact that the  $K$  level in the diagram represents  $\frac{1}{h}$  times the energy of the atom when an electron is removed from the  $K$  group; the  $L$  level represents the same thing when an electron is removed from the  $L$  group, etc. Finally, the level marked "normal state" represents  $\frac{1}{h}$  times the energy of the atom when all the electron groups are fully occupied.



The  $K$  excitation consists in the complete removal of an electron from the  $K$  group; graphically this signifies a transition from the normal state level to the  $K$  level, as indicated by the first vertical stroke. The return from the  $K$  level to the adjacent  $L$  level corresponds to the emission of  $K_\alpha$ , the softest and most intense of the  $K$  lines, whilst a drop from the  $K$  level directly to the  $M$  level is accompanied by the emission of the  $K\beta$  line. The further extension of this scheme to illustrate by means of the levels the production of the various characteristic lines of the series is too evident to require further explanation. Since distances along the energy axis represent frequencies, so that the frequencies of the lines concerned may be read off directly, we see at once the truth of the equation (34).

We have two methods of determining the energy difference between the level of the normal state and the  $K$  level. One of these methods consists in determining the *critical potential* ( $V_0$ ) for the  $K$  series, by which just enough energy is given to the impinging electron to enable it, on colliding with an atom, to eject an electron from the  $K$  group. The other method is based on the determination of the frequency of the  $K$  absorption discontinuity.

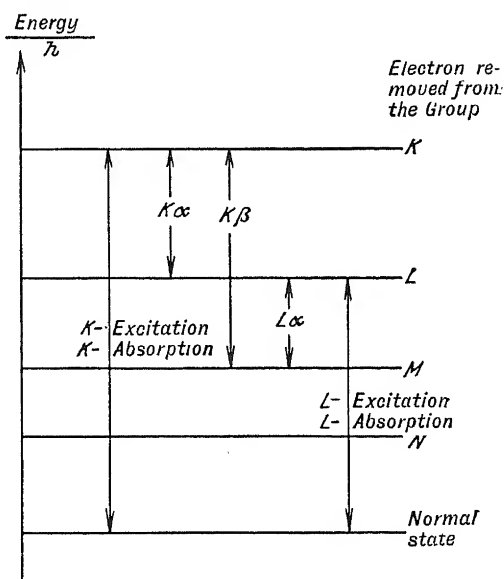


FIG. 83A.

According to the Einstein equation  $eV_0 = h\nu$  the atom absorbs at this frequency a quantity of energy just equal to the energy of an electron moving with a velocity corresponding to the critical voltage  $V_0$ .

It is a matter of considerable difficulty to determine the excitation voltages necessary to give the electrons these high velocities, and hence in only a few cases has the voltage been measured experimentally with the required degree of accuracy. The second method, on the other hand, as we have shown in Chapter V., is easily carried out, and the absorption spectra concerned have now been extensively investigated. We have stated the general result that there is one  $K$  absorption discontinuity, 3 in the  $L$  series, and 5 in the  $M$ . We must, accordingly, modify our level diagram in order to take account of these finer details afforded by experimental results. Thus we must introduce 3  $L$  levels and 5  $M$  levels in

place of the one of each kind shown in Fig. 83A. This enables us to explain in terms of energy levels why, as Duane has found in the case of tungsten, the  $K\alpha$  line is not a single line, as might be expected from the figure, but really consists of three very close components. The three components correspond to transitions from the three  $L$  levels to the single  $K$  level. In the same way, instead of one line corresponding to a transition from the  $M$  level to the  $L$  level, we have no fewer than 15 lines, corresponding to transitions from the 5  $M$  levels to the 3  $L$  levels. Nevertheless, not all of these 15 lines actually occur, for their number is limited in a manner expressed by certain selection rules, to be discussed later, just as in ordinary optics we find experimentally not all, but only a small fraction of the lines which may be calculated from the Ritz combination principle. The three components which Duane found in the case of tungsten, and which correspond to the three possible combinations of the  $L$  levels with the single  $K$  level, have been observed only for this one element; in all other cases only two of them are present. The third line belongs to a transition forbidden by the selection rule.

We shall now show, by a few examples, the quantitative agreement of the level diagram. From the tables of  $K$  absorption spectra and from the measurements of the absorption edges  $L_1$ ,  $L_2$  and  $L_3$  by Duane, we obtain the following values of the levels :

	$\frac{\nu}{R}$	
Tungsten $K$	5118	$\pm 2$ ,
$L_1$	750.9,	
$L_2$	849.6,	
$L_3$	889.9,	

$\frac{\nu}{R}$  is here chosen as the measure of the energy, where  $R=109,737$ , the Rydberg constant. From our level diagram we obtain for the three  $K$  lines

$$\begin{aligned} K_{a_1} &= K - L_1, \\ K_{a_2} &= K - L_2, \\ K_{a_3} &= K - L_3. \end{aligned}$$

In the following table the experimentally determined frequencies of the lines, divided by the Rydberg constant, are compared with the corresponding frequencies calculated from the diagram by the use of the absorption frequencies.

	$\frac{\nu}{R}$		$\frac{\nu}{R}$
$K_{a_1}$	$4368.7 \pm 0.6$	$K - L_1$	$4367 \pm 2$
$K_{a_2}$	$4270.3 \pm 0.6$	$K - L_2$	$4268 \pm 2$
$K_{a_3}$	$4239 \pm 20$	$K - L_3$	$4228 \pm 2$

The agreement is thus complete within the limit of error.

Let us now make use of the diagram of Fig. 83B to show the relations involved in transitions from the 5 *M* levels to the 3 *L* levels.

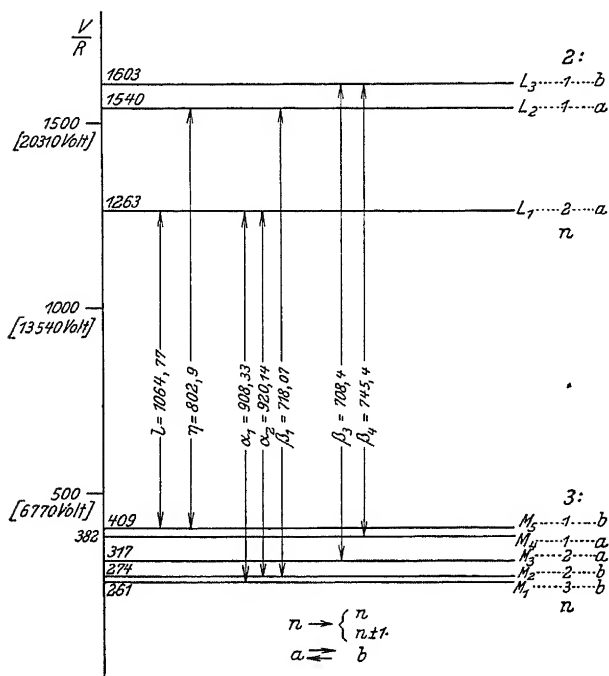


FIG. 83B. Diagram of the *L* and *M* levels of uranium, together with transitions which have been observed.

All the *L* and *M* levels are here drawn to proper scale on the  $\frac{\nu}{R}$  axis. The numerical values of the energy levels, expressed in terms of  $\frac{\nu}{R}$ , are:

$\frac{\nu}{R}$		$\frac{\nu}{R}$	
$L_3$	1603	$M_5$	409
$L_2$	1540	$M_4$	382
$L_1$	1263	$M_3$	317
		$M_2$	274
		$M_1$	261

The observed lines correspond to the transitions indicated in the diagram by the vertical arrows, on which are also recorded the designations of the lines and their wave-lengths. The values of  $\frac{\nu}{R}$  calculated from the energy levels are placed in the following table along with the observed values.

TABLE 27.

Transition.	$\frac{\nu}{R}$ calculated.	$\frac{\nu}{R}$ observed.	Designation of lines.
$L_1 - M_5$	854	855.8	$l$
$L_1 - M_2$	989	990.4	$\alpha_2$
$L_1 - M_1$	1002	1003.2	$a_1$
$L_2 - M_5$	1131	1134.9	$\eta$
$L_2 - M_2$	1266	1269.1	$\beta_1$
$L_3 - M_4$	1221	1222.5	$\beta_4$
$L_3 - M_3$	1286	1286.3	$\beta_3$

Here also the agreement is as good as could be expected. Furthermore, it is apparent that if we accept the level diagram as representing the facts, we may derive the values of the energy levels from the lines instead of from the absorption measurements. Since the lines may be determined throughout with greater accuracy than the absorption limits, we may in many cases prefer to calculate the levels in this manner.

It thus becomes quite certain that instead of working with the simple diagram of Fig. 83A all levels except the  $K$  level must be made multiple. The interpretation we have given to these energy levels is that the  $K$  level represents the energy of the atom when an electron has been removed from the innermost, or  $K$  group; the  $L$  level represents the energy when an electron is missing from the  $L$  group, etc. The question then arises as to how the multiplicity of the  $L$ ,  $M$ ,  $N$  levels is to be explained. Two explanations are possible: either we may suppose that when an electron is removed from one of the inner electron systems of the atom the remaining electrons arrange themselves in a somewhat changed configuration, which might take place in different ways; or it may be that the electrons of the same group (*i.e.* the  $L$  group, or the  $M$  group, etc.) *have not all the same energy value*, and hence the work required to remove different electrons of the same group is not the same. As will be shown later, there is strong support for the assumption that there is really truth in both these explanations. In the case of the  $K$  group, however, all of its electrons have the same energy value, and the removal of one of these electrons gives rise to a unique arrangement of those that remain.

### 30. Doublets in X-ray Spectra

Sommerfeld, who has applied himself to the theoretical investigation and explanation of Röntgen spectra with such fruitful results, very early called attention to the existence in the emission spectra of characteristic line doublets. Farther on we shall discuss the explanation which Sommerfeld has proposed for these doublets on the basis of the Bohr

theory. Here, however, we shall consider the numerical results which are afforded by the available wave-length measurements.

The upper portion of Fig. 84A represents the  $L$  spectrum of tungsten. For better comparison the frequencies ( $\frac{\nu}{R}$ ) from 500 to 900 are laid off

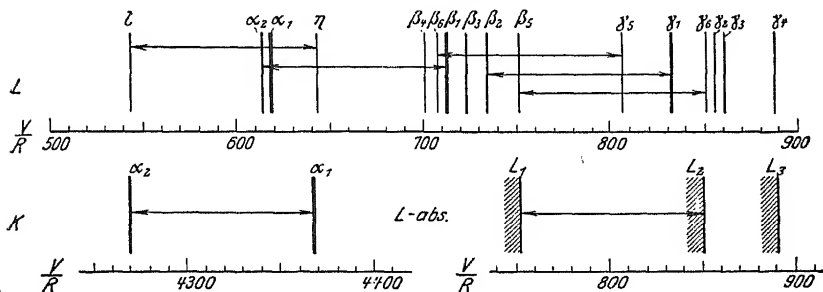


FIG. 84A.

upon a horizontal line. On examining these lines closely we find that no fewer than ten of them may be grouped in doublets which have the same frequency difference. In this same figure we have two  $K$  lines and the  $L$  absorption spectrum drawn on the frequency scale, and we observe that the same frequency difference enters here also. From the numerical values of  $\frac{\nu}{R}$  we obtain the following differences :

$L$ series :	$\eta$	642.78	$\beta_1$	712.39	$\gamma_5$	807.00	$\gamma_1$	831.81	$\gamma_6$	850.07
	$l$	544.03	$\alpha_2$	613.85	$\beta_6$	708.00	$\beta_2$	733.76	$\beta_5$	751.56
		<u>98.75</u>		<u>98.54</u>		<u>99.00</u>		<u>98.05</u>		<u>98.51</u>
$K$ series :	$\alpha_1$	4368.5	$L$ limits :		$L_2$	849.59				
	$\alpha_2$	4270.0			$L_1$	750.88				
		<u>98.5</u>				<u>98.71</u>				

Thus, within the limits of error, all these doublet differences from the  $K$  and the  $L$  series in the emission and absorption spectra have the same value. Table 28 shows in a similar way that this regularity obtains in general for analogous lines in the spectrum of other elements, but, of course, the magnitude of the doublet difference varies from element to element.

From the level diagram we derive at once the formal explanation of these doublets. The frequency differences which we have here calculated in various ways is simply the difference between the two energy levels  $L_1$  and  $L_2$ ; the last difference is, in fact, obtained directly from these levels. The two  $K$  lines are due to transitions from the  $L_1$  and  $L_2$  levels to the common  $K$  level, while the pairs of  $L$  lines correspond to transitions from a common level of origin to  $L_1$  and  $L_2$  as final levels. Herein we have an excellent means of determining by calculations to which levels the various lines belong.

TABLE 28.

Frequency differences of the  $L_1L_2$  doublets.

Element.	$K(a_1-a_2)$ .	$L(\eta-l)$ .	$L(\beta_1-a_2)$ .	$L(\gamma_3-\beta_6)$ .	$L(\gamma_1-\beta_2)$ .	$L(\gamma_3-\beta_5)$ .	$L_2-L_1$ .
17 Cl	0.13	—	—	—	—	—	—
19 K	0.22	—	—	—	—	—	—
20 Ca	0.26	—	—	—	—	—	—
21 Sc	0.34	—	—	—	—	—	—
22 Ti	—	—	—	—	—	—	—
23 Va	—	—	—	—	—	—	—
24 Cr	0.72	—	—	—	—	—	—
25 Mn	—	—	—	—	—	—	—
26 Fe	1.02	—	—	—	—	—	—
27 Co	1.19	—	—	—	—	—	—
28 Ni	1.30	—	—	—	—	—	—
29 Cu	1.49	—	—	—	—	—	—
30 Zn	1.69	—	—	—	—	—	—
32 Ge	1.69	—	—	—	—	—	—
33 As	2.62	—	—	—	—	—	—
34 Se	2.99	—	—	—	—	—	—
35 Br	3.40	—	—	—	—	—	—
37 Rb	4.38	—	—	4.44	—	—	—
38 Sr	5.0	4.90	—	5.00	—	—	—
39 Y	5.5	—	—	—	—	—	—
40 Zr	6.2	6.11	—	6.20	6.10	—	—
41 Nb	7.0	7.10	6.90	—	6.98	—	—
42 Mo	7.7	—	7.65	—	7.81	—	—
44 Ru	9.5	—	9.49	9.51	9.46	—	—
45 Rh	10.5	10.54	10.53	10.40	10.47	—	—
46 Pd	11.6	11.48	11.57	11.66	11.58	—	—
47 Ag	12.9	12.64	12.69	12.77	12.66	—	—
48 Cd	14.1	13.82	13.97	13.98	13.93	—	—
49 In	—	15.24	15.29	15.27	15.25	—	—
50 Sn	16.9	16.69	16.72	16.78	16.61	—	—
51 Sb	18.0	18.31	18.30	18.26	18.21	—	—
52 Te	20.2	—	20.00	20.03	19.86	—	—
53 I	—	—	21.70	—	36.71	—	—
55 Cs	—	—	25.59	25.77	25.43	—	—
56 Ba	—	27.69	27.74	27.95	27.63	—	—
57 La	—	29.55	30.01	30.19	29.83	—	29.4
58 Ce	—	—	32.35	32.56	32.31	—	31.7
59 Pr	—	35.47	35.02	35.11	34.79	—	34.1
60 Nd	—	37.77	37.86	37.76	37.72	—	37.2
62 Sm	—	43.70	43.95	44.17	43.65	—	—
63 Eu	—	—	47.17	47.29	46.88	—	—
64 Gd	—	—	50.64	51.08	50.47	—	—
65 Tb	—	—	54.36	54.41	54.18	—	—
66 Dy	—	58.53	58.27	58.25	57.46	—	—
67 Ho	—	62.48	62.43	61.66	61.60	—	—
68 Er	—	67.08	66.81	66.74	65.67	—	—

Element.	$K(\alpha_1-\alpha_2)$ .	$L(\eta-l)$ .	$L(\beta_1-\alpha_2)$ .	$L(\gamma_3-\beta_2)$ .	$L(\gamma_1-\beta_2)$ .	$L(\gamma_6-\beta_2)$ .	$L_2-L_1$ .
70 Yb	—	76.57	76.08	76.35	75.48	—	—
71 Lu	—	81.54	81.11	81.20	80.24	—	—
72 Hf	—	—	86.26	—	85.80	—	—
73 Ta	—	93.33	92.68	91.99	91.64	92.33	—
74 W	98.5	98.75	98.54	99.00	98.05	98.51	98.71
76 Os	—	—	111.08	—	110.67	—	—
77 Ir	—	—	118.64	—	117.57	119.49	—
78 Pt	—	126.18	125.92	—	—	—	146.39
79 Au	—	134.34	133.80	134.50	132.37	133.42	135.55
80 Hg	—	158.66	142.17	150.78	—	—	142.20
81 Tl	—	—	150.49	149.65	148.96	151.22	150.75
82 Pb	—	159.20	160.02	160.33	158.39	160.25	160.97
83 Bi	—	168.25	169.73	168.78	167.82	169.57	168.81
90 Th	—	—	250.86	—	247.81	251.26	250.0
92 U	—	279.11	278.71	—	276.28	279.33	276.6

TABLE 29.

Wave-length differences of the  $L_1L_2$  doublets.

Element.	$K(\alpha_2-\alpha_1)$ .	$L(l-\eta)$ .	$L(\alpha_2-\beta_1)$ .	$L(\beta_6-\gamma_3)$ .	$L(\beta_2-\gamma_1)$ .	$L(\beta_5-\gamma_6)$ .	$L_1-L_2$ .
17 Cl	3.15	—	—	—	—	—	—
19 K	3.39	—	—	—	—	—	—
20 Ca	3.26	—	—	—	—	—	—
21 Sc	3.37	—	—	—	—	—	—
22 Ti	3.64	—	—	—	—	—	—
23 Va	3.78	—	—	—	—	—	—
24 Cr	4.11	—	—	—	—	—	—
25 Mn	—	—	—	—	—	—	—
26 Fe	4.21	—	—	—	—	—	—
27 Co	4.28	—	—	—	—	—	—
28 Ni	3.93	—	—	—	—	—	—
29 Cu	3.86	—	—	—	—	—	—
30 Zn	3.81	—	—	—	—	—	—
32 Ge	2.91	—	—	—	—	—	—
33 As	3.97	—	—	—	—	—	—
34 Se	4.01	—	—	—	—	—	—
35 Br	4.04	—	—	—	—	—	—
37 Rb	4.12	—	—	228.9	—	—	—
38 Sr	4.17	316	—	224.2	—	—	—
39 Y	4.18	—	—	—	—	—	—
40 Zr	4.21	304.9	—	212.5	200.4	—	—
41 Nb	4.25	314	237.4	—	201.2	—	—
42 Mo	4.28	—	234.2	—	198.1	—	—
44 Ru	4.34	—	232.67	199.8	189.08	—	—
45 Rh	4.36	295.8	231.56	194.9	186.4	—	—
46 Pd	4.39	289.4	229.30	195.4	184.34	—	—
47 Ag	4.43	287.5	227.18	192.1	178.98	—	—

TABLE 29—*Continued.*

Element.	$K(a_2-a_1)$ .	$L(l-\eta)$ .	$L(a_2-\beta_1)$ .	$L(\beta_6-\gamma_5)$ .	$L(\beta_2-\gamma_1)$ .	$L(\beta_5-\gamma_5)$ .	$L_1-L_2$ .
48 Cd	4.43	283.8	226.28	189.2	178.40	—	—
49 In	4.43	283.2	224.59	186.2	175.91	—	—
50 Sn	4.47	281.5	233.16	184.8	172.97	—	—
51 Sb	4.55	280.7	222.39	182.2	171.53	—	163.5
52 Te	4.54	—	221.03	181.3	169.63	—	163.3
53 I	—	—	219.94	—	168.60	—	164.1
55 Cs	—	—	217.76	176.4	163.88	—	160.5
56 Ba	—	271.6	216.78	174.9	162.70	—	158.2
57 La	—	266.0	215.63	173.1	160.80	—	152
58 Ce	—	—	214.11	171.3	159.77	—	151
59 Pr	—	271.0	213.73	169.8	157.99	—	149
60 Nd	—	266.1	213.42	168.0	157.57	—	150
62 Sm	—	263.0	212.11	167.1	155.01	—	—
63 Eu	—	—	211.02	165.5	153.90	—	—
64 Gd	—	—	210.16	165.5	153.27	—	—
65 Tb	—	—	209.63	163.3	152.40	—	—
66 Dy	—	261.8	209.06	162.5	150.10	—	—
67 Ho	—	260.0	208.54	159.8	149.50	—	—
68 Er	—	260.3	207.96	160.6	148.30	—	—
70 Yb	—	259.0	206.4	159.7	148.00	—	—
71 Lu	—	258.0	205.66	158.3	146.90	—	—
72 Hf	—	—	204.60	—	146.70	—	—
73 Ta	—	258.7	205.86	156.7	146.29	140.6	—
74 W	—	257.35	205.35	157.9	146.38	140.5	141
76 Os	—	—	203.61	—	145.91	—	—
77 Ir	—	—	204.44	—	144.46	139.4	—
78 Pt	—	257.13	203.99	154.3	144.05	148.4	138.3
79 Au	—	257.04	203.96	156.4	143.38	136.92	139.0
80 Hg	—	256.4	203.90	163.0	—	—	136.7
81 Tl	—	—	203.37	153.8	142.57	136.6	136.1
82 Pb	—	256.42	203.62	154.9	142.82	135.82	136.4
83 Bi	—	255.95	204.00	153.8	142.28	134.9	134.4
90 Th	—	—	202.65	—	140.05	132.49	131.0
92 U	—	261.87	202.07	—	139.85	131.53	129.6

A second characteristic feature of these doublets appears from Fig. 73 (p. 110). The  $L$  series of spectra are here represented on a scale of wave-lengths instead of frequencies as in Fig. 84A, and it may be seen at once that the *wave-length difference* of the doublets  $l\eta$ ,  $a_2\beta_1$ , etc., *remains practically constant from element to element*. A collection of these doublet wave-length differences for elements ranging from Cl (17) to U (92) is presented in Table 29.

These doublets, which, according to the energy level diagrams, arise from the *two* levels  $L_1$  and  $L_2$  in the  $L$  group, are explained by Sommerfeld in terms of the relativistic variation of mass of the electron. For this reason they are often called *relativity doublets*. Sommerfeld and Wentzel



TABLE 30.

Wave-length differences of several relativity doublets in the  $M$  and  $N$  groups of levels.

	$L(a_2-a_1)$ ( $M_1M_2$ ).	$L(\beta_1-\beta_3)$ ( $M_3M_4$ ).	$M(a_2-\beta)$ ( $M_1M_2$ ).	$M(a_2-a_1)$ ( $N_1N_2$ ).	$L(\gamma_1-\gamma_3)$ ( $N_3N_6$ ).
92 U	11.81	37.0	204	12	7.4
90 Th	11.82	36.9	207	9	—
83 Bi	12.1	39.7	223	10	5.5
82 Pb	11.50	38.7	—	—	4.5
81 Tl	11.32	39.3	—	—	6.8
80 Hg	11.2	38.5	—	—	—
79 Au	11.34	—	—	—	5.6
78 Pt	11.13	40.3	—	—	6.1
77 Ir	11.05	38.5	—	—	7.0
76 Os	10.04	37.8	—	—	—
74 W	11.04	38.7	—	—	6.2
73 Ta	11.15	38.9	—	—	5.8
72 Hf	10.5	—	—	—	—
71 Lu	10.85	39.0	—	—	5.7
70 Yb	11.11	38.8	—	—	5.8
68 Er	11.00	38.5	—	—	6.6
67 Ho	11.08	39.3	—	—	6.4
66 Dy	11.04	39.0	—	—	6.4
65 Tb	10.82	38.9	—	—	5.5
64 Gd	10.69	38.4	—	—	5.1
63 Eu	11.00	39.4	—	—	6.2
62 Sm	10.67	38.4	—	—	4.2
60 Nd	10.32	40.0	—	—	4.9
59 Pr	9.93	37.7	—	—	5.1
58 Ce	9.11	38.3	—	—	5.0
57 La	9.25	38.5	—	—	5.0
56 Ba	9.38	38.8	—	—	4.5
55 Cs	9.50	37.57	—	—	5.2
53 Tl	9.21	39	—	—	—
52 Te	9.01	38.7	—	—	—
51 Sb	8.98	39.16	—	—	—
50 Sn	8.90	37.4	—	—	—
49 In	8.75	37.1	—	—	—
48 Cd	8.54	37.83	—	—	—
47 Ag	8.18	36.65	—	—	—
46 Pd	8.10	36.6	—	—	—
45 Rh	7.78	36.5	—	—	—
44 Ru	8.00	36.2	—	—	—
42 Mo	5.7	35.6	—	—	—
41 Nb	5.7	35.5	—	—	—
40 Zr	—	34.5	—	—	—
39 Y	—	34.1	—	—	—
38 Sr	—	35.6	—	—	—
37 Rb	—	32.9	—	—	—

have also proposed the name "regular" doublets. Quantitatively, the characteristic of relativity doublets is that *wherever a certain doublet appears in the spectrum of a given element, its frequency difference is a constant, while the wave-length difference of a given doublet remains nearly constant from element to element.*

There are a number of relativity doublets among the lines of the several series. We have explained those given in Tables 28 and 29 in

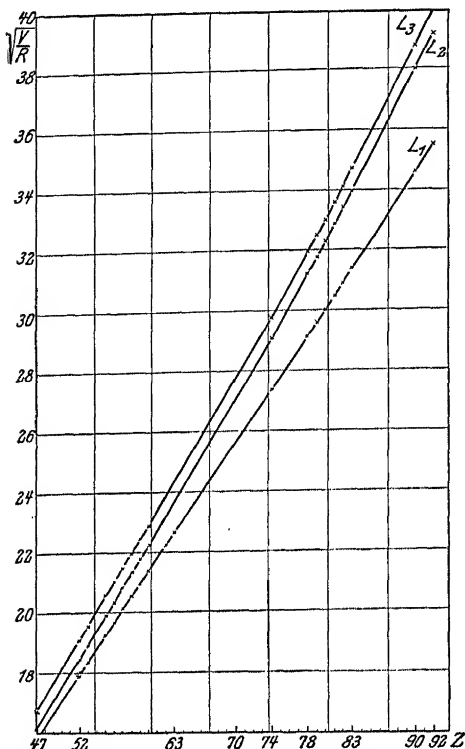


FIG. 84B. Moseley diagram for the  $L$  absorption limits.

terms of the energy level diagram as depending on the  $L_1$ ,  $L_2$  levels, which have the character of a relativity doublet, and this characteristic enters into all transitions in which these two levels play a part. Several such pairs appear in other energy level groups. Table 30 contains the wave-length differences of five of these doublets, and at the top of each column not only the lines are indicated but also the energy levels giving rise to the doublets.

We see from this table that the difference in wave-length of two lines forming a doublet is in reality very nearly constant for different elements. Nevertheless, it is to be expected that there are some pairs of lines which manifest this same characteristic but which are not truly relativity doublets.

A second type of very characteristic doublets in Röntgen spectra was discovered by Hertz. These doublets also indicate a doubling of the energy levels within the same groups ( $L$ ,  $M$  and  $N$ ). In the emission spectra this doubling is never manifested by simple line doublets, because, as we shall see later, such transitions are excluded by the selection rule. In the absorption spectra, however, where we obtain values of the energy levels directly, Hertz was able to demonstrate this doublet property. In Fig. 84B the  $L$  limits are represented in a Moseley diagram, in which, as usual, the values of  $\sqrt{\frac{\nu}{R}}$  are plotted as a function of the atomic

number. To the measurements of Hertz in this figure are added those of Lindsay and of Duane and Patterson. From this diagram it appears that the slightly curved lines, which represent the  $L_2$  and  $L_3$  limits run parallel to each other, and hence the difference  $\Delta \sqrt{\frac{\nu}{R}}$  between these two energy levels is a constant.

In Table 20 we have numerical values for the  $L$  series and in Table 21 for the  $M$  series which show the constancy of this difference  $\sqrt{\frac{\nu}{R}}$ . In the  $M$  group there are two pairs of energy levels,  $M_2 M_3$  and  $M_4 M_5$ , which form the Hertz doublets. Sommerfeld and Wentzel, to distinguish them from the former type, called these ones "irregular" doublets. Another term which expresses better their physical significance is "screening doublets." We have already stated that the multiple nature of a given group level, such as the  $L$ , may be explained on two separate bases. In the first place the electrons belonging to the group have different orbits, and hence, on account of the relativistic masses of the electrons, possess different quantities of energy; in the  $L$  group, for example, we have two such sub-groups of electrons, which give rise to a relativity doublet. In the second place we mentioned the possibility that when an electron is removed from a group those electrons which remain may arrange themselves in different ways and thus give rise to different energy levels. The Hertz doublets just mentioned are formed by levels which differ for this latter reason. Later we shall show how these doublets may be roughly explained by the screening of the nuclear charge.

### 31. Sommerfeld's Theory

A great service was rendered by Sommerfeld when he drew attention to the fact that certain characteristic features of Röntgen spectra may be explained by the aid of very simple atomic models, which even afford to some extent a quantitative agreement with the results of experiment. His theory also bridged over the gap between optical and X-ray spectra, even though their general structures differ so much from each other.

We have already referred several times to Moseley's discovery of the very simple law which holds for all X-ray spectral lines, that  $\sqrt{\frac{\nu}{R}}$  is nearly a linear function of the atomic number. For the strongest line of the  $K$  series this relation, with numerical values of the constants inserted, takes the following form :

$$\sqrt{\frac{\nu}{R}} = \sqrt{\frac{3}{4}} (Z - 1), \quad (42)$$

$$\text{or} \quad \frac{\nu}{R} = (Z - 1)^2 \left( \frac{1}{1^2} - \frac{1}{2^2} \right). \quad (43)$$

On the other hand, Bohr, in the work in which he laid down the fundamental principles of atomic radiation, showed that the line spectrum emitted by an atom consisting of a nucleus of positive charge  $Z$  and a single electron may be represented by the law

$$\frac{\nu}{R} = Z^2 \left( \frac{1}{1^2} - \frac{1}{n^2} \right) \quad (44)$$

where

$$R = \frac{2\pi^2 m e^4}{h^3}.$$

This formula applies only to transitions from the  $n$ th to the innermost orbit. For the first line of this series we have

$$\frac{\nu}{R} = Z^2 \left( \frac{1}{1^2} - \frac{1}{2^2} \right), \quad (45)$$

which has the same form as the law which Moseley found for the  $K\alpha$  line. In the special case  $Z=1$ , the latter Bohr formula gives the first line of the ultra-violet or Lyman hydrogen spectrum; when  $Z=2$  it gives the corresponding line for ionized helium. For  $Z=3$  the formula should represent the line for doubly ionized lithium, but the corresponding spectrum has not yet been observed experimentally.

Experiments show that these lines of hydrogen and helium, as well as the  $K\alpha$  line of X-ray spectra, are not single lines but double ones. Now when Sommerfeld, by an extension of the Bohr formula for hydrogen, was able to explain the optical doublets, he suggested that the  $K\alpha$  doublet might be explained in the same way.

For the generalized case of the hydrogen atom model, that is, a nucleus of positive charge  $Z$ , accompanied by a single electron which describes a Kepler ellipse of quantum number  $n$ , the energy  $W$  is given by

$$\frac{W}{R\hbar} = \frac{Z^2}{n^2}, \quad (46)$$

and this formula combined with the Bohr frequency condition

$$\nu = \frac{W_1}{h} - \frac{W_2}{h} \quad (47)$$

results at once in the above formula (44) for the transition from quantum orbit  $n$  to quantum orbit 1.

In establishing the energy expression (46) the variation of mass as required by the theory of relativity was ignored. Sommerfeld, however, carried out the calculation of the energy of the generalized hydrogen atom, taking into consideration this relativistic mass of the electron. The expression (46) then becomes, if we neglect all terms of the series after the first two,

$$\frac{W}{R\hbar} = \frac{Z^2}{n^2} + a^2 \frac{Z^4}{n^4} \left( \frac{n}{k} - \frac{3}{4} \right), \quad (48)$$

where  $\alpha$  is a small constant given by

$$\alpha^2 = \left( \frac{2\pi e^2}{\hbar c} \right)^2 = 5.315 \cdot 10^{-5}. \quad (49)$$

$n$  denotes the principal quantum number, and  $k$  the auxiliary quantum number; the latter has reference to the departure of the Kepler motion from the simple periodic orbit, and  $k$  cannot be greater than  $n$ .

In the case of the one quantum orbit, where  $n=k=1$ , the energy expression (48) is uniquely determined. *There is only one type of one quantum orbit—the circular orbit—and the energy content has but one value.* If the principal quantum number is 2 the auxiliary quantum number may be either 1, corresponding to an elliptic orbit, or 2, corresponding to a circular orbit. The principal term  $\frac{Z^2}{n^2}$  in the energy expression has, of course, always the same value, regardless of  $k$ , but the smaller second term has two separate values, so that in the two quantum orbit the relativity effect is manifested in two ways. In the same manner the principal quantum number 3 gives rise to a threefold energy level on account of the three possible values of  $k$ .

We may now compare the energy levels calculated for the generalized hydrogen atom with the  $K$ ,  $L$ , and  $M$  levels of the X-ray spectra. The relations for X-ray spectra are considerably more complicated, because more than one electron is revolving round the nucleus. In addition to the electron which gives rise to the radiation by its transition from one quantum orbit to another, we have to consider always the entire system of electrons, which are not entirely undisturbed by the changes taking place. More important still is the fact that the electric field, which determines the energy of the radiating electron, is also modified in a very great degree by the presence of the other electrons. We can take account of the effect of these surrounding electrons by introducing, instead of the actual nuclear charge, a corrected value which is called the *effective* nuclear charge. Further, we make the reservation that the correction to the nuclear charge is not necessarily the same in both terms of the energy equation (48). In the first term, which represents the greater part of the energy, we have the influence of the entire orbit, the outer portion of which is "screened" from the nucleus much more than the inner. For the second term, in which the variation of mass of the electron is the important factor, the inner portion of the orbit, where the greatest change in velocity occurs, will exercise the greatest influence.

In the energy expression (48) we therefore replace  $Z$  in the first term by  $Z - s_n$ , in the second term by  $Z - d$ , and thus obtain for the energy necessary to remove an electron from an  $n_k$  orbit the expression:

$$\frac{W}{\hbar} = \frac{(Z - s_n)^2}{n^2} + \alpha^2 \frac{(Z - d)^4}{n^4} \left( \frac{n}{k} - \frac{3}{4} \right). \quad (50)$$

For the transition from a two quantum to a one quantum orbit, introducing the Bohr frequency condition

$$\nu = \frac{W_1}{h} - \frac{W_2}{h},$$

we obtain as a first approximation, by neglecting the second term,

$$\frac{\nu}{R} = \frac{(Z - s_1)^2}{1^2} - \frac{(Z - s_2)^2}{2^2}. \quad (51)$$

We have denoted the screening constants by  $s_1$  and  $s_2$ , since they must depend in general on the quantum number, and on the magnitude and form of the orbit determined by it. Moreover, it must be supposed that these corrections to the nuclear charge depend not only on the principal quantum number but also on the auxiliary quantum number, as well as on the total number of electrons in the atom. According to the hypotheses of Bohr the electrons, particularly of higher quantum number, move in orbits extending from the surface of the atom even to its innermost parts near the nucleus. The form and size of the orbit, being determined by the two quantum numbers and the total number of electrons, will also have an influence on the screening.

A comparison of equation (51) with the empirical Moseley formula (43) shows, however, that for the first two quantum orbits we may put as a first approximation  $s_1 = s_2 = 1$ . The two equations then become identical. But we know that the  $K\alpha$  line is double and not single, as is assumed in the Moseley formula. Sommerfeld has shown that the fine structure of the hydrogen lines may be explained by formula (48), which takes account of the relativity effect. In particular, he showed that the first line of the ultra-violet series, which represents a transition from a two quantum to a one quantum orbit, is double on account of the two possible values of  $k$ . In spite of the numerous electrons in the atom, the disturbing influence of which would certainly complicate matters for X-ray spectra, we may yet undertake to explain the double nature of the  $K\alpha$  line in the same manner. The agreement of the Moseley formula with the general formula (51) seems to afford very strong support for this view.

Let us again turn to the general Sommerfeld formula (50) and consider the significance of the relativity term, for the transition from the two quantum to the one quantum orbit. For the one quantum orbit we get only one value for the energy, since in this case  $n$  and  $k$  are each unity. The two quantum orbit, however, affords two values of the energy differing slightly from each other. They correspond to the two possibilities

$$1. \quad n=2, \quad k=1;$$

and

$$2. \quad n=2, \quad k=2.$$

The doubling of the energy level means, however, that the associated lines must also be double.

We obtain the frequency difference directly from the difference of the two energy expressions for the two quantum orbit, *i.e.*

$$\Delta \frac{\nu}{R} = \alpha^2 \frac{(Z-d_1)^4}{2^4} \frac{5}{4} - \alpha^2 \frac{(Z-d_2)^4}{2^4} \frac{1}{4}. \quad (52)$$

We have here denoted the screening constant for the auxiliary quantum number 1 by  $d_1$  and for the auxiliary quantum number 2 by  $d_2$ , since they depend in general on the form of the orbit (and really also on the number of electrons in the atom). If we assume provisionally with Sommerfeld that  $d_1 = d_2 = d$  we have for the frequency difference the simple expression

$$\Delta \frac{\nu}{R} = \alpha^2 \frac{(Z-d)^4}{2^4}. \quad (53)$$

An analogous calculation for the simple hydrogen atom gives

$$\Delta \frac{\nu_H}{R} = \frac{\alpha^2}{2^4} = 0.332 \cdot 10^{-5}, \quad (54)$$

which, of course, results as a special case of (53), for the nuclear charge is here  $Z=1$ , and, since there is no screening effect,  $d=0$ . As Sommerfeld points out, we find the hydrogen doublet repeated in the X-ray spectrum and increased by the factor  $(Z-d)^4$ . It is the numerical agreement with the measurements which really gives confidence in the validity of these energy calculations, for, as has been stated several times, such idealized conditions are assumed in the derivations that, logically speaking, any lack of agreement should hardly occasion surprise. Sommerfeld's intuition was particularly fortunate in this case, however, and the agreement with the values obtained from the empirical formula is astonishingly close.

Since the frequency difference of equation (53) depends on the dual nature of the two quantum energy level, according to the general Bohr hypotheses and the resulting frequency equation, it should make no difference whether the two quantum orbit is the initial or the final orbit of the electron concerned in the emission process. In the preceding discussion we have assumed exclusively the former case, in which the transition is from the double two quantum to the single one quantum energy level. But for numerical comparisons we may just as well use the doublet lines which arise when the two quantum orbits are the final ones, and the initial orbit is one and the same orbit of higher quantum number. The frequency difference in this case must be exactly the same. That this is actually the case appears from our discussion of the doublets as calculated from the line measurements. For example, the frequency difference for a given element of the two lines  $K\alpha_1$  and  $K\alpha_2$  was shown to be the same within the limits of error as that of the two lines  $L_{\beta_1}$  and  $L_{\alpha_2}$  of the  $L$  series. A recent series of measurements of the  $K$  doublet

TABLE 31.  
Measurements by Leide.

	$\Delta \frac{\nu}{R}$	$K_{a_1} - K_{a_2}$	$L_{\beta_1} - L_{a_2}$
41	Nb	6.94	6.89
42	Mo	7.74	7.70
43	—	—	—
44	Ru	9.55	9.49
45	Rh	10.53	10.48
46	Pd	11.63	11.56
47	Ag	12.85	12.69
48	Cd	14.13	14.07
49	In	15.33	15.29
50	Sn	16.91	16.73
51	Sb	18.59	18.29
52	Te	20.18	19.94

in a region where the corresponding  $L$  doublet has also been accurately measured is shown alongside, with the permission of Mr. Leide. Throughout this region only the old and less accurate measurements of the  $K$  series were until recently available, while for the lighter elements, whose  $K$  series is well determined, the  $L$  series doublets cannot be obtained by present methods. Leide's results show that we are quite justified, both theoretically and experimentally, in obtaining the frequency difference of equation (53) from either the  $K\alpha$  doublet or the corresponding doublets in the  $L$  series.

In Table 32 the second column contains the values of  $\Delta \frac{\nu}{R}$  calculated from the  $L$  doublets (since these are more accurate than the  $K$  doublet). In the third column are these values of  $\Delta \frac{\nu}{R}$  divided by  $(Z-d)^4$ , where the screening constant  $d$  is taken to be 3.5. From formula (53) this

TABLE 32.

$Z$	$\Delta \frac{\nu}{R}$	$\frac{1}{(Z-3.5)^4} \Delta \frac{\nu}{R}$	$d$	$Z$	$\Delta \frac{\nu}{R}$	$\frac{1}{(Z-3.5)^4} \Delta \frac{\nu}{R}$	$d$
41 Nb	6.89	0.349	3.50	64 Gd	50.64	0.378	3.52
42 Mo	7.70	0.351	3.47	65 Tb	54.36	0.380	3.51
44 Ru	9.49	0.355	3.46	66 Dy	58.27	0.382	3.51
45 Rh	10.48	0.355	3.47	67 Ho	62.43	0.384	3.50
46 Pd	11.56	0.348	3.48	68 Er	66.81	0.386	3.50
47 Ag	12.69	0.354	3.51	70 Yb	76.08	0.389	3.5
48 Cd	14.07	0.358	3.48	71 Lu	81.11	0.391	3.3
49 In	15.29	0.357	3.50	72 Hf	86.26	0.392	—
50 Sn	16.73	0.358	3.50	73 Ta	92.68	0.397	3.48
51 Sb	18.29	0.359	3.50	74 W	98.54	0.399	3.51
52 Te	19.94	0.361	3.50	76 Os	111.08	0.402	3.49
53 I	21.70	0.361	3.51	77 Ir	118.64	0.406	3.50
55 Cs	25.59	0.356	3.52	78 Pt	125.92	0.409	3.51
56 Ba	27.74	0.365	3.54	79 Au	133.80	0.412	3.49
57 La	30.01	0.366	3.54	80 Hg	142.17	0.415	—
58 Ce	32.35	0.367	3.56	81 Tl	150.49	0.417	3.50
59 Pr	35.02	0.369	3.54	82 Pb	160.02	0.421	3.44
60 Nd	37.86	0.372	3.51	83 Bi	169.73	0.425	3.42
62 Sm	43.95	0.375	3.50	90 Th	250.86	0.448	3.43
63 Eu	47.17	0.378	3.52	92 U	278.71	0.465	3.49



should give the constant  $\frac{\alpha^2}{24}$ , the value of which is  $0.332 \cdot 10^{-5}$ . It may be seen from the table, and even better from the plotted values of Fig. 85, that this number is approached asymptotically for the lower atomic numbers. The simple formula (53) was obtained, however, by considering only the first term of the development which expresses the relativity effect. Sommerfeld carried the comparison a step farther by bringing in the second term of the series. The excellence of the numerical

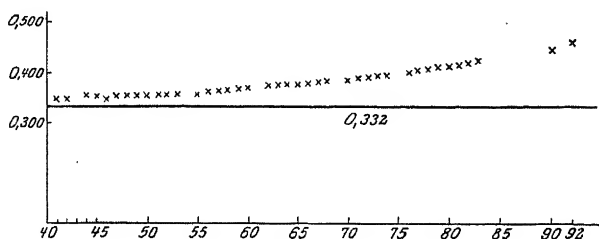


FIG. 85.

agreement then obtained is shown in column *d* of Table 32. Sommerfeld calculated these values, using the complete formula

$$\Delta \frac{\nu}{R} = \frac{\alpha^2}{24} (Z-d)^4 \left[ 1 + \frac{5}{2} \frac{\alpha^2}{24} (Z-d)^2 + \frac{53}{8} \frac{\alpha^4}{24} (Z-d)^4 + \dots \right] \quad (55)$$

and obtaining from it the screening constant *d* for the various elements. The value of  $\alpha^2$  used was the theoretical one,  $\alpha^2 = 5.315 \cdot 10^{-5}$ . It is seen that *d* varies from 3.50 only within the limits of error, and that by using the entire relativity correction a full and numerically complete explanation of the doublets in the *L* series is obtained.

The first approximation to the doublet difference, equation (53), shows that, neglecting the screening effect, the frequency difference  $\Delta \frac{\nu}{R}$  is nearly proportional to  $Z^4$ . According to Moseley's law  $\frac{\nu}{R}$  for all the lines is approximately proportional to  $Z^2$ , the screening effect being again neglected. Further, since

$$\nu = \frac{1}{\lambda},$$

and hence

$$\Delta \lambda = - \frac{\Delta \nu}{\nu^2},$$

it is at once evident that  $\Delta \lambda$  must be nearly constant from element to element. This is, in fact, the second characteristic of relativity doublets which we have found empirically; it is the result of the combination of the Moseley formula and of Sommerfeld's equation (53).

It may be mentioned that several investigators have also made the attempt to calculate the screening constant from assumptions as to the number and position of the electrons in the innermost shells of the atom. Besides Sommerfeld himself, Kroo, Vegard, Debye and others have attacked the problem, and have arrived in this way at results which are numerically quite satisfactory. There are now such strong grounds, however, for opposition to some of the assumptions they make concerning the structure of the atom that we shall omit any review of the calculations or results.

If we may apply Sommerfeld's theory of the fine structure of X-ray spectra to higher quantum numbers, we should expect a division of the three quantum  $M$  level into three subordinate levels, because there are here the three possibilities :

$$1. \quad n=3, \quad k=1 ;$$

$$2. \quad n=3, \quad k=2 ;$$

and

$$3. \quad n=3, \quad k=3.$$

Each such combination of quantum numbers requires a separate relativity correction. We should then have the following arrangement of quantum numbers and levels in the energy level scheme of Röntgen spectra :

$$K \dots\dots 1_1$$

$$L \dots\dots \begin{cases} 2_1 \\ 2_2 \end{cases}$$

$$M \dots\dots \begin{cases} 3_1 \\ 3_2 \\ 3_3 \end{cases}$$

$$N \dots\dots \begin{cases} 4_1 \\ 4_2 \\ 4_3 \\ 4_4 \end{cases}$$

$$O \dots\dots \begin{cases} 5_1 \\ 5_2 \\ 5_3 \end{cases}$$

In the higher levels the disturbing effect of the other electrons becomes so great that the analogy fails to a considerable extent. Instead of a triplet in the  $M$  level we find experimentally two doublets of a character similar to those which we have discussed in the case of the  $L$  level. In the same way experiment reveals three doublets of this type for the  $N$  level and two for the  $O$  group.

The results of experiments show that the  $L$  level, for example, is not double but triple, and Hertz has pointed out that, in addition to the relativity doublet, there is yet a third energy level, which forms with one of the levels first named a doublet of different character. The same

author indicated the explanation of this new doublet in terms of the atomic model. The characteristic of the Hertz doublet is that  $\Delta\sqrt{\frac{\nu}{R}}$  is nearly constant from element to element. In the Moseley diagram the energy levels  $L_2$  and  $L_3$  which represent  $\sqrt{\frac{\nu}{R}}$  as a function of the atomic numbers of the elements are nearly parallel straight lines. Starting from the expression (50) for the work required to remove an electron from the  $n$ -quantum orbit, which, neglecting the relativity term, becomes

$$\frac{W}{R\hbar} = \frac{(Z-s)^2}{n^2}, \quad (56)$$

we obtain for the frequency associated with the level, replacing  $W$  by  $h\nu$ ,

$$\frac{\nu}{R} = \frac{(Z-s)^2}{n^2}, \quad (57)$$

or in agreement with the Moseley diagram,

$$\sqrt{\frac{\nu}{R}} = \frac{Z-s}{n}. \quad (58)$$

The screening constant  $s$ , however, in general, depends on the quantum numbers  $n$  and  $l$ . If we take, for the same  $n$  in the denominator, two different values  $s_1$  and  $s_2$  of the screening constant, we obtain by subtraction a doublet in which

$$\Delta\sqrt{\frac{\nu}{R}} = \frac{s_1 - s_2}{n},$$

which shows that  $\Delta\sqrt{\frac{\nu}{R}}$  is a constant, independent of the atomic number.

Of the three empirically discovered  $L$  levels,  $L_1$  and  $L_2$  form together a doublet of the first type, viz. a relativity doublet, while  $L_2$  and  $L_3$  form one of the second type, a screening doublet. On the whole, as has been shown particularly by Wentzel, we may build up the energy level diagram in such a way that the relativity and screening doublets occur alternately.

### 32. The Complete Energy Level Diagram

The entire mass of experimental data on X-ray spectra may be built up into an orderly constructed level diagram, which we will now discuss more fully, using uranium as an example. When we have once arranged in order all the lines and absorption limits for a given element, it follows from Moseley's law, which connects lines and limits from element to element, that the same scheme must be applicable to other elements also.

Various investigators have from time to time applied themselves to the task of constructing the level diagram from the available data.

Among these we may mention especially Vegard, Smekal, Sommerfeld and Wentzel, and Dauvillier. The most exhaustive research in this line, however, is due to Coster, who himself contributed much of the data, and throughout made new photographs and measurements of spectra in cases where the material at hand was most meagre and unsatisfactory. For this reason, in the subsequent discussion, we shall for the most part follow the work of Coster. It must be said, however, that the results arrived at by other authors, in particular Wentzel, are almost identical with those reached by Coster. Dauvillier is an exception to this statement, for he has postulated a level diagram with a larger number of levels in the principal groups, and has thereby, in the opinion of the author, introduced unnecessary complications. The placing of the so-called spark lines in the normal level scheme also seems unjustifiable.

The spectrum of uranium has been the most fully investigated, and we shall therefore have this element continually in mind in our study of the level diagram. In the absorption spectrum one  $K$ , three  $L$  and five  $M$  edges have been experimentally found and measured. From the  $L$  and  $M$  edges we may, as already shown on page 156, calculate seven of the  $L$  lines by differences, with a high degree of accuracy. The greatest aid in the further construction of the diagram is afforded by the relativity doublets, which are formed among the lines as shown above on page 156 ff. Of the line doublets showing the  $L_1 L_2$  frequency difference, it is evident that one line must be associated with  $L_1$ , the other with  $L_2$ . By forming differences we then obtain frequencies for the higher levels. Among the  $L$  lines we find other doublet pairs which have the character of relativity doublets, but their frequency difference is quite different from that of  $L_1 L_2$ . For such lines we must suppose that they correspond to a common  $L$  level, and that their doublet nature is due to two higher quantum energy levels, which themselves form a relativity doublet. In this way one may easily build up by trial a system of levels which, together with the experimentally known  $K$ ,  $L$ , and  $M$  levels, suffice for the calculation of all known lines by means of frequency differences between levels.

Fig. 86 shows an energy level diagram for uranium constructed in this way by Coster. The  $M$  and  $N$  lines recently measured by Hjalmar are included in this figure. Of these latter lines only the first known and strongest lines  $\alpha_1$ ,  $\alpha_2$ ,  $\beta$ ,  $\gamma$  are designated by letters, while the others are indicated in the tables by their initial and final levels.

As may be seen from Fig. 86, all the lines of the  $K$ ,  $L$ ,  $M$ , and  $N$  series which have been found experimentally may be calculated from one  $K$ , three  $L$ , five  $M$  levels, all of which have been found experimentally, and seven  $N$ , five  $O$ , and one  $P$  level, which are of a hypothetical character. Of these levels it may be proved in many cases, and in others shown to be

probable, that they are associated in pairs to form relativity doublets or screening doublets. Wentzel has pointed out that the two classes of doublets occur alternately. Thus in the diagram  $L_3$  and  $L_2$  form a screening doublet, represented in the left side of the figure by  $s$ ,  $L_2$  and  $L_1$ , a relativity doublet  $r$ ,  $M_5$  and  $M_4$  form a screening doublet,  $M_4$  and  $M_3$  a relativity doublet, and so on throughout the entire scheme. To the right are the quantum numbers which are assigned to the various levels

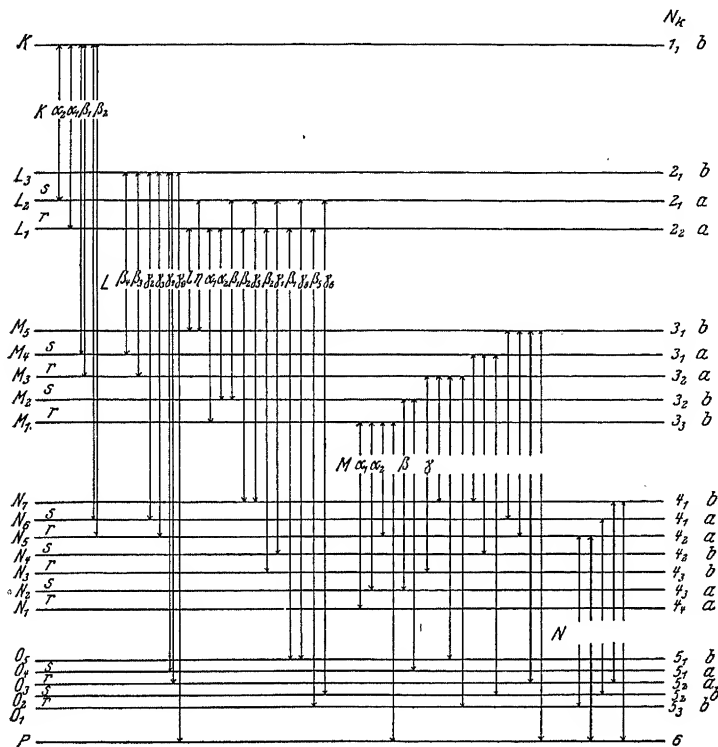


FIG. 86. Level diagram for uranium.

Requirement of selection rule:  $k \rightarrow \begin{cases} k \\ k \pm 1 \end{cases}$  $\alpha \leftrightarrow b$ 

in accordance with Sommerfeld's theory. The principal quantum number  $n$  increases by unity from one group to another, beginning with  $n$  equal to unity for the  $K$  group, and increasing up to  $n$  equal to 6 for the  $P$  level. The rule for the auxiliary quantum number is that it shall have the same value for the two levels of a screening doublet, while for a relativity doublet it differs by unity for the two components.

It is at once evident on inspection of the diagram that there are many possible transitions between levels which are not represented by any lines, and among these we observe first that no transitions occur between levels belonging to the same group. Coster has made exceedingly careful investigations of the spectrum in the regions where lines corresponding to transitions between  $L$  levels might be expected, but he found no traces of such lines.

A first *selection rule* that was discovered experimentally may be stated thus: in an electron-transition *the principal quantum number must change*. In the domain of optical spectra this is known not to be the case.

A second selection rule which also appears from the experimental data, and which is identical with that in optical spectra, is the one first theoretically derived by Rubinowicz, and then by Bohr, on general considerations arising from his correspondence principle. According to this second selection rule only those transitions occur in which the *auxiliary quantum number either remains constant or changes by one unit*. Experiment further shows that in general the transitions in which the *auxiliary quantum number diminishes by unity* give rise to lines of greater intensity.

These two selection rules, however, will not suffice, for we should still expect many more lines than are actually found. We must, therefore, have some additional restriction on the transitions from one orbit to another. The third selection rule was discovered independently by Coster and Wentzel. In order to express the rule clearly Coster made use of the letters  $a$  and  $b$ , assigning in a suitable way one or the other of them to each of the levels, while Wentzel stated it numerically, in a way similar to that in which the second rule is expressed above. Of course it is immaterial which form is adopted, since they are only symbolic methods of representing briefly the empirical facts, of which we are as yet unable to explain the real meaning. It may be stated, however, that Coster and Bohr, in a recent joint paper, have also formulated the third selection rule in numerical terms. All three systems of representation are essentially identical. The first system of Coster is used in this book, because on the whole it seems to the author to be the clearest, and to bring out better the *purely empirical nature* of the rule.

According to Coster's notation all relativity doublets are denoted by the same letter, either  $a$  or  $b$ , while the screening doublets are designated by different letters. The complete notation appears in Fig. 86. By comparing these designations of the levels with the observed lines in the level diagram, we see that the selection rule may be expressed as

$$a \rightarrow b.$$

TABLE 33.

Evaluation of energy levels for uranium.

	Calculation.	Experimental value.	Weighted mean.
$M_1$		$261.01 \pm 0.3$	
$M_2$	$M\beta_1 - Ma_2 = 12.8 \pm 0.5$ $La_1 - La_2 = 12.8 \pm 0.1$ $M_2 - M_1 = 12.8 \pm 0.1$ $= 261.01 \pm 0.3$ $+ 12.8 \pm 0.1$ $\hline 273.8 \pm 0.4$	$273.99 \pm 0.3$	$273.9 \pm 0.3$
$M_3$		$317.2 \pm 0.9$	
$M_4$	$L\beta_3 - L\beta_4 = 63.8 \pm 1.8$ $M_4N_7 - M_3N_7 = 63.7 \pm 1.7$ $M_4 - M_3 = 63.7 \pm 1.0$ $= 317.2 \pm 0.9$ $+ 63.7 \pm 1.0$ $\hline 380.9 \pm 1.9$	$382.1 \pm 2.5$	$381.3 \pm 1.9$
$L_1$	$M_1 + La_1 = 261.0 \pm 0.3$ $+ 1003.2 \pm 0.1$ $\hline = 1264.2 \pm 0.4$ $M_2 + La_2 = 273.9 \pm 0.3$ $+ 990.4 \pm 0.2$ $\hline = 1264.3 \pm 0.5$	$[1263.2 \pm 0.5]^*$	$1264.2 \pm 0.4$
$L_2$	$M_2 + L\beta_1 = 273.9 \pm 0.3$ $+ 1269.1 \pm 0.1$ $\hline = 1543.0 \pm 0.4$	$[1539.8 \pm 0.5]^*$	$1543.0 \pm 0.9$
$M_5$	$L_1 - L_1 = 1264.2 \pm 0.4$ $- 855.8 \pm 0.2$ $\hline = 408.4 \pm 0.6$ $L_2 - L_1 = 1543.0 \pm 0.4$ $- 1135.0 \pm 0.4$ $\hline = 408.0 \pm 0.8$	$408.9 \pm 3.0$	$408.3 \pm 0.6$
$L_3$	$M_3 + L\beta_3 = 317.2 \pm 0.9$ $+ 1286.3 \pm 0.9$ $\hline = 1603.5 \pm 1.8$	$[1602.9 \pm 2.1]^*$	$1603.5 \pm 1.8$
$N_1$	$M_1 - Ma = 261.0 \pm 0.3$ $- 233.6$ $\hline = 27.4$		$27.4$

etc.

\*The  $L$  absorption limits were measured by Daune and Patterson by the ionization method; these values seem to show a slight discrepancy throughout.

We will now make a numerical test of this level scheme which will demonstrate its applicability. In this test we may start from the eight experimentally determined energy levels (one  $K$ , three  $L$ , and five  $M$  levels), and first calculate the  $N$ ,  $O$ , and  $P$  values from certain lines which terminate at those levels, then we may use these latter levels, together with those experimentally determined, to calculate the entire system of lines. But since the experimental determination of the levels is subject to considerably larger error than are the line measurements, we make use of lines and certain absorption limits together, taking into consideration the accuracy of measurement in each case, and so arrive at a system of levels in which the uncertainty has been reduced to as small an amount as possible. Table 33 shows how, starting from the experimentally accurate value of the  $M_1$  limit, certain others of the energy levels may be evaluated. Of course we might proceed here in various ways, and the table only serves to demonstrate one of them.

As a final result we obtain for the energy levels of the uranium spectrum the following :

$K$	8447.0	$N_7$	106.6	$O_5$	23.9
		$N_6$	95.2	$O_4$	18.1
$L_3$	1603.5	$N_5$	76.4	$O_3$	11.8
$L_2$	1543.0	$N_4$	56.2	$O_2$	7.5
$L_1$	1264.2	$N_3$	53.8	$O_1$	5.8
		$N_2$	28.2		
$M_5$	408.3	$N_1$	27.4	$P$	1.7
$M_4$	381.3				
$M_3$	317.2				
$M_2$	273.9				
$M_1$	261.0				

For the levels which lie out beyond  $O_1$  we obtain no values differing perceptibly from the 1.7 given above. By reasons of analogy, and under the very probable assumption that the same rules of selection hold here also, we may resolve the  $P$  group, with the help of the five lines which arise from combination of a  $P$  level with one of lower quantum number. Since this would be rather an arbitrary proceeding, all  $P$  levels are replaced by a single one in the diagram. The following table shows what  $P$  levels would be necessary to explain the lines according to the above hypotheses. On the left we have the lower levels to which the observed lines are attributed, while above are the possible  $P$  levels, from analogy with the other groups of levels. Transitions to which the observed lines might be due are indicated by crosses.



TABLE 34.

Lines which correspond to transitions from  $P$  levels.

	$6_1b.$	$6_1a.$	$6_2a.$	$6_2b.$	$6_3b.$	$6_3a.$	$6_4a.$	$6_4b.$
$2_1b$	—	×	×	—	—	—	—	—
$3_1b$	—	×	×	—	—	—	—	—
$3_3b$	—	—	×	—	—	×	×	—
$4_1b$	—	×	×	—	—	—	—	—
$4_2a$	×	—	—	×	×	—	—	—

It may be seen at once that three  $P$  levels suffice to account for the observed lines, namely :

$$\begin{aligned} &6_1b, \\ &6_1a, \\ &6_2a, \end{aligned}$$

and we thus observe that the group of three  $P$  levels is analogous to the triple  $L$  group, just as the  $O$  group resembles the  $M$  group.

Table 35 shows the extent of the agreement between numerical values of  $\frac{\nu}{R}$  for the spectral lines and the energy level values given above; it also illustrates the application of the selection rule. The lines which are prohibited by the selection rule are indicated by  $\nu$ , and those not found experimentally by a horizontal stroke. In the  $L$  series the agreement is almost complete, although in certain cases, where weak lines are supposed to exist, they would lie so near to other lines that their presence is not yet definitely proved; apart from this, all the lines conforming to the selection rule have been found. Among the lines of the  $L$  series of uranium which have been measured accurately, there are none which do not fit into the energy level scheme, but for several other elements Coster has found the very weak lines  $\beta_9$  and  $\beta_{10}$  which are contrary to the selection rule, for they apparently correspond to the transitions  $L_3M_1$ , and  $L_3M_2$ . Since these transitions are of the type

$$\begin{aligned} \beta_9 & \quad . \quad . \quad . \quad 2_1b \rightleftharpoons 3_3b, \\ \beta_{10} & \quad . \quad . \quad . \quad 2_1b \rightleftharpoons 3_2b, \end{aligned}$$

they both transgress the  $ab$  rule. The line  $\beta_9$  is also contrary to the other selection rule, which requires that the auxiliary quantum number shall either remain constant or change at most by unity. As already stated, however, the lines are extremely faint, and perhaps they may be explained otherwise.

TABLE 35. Numerical representation of the level diagram for uranium containing values of  $\bar{\nu}$  for all transitions to be expected according to the selection rule and for the corresponding emission and absorption frequencies found by experiment.

	Surf. abs. freq.	P	O <sub>1</sub> 5-8	O <sub>2</sub> 7-5	O <sub>3</sub> 11-8	O <sub>4</sub> 18-1	O <sub>5</sub> 23-0	N <sub>1</sub> 27-4	N <sub>2</sub> 28-2	N <sub>3</sub> 53-8	N <sub>4</sub> 56-2	N <sub>5</sub> 76-4	N <sub>6</sub> 95-2	N <sub>7</sub> 100-6	M <sub>1</sub> 261-0	M <sub>2</sub> 273-0	M <sub>3</sub> 317-2	M <sub>4</sub> 381-3	M <sub>5</sub> 408-3
<i>L</i> series	L <sub>3</sub> c <sub>1</sub>	1603-5	1601-8	—	1591-7	1585-4	—	—	—	—	—	1527-1	1508-3	—	—	—	1286-3	1222-5	—
	L <sub>2</sub> c <sub>1</sub>	1602-9	1601-8	—	1588-1	—	—	—	—	—	—	1526-41	1507-82	—	—	—	1286-29	1222-53	—
	L <sub>2</sub> c <sub>2</sub>	1543-0	—	—	—	—	1519-1	—	—	—	—	—	—	1436-4	—	—	—	—	1134-7
	L <sub>1</sub> c <sub>1</sub>	1539-8	—	—	1537-76	—	—	—	—	—	—	1486-98	—	1436-4	—	—	1269-1	—	1134-95
<i>M</i> series	L <sub>1</sub> c <sub>2</sub>	1264-2	—	—	1258-5	—	—	—	—	—	—	—	—	1157-6	—	—	1269-08	—	855-9
	L <sub>1</sub> c <sub>3</sub>	1263-2	—	—	1258-4	—	—	—	—	—	—	—	—	1158-7	—	—	—	—	855-84
	M <sub>6</sub> c <sub>1</sub>	408-3	406-6	—	—	—	—	—	—	—	—	—	—	—	—	—	—	—	—
	M <sub>6</sub> c <sub>2</sub>	408-9	406-5	—	—	—	—	—	—	—	—	—	—	—	—	—	—	—	—
<i>N</i> series	M <sub>6</sub> c <sub>3</sub>	381-3	—	—	—	—	—	—	—	—	—	—	—	—	—	—	—	—	—
	M <sub>6</sub> c <sub>4</sub>	382-1	—	—	—	—	—	—	—	—	—	—	—	—	—	—	—	—	—
	M <sub>6</sub> c <sub>5</sub>	317-2	—	—	—	—	—	—	—	—	—	—	—	—	—	—	—	—	—
	M <sub>6</sub> c <sub>6</sub>	317-2	—	—	—	—	—	—	—	—	—	—	—	—	—	—	—	—	—
<i>N</i> series	M <sub>6</sub> c <sub>7</sub>	273-9	—	—	—	—	—	—	—	—	—	—	—	—	—	—	—	—	—
	M <sub>6</sub> c <sub>8</sub>	274-0	—	—	—	—	—	—	—	—	—	—	—	—	—	—	—	—	—
	M <sub>6</sub> c <sub>9</sub>	261-0	259-3	—	—	—	—	—	—	—	—	—	—	—	—	—	—	—	—
	M <sub>6</sub> c <sub>10</sub>	261-0	259-3	—	—	—	—	—	—	—	—	—	—	—	—	—	—	—	—
<i>N</i> series	N <sub>7</sub> c <sub>1</sub>	106-6	104-9	—	—	—	—	—	—	—	—	—	—	—	—	—	—	—	—
	N <sub>6</sub> c <sub>1</sub>	—	104-8	—	—	—	—	—	—	—	—	—	—	—	—	—	—	—	—
	N <sub>6</sub> c <sub>2</sub>	95-2	—	—	—	—	—	—	—	—	—	—	—	—	—	—	—	—	—
	N <sub>5</sub> c <sub>1</sub>	76-4	74-7	—	—	—	—	—	—	—	—	—	—	—	—	—	—	—	—
<i>N</i> series	N <sub>5</sub> c <sub>2</sub>	—	74-43	—	—	—	—	—	—	—	—	—	—	—	—	—	—	—	—
	N <sub>4</sub> c <sub>1</sub>	56-2	—	—	—	—	—	—	—	—	—	—	—	—	—	—	—	—	—
	N <sub>4</sub> c <sub>2</sub>	—	—	—	—	—	—	—	—	—	—	—	—	—	—	—	—	—	—
	N <sub>3</sub> c <sub>1</sub>	53-8	—	—	—	—	—	—	—	—	—	—	—	—	—	—	—	—	—
<i>N</i> series	N <sub>3</sub> c <sub>2</sub>	—	—	—	—	—	—	—	—	—	—	—	—	—	—	—	—	—	—
	N <sub>2</sub> c <sub>1</sub>	28-2	—	—	—	—	—	—	—	—	—	—	—	—	—	—	—	—	—
	N <sub>2</sub> c <sub>2</sub>	—	—	—	—	—	—	—	—	—	—	—	—	—	—	—	—	—	—
	N <sub>1</sub> c <sub>1</sub>	27-4	—	—	—	—	—	—	—	—	—	—	—	—	—	—	—	—	—

<i>Remarks on the L series:</i>														
$L_3P$ 1601-8 } (measured for														
$L_3O_3$ 1588-1 } uranium by														
$L_2N_7$ 1436-4 } Dauvillier.)														
$L_2O_6 = \gamma_s$ found for lighter elements.														
$L_3M_1 = \beta_0$ } Very weak and														
$L_3M_2 = \beta_{10}$ } lines, contrary														
selection to rule:														
found for cer-														
tain elements by														
Coster.)														
<i>Remarks on the M series:</i>														
$M_1O_2$ missing ( $k \rightarrow k$ )														
$M_2O_3$ nearly coincides with														
$M_3N_3$ ( $k \rightarrow k$ )														
$M_3O_3$ missing ( $k \rightarrow k+1$ )														
$M_4O_4$ missing ( $k \rightarrow k$ )														
$M_4O_5$ missing ( $k \rightarrow k$ )														
<i>Remarks on the N series:</i>														
$N_7O_4$ missing ( $k \rightarrow k$ )														
$N_6O_5$ missing ( $k \rightarrow k$ )														
$N_5O_2$ missing ( $k \rightarrow k$ )														

<i>Meaning of Symbols:</i>														
v = contrary to selection rule.														
x = nearly coincides with another observed line.														
— = not found experimentally.														
[ ] = wave-length too long to be observed.														
/ = uncertain because the P level is not yet resolved.														

Remarks on the *L* series:

$L_3P$  1601-8 (measured for  
 $L_3O_3$  1588-1 } uranium by  
 $L_2N_7$  1436-4 } Dauvillier.)  
 $L_2O_5 = \gamma_8$  found for lighter  
elements.

$L_3M_1 = \beta_9$  } Very weak and  
 $L_3M_2 = \beta_{10}$  } rather uncertain  
lines, contrary  
selection to rule:  
found for cer-  
tain elements by  
Coster.)

Remarks on the *M* series:

$M_3O_2$  missing ( $k \rightarrow k$ )  
 $M_2O_3$  nearly coincides with  
 $M_3N_3$  ( $k \rightarrow k$ )  
 $M_1O_3$  missing ( $k \rightarrow k+1$ )  
 $M_5O_4$  missing ( $k \rightarrow k$ )  
 $M_4O_5$  missing ( $k \rightarrow k$ )

Remarks on the *N* series:

$N_7O_4$  missing ( $k \rightarrow k$ )  
 $N_6O_5$  missing ( $k \rightarrow k$ )  
 $N_5O_2$  missing ( $k \rightarrow k$ )

Meaning of Symbols:

v = contrary to selection rule.

x = nearly coincides with another  
observed line.

— = not found experimentally.

[ ] = wave-length too long to be  
observed.

/ = uncertain because the *P* level is  
not yet resolved.

For some elements, Auger and Dauvillier have found a doublet ( $s, t$ ) corresponding to the transitions  $L_1M_4$  and  $L_1M_3$ . Both lines, which are rather faint, are contrary to the  $ab$  rule. The wave-lengths and the experimental values  $\frac{\nu}{R}$  are given in the following table, together with the values of  $\frac{\nu}{R}$  calculated from the energy levels in Table 37.

		$\lambda$	$\Delta\lambda$	$\frac{\nu}{R}$ obs.	$\frac{\nu}{R}$ calc.
73 Ta	- -	$t (L_1M_4)$	1671.7	545.1	547.6
		$s (L_1M_3)$	1608.6	566.5	567.9
74 W	- -	$t (L_1M_4)$	1621.6	562.0	562.7
		$s (L_1M_3)$	1561.0	583.8	584.2
77 Ir	- -	$t (L_1M_4)$	1490.0	611.6	610.3
		$s (L_1M_3)$	1429.5	637.5	636.5
78 Pt	- -	$t (L_1M_4)$	1449.0	628.9	624.7
		$s (L_1M_3)$	—	—	—
79 Au	- -	$t (L_1M_4)$	1410.0	646.3	643.4
		$s (L_1M_3)$	1348.1	676.0	675.7
92 U	- -	$t (L_1M_4)$	—	—	—
		$s (L_1M_3)$	961.7	947.6	947.1

As seen from this table the doublet is a relativity doublet, with constant  $\Delta\lambda$ .

In the  $M$  and the  $N$  series certain lines are missing which would be expected according to the selection rule. In the case of the  $N$  series this is not surprising, for here, on account of the long wave-length, all the lines are so faint that they are observed only with great difficulty. In the  $M$  series it happens that the lines which have not been found correspond to just those transitions  $k \rightarrow k$  and  $k \rightarrow k+1$  which, throughout the spectra, give rise to fainter lines than the transition  $k \rightarrow k-1$ .

Thus we see that, on the whole, the level diagram with its selection rules gives a very complete and comprehensive representation of the entire empirical material, both for the emission spectra and for the absorption spectra. The energy levels, which we are able to evaluate from both kinds of spectra, are, of course, fundamental for the structure of the atom, and in this respect are more important than the directly measurable *transitions* between these levels. There is no doubt that the knowledge of the energy levels, which characterise an atom, is a much more valuable thing for the investigation of the atom than, for example, the *atomic weight* of the element concerned, and we therefore see how important the determination of these levels is for the physics of the atom. But just in

those places in the periodic system where they are of the greatest interest, namely, where, as Bohr has shown, changes occur in the outer shell of the atom, the data are at present not nearly as satisfactory as might be desired. X-ray spectroscopy has here an important gap to fill.

Proceeding from uranium, we might now introduce into such a diagram the corresponding lines and limits connected by the Moseley law for all the other elements. A glance at the table of wave-lengths shows, however, that the great wealth of lines which we have in the case of uranium does not continue far down the periodic system of the elements. Several lines disappear even for the next few elements, and only a very few may be followed down to the first elements of the system. This decrease in the number of lines results in a corresponding simplification of the level

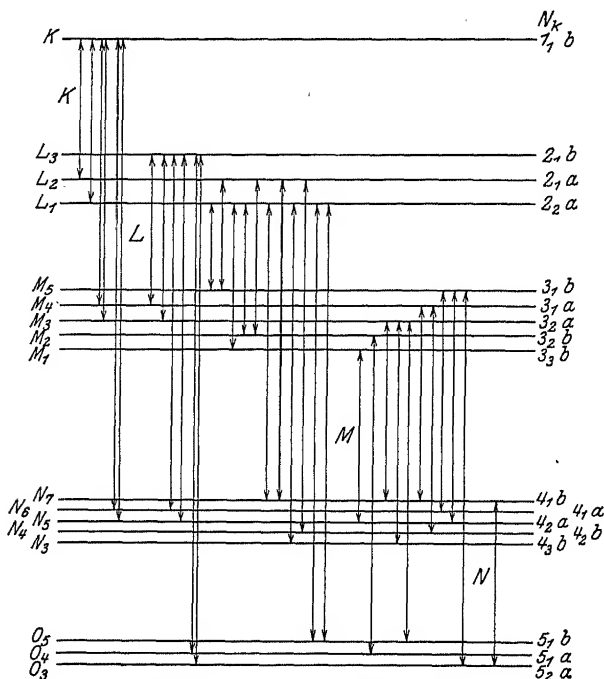


FIG. 87. Energy level diagram for Xenon.

diagram. Here we experience the great difficulty that we are unable to determine experimentally with certainty at what element a given line really ceases to exist. As a rule the intensity gradually decreases, until we are no longer certain whether the line is merely indistinguishable against the background of diffuse blackening, or whether it actually does not exist. In any case it is very evident that a diagram of much more simple construction suffices for the lighter elements. In consideration of

this point, we introduce the following table containing the atomic number of the last element for which the existence of the lines belonging to the different levels has been observed.

TABLE 36.

Elements of lowest atomic number for which the lines belonging to the levels indicated have definitely been shown to exist. (From results of Coster and Hjalmar.)

Level.	<i>P</i>	<i>O</i> <sub>1</sub>	<i>O</i> <sub>2</sub>	<i>O</i> <sub>3</sub>	<i>O</i> <sub>4</sub>	<i>O</i> <sub>5</sub>	<i>N</i> <sub>1</sub>	<i>N</i> <sub>2</sub>	<i>N</i> <sub>3</sub>	<i>N</i> <sub>4</sub>	<i>N</i> <sub>5</sub>	<i>N</i> <sub>6</sub>	<i>N</i> <sub>7</sub>
Line of <i>L</i> series - -	92	73*	73	49	49	73	—	—	40	40	37	37	37
Line of <i>M</i> series - -	90	90	90	90	81	90	67	66	71	76	76	92	76
Line of <i>N</i> series - -	90	92	90	90	—	—	—	—	—	—	90	90	90
	90	73	73	49	49	73	67	66	40	40	37	37	37

From Table 36 it appears that, to account for the spectra, the *P* levels are necessary only for atomic numbers 92 and 90, *O*<sub>1</sub> and *O*<sub>2</sub> are necessary only as far as element 73, *N*<sub>1</sub> and *N*<sub>2</sub> to 66, and *O*<sub>3</sub>, *O*<sub>4</sub>, and *O*<sub>5</sub> not farther than 49. As a matter of fact, *O*<sub>5</sub> has not been detected experimentally beyond 73, but since *O*<sub>3</sub> and *O*<sub>4</sub> lie farther out than *O*<sub>5</sub>, and they have been traced as far as 49, it is reasonable to assume that *O*<sub>5</sub> exists at least to the same limit. Hence the levels disappear with decreasing atomic number of the elements in the following order :

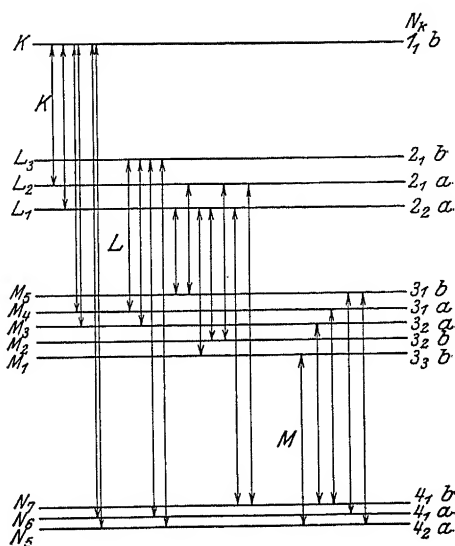
*P**O*<sub>1</sub>*O*<sub>2</sub>*N*<sub>1</sub>*N*<sub>2</sub>*O*<sub>3</sub>*O*<sub>4</sub>*O*<sub>5</sub>*N*<sub>3</sub>*N*<sub>4</sub>

FIG. 88. Level diagram for Krypton.

It is very probable, indeed, that the number of levels present is closely related to the development of the atoms of the noble gases, and Coster has drawn the diagrams which might be supposed to represent the noble gases niton 86, xenon 54, and krypton 36. Fig. 87 is the diagram for xenon, Fig. 88 that for krypton, while that for niton may be assumed to be identical with that of uranium shown in Fig. 86.

\* 51 according to Dauvillier.

The chief results of spectroscopic measurements are embodied in Tables 37 and 38, which consist of a collection of energy level values of the various elements, revised by Nishina from an article by Bohr and Coster. In these tables  $\frac{1}{R}$  is taken as a measure of the energy of the levels.

It has been shown in the preceding chapters that the theory of Sommerfeld, which started from the general atomic model for hydrogen, namely, a positively charged nucleus round which a single electron revolves, could give in an astonishingly high degree a numerical representation of many facts found experimentally. The influence of the electrons belonging to the different shells was accounted for in a fairly simple manner.

Landé has recently pointed out that another view seems in some respects better adapted to serve as a basis for a theory of X-ray spectra. If the system for the energy levels of the atom as found by X-ray spectra be represented in a way usually applied in the case of ordinary spectra, and first used in this field by Grotrian, we obtain the scheme shown in Fig. 88B. In this system every energy level is represented by three quantum numbers,  $n$ ,  $k$ ,  $j$ , as generally used in optical spectra. The azimuthal quantum number  $k$  does not agree with the  $k$  which was used in the former schemes, and which was supported by the relativity character of the doublets in the theory of Sommerfeld. " $j$ " is the "inner" quantum number which in ordinary spectra gives the orientation of the orbit. It may be seen that this representation of X-ray spectra is quite analogous to that of the *optical arc-spectra of the alkali group*. In analogy with the notation used in that connection, one may call the  $K$  level  $1s$ , whereas the three  $L$  levels correspond to  $2s$ ,  $2p_2$ , and  $2p_1$ ; the  $M$  levels to  $3s$ ,  $3p_2$ ,  $3p_1$ ,  $3d_2$ ,  $3d_1$ , and so on. The most satisfactory way, then, of denoting the levels by means of indices to the letters  $L$ ,  $M$ , etc., is to change the numbering formerly used. To distinguish these notations from the previous one, we shall—following the notation introduced by Bohr and Coster—denote the indices by the Roman numerals. The different notations are collected in the following table :

Earlier notation :

$K$	$L_3$	$L_2$	$L_1$	$M_5$	$M_4$	$M_3$	$M_2$	$M_1$	$N_7$	$N_6$	$N_5$	$N_4$	$N_3$	$N_2$	$N_1$
$1_1$	$2_1$	$2_1$	$2_2$	$3_1$	$3_1$	$3_2$	$3_2$	$3_3$	$4_1$	$4_1$	$4_2$	$4_2$	$4_3$	$4_3$	$4_4$
$b$	$b$	$a$	$a$	$b$	$a$	$a$	$b$	$b$	$b$	$a$	$a$	$b$	$b$	$a$	$a$

Present notation :

$K$	$L_I$	$L_{II}$	$L_{III}$	$M_I$	$M_{II}$	$M_{III}$	$M_{IV}$	$M_V$	$N_I$	$N_{II}$	$N_{III}$	$N_{IV}$	$N_V$	$N_{VI}$	$N_{VII}$
$1_{11}$	$2_{11}$	$2_{21}$	$2_{22}$	$3_{11}$	$3_{21}$	$3_{22}$	$3_{32}$	$3_{33}$	$4_{11}$	$4_{21}$	$4_{22}$	$4_{32}$	$4_{33}$	$4_{43}$	$4_{44}$
$1s$	$2s$	$2p_2$	$2p_1$	$3s$	$3p_2$	$3p_1$	$3d_2$	$3d_1$	$4s$	$4p_2$	$4p_1$	$4d_2$	$4d_1$	$4b_2$	$4b_1$

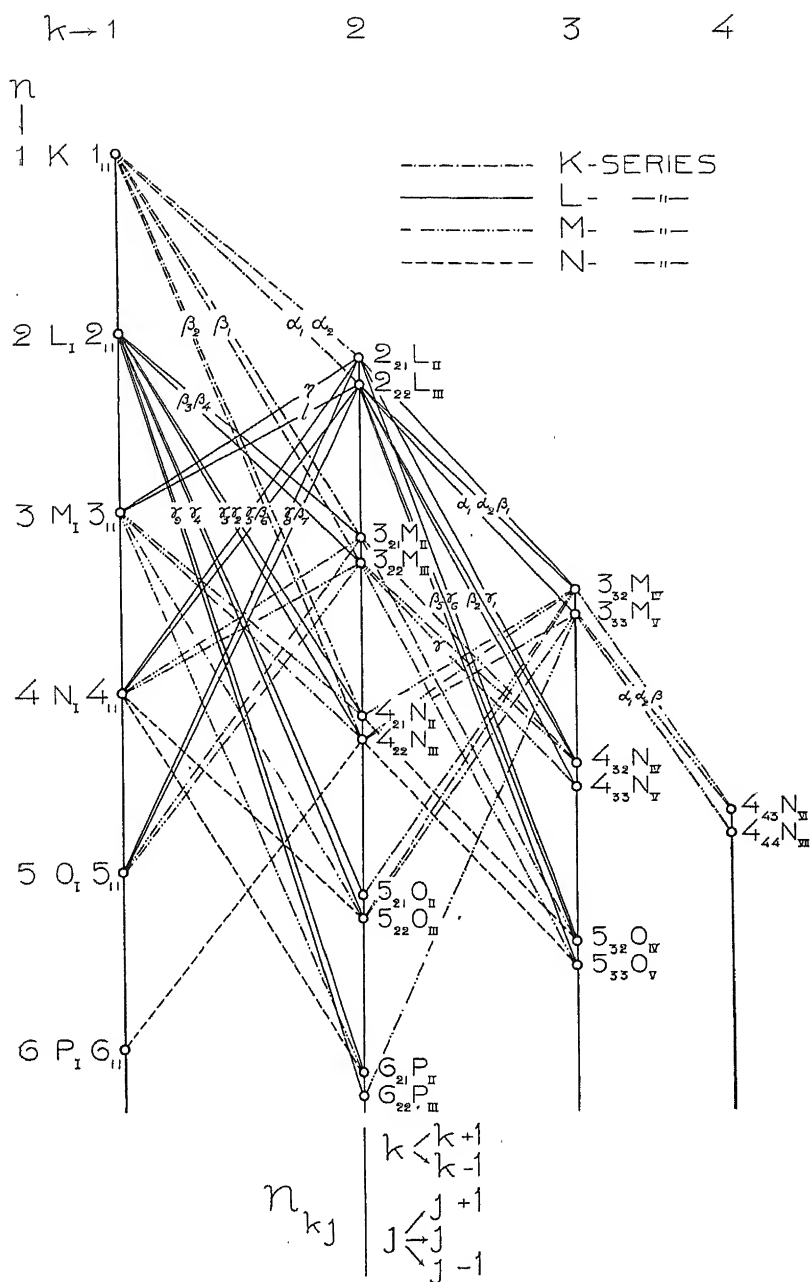


FIG. 88B.

TABLE 37.

	K	$L_3$	$L_2$	$L_1$	$M_5$	$M_4$	$M_3$	$M_2$	$M_1$
92 U	8477.0	1603.5	1543.1	1264.3	408.9	382.1	317.2	274.0	261.0
90 Th	8073.5	1509.7	1451.5	1200.6	381.6	354.4	298.0	256.6	244.9
83 Bi	6646.7	1207.9	1159.4	990.0	295.9	273.6	234.0	199.4	191.4
82 Pb	6463.0	1169.3	1121.9	960.5	283.8	262.3	226.0	190.5	183.0
81 Tl	6289.0	1132.4	1084.2	933.2	273.9	253.8	219.2	184.8	176.8
80 Hg	6115.9	1094.6	1048.6	906.1	—	—	—	—	—
79 Au	5940.4	1060.2	1014.4	878.5	252.9	235.1	202.8	169.3	163.0
78 Pt	5764.0	1026.8	978.7	852.0	243.4	227.3	198.0	162.3	156.4
74 W	5113.8	893.0	850.6	752.1	208.1	191.3	169.8	138.3	133.7
73 Ta	—	862.2	820.8	728.0	199.5	183.2	162.9	132.2	127.8
72 Hf	—	830.7	791.4	704.6	191.9	174.8	155.5	126.8	122.7
71 Lu	—	802.6	762.9	681.2	183.8	168.6	150.9	120.9	117.2
70 Yb	—	774.6	735.4	659.2	177.1	162.2	145.8	116.4	112.8
69 Tm	—	746.8	708.6	637.3	170.3	155.5	140.2	111.7	108.4
68 Er	—	719.6	682.6	615.9	163.6	148.8	134.7	107.2	104.0
67 Ho	4115.9	693.2	657.1	594.7	157.1	142.7	129.3	102.7	99.8
66 Dy	3972.5	667.7	632.2	574.2	151.2	136.9	124.5	98.5	95.8
65 Tb	—	642.6	608.3	553.9	145.0	131.0	119.6	94.2	91.6
64 Gd	3711.9	618.2	584.6	533.9	139.0	125.5	115.0	90.0	87.7
63 Eu	3583.4	594.3	561.5	514.4	133.1	120.2	110.3	86.0	83.8
62 Sm	3457.0	571.2	538.9	495.0	127.2	114.7	105.8	81.9	79.9
60 Nd	3214.2	526.2	495.5	457.8	116.5	104.8	96.8	74.2	72.5
59 Pr	3093.3	504.3	474.6	439.6	111.6	99.3	92.4	70.3	68.9
58 Ce	2972.2	483.3	454.1	421.9	106.2	94.6	88.1	66.7	65.4
57 La	—	462.9	434.2	404.4	100.7	90.0	84.0	62.9	61.7
56 Ba	2756.4	441.9	414.3	386.7	95.4	84.6	79.0	58.8	57.6
55 Cs	2649.1	421.8	394.9	369.3	89.8	79.3	74.4	54.6	53.6
53 I	2448.3	382.6	357.6	336.0	79.3	69.0	64.9	46.8	45.9
53 Te	2345.0	364.1	340.3	320.1	74.5	64.4	60.5	43.2	42.4
51 Sb	2241.7	346.1	323.6	305.3	70.4	60.0	56.4	40.4	39.7
50 Sn	—	329.4	306.2	289.5	65.3	56.2	53.1	36.5	35.9
47 Ag	1878.9	279.5	260.0	247.3	53.3	43.5	41.2	27.9	27.5
45 Rh	1709.1	253.4	231.4	220.9	45.8	39.7	38.5	22.5	22.2
42 Mo	1473.1	211.9	193.9	186.2	37.6	30.5	29.7	17.4	17.2
41 Nb	1401.3	—	181.4	174.4	35.1	—	—	15.0	14.9
40 Zr	1325.8	—	169.6	163.5	31.4	—	—	13.0	
29 Cu	661.1	—	71.3	69.8	—	5.2	—	0	—
28 Ni	612.0	—	62.6	61.3	—	3.3	—	—	—
27 Co	568.9	—	59.7	58.5	—	5.3	—	—	—
26 Fe	523.8	—	53.2	52.2	—	4.0	—	—	—
25 Mn	482.4	—	48.7	47.9	—	4.2	—	—	—
24 Cr	441.1	—	43.0	42.3	—	3.5	—	—	—
23 Va	402.3	—	38.2	37.6	—	2.6	—	—	—
22 Ti	365.4	—	32.6	32.2	—	2.2	—	—	—
21 Sc	331.2	—	30.3	30.0	—	2.7	—	—	—
20 Ca	297.5	—	25.9	25.6	—	2.0	—	—	—
19 K	265.3	—	21.4	21.2	—	0.9	—	—	—
17 Cl	207.8	—	14.8	14.7	—	0.4	—	—	—
16 S	181.8	—	11.8		—	0.3	—	—	—
15 P	158.3	—	9.9	—	—	0.8	—	—	—
13 Al	114.7	—	5.2	—	—	0	—	—	—
12 Mg	95.8	—	3.5	—	—	—	—	—	—



Energy level values ( $\nu/R$ ).[illegible]

TABLE 38.

	$K$	$L_3$	$L_2$	$L_1$	$M_5$	$M_4$	$M_3$	$M_2$	$M_1$
92 U	92.07	40.04	39.28	35.56	20.22	19.55	17.81	16.55	16.16
90 Th	89.85	38.85	38.10	34.65	19.53	18.83	17.26	16.02	15.65
83 Bi	81.53	34.75	34.05	31.46	17.20	16.54	15.32	14.12	13.83
82 Pb	80.39	34.19	33.50	30.99	16.85	16.20	15.08	13.80	13.53
81 Tl	79.31	33.65	32.92	30.55	16.55	15.93	14.81	13.60	13.30
80 Hg	78.20	33.08	32.38	30.10	—	—	—	—	—
79 Au	77.07	32.54	31.85	29.64	15.90	15.33	14.25	13.01	12.77
78 Pt	75.92	32.01	31.28	29.19	15.60	15.08	13.99	12.74	12.51
74 W	71.51	29.883	29.166	27.425	14.43	13.83	13.03	11.76	11.56
73 Ta	—	29.362	28.650	26.982	14.13	13.54	12.76	11.50	11.31
72 Hf	—	28.822	28.131	26.545	13.85	13.22	12.47	11.26	11.08
71 Lu	—	28.331	27.620	26.101	13.56	12.98	12.28	11.00	10.82
70 Yb	—	27.831	27.118	25.675	13.31	12.74	12.08	10.79	10.62
69 Tm	—	27.331	26.630	25.245	13.05	12.47	11.84	10.57	10.41
68 Er	—	26.826	26.127	24.816	12.79	12.20	11.61	10.35	10.20
67 Ho	64.16	26.328	25.634	24.387	12.53	11.94	11.37	10.14	9.99
66 Dy	63.03	25.840	25.144	23.963	12.29	11.70	11.16	9.93	9.79
65 Tb	—	25.349	24.664	23.534	12.04	11.45	10.94	9.70	9.57
64 Gd	60.93	24.864	24.179	23.107	11.79	11.20	10.73	9.49	9.36
63 Eu	59.86	24.379	23.697	22.679	11.54	10.97	10.50	9.27	9.15
62 Sm	58.80	23.899	23.214	22.249	11.28	10.71	10.28	9.05	8.94
60 Nd	56.69	22.939	22.260	21.395	10.79	10.24	9.84	8.61	8.52
59 Pr	55.62	22.456	21.785	20.967	10.57	9.96	9.61	8.39	8.30
58 Ce	54.52	21.984	21.310	20.541	10.30	9.72	9.39	8.17	8.09
57 La	—	21.514	20.837	20.108	10.03	9.49	9.17	7.93	7.86
56 Ba	52.50	21.029	20.355	19.664	9.77	9.20	8.89	7.67	7.59
55 Cs	51.47	20.537	19.872	19.218	9.47	8.90	8.62	7.39	7.32
53 I	49.48	19.560	18.910	18.330	8.90	8.31	8.05	6.84	6.78
52 Te	48.43	19.082	18.446	17.890	8.63	8.02	7.78	6.58	6.51
51 Sb	47.35	18.605	17.988	17.472	8.39	7.74	7.51	6.36	6.30
50 Sn	—	18.149	17.499	17.016	8.08	7.50	7.29	6.04	5.99
47 Ag	43.35	16.72	16.12	15.73	7.30	6.60	6.42	5.28	5.24
45 Rh	41.34	15.90	15.20	14.86	6.76	6.30	6.16	4.74	4.71
42 Mo	38.38	14.54	13.92	13.64	6.13	5.52	5.40	4.17	4.15
41 Nb	37.43	—	13.47	13.21	5.92	—	—	3.87	3.86
40 Zr	36.41	—	13.02	12.79	5.60	—	—	3.61	
29 Cu	25.71	—	8.44	8.36	—	2.28		0	
28 Ni	24.74	—	7.91	7.83	—	1.82		—	
27 Co	23.85	—	7.73	7.65	—	2.30		—	
26 Fe	22.89	—	7.29	7.23	—	2.00		—	
25 Mn	21.96	—	6.98	6.92	—	2.05		—	
24 Cr	21.00	—	6.56	6.50	—	1.87		—	
23 Va	20.06	—	6.18	6.13	—	1.61		—	
22 Ti	19.11	—	5.71	5.66	—	1.48		—	
21 Se	18.20	—	5.51	5.48	—	1.64		—	
20 Ca	17.25	—	5.09	5.06	—	1.42		—	
19 K	16.29	—	4.63	4.61	—	0.95		—	
17 Cl	14.42	—	3.85	3.84	—	0.63		—	
16 S	13.48	—	3.44		—	0.55		—	
15 P	12.58	—	3.15		—	0.89		—	
13 Al	10.71	—	2.28		—	0		—	
12 Mg	9.79	—	1.87		—	—		—	



Landé has given many arguments in favour of this arrangement of the X-ray spectra in a system *analogous to the term-systems for the arc-spectra of the alkalis*, instead of the general hydrogen term-system used in the theory of Sommerfeld. We shall first note one great formal advantage of this arrangement: the selection-rules for the transitions between the different energy levels are exactly the same in this notation as those met with in ordinary optics. (It is only necessary to remember that transitions within one and the same group are not permissible. In this respect the analogy is incomplete.) But the analogy can be pushed a step farther. The relative intensities of lines in the optical spectra of the alkalis and in X-ray spectra, resulting from analogous transitions, seem to show agreement. For instance, the  $K\alpha$  doublet, which corresponds to the yellow lines in the Na spectrum, has an intensity relation of 2 : 1. The same seems to hold for the three lines corresponding to the triplet of the diffuse series in the spectra of the alkalis, namely,  $L_{a_1} L_{a_2} L_{\beta_1}$ .

We must emphasize the fundamental difference in the views of Sommerfeld and of Landé as to the character of the so-called relativity doublet. According to Sommerfeld, this doublet arises from the energy difference between the circular and the elliptical two quantum orbits (for the  $K\alpha$  doublet and corresponding doublets of the  $L$  series), and is of the same kind as the analogous doublet in the hydrogen spectrum. Landé considers that this doublet is of the same nature as the doublets in the sharp series of the alkali spectra, and is thus due to the different orientation of the orbits, or to different "inner" quantum numbers. A characteristic feature of the relativity doublets is that the frequency difference varies as  $(Z-d)^4$  (cf. equation 55), a fact in exact agreement with the experimental results. But Landé remarks that this same law also holds for the alkali doublets ( $p_2 - p_1$ ). This is shown by the recent investigations of Paschen and Fowler on the spectra of NaI, MgII, AlIII and SiIV. The spectra of these four ionized atoms are emitted by an atomic configuration of quite the same structure but of nuclear charge, differing by unity from one element to the next. The following table gives the values of  $(Z-9)^4$ , and in the last column the values of  $d$  if  $(Z-d)^4$  be equated to the observed frequency-difference.

Element.	Z	$\Delta\nu$ obs.	$(Z-9)^4$ .	$d$
Na I	11	17.2	16	9.0
Mg II	12	91.5	81	8.9
Al III	13	238	256	9.1
Si IV	14	460	625	9.4

Another interesting point in favour of this scheme has been indicated by Sommerfeld and Grottrian. The two lines belonging to the "rela-

tivity " doublets always appear—as far as can be tested experimentally—at the same element in the periodic table. This is difficult to understand if, as is supposed in the theory of Sommerfeld, they should belong to orbits of *different* shells in the atom. Recent researches of Mr. Ray and the author on the displacement of the *K* doublet lines for lower elements point to the same conclusion. If these two lines belonged to orbits of very different shape, *e.g.* to circular and elliptical orbits, the influence of the other electrons on the two lines should have greatly different values. But experiments show that both lines are displaced in the same manner.

As compared with the previous scheme, that of Landé has the advantage of being more readily pictured, and it makes use of the ordinary optical selection rules. The analogy with the spectra of the alkalis may stimulate to further investigations in many directions. But at the same time it must be emphasized that there are essential differences in these two types of scheme, and that analogy does not constitute identity. This may be clear if we recall the fact that the levels in the X-ray diagram correspond to the energy of the atom which has lost one electron from a *K*, an *L* or an *M* group, etc. In the scheme for the spectra of the alkalis the first level in the *s*-term series corresponds to the energy of the *undisturbed* atom. The *1s* level in the X-ray scheme corresponds to an atom in which one electron has been removed from the *K* group of electrons, and so on. There is also no continuous transition from the X-ray scheme to the optical one. The X-ray lines of the ordinary kind are due to transitions between such groups of electrons in the atom as are normally occupied by electrons; experiment seems to show that the disappearance of an electron group at a particular element in the periodic table is accompanied by the disappearance of those lines which are associated with that group.

From this point of view there is no reason for designating purely optical spectral lines by names taken from the X-ray field. This has reference to those lines which belong to more highly ionized atoms, which fit excellently in the ordinary optical schemes. The X-ray lines correspond to transitions between orbits *within* groups ordinarily occupied by electrons; the optical lines correspond to transitions between orbits not occurring in the undisturbed atom. It may also be remembered that the X-ray spectra are emitted by atoms contained in solids, whereas the ordinary spectra are emitted only from free atoms.

Finally, we know that the optical spectrum emitted by one and the same atom changes very much if one or more electrons are removed from the neutral atom. A general law for these changes has been formulated by Sommerfeld and Kossel, and is known as the "displacement law." With very few exceptions all the X-ray lines which have been found correspond to an atom from which only one electron has been removed

from its normal orbit. All X-ray spectral lines collected in the energy diagrams previously given are of this kind. To trace the sequence of these lines down to the wave-length region of ordinary optics, it is thus necessary to restrict our choice to lines belonging to spectra of the arc type.

The few lines in the domain of X-ray spectra which must doubtless be ascribed to a higher state of ionization have not yet been sufficiently studied to permit the construction of an energy system like that given for the normal X-ray spectral lines. The analogy of the latter spectrum to a doublet spectrum may possibly indicate that the X-ray spectrum of the "spark" type has a triplet structure.

### 33. X-ray Spectra of Multiply-Ionized Atoms according to Wentzel

Although the great majority of known spectral lines may be classified according to the general energy level scheme, there are, nevertheless, groups of lines which evidently cannot be brought into this system. The first example of lines of such a type was that pointed out by the author jointly with Stenström as early as 1916, in an investigation of the  $K$  series for the lightest elements. In the neighbourhood of the element Zn a faint component apparently becomes separated from the short wave-length side of the  $K\alpha$  doublet, and for lower elements itself becomes resolved into a doublet which we have called  $a_3 a_4$ . This separation has been recently demonstrated below Ca by Dolejšek, and it has been measured as far down as Na.

In addition to this  $a_3 a_4$  doublet Hjalmar discovered a second doublet  $a_5 a_6$  in the  $K$  series for the very light elements, and also a single line between  $a_1 a_2$  and  $a_3 a_4$ , which he called  $a'$ , and which apparently belongs to this group of non-diagram lines. Similar conditions obtain in the  $\beta$  group of the  $K$  series.

An explanation of the presence of these lines has been given by Wentzel, and rough calculations lend such good support to the theory that we need not doubt its validity. According to Wentzel these lines arise from *an excitation process in which more than one electron is removed from the inner energy levels of the atom*. Since this condition bears a certain resemblance to the condition requisite for the production of the so-called spark lines in ordinary optical spectra, Wentzel called these lines *spark lines*. In the case of ordinary spectra it had not been shown with certainty that more than singly ionized atoms serve as radiators, but quite recently Paschen demonstrated the existence of a spectral series corresponding to the doubly ionized atom of Al, and Fowler a series for triply ionized Si. Wentzel has made it seem probable that in the case of these lines of the  $K$  series of X-rays we have to do with two-

and three-fold ionization. In order to make the nomenclature orderly, the proposal of Bohr and Coster seems to me worthy of acceptance; namely, that the spectra arising from the removal of one electron from its normal position in the atom shall be called spectra of the first degree, while those due to the removal of two or more electrons shall be called spectra of the second or higher degrees. The regular energy level diagram thus depicts spectra of the first degree.

In order to give a general representation of the X-ray spectra of different degrees, we present a scheme giving the number of electrons which are present at the beginning and at the end of the radiation process in the  $K$ ,  $L$  and  $M$  groups. We denote by  $k$ ,  $l$  and  $m$  the normal number of electrons belonging to the  $K$ ,  $L$  and  $M$  groups respectively. The excitation of the  $K$  series is due, then, to the removal of an electron from the  $K$  group; according to the preceding theory the emission of the  $K\alpha_{1,2}$ -line corresponds to the falling back of an electron from the  $L$  group to the  $K$  group. At the close of the emission process the  $L$  group lacks one electron of its normal number, while the  $K$  group is fully occupied.

According to Wentzel, spectra of the *second* degree presuppose the removal of *two* electrons from the electron shells. Both may be taken from the  $K$  group, or one may be taken from the  $K$ , the other from an outer group. If we restrict ourselves to the cases involving only the  $K$  and the  $L$  series, we have two possible initial conditions, and the two transitions indicated in the following scheme. Corresponding conditions and transitions may be supposed for the case of threefold ionization, in which, however, the possibility that three electrons have been removed from the  $K$  group is excluded, since the theory of the manner in which the periodic system is built up permits of only two electrons in the first group. The absence of a line in the X-ray spectrum corresponding to such a state is very direct evidence of the truth of the theory.

No. of electrons in	$K$ group.	$L$ group.	$M$ group.
Spectra of 1st degree	$\alpha_{1,2} \begin{cases} k-1 \\ k \end{cases}$	$\begin{cases} l \\ l-1 \end{cases}$	$\begin{cases} m \\ m \end{cases}$
Spectra of 2nd degree	$\alpha_3 \begin{cases} k-2 \\ k-1 \end{cases}$ $\alpha_4 \begin{cases} k-1 \\ k \end{cases}$	$\begin{cases} l \\ l-1 \\ l-2 \end{cases}$	$\begin{cases} m \\ m \\ m \end{cases}$
Spectra of 3rd degree	im- possible $\begin{cases} k-3 \\ k-2 \\ k-1 \end{cases}$ $\alpha_6 \begin{cases} k-1 \\ k \end{cases}$ $\alpha_5 \begin{cases} k \end{cases}$	$\begin{cases} l \\ l-1 \\ l-2 \\ l-3 \end{cases}$	$\begin{cases} m \\ m \\ m \\ m \end{cases}$

We have here taken no account of the multiple nature of the  $L$  and the  $M$  groups. We are quite justified in ignoring it, however, for it is

not yet possible to detect the fine structure of the lines due to this cause. As may be seen from the tables of wave-lengths, the separation of the lines  $\alpha_1$  and  $\alpha_2$  has been obtained only as far down as sulphur, while the separation of  $\alpha_3$  and  $\alpha_4$  begins only about in this region. These last two lines are less sharp than the  $\alpha_1$ ,  $\alpha_2$  lines, and their further resolution has therefore not been possible up to the present.

From the explanation given above we may draw certain semi-quantitative conclusions which support Wentzel's theory. If we compare the transitions corresponding to the lines  $\alpha_5$ ,  $\alpha_3$ , and  $\alpha_1$ , we observe that in all three cases the change in the  $K$  group is the same, but that the changes in the  $L$  group are in the regular steps  $l-2$  to  $l-3$ ,  $l-1$  to  $l-2$ , and  $l$  to  $l-1$ . As a first approximation we might therefore assume

$$\alpha_5 - \alpha_3 = \alpha_3 - \alpha_1.$$

Similarly, an examination of the transitions  $\alpha_6$  and  $\alpha_4$  shows identical changes in the  $K$  group, while the changes in the  $L$  group are the same as those for  $\alpha_3$  and  $\alpha_1$ ; hence we are justified in writing the approximation

$$\alpha_6 - \alpha_4 = \alpha_3 - \alpha_1.$$

A numerical test of these approximate relations is possible only for three elements, but in these cases the agreement as shown in Table 39 is relatively good.

TABLE 39.

$\Delta \nu_{\alpha}$	$\alpha_6 - \alpha_4$	$\alpha_5 - \alpha_3$	$\alpha_3 - \alpha_1$
12 Mg	0.72	0.66	0.65
13 Al	0.86	0.79	0.73
14 Si	0.94	0.90	0.84

The line  $\alpha'$  which Hjalmar found between  $\alpha_{1,2}$  and  $\alpha_{3,4}$  for the elements Na to Ca, Wentzel believed to be an example of spectra of the second degree in which the initial and final states should be

$$\alpha'_1 \begin{cases} k-1=l & m-1 \\ k & l-1 \quad m-1 \end{cases}$$

This assumption is not so well verified numerically as the previous case.

In the  $\beta$  group of the  $K$  series of the lighter elements there are also a number of lines which are doubtless to be explained on the basis of Wentzel's theory. Further, Wentzel points out that certain lines in the  $L$  series come under the same classification, as, for example, the harder component of  $\alpha_1$  found by Friman, and called by him  $\alpha_3$ . Investigations of the author (1918) in a region of greater wave-lengths, as for Sn, Ag, and



Mo, showed that this  $\alpha_3$  line is probably not a separate and simple line, but is rather to be regarded as a complex structure of the short wave-length side of  $\alpha_1$ . In the same way Stenström has shown experimentally that the fine structure of the  $M$  series requires for its explanation a consideration of multiple ionization.

In their studies of the  $L$  series, Coster and Dauvillier have also confirmed this view, and have discovered several other lines which are probably to be attributed to spectra of higher degree. Coster is of the opinion that on the short wave-length side of the  $La$  line there are at least three of these lines, partly veiled by the blackening of the continuous spectrum. He also pointed out several satellites of the line  $L\beta_1$  (see Figs. 74A, 74B, p. 111).

In a closer study of the above explanation of the satellites, an interesting and important question is whether the multiple ionization takes place all at once, or whether the electrons are removed by separate absorptions of energy. Wentzel believes the latter to be the case, and regards it as an explanation of the fine structure of the absorption edges observed by Stenström, Fricke, Hertz and others. Since the work which is necessary to eject an electron from the  $K$  group, for example, is slightly different according as to whether the atom possesses its normal number of electrons, or has already lost one or more, we might expect in multiple ionization to find the corresponding absorption edge somewhat displaced from its normal position.

As Coster and Rosseland have remarked, however, the number of atoms which are at any one time in the excited state is so very small compared with the number of those in the normal state, that this effect, if it exists, will be too small to detect in absorption spectra. Hence to explain the fine structure of absorption edges we must turn to other possibilities.

One might determine experimentally whether the excitation of spectra of higher degree is a simple process, or whether it takes place in several steps, by making a comparison of the voltage necessary to excite the satellites with that required for the principal line associated with them. If the satellites are excited by the simultaneous ejection of several electrons, then they should require a considerably higher exciting voltage. The double ionization of the  $K$  group, for example, would require a little more than twice the voltage necessary to remove one electron. Coster sought to answer this question experimentally by photographing the principal line of the  $L$  series, using greatly different excitation voltages. Although the experimental conditions were not so satisfactory as might have been desired, the results indicated that when the exciting voltage was kept low the satellites were repressed. This indicates that *the most probable process is that of simultaneous multiple ionization.*

This question has recently been studied in more detail and with a better equipment by E. Bäcklin, and by the author in collaboration with Mr. Axel Larsson. In both cases the tube was worked at a constant high voltage. Bäcklin investigated the spark lines of the  $K$  series for Al, with which element five such lines belonging to the  $\alpha$  group are known :  $\alpha'$ ,  $\alpha_3$ ,  $\alpha_4$ ,  $\alpha_5$ ,  $\alpha_6$ .

If the detailed scheme proposed by Wentzel for these different lines were quite valid, then the excitation of  $\alpha_3$  and  $\alpha_4$ , for instance, would require greatly differing minimum potentials— $\alpha_3$  about 1.62 kv. and  $\alpha_4$  about 3.10 kv.—if we suppose both electrons to be displaced in one process. The tube was worked at a potential nearly equal to the second value. Some of Bäcklin's results are collected in the following table :

Potential K.V.	Current M.A.	Time of exposure. Hours.	Lines visible on the plate.
$3.20 \pm 0.05$	70	$1\frac{1}{2}$	$\alpha_{1,2}, \alpha', \alpha_3, \alpha_4$
$2.90 \pm 0.05$	100	1	$\alpha_{1,2}, \alpha_3, \alpha_4$
$4.00 \pm 0.05$	70	1	$\alpha_{1,2}, \alpha', \alpha_3, \alpha_4, \alpha_5, \alpha_6$
$3.10 \pm 0.05$	80	1	$\alpha_{1,2}, \alpha', \alpha_3, \alpha_4, \alpha_5, \alpha_6$

Moreover, Bäcklin remarks that the relative intensities of the  $\alpha_3$  and  $\alpha_4$  lines are about the same at different potentials. These experiments seem to indicate that the proposed scheme cannot be quite right. Not only does the  $\alpha_4$  line appear at a lower potential than that necessary for a double ionization of the  $K$  shell, but the  $\alpha_6$  line is also visible at that potential.

The measurements of Mr. Larsson and the author were made in the  $L$  series of molybdenum. The spark lines in the neighbourhood of the  $\alpha$  line were photographed and compared photometrically at potentials ranging from 3 kv. to 40 kv. The minimum potential of the  $La$  line is about 2.9 kv. At 3.0 kv. only the ordinary lines  $\alpha_1$  and  $\alpha_2$  were seen on the plate, but at 4 kv. many faint satellites were already registered. No new satellites could be found at twice the potential, so it seems to be impossible in one process to eject two electrons from the  $L$  shell. At about 20 kv. a new satellite first appeared on the plate. This potential is a little too small for a simultaneous ionization of both the  $K$  and the  $L$  shells. At 40 kv. no more lines were visible than at 20 kv.

In all these cases it thus seems to be the rule that two electrons are never ejected from the same shell. This suggests that only with configurations in which two or more electrons from different shells are near together, they may be ejected by the same exciting electron.

### 34. X-ray Spectra and Atomic Structure

It is now generally recognized that the electron transitions which give rise to X-ray spectra take place between those quantum orbits which, in the normal state of the atom, are occupied by electrons. For this reason it is readily understood that X-ray spectra afford one of the most direct sources of information concerning the inner structure of the atom. The results of early investigations were, therefore, eagerly scanned with this end in view. Many authors, among whom we may mention especially Sommerfeld, Debye, Kroo, and Vegard, proceeded on the hypothesis that the electrons move in circular orbits, and they then endeavoured to determine the number of electrons in the rings so as to agree with experimental results, *e.g.* so as to give the proper magnitude for the screening effect of the electrons on the nucleus. In this way they arrived at formulae by which certain series of lines could be calculated, in extraordinary agreement with the measured values. But in the first place the number of electrons determined in this way, *e.g.* in the *K* ring, was different from that which one is forced to assume from considerations of the chemical properties of the elements; and, in addition, various other results of experiment speak *very definitely* against a simple ring arrangement of the electron groups. For these reasons the ring hypothesis has now been generally abandoned. We will cite here only one point further in connection with these earlier theories; Vegard first definitely expressed the condition that the electron groups reckoned from within outwards must be associated with the quantum numbers 1, 2, 3, 4, etc.

The Bohr theory of the atom differs considerably from the atomic hypotheses just mentioned, and from its commencement it has occupied an important position with regard to X-ray spectroscopy. As is now well known, Bohr's conception is that the atom is built up, starting from the nucleus, by the successive binding of one electron after another, until each element has a number of electrons equal to its atomic number. The atomic system thus built up by Bohr from entirely general principles has proved itself very satisfactory and very fruitful in a somewhat thorough study and discussion of phenomena in the domain of X-ray spectroscopy. That the theory is in accord with the fundamental features of X-ray spectra is evident from a comparison of the general level diagram of Röntgen spectra with the Bohr atomic table. In Table 40, which is Bohr's representation of the electron orbits for a series of elements, we find all the characteristics of X-ray spectra represented; the innermost group has two electrons, as we would be led to expect for several reasons, among others by Wentzel's theory of the *K* spectra of higher degree in the case of the light elements; the *K* group is a one quantum group, and both electrons have equal energies, which agrees with the fact that the

$K$  level is single ; in the two quantum  $L$  group we have two electron orbits of different energies, corresponding to the auxiliary quantum numbers 1 and 2 ; in the three quantum  $M$  group there are three types of orbit, represented by  $3_1$ ,  $3_2$  and  $3_3$  ; then the quantum number continues to rise for the outer groups until it reaches six for the  $P$  electrons. We need only compare the quantum numbers at the top of the table with the quantum numbers of the level diagram of p. 173 to see how completely the two systems agree. The only difference lies in the fact that we find that the presence of the screening doublet necessitates in the energy level scheme the doubling of certain levels which have the same principal and auxiliary quantum numbers. But this arises from causes which we have already discussed several times ; the general reasons underlying it are easily understood, and, as Bohr has pointed out, it is quite in accord with the atomic system. The table represents the types of orbits and the grouping of electrons for the normal atom which has its full quota of electrons. If *one electron be removed* from one of these subgroups, the remaining electrons have the possibility of arranging themselves in different ways. Why this occurs only in certain cases, and then in only *two* ways, is not yet properly understood.

A significant point in the Bohr theory of atomic structure is that the electron orbits of the outer groups penetrate deeply into the electron system. This circumstance, which gives rise directly to the characteristic doublet features, has already been discussed under the Sommerfeld doublet theory. A detailed analysis of this question may be found in a recent article by Bohr and Coster,\* where the effect of this penetration of the electron orbits upon the *principal quantum number* is also considered, since this number may be considered as being modified by the presence of the electron for a portion of its path among the innermost orbits.

It is very important to enquire whether the beginning of orbits of higher quantum number at certain elements, or the completion of groups of inner quantum orbits in certain groups of elements can be observed in Röntgen spectra. We have already stated in the discussion of the general scheme of energy levels that a smaller number of energy levels suffices for the explanation of the experimental results in the case of the lighter elements, than for the heavier elements. On account of experimental difficulties it has so far been impossible to demonstrate just at which element a new level begins. In no case, however, has an energy level been found which is not represented in the Bohr table by the corresponding type of electron orbit. The possibility is not excluded, however, that there may be lines, especially in the case of the lighter elements, representing transitions from unoccupied orbits.

\* *Zeitschrift für Physik*, vol. 12, p. 342 1923.

TABLE 40.

Types of electron orbits of the elements.

$nk$ $N$	$K$ $1_1$	$L$ $2_1 2_2$	$M$ $3_1 3_2 3_3$	$N$ $4_1 4_2 4_3 4_4$	$O$ $5_1 5_2 5_3 5_4 5_5$	$P$ $6_1 6_2 6_3 6_4 6_5 6_6$	$7_1 7_2$
1 H	1						
2 He	2						
3 Li	2	1					
4 Be	2	2					
5 B	2	2 (1)					
10 Ne	2	4 4					
11 Na	2	4 4	1				
12 Mg	2	4 4	2				
13 Al	2	4 4	2 1				
18 A	2	4 4	4 4				
19 K	2	4 4	4 4	1			
20 Ca	2	4 4	4 4	(2)			
21 Sc	2	4 4	4 4 1	(2)			
22 Ti	2	4 4	4 4 2	(2)			
29 Cu	2	4 4	6 6 6	1			
30 Zn	2	4 4	6 6 6	2			
31 Ga	2	4 4	6 6 6	2 1			
36 Kr	2	4 4	6 6 6	4 4			
37 Rb	2	4 4	6 6 6	4 4	1		
38 Sr	2	4 4	6 6 6	4 4	2		
39 Y	2	4 4	6 6 6	4 4 1	(2)		
40 Zr	2	4 4	6 6 6	4 4 2	(2)		
47 Ag	2	4 4	6 6 6	6 6 6	1		
48 Cd	2	4 4	6 6 6	6 6 6	2		
49 In	2	4 4	6 6 6	6 6 6	2 1		
54 X	2	4 4	6 6 6	6 6 6	4 4		
55 Cs	2	4 4	6 6 6	6 6 6	4 4	1	
56 Ba	2	4 4	6 6 6	6 6 6	4 4	2	
57 La	2	4 4	6 6 6	6 6 6	4 4 1	(2)	
58 Ce	2	4 4	6 6 6	6 6 6 1	4 4 1	(2)	
59 Pr	2	4 4	6 6 6	6 6 6 2	4 4 1	(2)	
71 Lu	2	4 4	6 6 6	8 8 8 8	4 4 1	(2)	
72 Hf	2	4 4	6 6 6	8 8 8 8	4 4 2	(2)	
79 Au	2	4 4	6 6 6	8 8 8 8	6 6 6	1	
80 Hg	2	4 4	6 6 6	8 8 8 8	6 6 6	2	
81 Tl	2	4 4	6 6 6	8 8 8 8	6 6 6	2 1	
86 Nt	2	4 4	6 6 6	8 8 8 8	6 6 6	4 4	
87 —	2	4 4	6 6 6	8 8 8 8	6 6 6	4 4	1
88 Ra	2	4 4	6 6 6	8 8 8 8	6 6 6	4 4	(2)
89 Ac	2	4 4	6 6 6	8 8 8 8	6 6 6	4 4 1	(2)
90 Th	2	4 4	6 6 6	8 8 8 8	6 6 6	4 4 2	(2)
118 ?	2	4 4	6 6 6	8 8 8 8	8 8 8 8	6 6 6	4 4

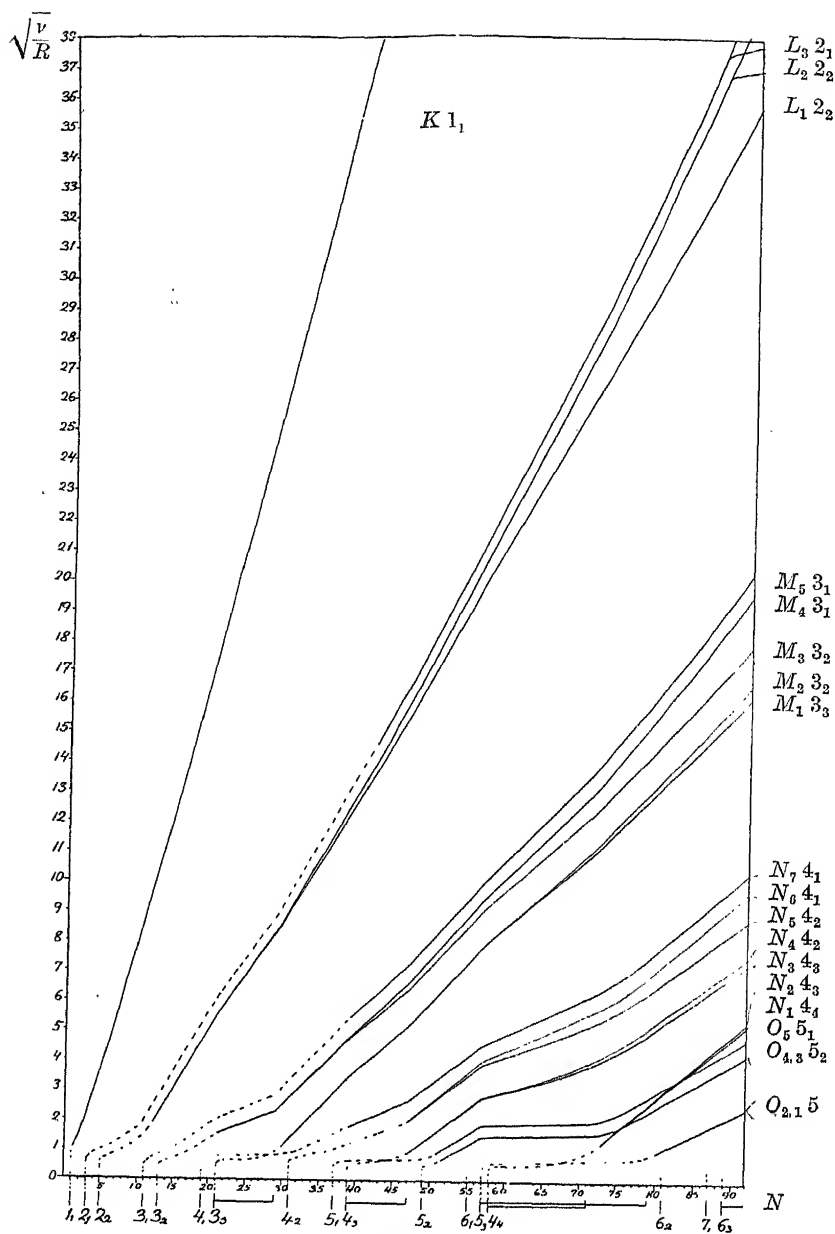


FIG. 80.

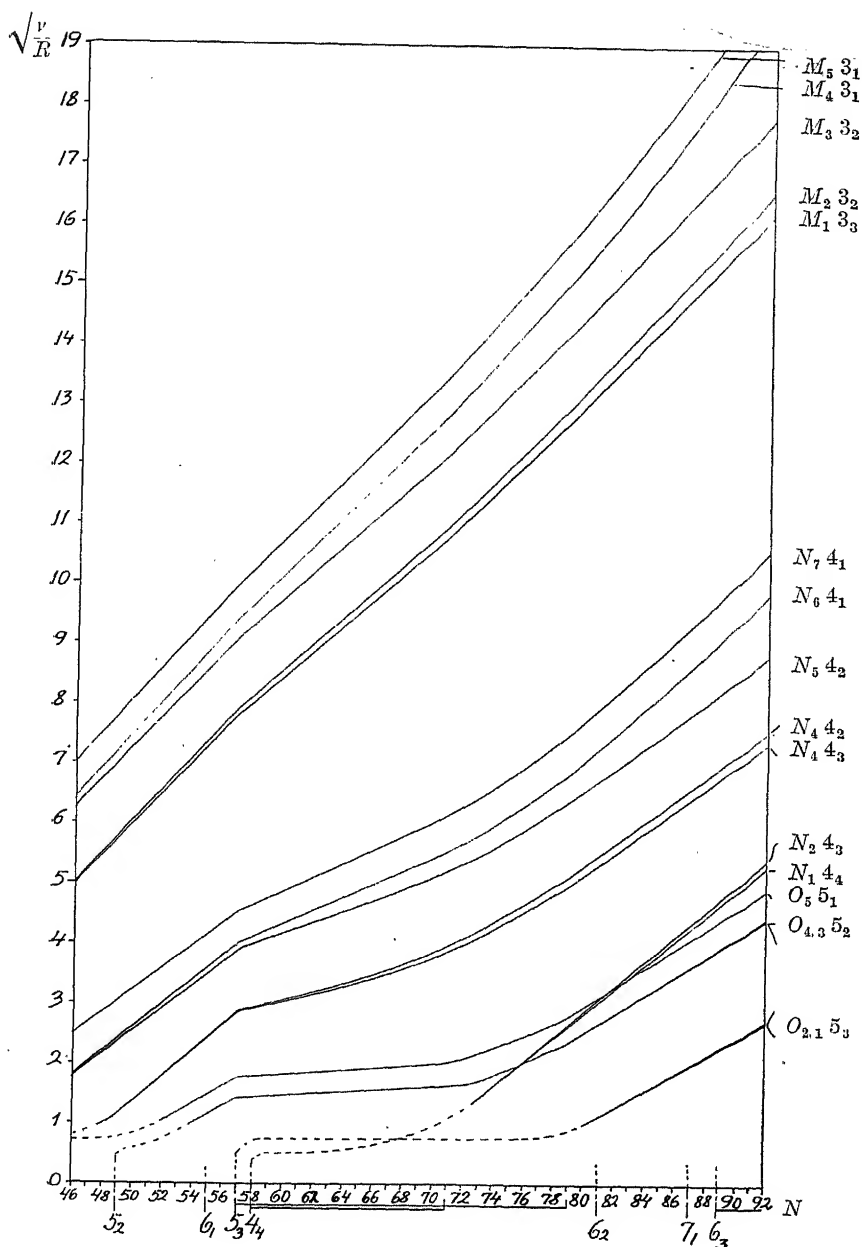


Fig. 90.

Though the empirical material yields little that is conclusive concerning the building up of the outermost electron groups, conditions are more favourable, as Bohr and Coster have shown, when we come to examine the spectra for evidence of the completion of an inner group of electrons. From Bohr's table we observe that such a completion of the  $M$  group occurs in the neighbourhood of the iron group, in the  $N$  group a similar phenomenon takes place in the palladium family. A more striking remodelling of the  $N$  group occurs in the rare earth group of elements.

Figs. 89 and 90, taken from Bohr and Coster's paper, show that this building up of the electron groups in two or more steps may be recognized from the shape of the energy level curves, which are drawn from the values of  $\sqrt{\frac{\nu}{R}}$  in Table 38.

Of the three levels in the  $L$  group,  $L_2$  and  $L_3$  form a screening doublet, and their curves run nearly parallel, while  $L_1$  and  $L_2$  constitute a relativity doublet whose separation  $\Delta\sqrt{\frac{\nu}{R}}$  steadily decreases with decreasing atomic number. Likewise in the  $M$  and  $N$  groups we find alternately the two types of doublets.

That the course of the curves is actually in agreement with this qualitative assertion of the Bohr atomic table concerning the completion of inner orbits, is shown in the  $L$  and  $M$  levels at the iron group, in several of the levels at the palladium group, but especially clearly in the rare earth group. This latter region may best be observed in the enlarged Fig. 90. Moreover, the measurement of the levels concerned is most easily carried out in this portion of the table. It is yet too soon to enter into details here, for further investigations will certainly yield important results along these lines.

We may call attention here to an interesting point, which is beautifully shown in the diagrams reproduced above. We have found the levels, which have been well determined numerically in the case of uranium, to be associated in groups, and always in such a manner that the lowest level of one group lay above the highest level of the group next below. This is not always the case, as is shown by the course of the level curves for  $N_1$  and  $N_2$ , which for lower elements cross over the highest  $O$  levels. This fact is easily understood in the light of Bohr's ideas, for in the course of the building up of the atom it happens several times that higher quantum orbits build up before the lower, since in the former the binding is stronger.

A more direct way of studying the connection between the process of atomic building and X-ray spectra has been followed by Mr. Ray and the author. As may be seen from Table 40, the three inner groups ( $K$ ,  $L$



and  $M$ ) in the Bohr scheme are unaffected by the building-up process from the element Cu 29 upwards. But below copper the re-arrangements of the outer electrons affect the  $M$  group. It must be supposed that this variation in the  $M$  group may have such a great influence on the two inner groups ( $K$  and  $L$ ), that irregularities in the spectral lines corresponding to transitions between these two groups may be revealed by measurements. As shown by the following Table (40B) and Fig. 90B, this

TABLE 40B.

$Z$	$\lambda$ in X.U.	$\frac{\Delta\nu}{R \cdot (z-3.5)^2}$	$Z$	$\Delta\lambda$ in X.U.	$\frac{\Delta\nu}{R \cdot (z-3.5)^2}$
16 S	2.85	.3686	34 Se	4.03	.3455
17 Cl	3.15	.3868	35 Br	4.04	.3453
19 K	3.38	.3820	37 Rb	4.12	.3477
20 Ca	3.26	.3565	38 Sr	4.17	.3529
21 Sc	3.37	.3576	39 Y	4.18	.3463
22 Ti	3.45	.3643	40 Zr	4.21	.3493
23 Va	3.60	.3763	41 Nb	4.25	.3509
24 Cr	3.89	.3836	42 Mo	4.28	.3523
25 Mn	4.08	.3949	44 Ru	4.34	.3549
26 Fe	4.22	.4019	45 Rh	4.36	.3550
27 Co	4.19	.3920	46 Pd	4.39	.3564
28 Ni	3.90	.3588	47 Ag	4.43	.3588
29 Cu	3.86	.3514	48 Cd	4.43	.3603
30 Zn	3.82	.3475	49 In	4.43	.3576
32 Ge	3.91	.3439	50 Sn	4.47	.3617
33 As	3.97	.3459	74 W	4.67	.3987

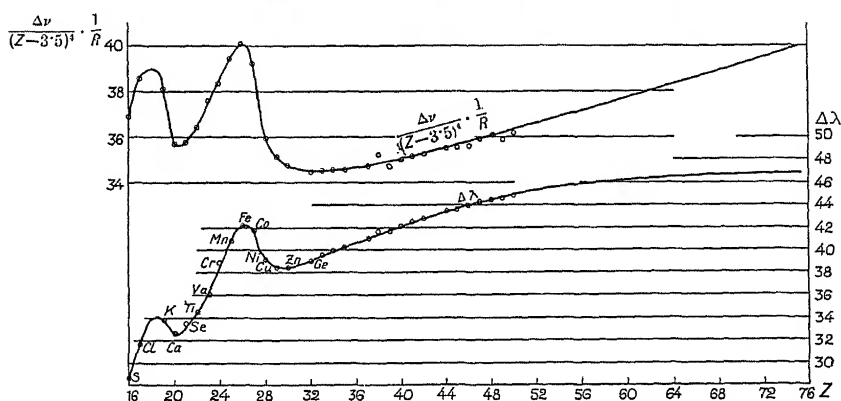


FIG. 90B.

supposed effect is actually found when we measure the distance between the  $K\alpha_1$  and  $\alpha_2$  lines. As best seen from the curve for the wave-length

differences  $\Delta\lambda$ , this difference follows a regular and smooth curve from W 74 down to Zn 30, where it begins to deviate from this regular form and attains a first maximum at Fe 26. At Ca 20 a point on the curve is reached which nearly corresponds to the value extrapolated from the smooth curve for the higher elements. After this a second periodic rise sets in.

TABLE 40c.

Z	$\Delta\lambda$ in X.U.	Z	$\Delta\lambda$ in X.U.	Z	$\Delta\lambda$ in X.U.	Z	$\Delta\lambda$ in X.U.
41 Nb	7.58	51 Sb	9.22	60 Nd	10.05	71 Lu	10.69
42 Mo	8.23	52 Te	9.40	62 Sm	10.35	73 Ta	10.93
44 Ru	8.15	53 I	9.48	63 Eu	10.50	74 W	11.02
45 Rh	7.78	55 Cs	9.42	64 Gd	10.81	78 Pt	11.39
46 Pd	7.72	56 Ba	9.33	66 Dy	10.95	79 Au	11.45
47 Ag	8.16	57 La	9.22	67 Ho	11.02	81 Tl	11.53
48 Cd	8.51	58 Ce	9.18	68 Er	11.10	82 Pb	11.54
49 In	8.80	59 Pr	9.74	70 Yb	11.12	92 U	11.81
50 Sn	8.95						

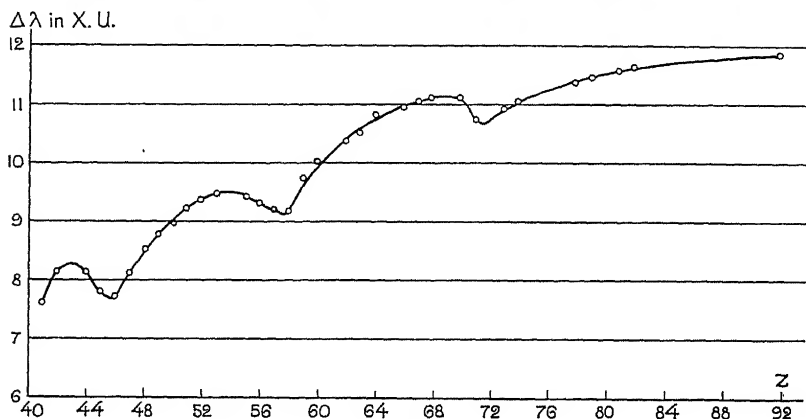


FIG. 90c.

All these measurements were carried out with the pure elements. As the outer group is strongly affected by the chemical binding for the lower elements, it was presumed that the same element in different chemical compounds would give slightly different values. Mr. Ray has made some preliminary investigations on this question, and has found that such an effect really exists. It may be remembered in this connection that it is a rather difficult matter to study the X-ray emission spectrum of an element in a specified chemical compound, as one can never be sure that the substance placed on the anticathode is really the same as that emitting

the observed spectrum. The strong bombardment with cathode rays, and the intense heating that inevitably accompanies this process, will in most cases cause a disintegration of the substance.

In the table and in the figure are also given the values of the function

$$\frac{\Delta\nu}{(Z-3.5)^4} \frac{1}{R}$$

calculated from the wave-lengths differences found experimentally. This function plays an important part in the doublet theory of Sommerfeld (§ 31). As we pass from the highest element down to atomic number 40 the numerical value of this function as shown in Table 32 and Fig. 85 decreases and approaches asymptotically the value  $0.332 \times 10^{-5}$ , which is the theoretical value for the corresponding doublet of the hydrogen spectrum, where the screening constant  $d$  is zero. The large variations of the above expression are naturally due to the fact that the screening constant cannot be taken to have the same value, 3.5, for the lower elements here investigated, for it varies with the different arrangement of the electrons in the nearest outer group.

Phenomena of this kind may also arise in other series in X-ray spectra. Ray has carried out an investigation of the doublet  $La_1a_2$ , which represents a transition of an electron from the  $M$  group to the  $L$  group. As seen from Table 40, the Bohr scheme makes it probable that irregularities are to be expected in at least two places between the elements 40 and 92. The experimental results, which are given in Table 40c and Fig. 90c, show some obvious deviations from the smooth curve, but the general character of the curve is not as simple and definite as for the  $K\alpha$  doublet.

## VII

### THE CONTINUOUS X-RAY SPECTRUM

#### 35. The General Character of the Continuous Spectrum

Just as in the ordinary optical domain we meet with line spectra and a continuous spectrum extending over a long range for wave-lengths, so we also find these two types of spectra in the region of X-rays. The continuous X-ray spectrum is often called the "white" spectrum, from the optical analogy. In fact, in the application of X-ray tubes to medical work the white radiation plays the most important part, for it usually contains by far the greater part of the intensity. In many cases the line spectrum does not even get out of the tube, as, for example, in the case of a tube with a tungsten anticathode actuated by a maximum voltage of 70 kv. At this voltage the *K* radiation is not yet excited, and though, of course, the *L*, *M*, etc., line radiations are produced, the *M* and higher groups do not pass through the walls of the tube at all, and even the *L* group is so strongly absorbed by the glass wall that its intensity outside the tube is negligible compared with that of the continuous radiation.

Conditions are different in the case of tubes having anticathodes of materials such as Ag, Pd, Rh and Mo, which are often used in commercial tubes. The characteristic radiation from these elements, as we have already stated, and as may also be seen from the tables, lies just in the region of radiation which is most used in professional work, namely, between wave-length limits of about 100 to 800 X.U. In general, a potential of 70 kv. is ample for exciting the radiations in question. These tubes, therefore, afford a composite radiation, consisting partly of white and partly of characteristic radiation. Since the characteristic radiation is localized in a very narrow region of wave-lengths, namely, the four lines  $\alpha_2$ ,  $\alpha_1$ ,  $\beta_1$ ,  $\beta_2$ , the white, rather than the characteristic radiation, should in this case also constitute the greater part of the total energy. This is a point which is often overlooked, because when measurements are made with the Bragg spectrometer in the usual way, the ionization current, when a setting is made on a line, causes a very large deflection of the electrometer in comparison with that due to the white radiation.

The large range of wave-lengths in the white radiation, however, counts more heavily for the total radiation than do the characteristic rays which are strongly concentrated into a few homogeneous lines.

In this connection we may mention an analogous phenomenon which is not always properly represented in the literature. For the production of homogeneous rays many experimenters expose a secondary radiator, such as silver, to the radiation from a commercial tube, and assume the resulting characteristic radiation from the silver to be monochromatic. The radiation obtained in this way indeed manifests the properties of monochromatic rays to a degree sufficient for many purposes, especially if a filter is used which absorbs strongly all radiation softer than the characteristic radiation. If one determines the absorption coefficient in Al, according to the method used some time ago by Barkla, the result is a tolerably constant absorption coefficient which leads one to suppose that the radiation is really monochromatic. This is not really the case, however, as will appear from what follows, and one must be careful in drawing conclusions from such experiments, which presuppose a really monochromatic radiation. The continuous spectrum, which has not so much effect on absorption measurements, is nevertheless always present, and in other respects may be of much greater consequence.

A typical continuous spectrum from an X-ray tube, in which the line spectrum does not appear, is shown in Fig. 91. This curve was obtained by the Bragg spectrometer method, in which crystal and ionization chamber are set at frequent intervals throughout the range of wave-lengths present, and the ionization current measured for each setting. This curve does not really give the true intensity distribution, for several reasons which we will discuss in detail later, but of which we will here mention the two most important. The first is, we cannot assume the ionization current to be proportional to the intensity of radiation for different wave-lengths. The second reason is that the ionization current gives, *e.g.* in the position corresponding to a wave-length of  $0.8 \text{ \AA}$ ., not only the ionizing effect of the radiation of this wave-length, but also in part that due to a wave-length of  $0.4 \text{ \AA}$ . reflected in the second order. At greater wave-lengths the curve is further disturbed by orders still higher than the second. Since the curve begins at  $0.34 \text{ \AA}$ . the spectrum of the second order will appear first at about  $0.68 \text{ \AA}$ ., so that the deformation of the curve due to this cause does not occur below the latter wave-length.

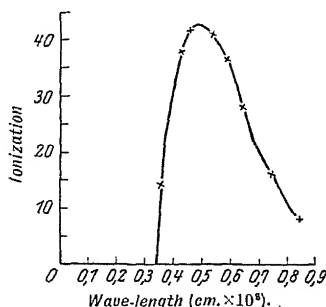


FIG. 91. The continuous radiation from an X-ray tube recorded by the Bragg ionization method.

In spite of the many distorting influences this curve still shows certain general features of the continuous radiation. One of the most important of these is that *the curve rises abruptly on the short wave-length side*. In this respect the curve differs fundamentally from the curve for the radiation of a "black" body, though otherwise the curves have an external resemblance.

The fact of the abrupt beginning of the ionization curve has been definitely established by a considerable number of experimenters, and thereby the validity of the fundamental Einstein photo-electric law has been proved for this region of wave-lengths. This well-known law, which gives a general quantum relation between the radiation emitted or absorbed and the energy of the incident or the ejected electrons, is expressed thus :

$$eV = h\nu.$$

In the case in hand this means that the energy  $eV$ , acquired by the electron in falling through the difference of potential  $V$  (the voltage on the tube), is transformed by collision with the anticathode into the energy of a homogeneous wave-train of frequency  $\nu$ . According to the theory of Röntgen radiation, which assumes the sudden change in velocity of an electron to be the cause of the radiation, there is a maximum frequency corresponding to the complete stoppage at a single collision of electrons possessing the maximum velocity afforded by the applied voltage. This maximum frequency is manifested in the sudden beginning of the curve on the short wave-length side.

The experimental determination of the position of this limiting frequency has shown it to be, in agreement with the theory, independent of the material of the anticathode. Wagner has also shown, in an investigation carried out with great accuracy, that this limiting frequency is quite independent of the direction of the emitted radiation with respect to the cathode ray stream. This was of special interest because the æther pulse theory requires a smaller width for the pulse in the direction of motion of the cathode rays than in other directions. Wagner's measurements extended to a tube potential of 10 kv., and Webster later showed the independence of limiting frequency and direction up to 67 kv. There have also been investigations of the validity of the Einstein relation for widely different voltages. The result is that the equation has been found to be true even for the very highest electron velocities attained. For example, Wagner carried out very accurate measurements in the interval 4500 to 10,500 volts; Müller, by a photographic method, worked with voltages between 18,000 and 28,000; Duane and Hunt, who were the first to make accurate measurements to solve this question, used potentials from 25,000 to 39,000 volts. Webster made his investigations in about the same region of from 20,000 to 40,000 volts, whilst Hull and

Rice verified the relation to 100,000 volts, and made some measurements as high as 150,000 volts. On the whole we can, therefore, say that the equation has been demonstrated to hold in the entire region extending from a few volts in the photo-electric effect up to the highest voltages which can be attained and measured in X-ray work.

The first characteristic of the continuous Röntgen radiation, namely, its limit on the short wave-length side, has thus now become well known, and is subject to a very simple law. The second fundamental feature of the white radiation, which is also very important for practical work, is the total intensity. We shall take the third to be the distribution of intensity among the different wave-lengths.

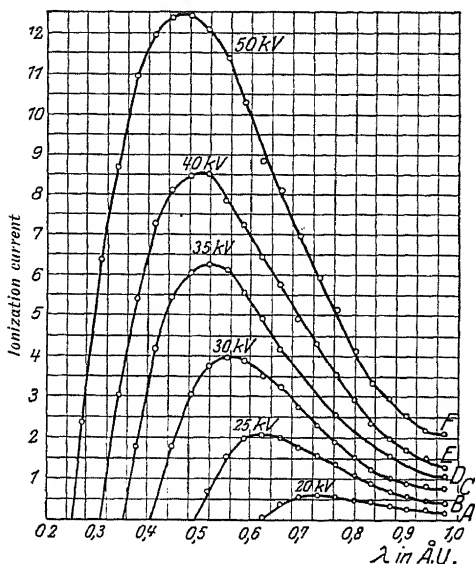


FIG. 92. Intensity distribution (uncorrected) of the continuous radiation from a tungsten anticathode at various voltages, taken by Ulrey.

Between the last two there is, of course, the simple relation that the former may be obtained from an integration of the latter. As a matter of measurement, the total intensity can be determined directly, thus avoiding certain sources of error which are introduced when the radiation is resolved into a spectrum. In both cases, as we shall show later, it is not the energy of the radiation itself which is determined, but rather a measure of its ionizing action. Just how these two quantities are related for different wave-lengths is yet an open question.

As an illustration of the intensity distribution, we reproduce in Fig. 92 the curves which were obtained by Ulrey by the ionization method from an X-ray tube with

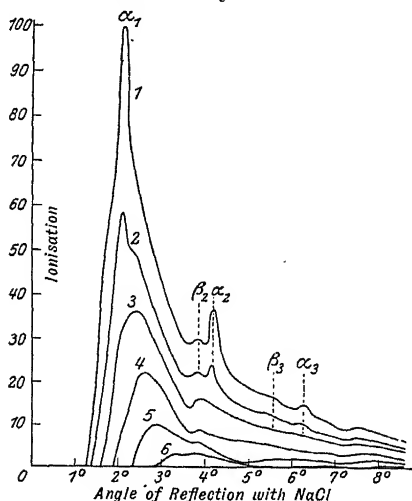


FIG. 93. Intensity distribution (uncorrected) of the continuous and line radiation from a tungsten anticathode, by Hull and Rice.

tungsten anticathode, using the constant voltages 20, 25, 30, 35, 40 and 50 kilovolts, and making no correction for the various sources of error. In addition to the displacement towards short wave-lengths with increasing voltage demanded by the Einstein relation, we observe also a marked increase in the intensity for all wave-lengths. In this work the voltage

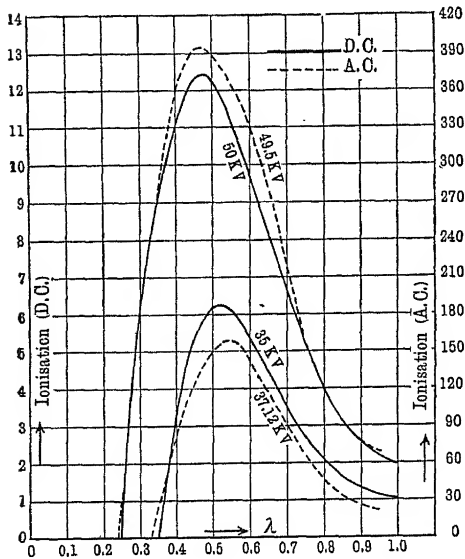


FIG. 94.

was kept low enough to ensure that the characteristic *K* radiation of tungsten was not excited. If the voltage be increased sufficiently the curves take on a complicated appearance, due to the superposition of the characteristic spectrum. Fig. 93 represents a set of such curves taken by Hull and Rice under the same conditions, but with voltages of from 40 to 90 kv. Particularly with the highest voltage the characteristic radiation shows very strongly and is visible in the first three orders. In a later paragraph we shall return to these experiments and to a study of the curves.

Finally, we reproduce in Fig. 94 some spectrometric measurements by Behnken which may be of interest from the practical standpoint, because they were not obtained like the former ones with a direct current voltage but from the A.C. commercial supply, which is the one ordinarily at hand. For direct comparison two of Ulrey's curves are reduced to the proper proportions in the ordinate scale and plotted beside those of Behnken for a corresponding A.C. voltage. Since the curves obtained by the alternating current voltage consist of a series of direct voltage curves with very different frequency limits, all combined into one, it is surprising how nearly identical the curves are. As Behnken pointed out, this comparison is not entirely justified, because the observations were taken under greatly different conditions. Among other things the crystals were different, Ulrey employing calcite and Behnken rocksalt.



### 36. Determination of the Limiting Wave-lengths of the Continuous Spectrum and the Evaluation of Planck's Constant $h$

The experimental determination of the limiting wave-length excited by a given tube voltage is not only of great significance for Röntgen spectroscopy, but it also affords a most excellent method for the evaluation of the constant  $h$ , which is of such great importance in the entire field of radiation. It is therefore not surprising that after Duane and Hunt had first demonstrated the validity of the Einstein equation in this region of wave-lengths, the problem of the constant  $h$  was attacked by a number of investigators with results ever increasing in accuracy.

There are two ways, which differ essentially in principle, for carrying out the measurements. In the first method the voltage on the tube is kept constant, while the crystal and the ionization chamber are turned over the region in which the wave-length limit is located; in other words, that part of the distribution curve is obtained which is necessary for the determination of the limiting wave-length. In the second method the crystal and ionization chamber are held fixed upon a certain wave-length, while the voltage is raised until a wave-length corresponding to the fixed position of the crystal is excited. Then the voltage is raised slightly and the ionization current measured. By subsequent extrapolation to the intensity zero of the ionization current the voltage is obtained which corresponds to the limiting wave-length given by the setting of the crystal and ionization chamber. In addition to these two methods, which require the use of a Bragg ionization spectrometer, the photographic method is also employed. In this method, that part of the spectrum in which the limiting wave-length lies is photographed, while the voltage on the tube is, of course, kept constant.

As an example of the first method we need only refer to the investigations of Webster already discussed on pp. 92-94, and especially to Fig. 70c. As indicated in that figure, the spectral curves were taken at 40.0, 31.8 and 23.2 kv., and the short wave-length limits were respectively 0.312, 0.387 and 0.531 Å. From Einstein's equation

$$eV = h\nu,$$

we have

$$h = \frac{eV\lambda}{300c},$$

where  $V$  is expressed in volts. Using Millikan's value of  $e = 4.774 \times 10^{-10}$  E.S.U. and the above values of  $V$  and  $\lambda$ , we find

$$\left. \begin{array}{l} h = 6.60 \\ h = 6.53 \\ h = 6.53 \end{array} \right\} \times 10^{-27} \text{ erg. sec.}$$

Another illustration is afforded by the numerical values of voltage and limiting frequency shown by Ulrey's curves for tungsten in Fig. 92. From these data the following values of  $h$  are calculated.

s.s.

o

Potential in kv.	Limiting wave-length in Å.	$h$ calculated.
20	0.615	6.53
25	0.490	6.50
30	0.405	6.45
35	0.355	6.59
40	0.310	6.58
50	0.250	6.63
Mean		$6.54 \times 10^{-27}$ erg. sec.

The second of the methods stated above, in which the intensity at a given wave-length is determined as a function of the tube voltage, is somewhat more accurate. Among the determinations of the constant  $h$  made in this manner we shall describe the very careful measurements of Blake and Duane, and also those of Wagner.

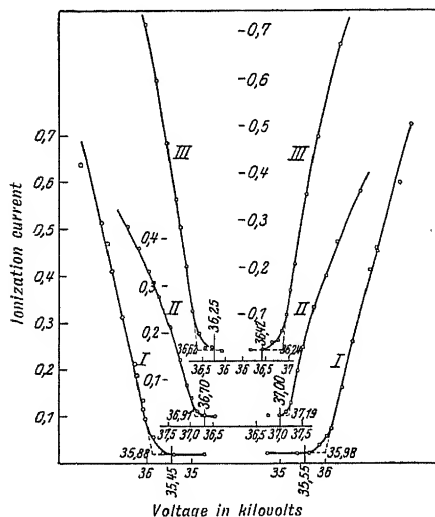


FIG. 95.

In both cases an ionization spectrometer of the Bragg type was employed, but while Blake and Duane worked with moderately high voltages, 36 to 42 kv., and therefore with wave-lengths of the order of 0.3 Å., Wagner used a gas-filled tube and much lower voltages, 4.5 to 10.5 kv., corresponding to wave-lengths from 2.0 to 1.1 Å.

These different ranges of voltage involve different sources of error, and consequently different methods of overcoming the errors.

In order to avoid electrostatic disturbances at the relatively high potentials used, Blake and Duane set up their ionization spectrometer in a large metal case. The X-ray tube, which was supplied with power from a storage battery, was placed in a special chamber together with the instruments for measuring the voltage applied to the tube. The special form of the ionization chamber—a sealed glass vessel—has been already described. One of the greatest difficulties here was the determination of the applied voltage. For this purpose Blake and Duane employed an electrostatic voltmeter consisting of four large metal spheres, of which two were fixed, while the other two were attached to a bifilar suspension. The rotation of the movable pair of spheres with the voltage used was sufficient to cause a deflection of 800 mm. on the scale, and this deflection could be estimated to 0.1 mm. The voltmeter was calibrated by direct

comparison with the fall of potential over a high resistance of 894,700 ohms, the current through which was read from a milliammeter.

The crystal was calcite, and since at these short wave-lengths the rays penetrate the crystal to a considerable extent, a correction is necessary on this account. Another correction must also be made for the finite width of the X-ray beam, which may be determined from the slit width. The result of this latter source of error is that the curves do not continue as straight lines down to the zero axis, but are rounded off as shown in Fig. 95. These curves were taken symmetrically on both sides, so that the wave-length might be determined independently of the direction of the incident beam.

As a mean value of these measurements, together with several made by the first method (constant voltage and rotating ionization chamber), Blake and Duane reported

$$h = 6.555 \times 10^{-27} \text{ erg. sec.}$$

Later (1921) Duane, together with H. H. Palmer and Chi-Sun Yeh repeated the determination, measuring the voltage by the potentiometer

method and a high resistance of 10 megohms. The result, which agreed very well with the previous one, was  $h = (6.556 \pm 0.009) \times 10^{-27} \text{ erg. sec.}$

In E. Wagner's very careful experiments for the determination of  $h$ , he used, as already stated, a gas-filled tube driven by a storage battery. It was shown by special tests that neither the gas pressure nor the kind of gas in the tube had any influence upon the results. Wagner also showed that the kind of crystal used had no effect, by making measurements with NaCl as well as with KCl. Finally, he used Cu and Pt as anticathodes in order to make certain that the value of the constant obtained was independent of the material used as radiator.

As voltmeter Wagner used the electrostatic index instruments of Hartmann and Braun in Frankfurt. The calibration was done by combining smaller voltages, which were measured by the help of 51 Weston standard cells.

The typical course of an intensity curve with increasing voltage is seen in Fig. 96. The sudden rise may be seen plainly here, and it is followed by a portion of the curve which is nearly straight. At a certain point, however, the curve suddenly changes its direction. For the

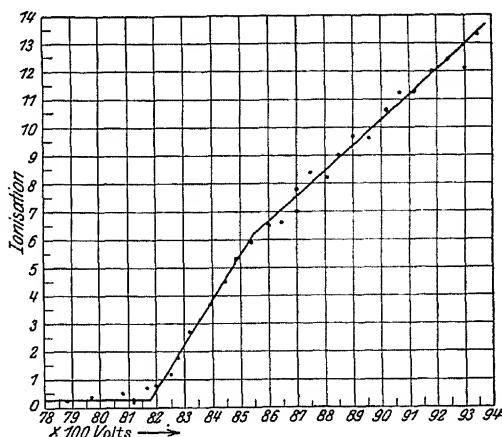


FIG. 96.

measurements desired this angle in the curve has, of course, no significance whatever, but it appears that the change of direction is something quite characteristic of the curves, as Wagner verified on a later occasion by measuring the total intensity. An explanation of this peculiarity has not yet been given.

For a final result of his first investigation Wagner found

$$h = 6.49 \times 10^{-27} \text{ erg. sec.}$$

and in a repetition of the experiment with improved technical facilities he obtained

$$h = 6.52 \times 10^{-27} \text{ erg. sec.}$$

The last determination of this constant which we will mention is that made by Müller, using the photographic method, in which he utilized an influence machine as the source of high potential, a gas-filled tube for the production of X-rays, and a number of different materials as anticathode. This method, if employed skilfully, without doubt affords a high degree of accuracy, but Müller's aim was not so much to measure  $h$  with the highest precision possible as to settle what was at that time a disputed point. From certain experiments which have since been shown not to be entirely free from objection, the question had been raised whether the characteristic radiation might not exercise some influence on the limiting frequency. Müller sought to prove that there was no such effect by using different materials, Cu, Ag, Pb and Pt as anticathode, and thus measuring the limiting frequency for different conditions as regards characteristic radiation. His measurements gave the expected result, namely, that the frequency limit is quite independent of the characteristic radiation of the anticathode, a fact which was also established beyond doubt by various other investigations. The mean value of Müller's measurements was

$$h = 6.57 \times 10^{-27} \text{ erg. sec.}$$

A summary of the values of  $h$  obtained by different authors is found in the following table:

TABLE 41.

Author.	Potential kv.	Crystal.	Anticathode.	$h \times 10^{27}$
Duane and Hunt	25—39	Calcite	W	6.50
Webster	23—40	„	Rh	6.55
Ulrey	20—50	„	W	6.54
Müller	15—28	Rocksalt	CuAgPbPt	6.57
Blake-Duane	40	Calcite	W	6.555
Wagner	4.5—10.5	KCl and NaCl	CuPt	6.52

For comparison with the results of measurements obtained by other means than X-rays a table is added which is taken from a report by Ladenburg on measurements of  $h$  (*Jahrb. d. Rad.* 17, 1920):

TABLE 42.

Method.	$h \cdot 10^{27}$ .
1. Radiation measurements :	
(a) Isochromatics of Warburg and co-workers ( $c_2=1.430$ ) - - - - -	$6.540 \pm 0.02$
(b) Stefan-Boltzmann constant of total radiation, $\sigma=5.8 \times 10^{-5}$ (Gerlach) - - - - -	$6.518 \pm 0.03$
2. From the quantum equation :	
(a) Photoelectric measurements of :	
Millikan for Na and Li - - - - -	6.571
Hennings and Kadesh for Mg, Al, Zn, Cu, Fe, Sn -	6.43
(b) Resonance and ionization potentials, mean of 16 values - - - - -	$6.58 \pm 0.03$
Ionization potential of He and Hg - - - - -	$6.54 \pm 0.03$
3. From Bohr's series formula :	
Paschen : measurement of the Rydberg constant $R_\infty=109,737$ - - - - -	$6.545 \pm 0.013$

### 37. Total Intensity and Intensity Distribution in the Continuous Spectrum

The early researches of Seitz, Carter, Whiddington, Beatty and others agree uniformly on the following simple approximate relation between the total energy of the X-radiation and the voltage applied to the tube : *The total energy is proportional to the square of the voltage.* The law presupposes that the current remains constant and that the characteristic radiation is not excited, or that it is deducted from the total radiation. Since the velocity of the cathode rays satisfies the equation

$$\frac{1}{2}mv^2 = eV,$$

we may express the law in another form : *The total energy is proportional to the fourth power of the velocity of the cathode rays exciting the radiation.* By

determining the area under Ulrey's curves (Fig. 92), which have already been discussed, we obtain results agreeing with the above law. The areas under these curves, taken as far as  $0.975 \text{ \AA}$ , are given, together with the corresponding voltages, in the following table. These values plotted in Fig. 97, show that the total energy is nearly proportional to the square of the voltage applied to the tube.

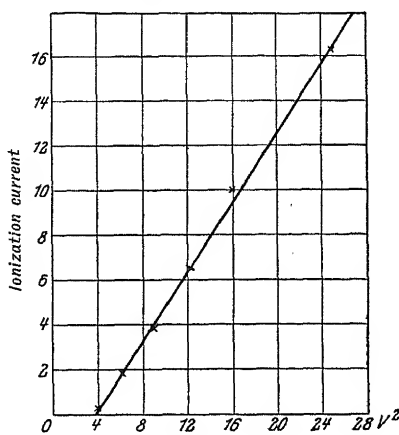


FIG. 97.

Tube voltage kv.	Area by integration.
20	0.46
25	1.85
30	3.96
35	6.78
30	10.06
50	16.34

This result is, indeed, not very convincing, because there are considerable sources of error for which no correction has been made. If one wishes merely to determine the total radiation, this roundabout method with the distribution curves is not to be recommended.

Duane and Shimizu made a direct measurement of intensity with modern apparatus, and although their primary object was to investigate the dependence of the total radiation on the atomic number of the element, yet their results also serve to show the relation between total

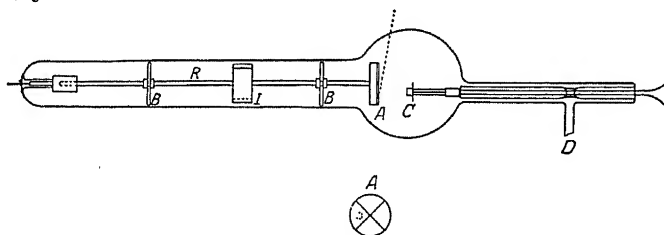


Fig. 98.

radiation and voltage. In the above measurements of Ulrey the anti-cathode was of tungsten. Duane and Shimizu, however, used the four light elements, Cu, Ni, Co and Fe. The range of voltage extended from 20 to 40 kv. They worked with the ionization method, and used the rays which came from the anode surface at almost the grazing angle, without dispersing them into a spectrum. The Coolidge tube, shown in Fig. 98, was provided with an anode consisting of a plate of four sectors composed of the metals named above, which could be brought in turn, by rotation of the anode, into the focus of the cathode rays. The results of the measurements are summarized in the following table :

TABLE 43.

Tube voltage kv.	Ionization current (volts/sec.).			
	29 Cu.	28 Ni.	27 Co.	26 Fe.
19.14	0.0248	0.0240	0.0227	0.0220
21.43	0.0386	0.0375	0.0344	0.0336
24.12	0.0544	0.0532	0.0502	0.0492
27.30	0.0812	0.0790	0.0792	0.0732
30.11	0.1088	0.1061	0.1021	0.0981
32.40	0.1327	0.1295	0.1251	0.1210
40.87	0.238	0.231	0.223	0.214

Fig. 99 represents, in the case of Cu, the intensity, measured by the ionization current, as a function of the square of the tube voltage, and as the curve shows, they are very nearly proportional. It is to be noted that the soft characteristic radiation was absorbed before reaching the ionization chamber, and hence was not measured.

Even though the conclusions of various authors, in their investigations of the relation of total intensity to voltage, are in good accord with each other in so far as they find the intensity to vary as the square of the voltage, independently of the absolute value of the voltage and of the material of the anticathode, yet the agreement is not so good when we pass to the question of the dependence of the total radiation on the atomic number of the element. It has been known since the first experiments of Röntgen that the X-radiation depends very greatly on the material of the anticathode. In a qualitative way it is also generally admitted that the heavier elements give a more intensive radiation than the lighter ones, a fact which is taken into consideration in the choice of materials such as platinum and tungsten for anticathodes in commercial tubes.

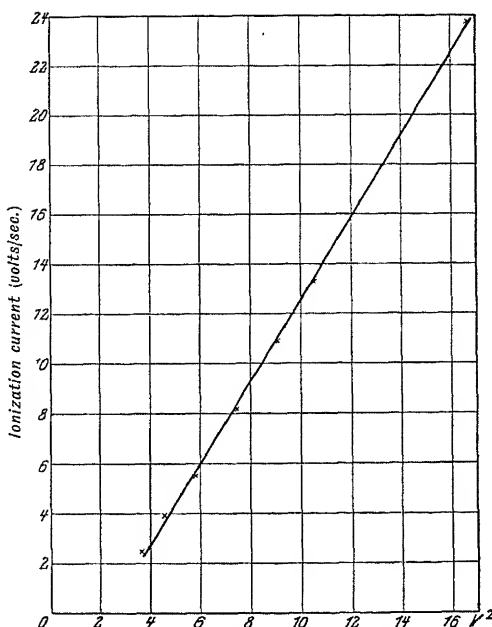


Fig. 99. Intensity of the X-radiation as a function of the square of the tube voltage for Cu and Shimizu.

The more definite quantitative relation between intensity and atomic number was not easily settled. Among the earlier investigations of this question we shall describe those of Kaye, which were carried out with great skill and in considerable detail. The apparatus used by him has already been reproduced in Fig. 21B, p. 34. The X-ray tube with changeable anticathode was driven by an induction coil at a voltage which was held as nearly constant as possible. By interposing a suitable filter, usually 2 mm. of Al, the characteristic radiation was mostly absorbed, and hence did not enter the ionization chamber. The ionization currents thus obtained are a measure of the relative total intensities of the radiation from the various elements, and are given in the following Table 44. In this table we have included the

atomic numbers of the elements as well as the densities and melting points.

TABLE 44.

Element.	Total intensity. (Ionization current) Pt = 100.	Density.	Melting point.
Au 79	101	19.3	1066
Pt 78	100	21.5	1750
Ir 77	98	22.4	2290
Os 76	97	22.5	2700
W 74	91	19.3	3200
Ta 73	90	16.6	2900
Pd 46	55	11.4	1550
Rh 45	54	12.4	1900
Ru 44	53	12.3	1950 ?
Mo 42	50	8.6	2500
Nb 41	49	12.7	2200 ?
Zr 40	47	4.1	1300
Y 39	46	3.8	—
Cu 29	33	8.9	1084
Ni 28	30	8.8	1470
Co 27	30	8.6	1480
Fe 26	27	7.9	1530
Mn 25	26	7.4	1260
Cr 24	25	6.5	1520
Va 23	24	5.5	1720
Ti 22	22	3.5	1800

Kaye himself showed the relation of his measured values of the total intensity to the atomic weight, but since we now know, from the discoveries of recent years, that the atomic number is a more fundamental variable than the atomic weight for the theory of X-radiation, it seems more fitting to represent the total radiation as a function of the atomic number. This has accordingly been done in Fig. 100. It is evident that a relation very nearly linear exists between the two quantities.

We may state the result of Kaye's investigation as follows: *At a constant voltage the total radiation is proportional to the atomic number of the element used as anticathode.*

Further investigations along the same lines, such as those carried out by Whiddington and by Carter, made it appear that the relation was not so simple. Whiddington worked with very low voltages, between 1500 and 3000 volts, while Carter employed from 30,000 to 60,000 volts. Since this question has now been settled by the very fine researches of Wagner and Kulenkampff these earlier investigations have mainly a historical interest, and therefore we shall refrain from a further discussion of them.



Before entering on a description of the investigation last mentioned, let us consider two still more recent results. On page 214 there appears a table containing the measurements of Duane and Shimizu on the total radiation from four different anticathodes at constant voltage. In the

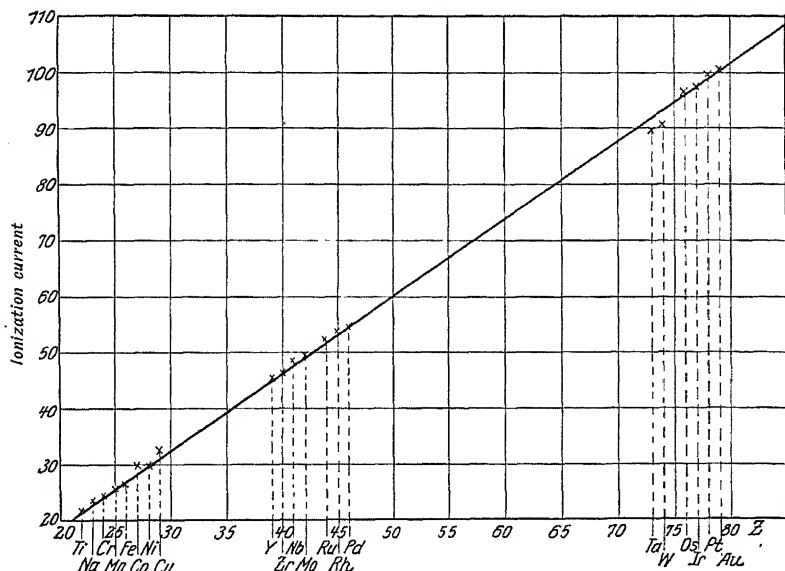


FIG. 100. Total radiation as a function of the atomic number of the material of the anticathode, from the earlier measurements of Kaye.

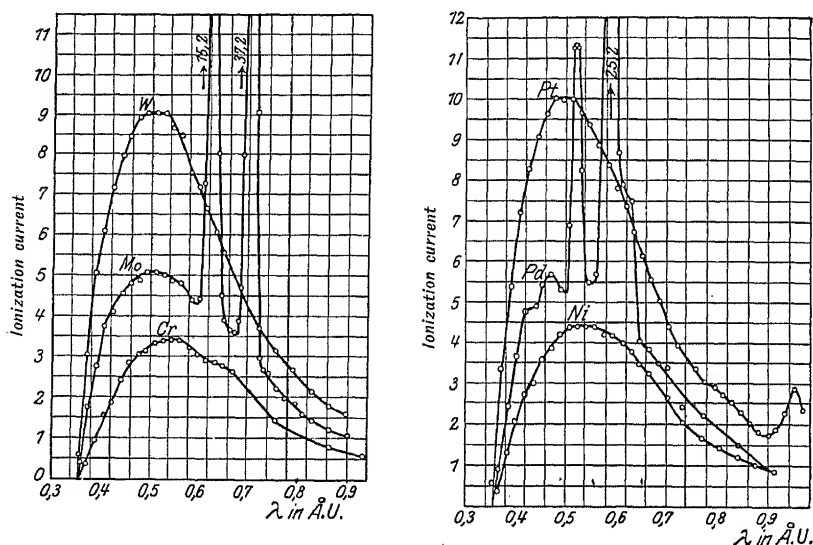
following table the same results are presented in a slightly different form, namely, by taking the ionization current in the case of iron as the unit. This table shows, therefore, the total radiation of the elements Cu, Ni and Co, referred to that of Fe as unity, for voltages ranging from 20 to 40 kv.

TABLE 45.

Tube voltage kv.	Ionization current (Fe=1.00).			
	Cu 29.	Ni 28.	Co 27.	Fe 26
19.14	1.127	1.091	1.032	1.00
21.43	1.149	1.116	1.024	1.00
24.12	1.106	1.081	1.020	1.00
27.30	1.109	1.079	1.041	1.00
30.11	1.109	1.082	1.041	1.00
32.40	1.097	1.070	1.034	1.00
40.87	1.110	1.079	1.042	1.00
Mean	1.115	1.085	1.033	1.00
Relative Atomic No.	1.115	1.077	1.038	1.00
Relative Atomic Wt.	1.138	1.051	1.056	1.00

In the first place it is apparent from this table that the *relative* total radiation is independent of the voltage applied to the tube. Secondly, the mean values are directly proportional to the atomic numbers of the elements. On the contrary, there is no direct proportionality between the total radiation and the atomic weight, as the last row of figures shows. In this connection the elements Ni and Co are especially desirable for investigation. (Compare the values of Kaye.)

The values obtained by integrating the areas under Ulrey's spectral distribution curves are not in agreement with the above results. On the contrary, Ulrey felt compelled to conclude from his measurements that a distinct periodicity, in accord with the chemical properties of the



FIGS. 101A, B. Uncorrected intensity distribution of the total radiation from several anticathodes, according to Ulrey.

elements, could be observed in the total Röntgen radiation. Considering all that we now know about X-ray emission this periodicity seems very improbable, and Ulrey's method of investigation, which neglected the effect on the curves of several disturbing factors, can hardly be deemed sufficiently reliable for such conclusions.

Ulrey worked with constant voltage according to the Hull method. The crystal used was calcite, and the ionization chamber, which was 750 mm. long and 75 mm. in diameter, was filled with ethyl bromide vapour. He calculated that this ionization chamber at 20° C. absorbs as strongly as one 1800 mm. long filled with air. In Figs. 101A, B we have the ionization curves for the anticathode substances W, Mo, Cr and Pt, Pd, Ni, taken at a voltage of 35 kv.

The evaluation of the areas gives, after deducting the characteristic radiation, the relative measures (uncorrected) of the total radiation shown in Table 46.

TABLE 46.

Element.		Total radiation (area under curves).
Pt	78	100
W	74	90.0
Pd	46	60.3
Mo	42	54.3
Ni	28	45.7
Cr	24	34.6

If we plot these values as a function of the atomic number, or of the atomic weight, in accordance with Fig. 100, the plots are found to be distributed quite irregularly, and it is impossible to recognize in them the expression of any simple relation. In the author's opinion we can only conclude from these results, that on account of the disturbing influence of the sources of error, the ionization curves are not sufficiently reliable to decide this question. Behnken has made an attempt to apply the necessary corrections.

This whole question has recently entered into quite a new phase as a result of the excellent researches of E. Wagner and Kulenkampff. They used in their investigations a considerable number of elements as anticathode—Al, Fe, Co, Ni, Cu, Ag, Sn, Pt—and applied in all cases a constant tension of 10,470 volts to the tube. In addition, they studied the intensity distribution for Ag and Pt as a function of the voltage between 7 and 12 kv. Very painstaking preliminary work was necessary in order to study and estimate the effect of all the sources of error which might affect the distribution curves.

When one wishes to evaluate the true intensity of radiation from the anticathode as a function of the wave-length, or better still of the frequency, utilising as a basis for that calculation the intensity curve which really represents the current measured directly in the ionization chamber, the principal factors to be considered are the following :

1. Reflecting power of the grating and its dependence on wave-length.
2. Absorption of the radiation in passing from the anticathode to the measuring chamber, including absorption in the aluminium window of the tube, in the air space between the aluminium window and the window of the chamber, and finally in the window of the chamber itself.
3. Absorption in the anticathode itself.
4. Finite length of the ionization chamber.
5. The relation between intensity of the radiation and ionizing action in respect of their dependence on wave-length.

Wagner and Kulenkampff did not enter into an investigation of the last factor, but assumed the ionizing action of the rays in the air-filled chamber to be a measure of the intensity, and hence in the following discussion, when reference is made to the intensity of radiation of a given frequency, it is to be understood as the ionizing effect of the radiation.

This is, moreover, the sense in which the term has been used in describing experiments in the preceding pages.

Corrections 2 and 4 may, of course, be calculated with no great difficulty from our present knowledge.

With 1 and 3 it is a different matter. Extended preliminary experiments were necessary to determine the reflecting power, since this depends to some extent on the particular crystal used. The coefficient of reflection was determined for the wavelengths 1.39, 1.54, 1.75 and 1.93 Å. (Cu and Fe radiation) by double reflection from calcite and from rock-salt crystals. The results indicated that the coefficient for calcite was nearly independent of the wavelength. The results of Wagner and Kulenkampff are in good agreement

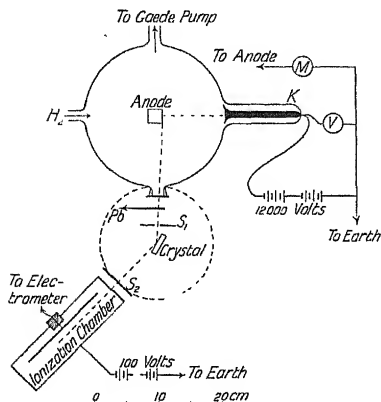


FIG. 102. Apparatus of Wagner and Kulenkampff.

with those of W. L. Bragg, James and Bosanquet, and of Davis and Stempel, which were obtained in the region of considerably shorter wave-lengths.

Finally, the correction factor 3 was estimated as follows: From

Fig. 102 it may be seen that the anode consisted of a parallelopiped, on the four sides of which various materials were placed. By turning the anode about an axis perpendicular to the plane of the figure each one of these substances could be brought into a position to act as radiator. The X-rays received into the ionization chamber proceeded in a direction at right angles to the cathode rays.

Nevertheless, it was possible with such a mounting of the anticathode to vary the angle  $\psi$  between the X-ray beam and the surface of the anticathode. In general, the measurements were made with very small values of this angle. On account of the characteristic absorption of the anticathode the X-radia-

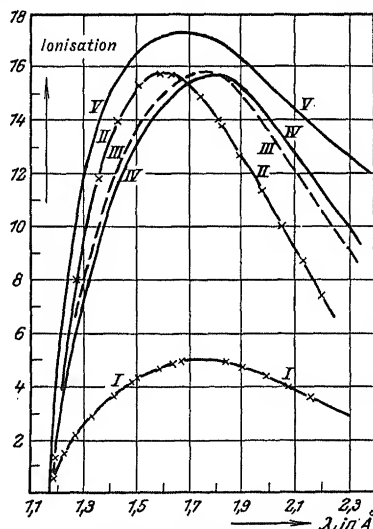


FIG. 103. Intensity distribution with silver anticathode and a potential of 10,500 volts.

I. = calcite crystal (uncorrected curve).  
 II. = rock-salt.  
 III. = I, magnified to accord with II.  
 IV. =  
 V. =

tion was diminished in intensity, and in varying degrees according to the angle  $\psi$ . It was possible, however, to establish a simple relation between the angle  $\psi$  and the decrease in intensity, by the help of which the correction was then made.

Fig. 103 shows how the curves obtained directly from experiment were modified in one particular case by the corrections mentioned above.

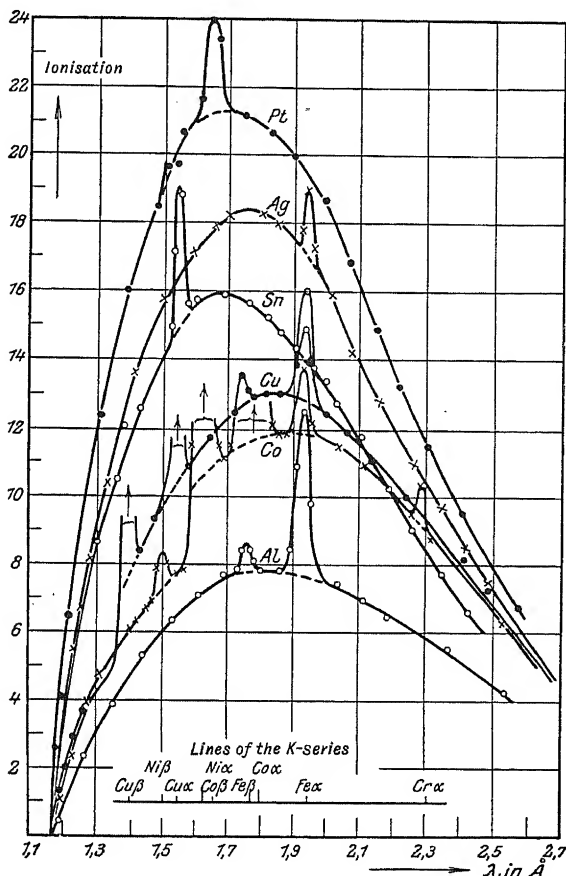


FIG. 104. Distribution curves (uncorrected) for various anticathode materials. Potential on tube, 10,470 volts. The superposed lines are due mostly to impurities.

It represents the distribution curve with silver as anticathode and 10,500 volts as the potential on the tube. Rocksalt and calcite were used as crystal gratings.

From distribution curves, such as those of Fig. 104 for Pt, Ag, Sn, Cu, Co and Al, which were measured directly at a tube voltage of 10.47 kv., the curves of Fig. 105 were obtained, showing the characteristic

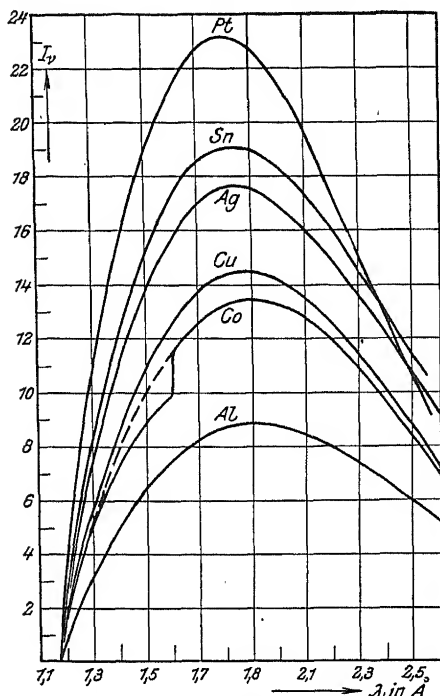


FIG. 105. The curves of Fig. 104, after making corrections.

measured by ionization as a function of the frequency, are straight lines.

One point on these curves is fixed by the Einstein relation  $h\nu = eV$ , namely, the point of intersection with the frequency axis. Since all the curves of Fig. 104 correspond to the same voltage, 10.47 kv., they have a common point of intersection on the axis of abscissae. One might expect, therefore, that the straight lines which represent the intensity as a function of the frequency would also pass through a common

absorption in the anticathode. After applying the corrections for absorption and reflection corresponding to the factors mentioned under 1, 2 and 4, and after recalculating in terms of frequency instead of wave-length, the curves of Fig. 106 were obtained. The calculations for the latter curves were made as follows: we have

$$\nu = \frac{c}{\lambda},$$

and hence

$$d\nu = -\frac{1}{c} \nu^2 d\lambda.$$

From the equation

$$I_\nu d\nu = I_\lambda d\lambda,$$

we therefore obtain

$$I_\nu = \frac{c}{\nu^2} I_\lambda.$$

The authors thus finally arrived at the very important result: *The curves which represent intensity,*

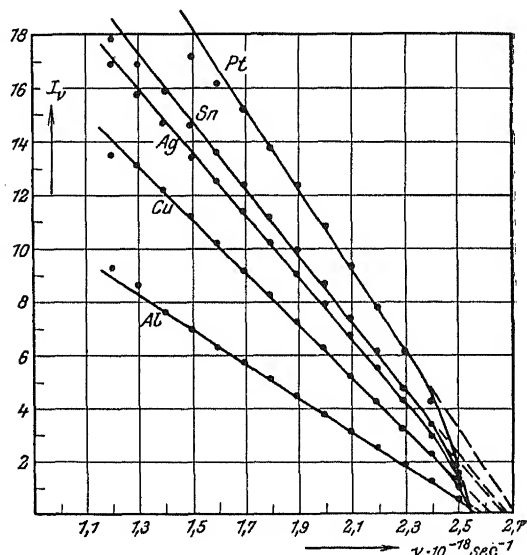


FIG. 106. The curves of Figs. 104 and 105 expressed in terms of frequency.

point on the frequency axis. They do not do so, however, for the lower parts of the curves are slightly bent towards the axis of abscissae, or they suffer there a break which results in a slight change in direction towards that end of the curves.

This slight discrepancy is still more apparent in the curves of Figs. 107 and 108, which represent the intensity distribution with various voltages, but with the same anticathode, which is

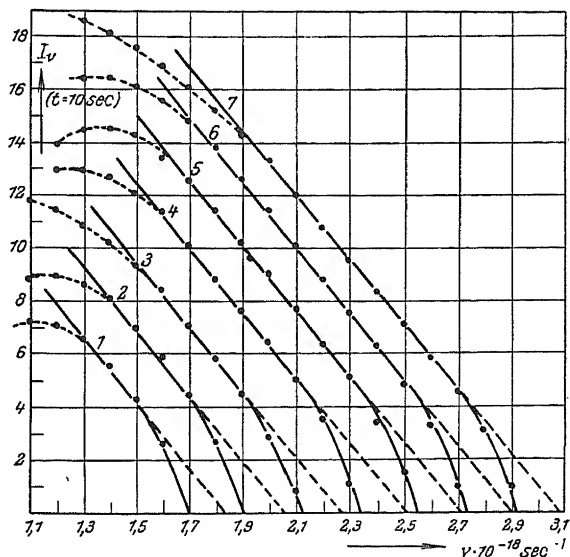


Fig. 107. Distribution curves in terms of frequency for platinum with various tube voltages.

1 = 7000 volts; 3 = 8750 volts; 5 = 10,470 volts; 7 = 11,980 volts.  
2 = 7850 „ 4 = 9600 „ 6 = 11,200 „

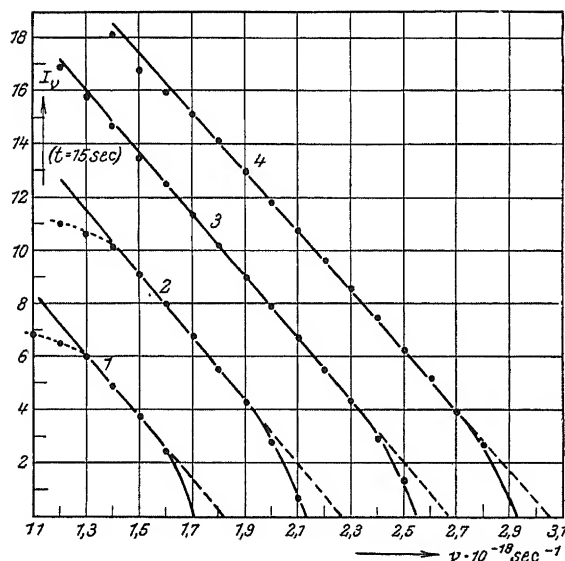


Fig. 108. Distribution curves in terms of frequency for silver with various tube voltages.

1 = 7000 volts; 3 = 10,470 volts;  
2 = 8750 „ 4 = 11,980 „

Pt in Fig. 107 and Ag in Fig. 108. According to the Einstein equation the intercepts are displaced towards greater frequencies with higher voltages. Under change of voltage the straight lines exhibit a parallel displacement. It is also to be observed from these figures that the curvature of the lower part of the lines is independent of the voltage. In particular, the frequency difference between the actual limiting frequency and that indicated by the

straight line produced is a constant. The values obtained for this frequency difference  $\Delta\nu$  are arranged in the following table. For different elements  $\Delta\nu$  is approximately proportional to the atomic number.

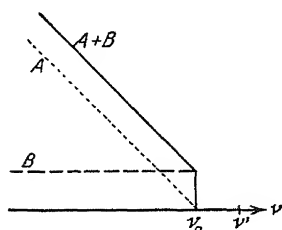


FIG. 109.

We may take account of this small departure of the curves from straight lines by constructing the curves in two distinct parts, as shown in Fig. 109. For the principal part *A* of the curve we have then

$$I_\nu = \text{const.} \times (\nu_0 - \nu), \quad (1)$$

where  $\nu_0$  is the maximum frequency calculated from the Einstein equation.

For this portion we obtain the *total radiation*.

$$I_A = \int_0^{\nu_0} I_\nu d\nu = \text{const.} \times \nu_0^2 = \text{const.} \times V^2,$$

which is in entire agreement with the earlier work described above.

The proportionality factor of equation (1) is independent of the voltage, but varies with the atomic number of the material of the anti-cathode. It may be found from the slope of the curves in Fig. 106. In this way the constant is found to be *directly proportional to the atomic number*, a relation which we had already deduced as the probable one from earlier measurements. Hence, for the part *A* of the curve, we may write

$$I_\nu = CZ(\nu_0 - \nu),$$

where *C* is a constant which is independent of the voltage and of the atomic number.

For the part *B* we have evidently

$$I_\nu = \text{const.},$$

independent of the voltage, from which we obtain immediately that the *total radiation* of this portion is directly proportional to the voltage. For different elements the portion *B* increases approximately as the square of the atomic number, so that we may write for the parts *A* and *B* combined

$$I_\nu = C[Z(\nu_0 - \nu) + bZ^2], \quad (2)$$

where *b* is also a constant independent of voltage and atomic number.

TABLE 47.

Voltage kv.	$\Delta\nu$	
	Pt.	Ag.
11.98	0.15	0.12
11.20	0.17	—
10.47	0.16	0.12
9.60	0.17	—
8.75	0.14	0.13
7.85	0.15	—
7.00	0.14	0.11
Mean	0.15 <sub>5</sub>	0.12



This important equation represents the final result of all the researches and it was found by Wagner and Kulenkampff to hold over an interval ranging from 7000 to 12,000 volts, and in a wave-length region from 1.0 to 2.8 Å. It embraces as special cases the laws deduced from the earlier investigations, namely, that the total energy increases as the square of the voltage, and as the first power of the atomic number. It seems very probable that this intensity distribution law, derived from the ionizing effect, is also valid for the voltages and wave-lengths employed with X-ray tubes for commercial purposes.

There is one more point in connection with these curves which was considered by Kulenkampff, and which we may take up here briefly. Several authors have occupied themselves with the question as to whether, in the curves showing the relation between intensity and wave-lengths for the continuous spectrum, the wave-length  $\lambda_m$  corresponding to the maximum intensity varies according to any simple law. The similarity between these curves and those of "black body" radiation in the optical spectrum has been pointed out, although the resemblance is purely external. The expression for  $\lambda_m$  is easily derived from the distribution law of equation (2). It is only necessary to transform from  $I_\nu$  to  $I_\lambda$  by the relation

$$I_\lambda = \frac{c}{\lambda^2} I_\nu,$$

to differentiate the resulting equation with respect to  $\lambda$  and to set the derivative equal to zero. If we denote by  $\lambda_0$  the wave-length corresponding to  $\nu_0$  we thus obtain

$$\lambda_m = \frac{3c}{2} \frac{\lambda_0}{c + bZ\lambda_0}.$$

If we neglect the part  $B$  of Fig. 109, *i.e.* if we put  $b=0$ , we have the simple relation

$$\frac{\lambda_m}{\lambda_0} = \frac{3}{2}.$$

In an investigation recently published, Kirkpatrick has studied the distribution of the energy, measured by ionization, of the continuous X-ray spectrum of tungsten at voltages higher than those used by Wagner and Kulenkampff. He has also thoroughly investigated all the sources of error in the directly measured ionization curve, and corrected the result for these errors. As he worked with higher voltages and correspondingly smaller angles of reflection it was necessary to study in detail the effect of the overlapping of the spectra in different orders. This was done in two different ways, the results of which gave satisfactory agreement. The other factors for which corrections were made were (1) the absorption in the walls of the tube, in the air, and in the window

of the ionization chamber; (2) for the reflecting power of the rocksalt crystal; (3) for incompleteness of absorption in the ionization chamber.

The ionization energy curve was determined at four voltages between 51 kv. and 71 kv. As Kirkpartick shows, his curve found experimentally does not agree at all with the corresponding curves from the theories of March, Behnken and Bergen Davis.

For the connection between the wave-length  $\lambda_m$  of the maximum point on the distribution curve and the minimum wave-length  $\lambda_0$ , Kirkpatrick gives the equation

$$\lambda_m = k + k'\lambda_0,$$

where  $k$  and  $k'$  are positive constants. The numerical values are not given, so it is difficult to say whether the difference between this formula and the relation found by Kulenkampff is of importance.

It does not fall within the scope of this book to discuss the theories of the continuous X-radiation which have been given hitherto by different authors. As stated above, none of those already mentioned are in accordance with the experimental ionization energy curves. But I may call attention to a theory of the phenomenon recently put forward by H. A. Kramers, which seems to be in good agreement with the measurements of Wagner and Kulenkampff. The theory of Kramers is based on the general principles of Bohr's quantum theory of spectra, and is developed in a manner first used by Einstein for black radiation. The resulting formula given by Kramers for the continuous spectrum is

$$I_\nu = i \frac{8\pi}{3\sqrt{3}l} \cdot \frac{e^2\hbar}{c^3m} \cdot Z(\nu_0 - \nu) \sim i 5 \cdot 10^{-50} Z(\nu_0 - \nu). \quad (3)$$

$i$  = number of electrons striking the target in unit time.

$l$  = numerical factor of the order of magnitude 6.

As may be seen, this agrees well with the experimental formula (2), if the term  $CbZ^2$ , corresponding to the part  $B$  in Fig. 109, be neglected. Concerning this last term, which is introduced to account for a bend in the observed curves, Kramers makes the interesting remark: "The electrons will not only lose kinetic energy at their collisions with the atoms, but they will also be deflected through large angles, so that, in general, they will penetrate much less deeply into the target than when their path was straight. Due to these deflections a fraction of the electrons will be able to leave the target, . . . some of them with very small velocities, but many of them also with velocities about equal to the initial velocity  $v$ . The latter effect increases considerably with the atomic number, and will materially contribute to the appearance of the bend in Kulenkampff's curves—for which the second term on the right hand of (2) gives an approximate expression."

It must be emphasized that the formula of Kramers also gives a numerical value of the constant, which is in good agreement with the experimental value.

The continuous spectrum emitted from a Coolidge tube with a molybdenum anticathode has been carefully examined by Webster and Hennings. In this investigation the "isochromatics" for different wave-lengths between 0.246 Å.U. and 1.23 Å.U. were determined at voltages ranging from the minimum voltage for each wave-length up to 70 kv. Both wave-lengths and voltages were measured to  $\frac{1}{10}$  of one per cent. A correction for absorption in the target was applied, and the error due to scattering from the crystal eliminated by taking readings on both sides of the reflecting angle.

The results are given in a graph, in which the intensities are plotted as a function of  $V/V_0$  for every wave-length. These wave-lengths are 0.247, 0.309, 0.415, 0.494, 0.588, 0.676, 0.823, 1.029 and 1.234 Å.  $V_0$  is the minimum potential for producing the wave-length in question. To get a suitable scale for the intensities these were given as  $\frac{I}{I_2}$  where  $I_2$  is in every case the intensity at  $2V_0$ . The graph for each wave-length is a straight line, with the exception of the first part of the curve, where it is slightly bent. In no case do the curves go farther than to the voltage  $2V_0$ , for at this point the reflection in the second order would disturb the measured values. Attempts to eliminate this disturbing influence by using a crystal which gives no reflection in the second order—such as fluorite—were without success, because no sufficiently perfect crystal could be found.

The isochromatic curves were found to agree well with an empirical equation formerly given by Webster :

$$I(V, \nu)d\nu = A\{(V - V_0) + B[1 - e^{C(V - V_0)}]\}d\nu.$$

$A$ ,  $B$  and  $C$  are constants depending only on the frequency.

Starting from this equation, an expression for the radiation from an infinitely thin target is derived, which shows that the probability of the emission of a quantum with the frequency  $\nu$  to  $\nu + d\nu$  in the distance  $ds$  is  $i \cdot ds \cdot \frac{d\nu}{h\nu}$ , where  $i \cdot ds \cdot d\nu$  is the intensity per cathode ray. In this it is supposed that the Thomson-Whiddington law for the decrease of the cathode ray energy, and the  $V^2$  law for the total intensity, hold good.

## VIII

### OTHER METHODS OF EVALUATING THE INNER ENERGY LEVELS OF THE ATOMS

#### 38. Electron Emission by Excitation with X-rays

IN the earliest period of X-ray investigation it was shown by Sagnac and Dorn that bodies exposed to X-rays, in addition to emitting secondary X-radiation, also give off electrons of high velocity. At that time the attempt was also made to determine the velocity of the emitted electrons. The methods employed were the three following :

1. By determination of the curvature of the electron paths in a known magnetic field.
2. By determination of the retarding electric field which is just strong enough to cause the electrons to return to the emitting body.
3. By determination of the coefficient of absorption of the electrons in an absorbing mass of gas.

The last of these three methods is ill-adapted to quantitative measurements, first, because the absorption of the electrons is no simple process, and also because the degree of accuracy in absorption measurements with swiftly moving electrons is very small. The second method also offers great difficulties in the X-ray region, for the necessary electric field involves voltages far too high to allow measurement to the required degree of precision. It is only in the as yet little investigated region lying between the X-ray and optical spectra that we might hope for success by this method.

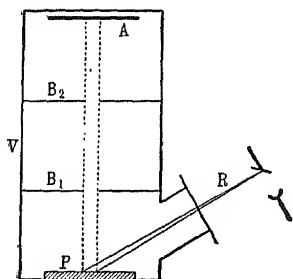


FIG. 110.

We are, therefore, reduced to the magnetic deflection method. This method was first employed by Dorn for electron emission. Fig. 110 is a diagram of the apparatus used. The body emitting the  $\beta$ -rays is at  $P$ , while a photographic plate is placed at  $A$ . The secondary X-rays and

the  $\beta$ -rays emitted by  $P$  pass together through two narrow windows and fall upon the plate  $A$ . By means of a magnetic field whose lines are at right angles to the plane of the figure the  $\beta$ -rays are deflected through a distance which is registered and measured on the plate. In order to prevent a diminution of the velocity of the electrons in passing over the distance  $PA$  the entire apparatus is evacuated.

The photographs thus obtained show an extended band of blackening on the plate, which indicates a corresponding distribution of velocities among the  $\beta$ -rays. Of course each point at which the plate is blackened represents a very definite curvature of the corresponding electron path, and, since all the electrons are subject to the same magnetic field, each position on the plate corresponds to a definite velocity of the electrons emitted.

By determining the radius of curvature  $r$  and the magnetic field intensity  $H$ , we may compute the value of the velocity  $v$  from

$$v = \frac{e}{m} Hr,$$

where  $e$  is the elementary electronic charge and  $m$  the mass of the electron. Since we are here dealing with relatively high velocities it is necessary to take account of the relativity correction to the mass, by making use of the expression

$$m = \frac{m_0}{\sqrt{1 - \beta^2}},$$

where

$$\beta = \frac{v}{c}.$$

The early investigations of Dorn, Bestelmeyer, Innes and others, by the photographic method, of Becker and Whiddington by the absorption method, and of Laub by the electrostatic method, showed that the velocity of the  $\beta$ -rays emitted is independent of the intensity of the primary X-rays, as might be expected from analogy with the ordinary photo-electric effect. These researches also gave the order of magnitude of the velocities involved; in particular, Whiddington showed that a simple relation exists between the velocity of the primary cathode rays in the X-ray tube and the velocity of the secondary electrons. But quite recently interesting and important facts have been discovered concerning the emission of secondary electrons, and the definite relation existing between the velocities and the X-ray absorption spectrum of the atoms serving as secondary radiators has been established.

The experiments by which Duane and Hunt proved the validity of the Einstein photo-electric equation for the process of emission of X-rays would seem in themselves to demonstrate that the velocity of the electrons emitted by a body exposed to X-rays is subject to the same law. Hence,

if a plate be irradiated with monochromatic X-rays, it is to be expected that electrons will be ejected with a very definite velocity (except for the loss of velocity in the emitting body itself). Indications of the truth of this are to be found in the work of Rawlinson and Robinson, as well as in that of Kang-Fuh-Hu. The first two authors, working in Rutherford's laboratory, made the first application to secondary X-ray electrons of the magnetic deflection method described by Rutherford, which is very suitable for faint effects on account of its focussing property. Fig. 111 is a diagram of the apparatus. X-rays from a powerful tube, whose anticathode is at *A*, pass through a slit *S* and fall upon the secondary radiator, which is mounted in an evacuated vessel. Directly above the

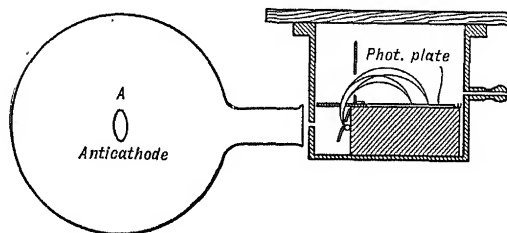


FIG. 111. Apparatus used by Rawlinson and Robinson for X-ray spectra.

radiator is a second slit, parallel to the first one, and lying in the same plane as the photographic plate *P*. All electrons of a given velocity travel in circles of the same radius through the magnetic field, which is at right angles to the plane of the figure.

As may be seen at once, even if the slit be rather wide, all electron paths of the same radius meet the plate at approximately the same distance from the slit. If there are groups of electrons with definite velocities among the electrons emitted then "lines" will appear on the plate. On account of the absorption in the secondary radiator itself, even when it is very thin, these lines will shade off gradually towards the side of smaller velocities. Rawlinson and Robinson succeeded in obtaining lines by exposing thin sheets of iron and lead to the radiation from a nickel anticathode. In spite of the focussing effect they found it necessary to expose as long as twelve hours, even with the maximum output of the tube. It was not possible, however, to identify the lines in a satisfactory way with the radiation from nickel, iron and lead.

### 39. $\beta$ -Ray Spectra

Employing the method of Rawlinson and Robinson, de Broglie succeeded in obtaining results which shed great light on the subject of  $\beta$ -ray spectra. De Broglie's explanation of the results of his experiments is in complete accord with the general hypotheses concerning the mechanism of radiation which have been stated above. When monochromatic Röntgen radiation of frequency  $\nu$  falls upon the surface of a secondary radiator, in the first place electrons are ejected according to

the laws governing the photo-electric effect, *i.e.* the liberated electrons have a velocity given by the equation

$$\frac{1}{2}mv^2 = h\nu.$$

The electrons concerned in this case are those which are so loosely bound that the work required to remove them from the atom is negligible. On the other hand, some electrons are removed from lower levels, and an appreciable amount of work must be done to remove them from the influence of the atom. If we denote this work by  $W$  it is apparent that the kinetic energy of the electron on leaving the atom is

$$\frac{1}{2}mv^2 = h\nu - W.$$

From the atomic theories already discussed we know that the energy necessary to eject an electron from one of the inner electron groups is nothing else than the quantity of energy representing the level in the energy level diagram of the atom. We have represented these quantities

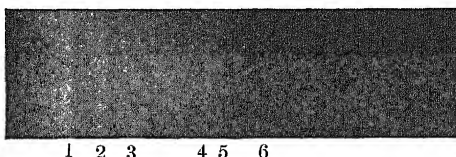


FIG. 112.  $\beta$ -ray spectrum from a silver radiator exposed to primary rays from tungsten. Photograph by de Broglie.

- |   |                                 |
|---|---------------------------------|
| 1. $K\alpha_{1,2}$ of Ag— $L_{Ag}$ ,                                    | 4. $K\alpha_2$ of W— $K_{Ag}$ , |
| 2. $\begin{cases} K\alpha_{1,2} \\ K\beta \end{cases}$ „ Ag— $M_{Ag}$ , | 5. $K\alpha_1$ „ W— $K_{Ag}$ ,  |
| 3. $K\beta$ „ Ag— $L_{Ag}$ ,  | 6. $K\beta$ „ W— $K_{Ag}$ ,     |

of energy by  $K$ ,  $L_1$ ,  $L_2$ ,  $L_3$ ,  $M_1$ , etc. If the exciting radiation is of frequency high enough to eject an electron from the  $K$  group, then the velocities involved in the following equations are to be expected, according as the electron is ejected from the  $K$ , the  $L$ , the  $M$  level, or from the surface of the atom.

$$\frac{1}{2}mv_1^2 = h\nu - K,$$

$$\frac{1}{2}mv_2^2 = h\nu - L,$$

$$\frac{1}{2}mv_3^2 = h\nu - M,$$

$$\dots\dots\dots$$

$$\frac{1}{2}mv_0^2 = h\nu.$$

De Broglie showed in a convincing manner that this is actually what occurs, and we shall consider in more detail the results from one of his photographs.

The “ $\beta$ -ray spectrum” (Fig. 112) was obtained by irradiating a thin silver plate with the  $K$  radiation from tungsten. Five distinct lines may be observed upon the plate, shading off towards smaller velocities on account of the absorption in the silver plate itself. The lines denoted

by 4 and 5 correspond to the removal of a  $K$  electron by the monochromatic tungsten radiation  $Ka_2$  and  $Ka_1$  respectively. The kinetic energies of the electrons for these two lines are given by

$$h\nu_{WKa_2} - K_{Ag},$$

$$h\nu_{WKa_1} - K_{Ag}.$$

The other three strong lines are due to the secondary silver  $K$  radiation, which in its turn gives rise to the emission of electrons. The lines 1,

2, 3, correspond to kinetic energies whose magnitude is given by the following equations:

$$1. h\nu_{AgK\alpha} - L_{Ag},$$

$$2. \begin{cases} h\nu_{AgK\beta} - L_{Ag}, \\ h\nu_{AgK\alpha} - M_{Ag}, \end{cases}$$

$$3. h\nu_{AgK\beta} - M_{Ag}.$$

De Broglie carefully tested the validity of the above expression by means of his photographs. In certain cases the  $\beta$ -ray spectra afford a

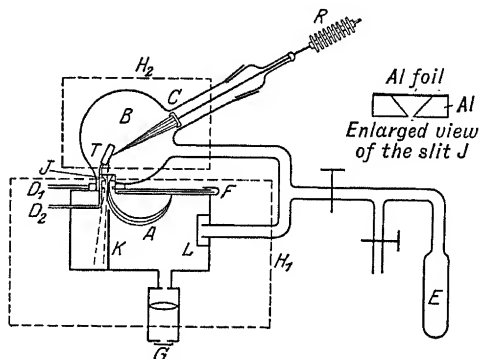


FIG. 113. Whiddington's apparatus for the photography of secondary  $\beta$ -ray spectra.

very good resolution which may even be superior to that of X-ray spectra. For example, we may notice the wide separation of the two  $Ka$  lines of tungsten in the spectrogram of Fig. 112, which in an ordinary X-ray spectrogram would be difficult to obtain. The disadvantages of the method are the feebleness of the radiation and the relatively low degree of accuracy of the measurements. In order to improve the latter de Broglie greatly increased the dimensions of his apparatus, and worked with radii of curvature of the deflected rays equal to about 12 cm. The magnetic field for these experiments was furnished by a large coil with air core.

Whiddington shortened considerably the time necessary for an exposure by placing the secondary radiator very close to the anticathode, as shown in Fig. 113. The X-ray tube was sealed directly to the  $\beta$ -ray spectrograph, and was provided with a water-cooled anticathode of rhodium. The substance to be used as secondary radiator was rubbed on the walls of a triangular chamber. The magnetic field was produced in this case, as in de Broglie's apparatus, by a coil free from iron. In order to prevent stray lines of the magnetic field from deviating the cathode ray beam away from the anticathode the field was compensated by a special coil. With this apparatus Whiddington was able to obtain a spectrogram in as short a time as five minutes. Fully-exposed plates were obtained in thirty minutes.



Some of Whiddington's results are reproduced in the two following tables. The first column contains the frequencies calculated from given velocities by means of the equation

$$h\nu = \frac{1}{2}mv^2.$$

The second column indicates the electron group of the radiator from which the electron in question is ejected; in the third is given the monochromatic primary or secondary radiation which gives rise to the electron emission concerned, and this radiation is either the rhodium  $K$  or the characteristic radiation of the secondary radiator itself, *e.g.* that of Cu. or of As. Finally, the last column gives the frequencies calculated from the known data contained in columns 2 and 3. (See Tables 48a and 48b.)

TABLE 48a.

Anticathode—rhodium; secondary radiator—arsenic.

$\nu$ Measured.	Frequency of arsenic level supplying electron.	Frequency of primary radiation.	$\nu$ Calculated.
222	$L$ (35)	As $K\alpha$ (252)	217
251 st.	$\left\{ \begin{array}{l} L \text{ (35)} \\ \text{Surface (0)} \end{array} \right.$	As $K\beta$ (285)	250
270 wk.	Surface (0)	As $K\alpha$ (252)	252
442 st.	$L$ (35)	As $K\beta$ (285)	285
507 wk.	$\left\{ \begin{array}{l} L \text{ (35)} \\ \text{Surface (0)} \end{array} \right.$	Rh $K\alpha$ (490)	455
563 very wk.	Surface (0)	Rh $K\beta$ (551)	516
		Rh $K\alpha$ (490)	490
		Rh $K\beta$ (551)	551

TABLE 48b.

Anticathode—rhodium; secondary radiator—copper.

$\nu$ Measured.	Frequency of copper level supplying electron.	Frequency of primary radiation.	$\nu$ Calculated.
172 st.	$L$ (22)	Cu $K\alpha$ (195)	173
193 st.	$\left\{ \begin{array}{l} L \text{ (22)} \\ \text{Surface (0)} \end{array} \right.$	Cu $K\beta$ (216)	194
217 wk.	Surface (0)	Cu $K\alpha$ (195)	195
270 st.	$K$ (217)	Cu $K\beta$ (216)	216
287 wk.	?	Rh $K\alpha$ (490)	273
313 st.	$K$ ? (217)	?	
461 st.	$L$ (22)	Rh $K\beta$ (551)	334
502 wk.	$\left\{ \begin{array}{l} L \text{ (22)} \\ \text{Surface (0)} \end{array} \right.$	Rh $K\alpha$ (490)	468
552 very wk.	Surface (0)	Rh $K\beta$ (551)	529
		Rh $K\alpha$ (490)	490
		Rh $K\beta$ (551)	551

With regard to the second table Whiddington remarks that the interpretation of the lines with the frequencies 287 and 313 is not clear.

The very remarkable observation was made that the incident radiation is able to eject an electron only when its frequency is double the value corresponding to the energy level of the electron concerned. As an example of this peculiar feature he calls attention to the line to be expected from the removal of an electron of the  $K$  group of arsenic by the  $K$  radiation of rhodium. The corresponding equation is

$$h\nu_{\text{RhK}\alpha} - K_{\text{As}} = 202,$$

in which

$$K_{\text{As}} = 288.$$

This line did not appear in the spectrograms.

In a recently published and very extensive study by the same method Robinson was unable to confirm the results on this point. Many lines, which by Whiddington's rule should not appear, were actually found. As a possible explanation of Whiddington's conflicting results Robinson suggests that the vacuum in the deflecting apparatus used by Whiddington was not sufficiently high to permit the passage of the slower electrons.

The work of Robinson marks a great step forward, both qualitatively and quantitatively. The results so far obtained are collected in the following Table 49, where the values of  $\frac{\nu}{R}$  for a large number of energy levels for different elements are reproduced. A comparison of these values with those of Table 37 shows a very good agreement. The electrons in all these determinations were expelled from the atoms by the  $K$  radiation from copper, previously filtered through nickel foil 0.015 to 0.025 mm. thick. This almost completely cuts out the  $K\beta$  radiation.

The magnetic field was produced by a pair of coils of the Helmholtz-Gauguin type.

Of especial interest is the result concerning the relative intensities which Robinson found for the different levels. As stated above, the three  $L$  levels in the ordinary absorption spectrum of an element have intensities diminishing in the sequence  $L_1, L_2, L_3$ . Robinson finds this sequence only when there is a small energy-difference between the exciting quantum and the levels. When this difference becomes larger the intensity sequence is reversed to  $L_3, L_2, L_1$ . This fact has an important bearing on the phenomena connected with the  $\gamma$  and  $\beta$  radiation of radioactive substances, as studied and interpreted by L. Meitner and by Ellis.

It is evident that this method is in principle a very important one, since, independently of crystal lattices, and in regions where crystals cannot be used because their lattice constants are either too large or too small, it permits the determination of the wave-length of monochromatic radiation, as well as the energy levels of the atom.

If we wish to use this method to determine an unknown frequency, then the energy levels of the atoms of the secondary radiator must be

TABLE 49.

Energy levels determined by H. Robinson.

	<i>K</i>	<i>L</i> <sub>3</sub>	<i>L</i> <sub>2</sub>	<i>L</i> <sub>1</sub>	<i>M</i> <sub>5</sub>	<i>M</i> <sub>4</sub>	<i>M</i> <sub>3</sub>	<i>M</i> <sub>2</sub>	<i>M</i> <sub>1</sub>	<i>N</i> <sub>7</sub>	<i>N</i> <sub>6</sub>	<i>N</i> <sub>5</sub>	<i>N</i> <sub>4</sub>	<i>N</i> <sub>3</sub>	<i>N</i> <sub>2,1,0</sub>
83 Bi	—	—	—	—	296.5	272.5	235.2	200.3	191.6	71.3	61.0	51.0	38.2	33.3	8.8
82 Pb	—	—	—	—	284.3	263.0	227.1	191.6	182.6	49.0			31.4		8.2
79 Au	—	—	—	—	253.6	232.9	202.2	167.9	161.5	54.2—38.6			22.6		1.8
74 W	—	—	—	—	208.5	189.4	167.5	139.0	133.2	31.4			17.2		—0.5
6 Ba	—	443.3	414.1	386.0	95.8	84.9	79.0	58.4		13.9			—0.4		
3 I	—	383.1	356.6	337.2	80.0	66.5		46.6		9.2					
0 Sn	—	329.8	307.8	290.7	65.3	52.7		35.5		7.6					
7 Ag	—	280.0	260.1	246.2	47.1—39.3			23.8		1.8					
2 Mo	—	212.1	193.4	186.1											
8 Sr	—	165.2	149.8	145.8											
9 Cu	—	82.0	69.7		6.5										
0 Ca	297.6	—	—	—											
9 K	266.2	—	—	23.8?											
6 S	183.3	—	—	16.5?											
2 Mg	99.6	—	—	8.0?											
1 Na	81.3	—	—	—											
8 O	42.3	—	—	—											

known in order to calculate the frequency from the observed electron velocities. Conversely, in order to evaluate energy levels, we must work with a known frequency.

So far the method has been applied only for very short wave-lengths, except in testing the principles on which the spectra are explained, and here, of course, data for both wave-lengths and energy levels were known. These investigations with very short wave-lengths lie in the realm of radioactivity, and as such are outside the borders of this discussion. The method affords great promise, however, for the study of those wave-length regions for which the dimensions of the crystal are too small to permit of its use as a grating. At present 13 Å. is about the greatest wave-length which has been measured by the crystal method. With a sugar crystal, whose grating constant  $2d$  is given on p. 85 as about 20 Å.U., the limit is reached at about the above wave-length. Certain

organic compounds whose grating spaces have recently been determined by Becker and Jancke, have considerably greater distances between their atoms, but as yet no study has been made of their applicability to wave-length measurements.

There are no such limitations in connection with  $\beta$ -ray spectra. On the other hand, the feeble photographic action of low velocity electrons is apparently an obstacle in obtaining and measuring these spectra, which at the best are comparatively faint. Since in this region the counter-voltage necessary for the second method of Section 38 is easier to control, perhaps something may be hoped for from the application of this method.

#### 40. Determination of Excitation Voltages by Means of the Photoelectric Action of the Emitted Radiation

Among the properties characteristic of X-rays, their ability to liberate electrons from a surface on which they fall is of great aid in the study of

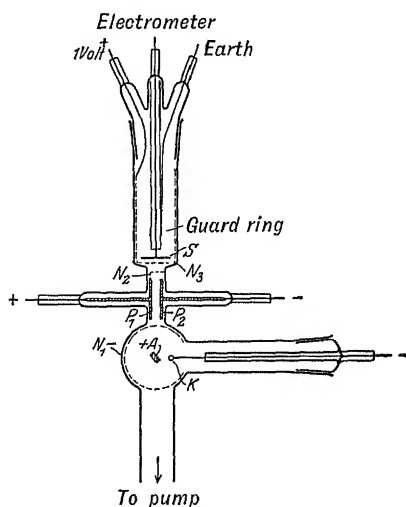


FIG. 114. Apparatus of Holtsmark.

very soft rays. We will here consider in detail only those recent investigations which aimed at bridging the gap in the spectral region between X-rays and ultra-violet rays, or, more properly, tracing the series of lines and absorption limits from X-ray spectra into the ultra-violet region. Certain earlier attempts had been made to demonstrate that with very low voltages—from 1000 volts down to a few tenths of a volt—a radiation may be produced which has the properties of very soft X-rays, and which represents an extension of the continuous X-ray spectrum down to a point corresponding to these low voltages.

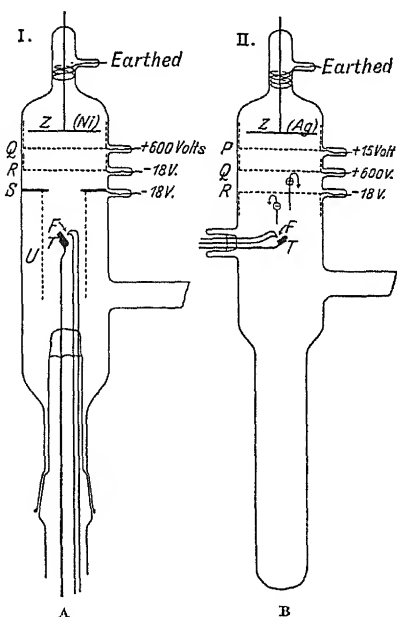
The principle of the method is very simple, and consists in allowing the radiation from the anticathode of a highly evacuated X-ray tube to fall upon a plate without passing through any absorbing substance. Electrons are thereupon liberated from this plate with a certain velocity, the maximum value of which is given by the Einstein photo-electric relation. By connecting the plate with an electrometer the quantity of electrons emitted may be measured and compared with the voltage applied to the tube. The strength of current through the X-ray tube is kept constant, while the voltage is changed by small steps, at each

of which the photo-electric current is measured. A discontinuity in the rate of change of the latter current is to be expected when the tube voltage becomes high enough to excite the characteristic radiation. Actually one finds that the curves representing the photo-electric current show a more or less distinct change in direction at certain points. In carrying out these experiments one is confronted by a series of difficulties which must be overcome by special precautions and appliances. In the first place, it is very necessary to have a high vacuum in the apparatus, in order to avoid disturbances arising from ionization of the gas present, as well as from the gas given off by the walls. Again, the rapidly moving charges from the X-ray tube proper must not be allowed to enter the portion of the vessel in which the photo-electric current is to be measured. In order to exclude them, Richardson and Bazzoni, as well as Holtsmark, introduced a strong transverse electrostatic field which deflected the electric charges to one side. Fig. 114 represents Holtsmark's apparatus as a sample of this type. The entire apparatus consisted of a quartz vessel with a spherical portion for the actual X-ray tube ( $K$  is the hot filament cathode and  $A$  the anode). The remaining part contains the photo-electric plate  $s$ , surrounded by a protecting gauze  $N_3$  which was kept at a potential of +1 volt. To prevent the conduction of charges to the plate an earthed guard ring is placed around the insulating support. The transverse field  $P_1P_2$  is between the two portions of the vessel.

The same protection of the plate may be attained by an electric field in the direction of the radiation, the sense of the field being such as to retard or throw back the charges coming from the X-ray tube. As an example of such an arrangement, the apparatus of Hughes in two slightly different forms is shown in Figs. 115A, 115B.

McLennan and Clark used a very similar arrangement in their work, to which we shall return later.

The experimental arrangement employed by Kurth, which was to some extent a combination of these two principal types, is to be seen in Fig. 116.



FIGS. 115A, B. Apparatus of Hughes.

The appearance of the curves representing the photo-electric current as a function of the exciting voltage applied to the X-ray tube often changes very greatly, and accidental circumstances play an important

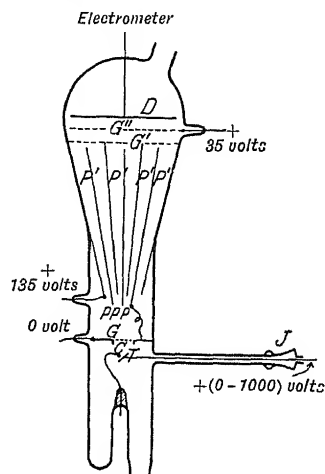


FIG. 116. Apparatus of Kurth.

part with one and the same apparatus. Under favourable conditions several authors have obtained curves consisting of several portions which are almost straight lines. Fig. 117 is a typical example, which gives the curves obtained by Hughes for boron. In the lower group of curves two were taken with increasing voltage on the tube and two with decreasing.

The upper curve gives the mean values, and shows very clearly a change in direction at 150 volts. Richardson and Bazzoni have published curves of this type, and Holtsmark has also found them to consist of straight line portions in the case of boron. In general, however, Hughes has obtained curves of quite different

appearance, and which give only slight indications of a discontinuity. Such a curve, also for the element boron, is shown in Fig. 118.

The curves obtained by McLennan and Clark from their experiments are still different in appearance. Their course is much more irregular, and the discontinuities are more marked.

Rollefson investigated iron by this method, and found altogether twelve discontinuities. He attributes three of them to the *L* series and nine to the *M* series. A comparison of his results with the recent direct measurements of the *L* series of iron by Thoraeus and the author shows that the results obtained by these two methods are inconsistent in this case.

The experiments so far described all relate to investigations of soft X-rays excited in solid bodies. Mohler and Foote have made some very interesting researches on X-rays emitted by gases. Fig. 119 represents an arrangement of apparatus modelled after those used in optical work, and consisting of a central filament surrounded by two gauze cylinders

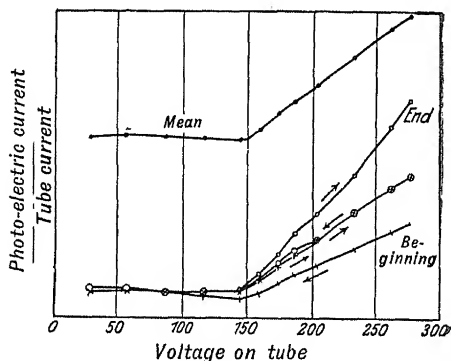


FIG. 117.

and by an outer cylindrical metal tube. The distance from the filament to the inner cylinder of gauze is made as small as possible in order that the electrons may attain their full velocity  $V_1$  before colliding with gas molecules. In the space between the two gauzes the electrons collide with the molecules of the gas under investigation, and the radiation thereby excited exercises a photo-electric effect on the outer gauze cylinder. The magnitude of this effect is then measured by the current between  $V_2$  and  $V_3$ . The strong retarding field  $-V_2 + V_1$  prevents all electrons from the filament, as well as all negative ions produced in the ionizing space, from reaching  $V_2$ . Positive ions are stopped in the field  $-V_2 + V_3$ .

With this apparatus Mohler and Foote studied the vapours of K, Na, Mg, P, S, as well as air (N, O), Cl, CO,  $\text{CCl}_4$ ,  $\text{CO}_2$ , and  $\text{C}_2\text{H}_2$ .

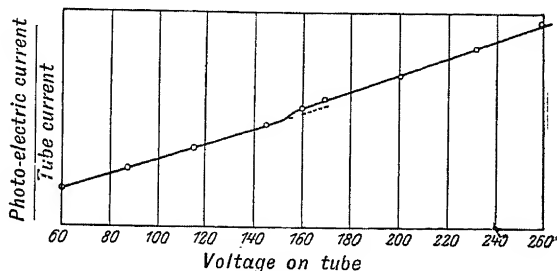


FIG. 118.

Table 50 contains the results hitherto obtained by many different authors using the method described above, in which they located the discontinuities in the slope of the curves representing the photo-electric current as a function of the exciting voltage. The column of voltages in the table is obtained from the curves. The succeeding columns contain the values of  $\frac{\nu}{R}$ ,  $\sqrt{\frac{\nu}{R}}$ , and  $\lambda$ . In

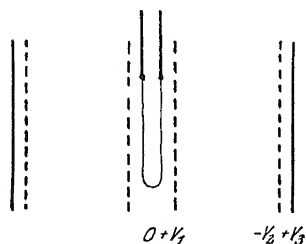


FIG. 119.

addition, the table contains, for comparison, the values for H, He, and  $\text{Ne}^*$  known from optical data and experiment.

In general, the various authors interpret the ionizing potentials to be the same as the limiting voltages for the  $K$  and  $L$  series known from X-ray data and continued down to these lighter elements. For example, if we plot in the Moseley diagram  $\sqrt{\frac{\nu}{R}}$ , found from absorption measurements, as a function of the atomic number, we obtain a straight line as far down as Mg (12). By producing this line we obtain what is apparently a fairly satisfactory value of the excitation potential for the lower elements in the  $K$  series. It should be remarked, however, that the gradual disappearance of the higher quantum electron orbits exerts a

\* Measurements by Horton and Davis, interpretation by Grotrian.

TABLE 50.

*Abbreviations* : Fr. and He=Franck and Hertz, Le.-Cl.=McLennan and Clark, Mo.-Fo.=Mohler and Foote, Hg.=Hughes, Ho.=Holtzmark, K.=Kurth, Ri.-Ba.=Richardson and Bazzoni, Ho.-Da.=Horton and Davies, R.=Rollefson.

	$\nu$	$\frac{\nu}{R}$	$\sqrt{\frac{\nu}{R}}$	$\lambda$ in Å.	Origin.	Author.
1 H	13.53	1.90	0.46	912		
2 He	25.23	1.86	1.36	493	1 S (K)	Fr. and He.
	21.85	1.61	1.27	569	1 S - 2P	Fr. and He.
3 Li	37.0	2.73	1.65	334		Le.-Cl.
	31.8	2.35	1.53	388		Le.-Cl.
	12.0	0.89	0.94	1029		Le.-Cl.
4 Be	93.0	6.87	2.62	133		Le.-Cl.
	78.2	5.77	2.40	158		Le.-Cl.
	20.3	1.50	1.22	608		Le.-Cl.
	16.0	1.18	1.09	772		Le.-Cl.
5 B	186	13.74	3.71	66.4	K	Mo.-Fo.
	148	10.93	3.31	83.5	K	Hg.
	147.5	10.90	3.30	83.7	K	Le.-Cl.
	147	10.86	3.30	84.0	K	Ho.
	125	9.23	3.04	98.7		Mo.-F.
	27.92	2.15	1.47	442		Le.-Cl.
	24.5	1.81	1.35	505	L	Hg.
	23.45	1.73	1.32	527		Le.-Cl.
6 C	290	21.42	4.63	42.6	K	K.
	287	21.19	4.60	43.0	K	Ho.
	286	21.12	4.60	43.2	K	Ri.-Ba.
	272±2	20.09	4.48	45.4	K	Mo.-Fo.
	234±3	17.28	4.16	52.8		Mo.-Fo.
	215	15.88	3.98	57.5	K	Hg.
	75	5.54	2.35	165		Mo.-Fo.
	74	5.46	2.34	167		Le.-Cl.
	34.5	2.55	1.60	358	L	Hg.
	32.9	2.43	1.56	375	L	K.
7 N	374±5	27.62	5.26	33.0	K	Mo.-Fo.
	352	25.99	5.10	35.1		Mo.-Fo.
8 O	518	38.25	6.18	23.8	K	K.
	478±2	35.30	5.94	25.8	K	Mo.-Fo.
	49.8	3.68	1.92	248	L	K.
10 Ne	22.8	1.68	1.30	541	(L <sub>3</sub> ? Gr.)	Ho.-Da.
	20.0	1.48	1.22	617	(? Gr.)	Ho.-Da.
	16.7	1.23	1.11	739	(L <sub>1</sub> L <sub>2</sub> ? Gr.)	Ho.-Da.
11 Na	35±1.4	2.58	1.61	353	L	Mo.-Fo.
	17±1.5	1.26	1.12	725	L	Mo.-Fo.
12 Mg	46±1	3.40	1.84	268	L <sub>1, 2</sub>	Mo.-Fo.
	33±1	2.44	1.56	374	(L <sub>5</sub> ?)	Mo.-Fo.
13 Al	123	9.08	3.01	100	L	K.
	37.9	2.80	1.67	326	M	K.
14 Si	150	11.08	3.33	82.5	L	K.



	$V$	$\frac{\nu}{R}$	$\sqrt{\frac{\nu}{R}}$	$\lambda$ in Å.	Origin.	Author.
15 P	163±2	12.04	3.47	75.8	$L_{1,2}$	Mo.-Fo.
	126±1	9.30	3.05	98		Mo.-Fo.
	110±1	8.12	2.85	112		Mo.-Fo.
	95±5	7.02	2.65	130		Mo.-Fo.
16 S	152±2.5	11.22	3.35	81.2	$L_{1,2}$ ( $L_5?$ )	Mo.-Fo.
	122±1	9.01	3.00	101		Mo.-Fo.
17 Cl	198±3	13.29	3.65	62.3	$L_{1,2}$	Mo.-Fo.
	175	12.92	3.59	70.5		Mo.-Fo.
	157±2	11.59	3.40	78.6		Mo.-Fo.
19 K	23.3±1	1.72	1.31	530		Mo.-Fo.
	19.3±0.7	1.43	1.19	640		Mo.-Fo.
22 Ti	504	37.22	6.10	24.5	$L$	K.
	145	10.71	3.27	85.3	$M$	K.
26 Fe	757	55.90	7.48	16.3	$L$	K.
	227	16.76	4.09	54.3	$M$	K.
	50	3.69	1.92	247	$N$	K.
	697	51.5	7.18	17.7	$L$	R.
	637	47.0	6.86	19.4	$L$	R.
	618	45.5	6.74	20.0	$L$	R.
	160.1	11.83	3.44	77.0	$M$	R.
	153.4	11.33	3.37	80.5	$M$	R.
	147.1	10.88	3.30	83.9	$M$	R.
	140.9	10.40	3.22	87.8	$M$	R.
	130.4	9.63	3.10	94.6	$M$	R.
	111.2	8.21	2.87	111.0	$M$	R.
	95.4	7.05	2.66	129.6	$M$	R.
	81.7	6.03	2.46	151	$M$	R.
	46.8	3.46	1.86	264	$M$	R.
29 Cu	1000	73.85	8.59	12.3	$L$	K.
	297	21.93	4.68	41.6	$M$	K.
	104	7.68	2.77	119	$N$	K.
42 Mo	356	26.29	5.13	34.7	$M$	Ri.-Ba.

marked influence on the slope of the curves, as shown in Figs. 89 and 90, so that we must not place too much faith in the values obtained by extrapolation.

Still more important is the fact that we are here just in a region in which the transition occurs from the simple relations found in X-ray spectra to the far more complicated ones encountered in optical spectra. While in X-ray spectra the unoccupied orbits with their comparatively small differences in energy cannot, in general, be distinguished, and the energy of dissociation is also relatively of no consequence, neither of these two factors can be neglected in the interpretation and classification of the lower voltages. Lindh's investigations of Cl, S and P show that the chemical nature of the element is also a significant factor.

In the sixth column of Table 50 we have the interpretation of the breaks in the photo-electric curves, as given by the various authors, and we observe that the agreement among them for different voltage values is not especially good. One author often reports a distinct break in a curve at a given voltage, whereas another finds only a straight line, and it has already been shown above that the same author may arrive at quite different results in different series of measurement.

In a recent publication Boyce has communicated some results obtained by the method of Kurth, which seem exceedingly interesting. In contrast to earlier work in this field Boyce worked with higher elements, from Ta (73) to Au (79). In this way he avoided the complication, probably arising from multiple ionization, which affects the results for the lower elements. Boyce was able to deduce most of the energy levels in the *N* group, and some in the *M* and *O* groups of the elements mentioned. There is fairly good agreement between his values of  $\frac{\nu}{R}$  and those contained in Table 37. The results are collected together in Table 51.

TABLE 51.

Values of  $\frac{\nu}{R}$  determined by Boyce compared with the values (calc.) from Table 37.

	<i>M</i>	<i>N</i> <sub>7</sub>	<i>N</i> <sub>6</sub>	<i>N</i> <sub>5</sub>	<i>N</i> <sub>4</sub>	<i>N</i> <sub>3</sub>	<i>N</i> <sub>2</sub>	<i>N</i> <sub>1</sub>	<i>O</i> <sub>3</sub>	<i>O</i> <sub>1</sub>	<i>O</i> <sub>2</sub>	<i>O</i> <sub>1</sub>
73 Ta {												
Exp.	101.0?	49.1	38.0	27.7	—	13.7	2.80	5.67	3.46	—	—	—
Calc.	—	41.7	33.0	30.0	—	17.2	2.5	5.3	2.6	—	—	—
74 W {												
Exp.	—	42.9		29.7	—	—	2.42	5.45	2.74	—	—	—
Calc.	—	43.6		30.6	—	—	2.5	5.2	2.9	—	—	—
76 Os {												
Exp.	104.5?	44.2	—	—	25.2	15.6	5.96	4.05	—	—	—	2.72
Calc.	—	44.4	—	—	21.3	20.1	3.4	3.6	—	—	—	—
77 Ir {												
Exp.	98.4?	43.0	—	27.7	17.7	13.8	4.42	3.46	—	—	—	2.65
Calc.	—	47.9	—	38.4	22.4	21.3	4.2	4.0	—	—	—	—
78 Pt {												
Exp.	111	54.2	—	40.4	—	15.2?	3.24	6.04	7.8?	—	—	—
Calc.	—	52.5	—	42.3	—	23.2	5.2	7.1	8.6	—	—	—
79 Au {												
Exp.	98.4?	65.6	—	40.4	32.8	18.9	6.68	—	—	—	4.56	—
Calc.	—	58.0	—	42.8	26.4	25.0	6.4	—	—	—	0.8	—

#### 41. Wave-length Measurements by Millikan in the Extreme Ultra-violet Region.

The measurements of ionizing potentials discussed in Section 40 refer mostly to the short wave-length end of the ultra-violet region. We must not forget, however, that the method there described does not really give the wave-lengths (even if we admit the validity of the Einstein photo-electric equation), but only the critical value of the voltage at which the radiation is excited. By analogy with X-ray spectra we should expect that the wave-length of the radiation emitted would be appreciably greater than the value calculated from the Einstein equation and contained in the fifth column of Table 50.

A direct measurement of wave-lengths in this region would be very valuable, as it might throw light on relations which are evidently very complicated. It is, therefore, of the greatest interest that Millikan has recently succeeded in improving the methods of ultra-violet spectroscopy to such an extent that a large part of the wave-length region here in question has been rendered accessible to direct measurement by the concave grating. It must, nevertheless, be admitted that the results so far obtained do not completely solve the problem. It can, however, be regarded as certain that the optical method developed by Millikan permits the measurement of wave-lengths down as low as  $114 \text{ \AA}$ . Measurements by X-ray methods have been extended by Hjalmar, as is well known, to about  $13 \text{ \AA}$ . Unfortunately, this gap is still too great to permit a reliable extrapolation of the series, but it does not seem entirely impossible to effect a junction by the method described in Section 39.

Millikan used as his source of radiation a high potential spark, which he obtained by the discharge of a battery of large Leyden jars. The vacuum in which the spark took place was as high as that in the spectrograph ( $10^{-4}$  mm. of Hg). In this way Millikan avoided any absorbing substance in the path of the rays. The concave gratings used were made in the Ryerson Laboratory at Chicago by Millikan and Fred Pearson, using the famous Michelson ruling engine. The number of lines on the gratings was from 500 to 1100 per mm. Millikan obtained the best spectra with a grating having 500 lines per mm., and a focal length of 835 mm. In all, eight different gratings were used, and the spectra obtained with them were compared, to eliminate individual peculiarities of the gratings. When one considers that the ratio between the grating constant and the wave-length is 70 in some cases, the necessity for these precautions is obvious. Since the angles of reflection were necessarily somewhat small, nearly normal spectra were obtained, so that it was possible to interpolate by means of known aluminium lines at  $1854.7$  and  $1862.7 \text{ \AA}$ . A very satisfactory check was afforded by a comparison

of measurements of the strongest lines in several orders. Millikan estimates the accuracy of his wave-length determinations to be 0.1 Å.

With the apparatus described, Millikan, partly in conjunction with Bowen, Sawyer and Shallenberger, investigated the wave-length region as far down as 144 Å. (for Al). Extended wave-length measurements are now available, among others, for iron from 271 to 2153 Å., for C from 360 to 1931 Å., for Ni from 200 to 1860 Å., for Zn from 316 to 2139 Å., and for Al and Li as far as lines could be found in that region of the spectrum. We shall consider these last measurements at greater length, since they are of interest in the extension of X-ray series.

There is a marked difference between the elements above and below neon (10). For Al, Mg and Na, Millikan found a single very short wave-length line, which he identified with *La*. With Al, for example, no other line was found on the plate from the single line just mentioned, with a wave-length of 144.3 Å., up to 1200 Å. With Mg the corresponding line is at 232.2, and it is followed by a region devoid of lines until 1700 Å., whilst for Na the corresponding wave-lengths are 376.5 and 2413 Å.

The three lines just cited are contained in the table below along with the corresponding values of  $\lambda$ ,  $\frac{\nu}{R}$ ,  $\sqrt{\frac{\nu}{R}}$  and  $V$ . It is difficult to see any direct connection between these voltages and the ionizing potentials of Table 50. The extrapolation of the *L* series for the higher elements, for which measurements by the crystal method are available, lead to numerical values of this order of magnitude, and Kossel's combination principle also gives wave-lengths of approximately the same value for the *L* series, which, of course, is to be looked for somewhere in this region. If we make use of the energy-level diagram of Bohr and Coster, and admit that the  $3_3$  electron orbit disappears at the atomic number 21, and the  $3_2$  orbit at 13, then so far as we may extrapolate according to the laws which hold for X-ray spectra we should identify the line with  $L\beta_3\beta_4$  rather than with *La*.

	$\lambda$ in Å.	$\frac{\nu}{R}$	$\sqrt{\frac{\nu}{R}}$	$V_{\text{Volts.}}$
11 Na - - -	372.2	2.449	1.57	33.1
12 Mg - - -	232.2	3.924	1.98	53.1
13 Al - - -	144.3	6.313	2.52	85.4

For the still lighter elements it is more difficult to establish the connection between the optical data and the X-ray series; nevertheless, Millikan has made an attempt to do so. Since the real X-ray lines arise from transitions between electron orbits which are occupied when the atom is in its normal state, and according to Bohr the elements below number 10 have only the one quantum and two quantum orbits occupied, we should expect to find in this region at most only the *K* series. In the wave-

length region where, according to extrapolation, the  $L$  series should lie, Millikan found a number of spectral lines; they constitute a complex line system, however, and have little outward resemblance to the  $L$  series. It seems much more fitting to compare them with ordinary optical spectra.

An idea of the difficulty of carrying the X-ray series over into this region may be gathered from Millikan's interpretation of several lines in the spectrum of carbon. In an article dated July, 1920, he identifies three lines of wave-lengths 384.4, 372.1 and 360.5 Å. with  $La$ ,  $L\beta$  and  $L\gamma$ , because their general appearance, relative positions, and intensities were thought to be suitable for those lines. In another paper, presented to the National Academy of Science in April of the same year, but evidently representing a later view-point of the author (the latter paper was printed in Oct. 1921), he considers it better, since the X-ray series cannot be *directly* carried over, to identify a strong line of wave-length 1335.0 Å. with  $La$ . There is, therefore, no general correspondence of this complicated system of many lines with the  $L$  series of X-ray spectra.

It is apparent that Millikan's first interpretation of the lines, in which he believed the well-known and very characteristic doublet of the  $L$  series reappeared, cannot be the right one, for the doublet difference, which may be calculated with great accuracy from the formula of Sommerfeld, should be about  $\frac{1}{7.66}$  of that found experimentally by Millikan.

In the opinion of the author, therefore, the results of this very important research belong more to the domain of optics than to that of X-rays, and for this reason the data, which have already become very extensive, are not presented here.

# APPENDIX

TABLE I.

Kilovolts required to excite the group of lines of highest frequency in the various X-ray series.

	K	L	M	N		K	L	M	N
92 U	115	21.7	5.54	1.44	47 Ag	25.5	3.79	0.72	0.10
90 Th	109	20.5	5.17	1.33	46 Pd	24.4	3.64	0.67	0.08
83 Bi	90.1	16.4	4.01	0.96	45 Rh	23.2	3.43	0.62	0.07
82 Pb	87.6	15.8	3.85	0.89	44 Ru	22.1	3.24	0.59	0.06
81 Tl	85.2	15.3	3.71	0.86	42 Mo	20.0	2.87	0.51	0.06
80 Hg	82.9	14.8	3.57	0.82	41 Nb	19.0	2.68	0.48	0.05
79 Au	80.5	14.4	3.43	0.79	40 Zr	18.0	2.51	0.43	0.05
78 Pt	78.1	13.9	3.30	0.71	39 Y	17.0	2.36	—	—
77 Ir	76.0	13.4	3.17	0.67	38 Sr	16.1	2.19	—	—
76 Os	73.8	13.0	3.05	0.64	37 Rb	15.2	2.05	—	—
74 W	69.3	12.1	2.81	0.59	35 Br	13.5	1.77	—	—
73 Ta	67.4	11.7	2.71	0.57	34 Se	12.7	1.64	—	—
72 Hf	65.4	11.3	2.60	0.54	33 As	11.9	1.52	—	—
71 Lu	63.4	10.9	2.50	0.51	32 Ge	11.1	1.41	—	—
70 Yb	61.4	10.5	2.41	0.50	31 Ga	10.4	1.31	—	—
69 Tu	59.5	10.1	2.31	0.47	30 Zn	9.65	1.20	—	—
68 Er	57.5	9.73	2.22	0.45	29 Cu	8.86	—	—	—
67 Ho	55.8	9.38	2.13	0.43	28 Ni	8.29	—	—	—
66 Dy	53.8	9.03	2.04	0.42	27 Co	7.71	—	—	—
65 Tb	52.0	8.70	1.96	0.40	26 Fe	7.10	—	—	—
64 Gd	50.3	8.37	1.88	0.38	25 Mn	6.54	—	—	—
63 Eu	48.6	8.04	1.80	0.36	24 Cr	5.98	—	—	—
62 Sm	46.8	7.73	1.72	0.35	23 Va	5.45	—	—	—
60 Nd	43.6	7.12	1.58	0.32	22 Ti	4.95	—	—	—
59 Pr	41.9	6.83	1.51	0.30	21 Sc	4.49	—	—	—
58 Ce	40.3	6.54	1.43	0.29	20 Ca	4.03	—	—	—
57 La	38.7	6.26	1.36	0.27	19 K	3.59	—	—	—
56 Ba	37.4	5.99	1.29	0.25	17 Cl	2.82	—	—	—
55 Cs	35.9	5.71	1.21	0.23	16 S	2.46	—	—	—
53 I	33.2	5.18	1.08	0.19	15 P	2.14	—	—	—
52 Te	31.8	4.93	1.01	0.17	14 Si	1.83	—	—	—
51 Sb	30.4	4.69	0.94	0.15	13 Al	1.55	—	—	—
50 Sn	29.1	4.49	0.88	0.13	12 Mg	1.30	—	—	—
49 In	27.9	4.28	0.83	0.12	11 Na	1.07	—	—	—
48 Cd	26.7	4.07	0.77	0.11					

TABLE II.

A. Shortest wave-lengths in X.U. excited at potentials from  
0.1 to 9.9 kilovolts.

	·0	·1	·2	·3	·4	·5	·6	·7	·8	·9
1	12340	123400	61700	41133	30850	24680	20567	17629	15425	13711
2	6170	11218	10283	9492	8814	8226	7712	7258	6855	6494
3	4113	5876	5609	5365	5141	4936	4746	4570	4410	4255
4	3085	3980	3856	3739	3629	3525	3427	3335	3247	3164
5	2468	3009	2938	2869	2804	2742	2682	2625	2571	2518
6	2057	2420	2373	2328	2285	2244	2204	2165	2127	2092
7	1763	2023	1990	1959	1928	1898	1870	1842	1815	1788
8	1543	1738	1714	1690	1668	1645	1624	1603	1582	1562
9	1371	1523	1504	1487	1469	1452	1435	1418	1402	1387
9	1371	1356	1341	1327	1313	1299	1285	1272	1259	1246

B. Shortest wave-lengths in X.U. excited at potentials from  
10 to 149 kilovolts.

	0	1	2	3	4	5	6	7	8	9
1	1234	1122	1028	949	881	823	771	725.8	686	649
2	617	587.6	560.9	536.5	514.1	493.6	474.6	457	441	425.5
3	411.3	398	385.6	373.9	362.9	352.5	342.7	333.5	324.7	316.4
4	308.5	300.9	293.8	286.9	280.4	274.2	268.2	262.5	257.1	251.8
5	246.8	242	237.3	232.8	228.5	224.4	220.4	216.5	212.7	209.2
6	205.7	202.3	199	195.9	192.8	189.8	187	184.2	181.5	178.8
7	176.3	173.8	171.4	169	166.8	164.5	162.4	160.3	158.2	156.2
8	154.3	152.3	150.4	148.7	146.9	145.2	143.5	141.8	140.2	138.7
9	137.1	135.6	134.1	132.7	131.3	129.9	128.5	127.2	125.9	124.6
10	123.4	122.2	121	119.8	118.7	117.5	116.4	115.3	114.3	113.2
11	112.2	111.1	110.2	109.2	108.2	107.3	106.4	105.5	104.6	103.7
12	102.8	102	101.2	100.3	99.5	98.7	97.9	97.2	96.4	95.7
13	94.9	94.2	93.5	92.8	92.1	91.4	90.7	90.1	89.4	88.8
14	88.1	87.5	86.9	86.3	85.7	85.1	84.5	83.9	83.4	82.8

C. Shortest wave-lengths in X.U. excited at potentials from  
150 to 245 kilovolts.

150	155	160	165	170	175	180	185	190	195
82.3	79.6	77.1	74.8	72.6	70.5	68.6	66.7	64.9	63.3

200	205	210	215	220	225	230	235	240	245
61.7	60.2	58.8	57.4	56.1	54.8	53.7	52.5	51.4	50.4

TABLE III.

Absorption coefficients and half-value thicknesses of several substances for a series of wave-lengths. ( $d_{\frac{1}{2}}$  is the thickness in cm. of the substance which reduces the intensity of the corresponding wave-length radiation to one-half its initial value.)

$\lambda$ in $\text{\AA}$ .	Alr at 0° C., 760 mm.		H <sub>2</sub> O		C		Al		Cu		Ag		Pb	
	$\mu/\rho$	$d_{\frac{1}{2}}$	$\mu/\rho$	$d_{\frac{1}{2}}$	$\mu/\rho$	$d_{\frac{1}{2}}$	$\mu/\rho$	$d_{\frac{1}{2}}$	$\mu/\rho$	$d_{\frac{1}{2}}$	$\mu/\rho$	$d_{\frac{1}{2}}$	$\mu/\rho$	$d_{\frac{1}{2}}$
0.1			0.17	4.0	0.14	2.1	0.17	1.5	0.32	0.25	1.0	0.066	1.7	0.037
0.2			0.20	3.3	0.17	1.8	0.26	0.98	1.5	0.051	6.2	0.011	4.0	0.015
0.3			0.26	2.6	0.20	1.5	0.54	0.48	4.6	0.017	18	0.0036	14	0.0043
0.4			0.36	1.9	0.24	1.3	1.1	0.24	10	0.0078	38	0.0017	33	0.0019
0.5	0.55	980	0.50	1.4	0.30	1.0	2.0	0.13	19	0.0040	12	0.0056	66	0.00093
0.6	0.88	610	0.71	0.97	0.40	0.76	3.2	0.080	32	0.0025	20	0.0034	120	0.00053
0.7	1.3	410	1.0	0.70	0.53	0.57	5.0	0.051	50	0.0016	30	0.0022	180	0.00034
0.8	1.8	300	1.4	0.48	0.71	0.43	7.3	0.035	72	0.0011	43	0.0015		
0.9	2.4	220	2.0	0.34	1.1	0.28	10	0.025	100	0.00074	61	0.0011		
1.0	3.2	170	2.7	0.25	1.3	0.24	14	0.018	140	0.00055	82	0.00081		
1.5	9.2	58	8.6	0.079	3.7	0.082	46	0.0056	52	0.0015	260	0.00026		
2.0	19	30	20	0.034	8.4	0.036	110	0.0024	120	0.00065	580	0.00011		
2.5	32	17	39	0.018	16	0.019	210	0.0012	210	0.00036				
3.0	53	10	66	0.010	26	0.012	360	0.00072	350	0.00022				
3.5	77	6.9	100	0.0068	40	0.0075	560	0.00046	520	0.00015				
4.0	110	4.9	150	0.0045	59	0.0052	830	0.00031						
4.5	140	3.9	210	0.0032	81	0.0037	1200	0.00022						
5.0	190	2.8	300	0.0023	110	0.0028	1600	0.00016						
6.0	310	1.7	500	0.0014	180	0.0017	2800	0.000094						
7.0	480	1.1	790	0.00086	280	0.0011	3400	0.000075						
8.0	630	0.86	1200	0.00058	400	0.00075	770	0.00035						
9.0	850	0.63	1700	0.00041	560	0.00054	1070	0.00025						
10.0	1100	0.49	2300	0.00030	760	0.00040	1450	0.00019						



TABLE IV.

D. Mendelejeff's Periodic Table of the Elements, with Atomic Weights.

Group of elements.										
Period.	0.	I.	II.	III.	IV.	V.	VI.	VII.	VIII.	
1		1 H 1.008								
2	2 He 4.00	3 Li 6.94	4 Be 9.02	5 B 10.82	6 C 12.00	7 N 14.008	8 O 16.000	9 F 19.00		
3	10 Ne 20.2	11 Na 23.00	12 Mg 24.32	13 Al 26.97	14 Si 28.06	15 P 31.04	16 S 32.07	17 Cl 35.46		
4	18 A 39.88	19 K 39.10	20 Ca 40.07	21 Sc 45.10	22 Ti 48.1	23 Va 51.0	24 Cr 52.01	25 Mn 54.93	26 Fe, 27 Co, 28 Ni 55.84 58.97 58.68	
5		29 Cu 63.57	30 Zn 65.37	31 Ga 69.72	32 Ge 72.60	33 As 74.96	34 Se 79.2	35 Br 79.92		
6	36 Kr 82.92	37 Rb 85.5	38 Sr 87.6	39 Y 89.0	40 Zr 91.2	41 Nb 93.5	42 Mo 96.0	43 —	44 Ru, 45 Rh, 46 Pd 101.7 102.9 106.7	
7		47 Ag 107.88	48 Cd 112.4	49 In 114.8	50 Sn 118.70	51 Sb 121.8	52 Te 127.5	53 I 126.92		
8	54 X 130.2	55 Cs 132.8	56 Ba 137.4	57 La 138.9	[58 Ce 140.25	59 Pr 140.9	60 Nd 144.3	61 —		
9		62 Sm 150.4	63 Eu 152.0	64 Gd 157.3	65 Tb 159.2	66 Dy 162.5	67 Ho 163.5	68 Er 167.7		
10		69 Tu 169.4	70 Yb 173.5	71 Lu 175.0	72 Hf 178.6	73 Ta 181.5	74 W 184.0	75 —	76 Os, 77 Ir, 78 Pt 190.9 193.1 195.2	
11		79 Au 197.2	80 Hg 200.6	81 Tl 204.4	82 Pb 207.2	83 Bi 209.0	84 Po 210	85 —		
12	86 Em 222	87 —	88 Ra 226.0	89 Ac	90 Th 232.1	91 Pa	92 U 238.2	93 —		

TABLE V.

Reflection angles and wave-lengths (in X.U.). Rocksalt.  $2d=5628$  X.U.

	0'	10'	20'	30'	40'	50'
1°	98.2	114.6	131.0	147.3	163.7	180.3
2°	196.4	212.8	229.1	245.5	261.9	278.2
3°	294.6	310.9	327.2	343.6	359.9	376.2
4°	392.6	408.9	425.3	441.6	457.9	474.2
5°	490.5	506.8	523.1	539.4	555.7	572.0
6°	588.3	604.6	620.8	637.1	653.4	669.6
7°	685.9	702.1	718.4	734.6	750.8	767.0
8°	783.2	799.5	815.7	831.9	848.1	864.2
9°	880.4	896.6	912.7	928.9	945.1	961.1
10°	977.3	993.4	1009.5	1025.6	1041.7	1057.8
11°	1073.9	1089.9	1106.0	1122.1	1138.1	1154.1
12°	1170.1	1186.2	1202.1	1218.1	1234.1	1250.1
13°	1266.0	1281.9	1297.9	1313.9	1329.7	1345.7
14°	1361.5	1377.4	1393.3	1409.1	1425.0	1440.8
15°	1456.6	1472.5	1488.2	1504.0	1519.8	1535.5
16°	1551.3	1567.0	1582.8	1598.5	1614.1	1629.8
17°	1645.5	1661.1	1676.8	1692.4	1708.0	1723.6
18°	1739.2	1754.7	1770.2	1785.8	1801.3	1816.8
19°	1832.3	1847.8	1863.2	1878.7	1894.1	1909.5
20°	1924.9	1940.3	1955.6	1971.0	1986.3	2001.6
21°	2016.9	2032.2	2047.4	2062.7	2077.9	2093.1
22°	2108.3	2123.4	2138.6	2153.7	2168.9	2183.9
23°	2199.0	2214.1	2229.1	2244.2	2259.2	2274.2
24°	2289.1	2304.0	2319.0	2333.9	2348.8	2363.6
25°	2378.5	2393.3	2408.1	2422.0	2437.7	2452.4
26°	2467.1	2481.8	2496.5	2511.2	2525.8	2540.5
27°	2555.1	2569.6	2584.2	2598.7	2613.2	2627.7
28°	2642.2	2656.6	2671.0	2685.5	2699.8	2714.2
29°	2728.5	2742.8	2757.1	2771.3	2785.6	2799.8
30°	2814.0	2828.2	2842.3	2856.4	2870.5	2884.6
31°	2898.6	2912.7	2926.7	2940.6	2954.6	2968.5
32°	2982.4	2996.2	3010.1	3023.9	3037.7	3051.5
33°	3065.2	3079.0	3092.6	3106.3	3119.9	3133.6
34°	3147.1	3160.7	3174.2	3187.8	3201.2	3214.7
35°	3228.1	3241.5	3254.8	3268.2	3281.5	3294.8
36°	3308.1	3321.3	3334.5	3347.6	3360.8	3373.9
37°	3387.0	3400.1	3413.1	3426.1	3439.1	3452.0
38°	3464.9	3477.8	3490.7	3503.5	3516.3	3529.1
39°	3541.8	3554.5	3567.2	3579.9	3592.5	3605.1
40°	3617.6	3630.1	3642.6	3655.1	3667.5	3679.9
41°	3692.3	3704.6	3717.0	3729.2	3741.5	3753.7
42°	3765.9	3778.0	3790.1	3802.2	3814.3	3826.3
43°	3838.3	3850.2	3862.2	3874.0	3885.9	3897.7
44°	3909.5	3921.3	3933.0	3944.7	3956.4	3968.0
45°	3979.6	3991.2	4002.7	4014.2	4025.7	4037.1
46°	4048.4	4059.8	4071.1	4082.4	4093.6	4104.9
47°	4116.0	4127.2	4138.3	4149.4	4160.4	4171.5

	0'	10'	20'	30'	40'	50'
48°	4182.4	4193.4	4204.3	4215.1	4226.0	4236.8
49°	4247.5	4258.2	4268.9	4279.6	4290.2	4300.7
50°	4311.3	4321.8	4332.3	4342.7	4353.1	4363.4
51°	4373.8	4384.0	4394.3	4404.5	4414.7	4424.8
52°	4434.9	4445.0	4455.0	4465.0	4474.9	4484.8
53°	4494.7	4504.5	4514.3	4524.1	4533.8	4543.5
54°	4553.2	4562.7	4572.3	4581.9	4591.3	4600.8
55°	4610.2	4619.6	4628.9	4638.2	4647.4	4656.7
56°	4665.8	4675.0	4684.1	4693.1	4702.1	4711.1
57°	4720.0	4728.9	4737.8	4746.6	4755.4	4764.1
58°	4772.8	4781.5	4790.1	4798.7	4807.2	4815.7
59°	4824.2	4832.5	4840.9	4849.3	4857.5	4865.8
60°	4874.0	4882.2	4890.3	4898.4	4906.4	4914.4

*Calcite.*  $2d=6058.08$  X.U.

1°	105.8	123.4	141.0	158.7	176.2	193.9
2°	211.5	229.1	246.7	264.3	281.9	299.5
3°	317.1	334.7	352.3	369.9	387.5	405.0
4°	422.7	440.2	457.8	475.4	492.9	510.5
5°	528.1	545.6	563.2	580.7	598.2	615.8
6°	633.3	650.8	668.3	685.8	703.3	720.9
7°	738.4	755.9	773.3	790.8	808.3	825.7
8°	843.2	860.6	878.1	895.5	913.0	930.3
9°	947.7	965.2	982.6	999.9	1017.3	1034.7
10°	1052.0	1069.4	1086.7	1104.1	1121.4	1138.7
11°	1156.0	1173.3	1190.9	1207.9	1225.1	1242.4
12°	1259.6	1276.9	1294.1	1311.3	1328.5	1345.7
13°	1362.8	1380.0	1397.2	1414.3	1431.4	1448.5
14°	1465.6	1482.7	1499.8	1516.9	1534.0	1551.0
15°	1568.0	1585.0	1602.0	1619.0	1636.0	1652.9
16°	1669.9	1686.8	1703.8	1720.7	1737.5	1754.4
17°	1771.3	1788.1	1804.9	1821.8	1838.6	1855.3
18°	1872.1	1888.8	1905.6	1922.3	1939.0	1955.7
19°	1972.4	1989.0	2005.6	2022.3	2038.9	2055.5
20°	2072.0	2088.6	2105.1	2121.7	2138.1	2154.6
21°	2171.1	2187.5	2203.9	2220.3	2236.8	2253.1
22°	2269.5	2285.8	2302.1	2318.4	2334.7	2350.9
23°	2367.1	2383.4	2399.5	2415.7	2431.9	2448.0
24°	2464.1	2480.2	2496.2	2512.3	2528.3	2544.3
25°	2560.3	2576.3	2592.2	2608.1	2624.0	2639.9
26°	2655.7	2671.6	2687.4	2703.2	2718.9	2734.7
27°	2750.4	2766.1	2781.7	2797.4	2813.0	2828.6
28°	2844.1	2859.7	2875.2	2890.7	2906.2	2921.6
29°	2937.1	2952.5	2967.9	2983.2	2998.5	3013.8
30°	3029.1	3044.4	3059.6	3074.8	3089.9	3105.1
31°	3120.2	3135.3	3150.4	3165.4	3180.4	3195.4
32°	3210.4	3225.3	3240.2	3255.1	3269.9	3284.8
33°	3299.5	3314.3	3329.0	3343.8	3358.4	3373.1
34°	3387.7	3402.3	3416.9	3431.4	3445.9	3460.4

	0'	10'	20'	30'	40'	50'
35°	3474.9	3489.3	3503.6	3518.0	3532.3	3546.6
36°	3560.9	3575.2	3589.4	3603.5	3617.7	3631.8
37°	3645.9	3660.0	3674.0	3688.0	2702.0	3715.9
38°	3729.8	3743.7	3757.5	3771.3	3785.1	3798.8
39°	3812.5	3826.2	3839.9	3853.5	3867.1	3880.6
40°	3894.1	3907.6	3921.0	3934.5	3947.9	3961.2
41°	3974.5	3987.8	4001.1	4014.3	4027.5	4040.6
42°	4053.7	4066.8	4079.8	4092.8	4105.8	4118.8
43°	4131.8	4144.5	4157.4	4170.1	4182.9	4195.6
44°	4208.4	4221.0	4233.6	4246.2	4258.8	4271.3
45°	4283.8	4296.2	4308.6	4321.0	4333.3	4345.6
46°	4357.9	4370.1	4382.3	4394.4	4406.5	4418.6
47°	4430.6	4442.6	4454.6	4466.6	4478.4	4490.3
48°	4502.1	4513.9	4525.6	4537.3	4549.0	4560.6
49°	4572.2	4583.7	4595.2	4606.7	4618.1	4629.5
50°	4640.8	4652.1	4663.4	4674.6	4685.8	4697.0
51°	4708.1	4719.1	4730.1	4741.2	4752.1	4763.0
52°	4773.9	4784.7	4795.5	4806.2	4817.0	4827.6
53°	4838.2	4848.8	4859.3	4869.8	4880.3	4890.7
54°	4901.1	4911.4	4921.7	4932.0	4942.2	4952.4
55°	4962.5	4972.6	4982.6	4992.6	5002.6	5012.5
56°	5022.4	5032.2	5042.0	5051.8	5061.5	5071.1
57°	5080.7	5090.3	5099.8	5109.3	5118.8	5128.2
58°	5137.6	5146.9	5156.2	5165.4	5174.6	5183.7
59°	5192.8	5201.8	5210.9	5219.8	5228.7	5237.6
60°	5246.5	5255.3	5264.0	5272.7	5281.3	5290.0

*Quartz.*  $2d = 8494$  X.U.

1°	148.2	172.9	197.7	222.4	247.0	271.7
2°	296.4	321.2	345.8	370.5	395.2	419.9
3°	444.6	469.2	493.8	518.6	543.2	567.8
4°	592.5	617.2	641.8	666.4	691.1	715.7
5°	740.3	764.9	789.5	814.1	838.7	863.3
6°	887.9	912.4	937.0	961.5	986.1	1010.6
7°	1035.2	1059.7	1084.2	1108.7	1133.2	1157.6
8°	1182.1	1206.6	1231.0	1255.5	1280.0	1304.3
9°	1328.7	1353.2	1377.6	1401.9	1426.3	1450.6
10°	1475.0	1499.3	1523.6	1547.9	1572.2	1596.4
11°	1620.7	1644.9	1669.2	1693.4	1717.7	1741.9
12°	1766.0	1790.2	1814.3	1838.4	1862.6	1886.7
13°	1910.7	1934.8	1958.9	1982.9	2006.8	2030.9
14°	2054.9	2078.8	2102.8	2126.7	2150.7	2174.5
15°	2198.4	2222.4	2246.1	2269.9	2293.7	2317.5
16°	2341.3	2365.0	2388.8	2412.5	2436.1	2459.8
17°	2483.4	2507.0	2530.6	2554.2	2577.8	2601.3
18°	2624.8	2648.3	2671.7	2695.1	2718.6	2742.0
19°	2765.4	2788.8	2812.0	2835.4	2858.7	2881.9
20°	2905.1	2928.3	2951.5	2974.7	2997.8	3020.9
21°	3044.0	3067.0	3090.0	3113.1	3136.1	3159.0

	0'	10'	20'	30'	40'	50'
22°	3181.9	3204.8	3227.6	3250.5	3273.3	3296.1
23°	3318.9	3341.6	3364.3	3387.0	3409.7	3432.3
24°	3454.8	3477.4	3499.9	3522.4	3544.9	3567.3
25°	3589.7	3612.1	3634.4	3656.8	3679.0	3701.3
26°	3723.5	3745.7	3767.9	3790.0	3812.1	3834.2
27°	3856.2	3878.2	3900.2	3922.1	3944.0	3965.8
28°	3987.7	4009.5	4031.3	4053.0	4074.7	4096.3
29°	4118.0	4139.6	4161.1	4182.6	4204.1	4225.6
30°	4247.0	4268.4	4289.7	4311.0	4332.3	4353.5
31°	4374.7	4395.9	4417.0	4438.1	4459.2	4480.2
32°	4501.1	4522.0	4542.9	4563.8	4584.6	4605.4
33°	4626.2	4646.9	4667.5	4688.2	4708.7	4729.3
34°	4749.8	4770.2	4790.7	4811.1	4831.4	4851.7
35°	4872.0	4892.2	4912.3	4932.5	4952.6	4972.6
36°	4992.7	5012.6	5032.5	5052.4	5072.3	5092.1
37°	5111.9	5131.6	5151.2	5170.8	5190.4	5210.0
38°	5229.4	5248.9	5268.3	5287.6	5307.0	5326.2
39°	5345.4	5364.6	5383.8	5402.9	5421.9	5440.9
40°	5459.9	5478.7	5497.6	5516.4	5535.2	5553.9
41°	5572.6	5591.2	5609.8	5628.3	5646.8	5665.2
42°	5683.6	5701.9	5720.2	5738.5	5756.6	5774.8
43°	5792.9	5810.9	5828.9	5846.8	5864.8	5882.6
44°	5900.4	5918.2	5935.9	5953.5	5971.1	5988.7
45°	6006.2	6023.6	6041.0	6058.3	6075.7	6092.9
46°	6110.1	6127.2	6144.3	6161.3	6178.3	6195.3
47°	6212.1	6228.9	6245.7	6262.5	6279.1	6295.8
48°	6312.2	6328.8	6345.3	6361.7	6378.0	6394.3
49°	6410.5	6426.6	6442.8	6458.9	6474.9	6490.9
50°	6506.7	6522.6	6538.4	6554.1	6569.9	6585.5
51°	6601.1	6616.1	6632.0	6647.5	6662.9	6678.2
52°	6693.4	6708.6	6723.7	6738.7	6753.7	6768.7
53°	6783.6	6798.4	6813.2	6828.0	6842.6	6857.2
54°	6871.8	6886.3	6900.7	6915.1	6929.4	6943.7
55°	6957.9	6972.0	6986.1	7000.2	7014.1	7028.0
56°	7041.9	7055.6	7069.4	7083.1	7096.7	7110.2
57°	7123.7	7137.1	7150.4	7163.8	7177.0	7190.2
58°	7203.3	7216.4	7229.4	7243.3	7255.2	7268.1
59°	7280.8	7293.5	7306.1	7318.7	7331.2	7343.7
60°	7356.1	7368.4	7380.6	7392.8	7404.9	7417.0

*Gypsum.*  $2d=15,155 \text{ X.U.}$

1"	264.5	308.6	352.7	396.8	440.7	484.8
2"	528.9	573.0	617.0	661.1	705.2	749.1
3"	793.2	837.2	881.1	925.2	969.2	1013.1
4"	1057.2	1101.2	1145.1	1189.1	1233.0	1277.0
5"	1320.9	1364.7	1408.7	1452.6	1496.4	1540.4
6"	1584.2	1628.0	1671.7	1715.5	1759.3	1803.1
7"	1846.9	1890.7	1934.4	1978.2	2021.8	2065.5
8"	2109.1	2152.8	2196.4	2240.1	2283.7	2327.2

	0'	10'	20'	30'	40'	50'
9°	2370.7	2414.3	2457.8	2501.3	2544.8	2588.2
10°	2631.7	2675.0	2718.4	2761.8	2805.0	2848.4
11°	2891.7	2934.9	2978.3	3021.5	3064.6	3107.8
12°	3150.9	3194.1	3237.1	3280.1	3323.2	3366.2
13°	3409.1	3452.0	3495.0	3537.9	3580.7	3623.6
14°	3666.3	3709.3	3751.8	3794.5	3837.2	3879.8
15°	3922.4	3965.0	4007.4	4050.0	4092.5	4134.9
16°	4177.3	4219.6	4262.0	4304.3	4346.5	4388.7
17°	4430.9	4473.0	4515.1	4557.3	4599.2	4641.2
18°	4683.2	4725.0	4766.9	4808.7	4850.5	4892.3
19°	4934.0	4975.7	5017.2	5058.9	5100.4	5141.9
20°	5183.3	5224.7	5266.1	5307.4	5348.7	5389.8
21°	5431.1	5472.2	5513.2	5554.3	5595.4	5636.3
22°	5677.2	5718.0	5758.7	5799.5	5840.3	5880.9
23°	5921.5	5962.1	6002.6	6043.1	6083.5	6123.8
24°	6164.1	6204.3	6244.5	6284.6	6324.8	6364.8
25°	6404.8	6444.7	6484.5	6524.4	6564.1	6603.8
26°	6643.5	6683.1	6722.6	6762.2	6801.6	6841.0
27°	6880.2	6919.5	6958.7	6997.8	7036.9	7075.9
28°	7114.8	7153.8	7192.6	7231.4	7270.0	7308.7
29°	7347.3	7385.8	7424.3	7462.6	7501.0	7539.3
30°	7577.5	7615.7	7653.7	7691.8	7729.7	7767.5
31°	7805.4	7843.2	7880.9	7918.5	7956.1	7993.5
32°	8030.9	8068.2	8105.5	8142.8	8179.9	8217.0
33°	8254.0	8291.0	8327.8	8364.7	8401.3	8438.0
34°	8474.5	8511.0	8547.6	8583.9	8620.2	8656.4
35°	8692.6	8728.7	8764.6	8800.5	8836.4	8872.2
36°	8908.0	8943.6	8979.0	9014.5	9050.0	9085.3
37°	9120.6	9155.7	9190.7	9225.8	9260.8	9295.6
38°	9330.3	9365.0	9399.7	9434.1	9468.7	9503.1
39°	9537.3	9571.6	9605.7	9639.8	9673.7	9707.7
40°	9741.5	9775.1	9808.8	9842.4	9875.9	9909.2
41°	9942.6	9975.8	10009.0	10042.0	10075.0	10107.9
42°	10140.7	10173.4	10206.0	10238.6	10271.0	10303.4
43°	10335.7	10367.8	10400.0	10431.9	10463.9	10495.7
44°	10527.6	10559.2	10590.8	10622.3	10653.7	10685.0
45°	10716.3	10747.3	10778.4	10809.3	10840.2	10871.0
46°	10901.6	10932.2	10962.7	10993.0	11023.3	11053.6
47°	11083.6	11113.6	11143.6	11173.5	11203.2	11232.9
48°	11262.3	11291.8	11321.2	11350.5	11379.6	11408.7
49°	11437.6	11466.4	11495.2	11524.0	11552.5	11581.0
50°	11609.3	11637.7	11665.9	11693.9	11721.9	11749.8
51°	11777.7	11805.3	11832.9	11860.5	11887.9	11915.2
52°	11942.3	11969.4	11996.4	12023.2	12050.0	12076.7
53°	12103.4	12129.8	12156.1	12182.5	12208.6	12234.6
54°	12260.7	12286.5	12312.2	12338.0	12363.4	12388.9
55°	12414.2	12439.5	12464.7	12489.7	12514.5	12539.4
56°	12564.1	12588.7	12613.2	12637.6	12661.9	12685.9
57°	12710.0	12734.0	12757.8	12781.6	12805.2	12828.7
58°	12852.2	12875.5	12898.7	12921.8	12944.8	12967.7

	0'	10'	20'	30'	40'	50'
59°	12990.4	13013.0	13035.6	13058.0	13080.3	13102.6
60°	13124.7	13146.7	13168.5	13190.3	13211.8	13233.5

*Sugar.*  $2d = 21,141 \text{ X.U.}$

1°	368.9	430.4	492.0	553.5	614.8	676.3
2°	737.8	799.3	860.7	922.2	983.7	1045.0
3°	1106.5	1167.8	1229.1	1290.7	1352.0	1413.3
4°	1474.8	1536.1	1597.4	1658.7	1720.0	1781.3
5°	1842.6	1903.7	1965.1	2026.4	2087.5	2148.8
6°	2209.9	2271.0	2332.1	2393.2	2454.3	2515.4
7°	2576.5	2637.6	2698.4	2759.5	2820.4	2881.3
8°	2942.2	3003.1	3064.1	3124.9	3185.7	3264.4
9°	3307.1	3368.0	3428.6	3489.3	3550.0	3610.5
10°	3671.1	3731.6	3792.1	3852.7	3913.0	3973.5
11°	4033.9	4094.2	4154.6	4214.9	4275.1	4335.4
12°	4395.4	4455.7	4515.7	4575.8	4635.8	4695.8
13°	4755.7	4815.5	4875.5	4935.4	4995.0	5054.8
14°	5114.4	5174.0	5233.7	5293.3	5352.9	5412.3
15°	5471.7	5531.1	5590.3	5649.7	5708.9	5768.1
16°	5827.3	5886.3	5945.5	6004.5	6063.2	6122.2
17°	6181.0	6239.8	6298.5	6357.3	6415.9	6474.4
18°	6533.0	6591.3	6649.7	6708.0	6766.4	6824.7
19°	6882.9	6941.0	6998.9	7057.1	7115.0	7172.9
20°	7230.6	7288.4	7346.1	7403.8	7461.3	7518.8
21°	7576.3	7633.6	7690.9	7748.2	7805.5	7862.5
22°	7919.6	7976.5	8033.4	8090.2	8147.1	8203.8
23°	8260.4	8317.1	8373.5	8430.0	8486.4	8542.7
24°	8598.9	8654.9	8710.9	8767.0	8823.0	8878.8
25°	8934.6	8990.2	9045.8	9101.4	9156.8	9212.2
26°	9267.6	9322.8	9377.9	9433.1	9488.1	9543.0
27°	9597.8	9652.6	9707.3	9761.9	9816.4	9870.7
28°	9925.1	9979.4	10033.5	10087.6	10141.5	10195.5
29°	10249.4	10303.1	10356.8	10410.3	10463.7	10517.2
30°	10570.5	10623.8	10676.8	10729.9	10782.8	10835.6
31°	10888.5	10941.1	10993.7	11046.2	11098.6	11150.8
32°	11203.0	11255.0	11307.1	11359.1	11410.9	11462.7
33°	11514.2	11565.8	11617.2	11668.6	11719.7	11770.9
34°	11821.8	11872.8	11923.7	11974.5	12025.0	12075.5
35°	12126.1	12176.4	12226.5	12276.6	12326.7	12376.6
36°	12426.5	12476.1	12525.6	12575.1	12624.6	12673.8
37°	12723.1	12772.1	12821.0	12869.8	12918.6	12967.3
38°	13015.7	13064.1	13112.5	13166.0	13208.7	13256.7
39°	13304.5	13352.2	13399.8	13447.4	13494.7	13542.1
40°	13589.2	13636.2	13683.1	13730.0	13776.7	13823.3
41°	13848.6	13916.1	13962.4	14008.4	14054.5	14100.4
42°	14146.1	14191.7	14237.2	14282.6	14327.9	14373.1
43°	14418.2	14463.0	14507.8	14552.4	14597.0	14641.4
44°	14685.8	14730.0	14774.0	14817.9	14861.7	14905.5
45°	14949.0	14992.4	15035.7	15078.8	15121.9	15164.9

	0'	10'	20'	30'	40'	50'
46°	15207.6	15250.3	15292.8	15335.0	15377.3	15419.6
47°	15461.5	15503.3	15545.2	15586.8	15628.3	15669.7
48°	15710.7	15751.9	15793.0	15833.8	15874.4	15914.9
49°	15955.3	15995.5	16035.7	16075.8	16115.6	16155.3
50°	16194.9	16234.4	16273.7	16312.8	16351.9	16390.8
51°	16429.7	16468.2	16506.7	16545.2	16583.4	16621.5
52°	16659.3	16697.2	16734.8	16772.2	16809.6	16846.8
53°	16884.0	16920.8	16957.6	16994.4	17030.8	17067.1
54°	17103.5	17139.4	17175.4	17211.3	17246.8	17282.3
55°	17317.7	17353.0	17388.0	17422.9	17457.6	17492.3
56°	17526.7	17561.0	17595.0	17629.3	17663.1	17696.7
57°	17730.3	17763.7	17796.9	17830.1	17863.1	17895.9
58°	17928.6	17961.2	17993.5	18025.7	18057.8	18089.7
59°	18121.4	18152.9	18184.4	18215.7	18246.8	18277.9
60°	18308.7	18339.4	18369.8	18400.3	18430.3	18460.5



TABLE VI.

The principal X-ray spectral lines of the elements arranged in order of their wave-lengths.

$\lambda, 10^{11}$ .	Element.	Series.	Line.	$\lambda, 10^{11}$ .	Element.	Series.	Line.	$\lambda, 10^{11}$ .	Element.	Series.	Line.
104	92 U	K	$\beta_1$	485	47 Ag	K	$\beta_2$	761	83 Bi	L	$\gamma_4$
154	92 U	K	$a_1$	489	50 Sn	K	$a_1$	763	90 Th	L	$\beta_1$
158	78 Pt	K	$\beta_2$	494	50 Sn	K	$a_2$	769	38 Sr	K	$\beta_2$
163	78 Pt	K	$\beta_1$	496	47 Ag	K	$\beta_1$	781	38 Sr	K	$\beta_1$
168	77 Ir	K	$\beta_1$	509	46 Pd	K	$\beta_2$	784	82 Pb	L	$\gamma_4$
179	74 W	K	$\beta_2$	511	49 In	K	$a_1$	784	40 Zr	K	$a_1$
184	74 W	K	$\beta_1$	515	49 In	K	$a_2$	787	92 U	L	$\beta_6$
185	78 Pt	K	$a_1$	519	46 Pd	K	$\beta_1$	787	83 Bi	L	$\gamma_3$
190	78 Pt	K	$a_2$	534	48 Cd	K	$a_1$	788	40 Zr	K	$a_2$
196	77 Ir	K	$a_2$	534	45 Rh	K	$\beta_2$	789	90 Th	L	$\beta_4$
209	74 W	K	$a_1$	538	48 Cd	K	$a_2$	791	90 Th	L	$\beta_2$
214	74 W	K	$a_2$	545	45 Rh	K	$\beta_1$	793	83 Bi	L	$\gamma_2$
292	60 Nd	K	$\beta_1$	558	47 Ag	K	$a_1$	803	92 U	L	$\eta$
301	59 Pr	K	$\beta_1$	563	47 Ag	K	$a_2$	810	81 Tl	L	$\gamma_4$
314	58 Ce	K	$\beta_1$	564	44 Ru	K	$\beta_2$	811	83 Bi	L	$\gamma_1$
329	57 La	K	$\beta_1$	574	44 Ru	K	$\beta_1$	814	82 Pb	L	$\gamma_3$
330	60 Nd	K	$a_1$	584	46 Pd	K	$a_1$	815	37 Rb	K	$\beta_2$
335	60 Nd	K	$a_2$	589	46 Pd	K	$a_2$	818	82 Pb	L	$\gamma_2$
342	59 Pr	K	$a_1$	593	92 U	L	$\gamma_6$	826	90 Th	L	$\beta_6$
343	56 Ba	K	$\beta_1$	597	92 U	L	$\gamma_3$	827	37 Rb	K	$\beta_1$
347	59 Pr	K	$a_2$	604	92 U	L	$\gamma_2$	827	39 Y	K	$a_1$
352	55 Cs	K	$\beta_1$	612	45 Rh	K	$a_1$	831	39 Y	K	$a_2$
355	58 Ce	K	$a_1$	613	92 U	L	$\gamma_1$	835	80 Hg	L	$\gamma_4$
360	58 Ce	K	$a_2$	616	45 Rh	K	$a_2$	837	82 Pb	L	$\gamma_1$
372	57 La	K	$a_1$	619	42 Mo	K	$\beta_2$	838	83 Bi	L	$\gamma_5$
375	53 I	K	$\beta_2$	630	90 Th	L	$\gamma_6$	838	81 Tl	L	$\gamma_3$
376	57 La	K	$a_2$	631	42 Mo	K	$\beta_1$	842	81 Tl	L	$\gamma_6$
388	56 Ba	K	$a_1$	642	44 Ru	K	$a_1$	845	81 Tl	L	$\gamma_2$
388	53 I	K	$\beta_1$	646	44 Ru	K	$a_2$	864	82 Pb	L	$\gamma_5$
390	52 Te	K	$\beta_2$	651	90 Th	L	$\gamma_1$	865	81 Tl	L	$\gamma_1$
393	56 Ba	K	$a_2$	652	41 Nb	K	$\beta_2$	866	79 Au	L	$\gamma_4$
398	55 Cs	K	$a_1$	664	41 Nb	K	$\beta_1$	870	80 Hg	L	$\gamma_2$
399	52 Te	K	$\beta_1$	688	40 Zr	K	$\beta_2$	873	38 Sr	K	$a_1$
402	55 Cs	K	$a_2$	700	40 Zr	K	$\beta_1$	877	38 Sr	K	$a_2$
407	51 Sb	K	$\beta_2$	708	42 Mo	K	$a_1$	894	80 Hg	L	$\gamma_1$
416	51 Sb	K	$\beta_1$	708	92 U	L	$\beta_3$	894	83 Bi	L	$\beta_9$
425	50 Sn	K	$\beta_2$	712	42 Mo	K	$a_2$	894	81 Tl	L	$\gamma_5$
434	50 Sn	K	$\beta_1$	718	92 U	L	$\beta_1$	895	78 Pt	L	$\gamma_4$
437	53 I	K	$a_1$	724	92 U	L	$\beta_5$	896	79 Au	L	$\gamma_3$
444	49 In	K	$\beta_2$	727	39 Y	K	$\beta_2$	901	79 Au	L	$\gamma_2$
450	52 Te	K	$a_1$	736	92 U	L	$\beta_7$	908	92 U	L	$a_1$
454	49 In	K	$\beta_1$	739	39 Y	K	$\beta_1$	914	80 Hg	L	$\gamma_5$
455	52 Te	K	$a_2$	745	41 Nb	K	$a_1$	918	35 Br	L	$\beta_2$
464	48 Cd	K	$\beta_2$	745	92 U	L	$\beta_4$	920	92 U	K	$a_2$
469	51 Sb	K	$a_1$	749	41 Nb	K	$a_2$	922	82 Pb	L	$\beta_9$
474	51 Sb	K	$a_2$	752	90 Th	L	$\beta_3$	922	83 Bi	L	$\beta_5$
474	48 Cd	K	$\beta_1$	753	92 U	L	$\beta_2$	924	37 Rb	K	$a_1$

$\lambda \cdot 10^{11}$	Element.	Series.	Line.	$\lambda \cdot 10^{11}$	Element.	Series.	Line.	$\lambda \cdot 10^{11}$	Element.	Series.	Line.
924	79 Au	L	$\gamma_1$	1057	78 Pt	L	$\beta_1$	1177	76 Os	L	$\beta_3$
926	78 Pt	L	$\gamma_3$	1060	74 W	L	$\gamma_3$	1177	33 As	K	$a_2$
928	37 Rb	K	$a_2$	1061	79 Au	L	$\beta_8$	1178	71 Lu	L	$\gamma_3$
931	35 Br	K	$\beta_1$	1062	73 Ta	L	$\gamma_4$	1182	70 Yb	L	$\gamma_4$
932	78 Pt	L	$\gamma_2$	1065	92 U	L	$l$	1183	71 Lu	L	$\gamma_2$
936	83 Bi	L	$\beta_3$	1066	74 W	L	$\gamma_2$	1184	82 Pb	L	$a_2$
949	83 Bi	L	$\beta_1$	1068	79 Au	L	$\beta_2$	1195	76 Os	L	$\beta_1$
950	82 Pb	L	$\beta_5$	1069	80 Hg	L	$\beta_4$	1200	79 Au	L	$\eta$
953	83 Bi	L	$\beta_2$	1070	78 Pt	L	$\beta_5$	1202	74 W	L	$\beta_9$
953	90 Th	L	$a_1$	1072	74 W	L	$\gamma_6$	1205	81 Tl	L	$a_1$
954	79 Au	L	$\gamma_5$	1077	80 Hg	L	$\beta_6$	1205	76 Os	L	$\beta_6$
955	78 Pt	L	$\gamma_1$	1079	78 Pt	L	$\beta_7$	1206	31 Ga	K	$\beta_1$
957	77 Ir	L	$\gamma_3$	1079	74 W	L	$\gamma_9$	1209	74 W	L	$\beta_{10}$
959	82 Pb	L	$\beta_7$	1081	79 Au	L	$\beta_1$	1213	74 W	L	$\beta_5$
964	77 Ir	L	$\gamma_2$	1090	82 Pb	L	$\eta$	1215	76 Os	L	$\beta_4$
965	90 Th	L	$a_2$	1093	78 Pt	L	$\beta_8$	1216	81 Tl	L	$a_2$
966	82 Pb	L	$\beta_3$	1096	74 W	L	$\gamma_1$	1220	70 Yb	L	$\gamma_3$
974	82 Pb	L	$\beta_8$	1096	73 Ta	L	$\gamma_3$	1220	71 Lu	L	$\gamma_1$
975	83 Bi	L	$\beta_4$	1100	78 Pt	L	$\beta_2$	1221	74 W	L	$\beta_7$
977	34 Se	K	$\beta_2$	1102	73 Ta	L	$\gamma_2$	1226	70 Yb	L	$\gamma_2$
978	81 Tl	L	$\beta_5$	1102	34 Se	K	$a_1$	1235	74 W	L	$\beta_8$
980	82 Pb	L	$\beta_1$	1103	77 Ir	L	$\beta_5$	1239	80 Hg	L	$a_1$
986	78 Pt	L	$\gamma_5$	1104	79 Au	L	$\beta_4$	1240	78 Pt	L	$\eta$
988	81 Tl	L	$\beta_7$	1106	34 Se	K	$a_2$	1242	74 W	L	$\beta_2$
988	77 Ir	L	$\gamma_1$	1110	73 Ta	L	$\gamma_6$	1243	73 Ta	L	$\beta_9$
990	34 Se	K	$\beta_1$	1111	79 Au	L	$\beta_6$	1250	80 Hg	L	$a_2$
992	83 Bi	L	$\beta_6$	1112	90 Th	L	$l$	1251	73 Ta	L	$\beta_5$
998	81 Tl	L	$\beta_3$	1114	32 Ge	K	$\beta_2$	1251	32 Ge	K	$a_1$
1005	82 Pb	L	$\beta_4$	1117	78 Pt	L	$\beta_1$	1254	32 Ge	K	$a_2$
1008	80 Hg	L	$\beta_5$	1125	81 Tl	L	$\eta$	1256	71 Lu	L	$\gamma_5$
1008	81 Tl	L	$\beta_2$	1126	32 Ge	K	$\beta_1$	1260	74 W	L	$\beta_2$
1013	81 Tl	L	$\beta_1$	1127	77 Ir	L	$\beta_8$	1260	73 Ta	L	$\beta_7$
1019	82 Pb	L	$\beta_6$	1129	74 W	L	$\gamma_5$	1265	70 Yb	L	$\gamma_1$
1019	79 Au	L	$\beta_9$	1133	77 Ir	L	$\beta_2$	1273	68 Er	L	$\gamma_4$
1022	76 Os	L	$\gamma_1$	1135	73 Ta	L	$\gamma_1$	1274	79 Au	L	$a_1$
1026	79 Au	L	$\beta_1$	1138	77 Ir	L	$\beta_3$	1274	73 Ta	L	$\beta_8$
1026	74 W	L	$\gamma_4$	1140	78 Pt	L	$\beta_4$	1279	74 W	L	$\beta_1$
1030	80 Hg	L	$\beta_3$	1140	76 Os	L	$\beta_5$	1281	73 Ta	L	$\beta_2$
1037	81 Tl	L	$\beta_4$	1141	71 Lu	L	$\gamma_4$	1281	30 Zn	K	$\beta_2$
1038	80 Hg	L	$\beta_2$	1141	83 Bi	L	$a_1$	1285	79 Au	L	$a_2$
1038	33 As	K	$\beta_2$	1153	83 Bi	L	$a_2$	1287	74 W	L	$\beta_6$
1038	35 Br	K	$a_1$	1155	77 Ir	L	$\beta_1$	1293	30 Zn	K	$\beta_1$
1038	79 Au	L	$\beta_5$	1162	80 Hg	L	$\eta$	1299	74 W	L	$\beta_4$
1042	35 Br	K	$a_2$	1168	76 Os	L	$\beta_2$	1303	70 Yb	L	$\gamma_5$
1046	80 Hg	L	$\beta_1$	1170	73 Ta	L	$\gamma_5$	1303	73 Ta	L	$\beta_3$
1047	79 Au	L	$\beta_7$	1172	77 Ir	L	$\beta_6$	1310	78 Pt	L	$a_1$
1048	81 Tl	L	$\beta_6$	1172	82 Pb	L	$a_1$	1312	68 Er	L	$\gamma_3$
1052	78 Pt	L	$\beta_9$	1173	33 As	K	$a_1$	1313	83 Bi	L	$l$
1055	33 As	K	$\beta_1$	1176	77 Ir	L	$\beta_4$	1318	68 Er	L	$\gamma_2$
1057	83 Bi	L	$\eta$	1177	72 Hf	L	$\gamma_1$	1320	67 Ho	L	$\gamma_4$

$\lambda, 10^{11}$	Element.	Series.	Line.	$\lambda, 10^{11}$	Element.	Series.	Line.	$\lambda, 10^{11}$	Element.	Series.	Line.
1321	78 Pt	L	$\alpha_2$	1474	65 Tb	L	$\gamma_2$	1631	70 Yb	L	$\eta$
1324	73 Ta	L	$\beta_1$	1482	64 Gd	L	$\gamma_4$	1636	67 Ho	L	$\beta_{13}$
1324	72 Hf	L	$\beta_2$	1482	68 Er	L	$\beta_9$	1638	64 Gd	L	$\gamma_5$
1327	73 Ta	L	$\beta_6$	1485	74 W	L	$\alpha_2$	1644	67 Ho	L	$\beta_1$
1333	71 Lu	L	$\beta_9$	1485	28 Ni	K	$\beta_2$	1644	63 Eu	L	$\gamma_7$
1338	31 Ga	K	$\alpha_1$	1488	70 Yb	L	$\beta_4$	1648	28 Ni	K	$\alpha_3$
1340	71 Lu	L	$\beta_{10}$	1489	68 Er	L	$\beta_7$	1652	62 Sm	L	$\gamma_3$
1342	31 Ga	K	$\alpha_2$	1497	28 Ni	K	$\beta_1$	1654	63 Eu	L	$\gamma_1$
1342	73 Ta	L	$\beta_4$	1497	78 Pt	L	$l$	1655	28 Ni	K	$\alpha_1$
1346	71 Lu	L	$\beta_7$	1499	28 Ni	K	$\beta'$	1655	67 Ho	L	$\beta_4$
1347	82 Pb	L	$l$	1501	68 Er	L	$\beta_{11}$	1656	65 Tb	L	$\beta_7$
1348	77 Ir	L	$\alpha_1$	1511	68 Er	L	$\beta_2$	1656	62 Sm	L	$\gamma_2$
1349	72 Hf	L	$\beta_3$	1512	68 Er	L	$\beta_{14}$	1659	63 Eu	L	$\gamma_9$
1359	71 Lu	L	$\beta_{11}$	1515	66 Dy	L	$\gamma_5$	1659	28 Ni	K	$\alpha_2$
1359	77 Ir	L	$\alpha_2$	1518	73 Ta	L	$\alpha_1$	1664	65 Tb	L	$\beta_{10}$
1361	67 Ho	L	$\gamma_3$	1526	64 Gd	L	$\gamma_3$	1668	70 Yb	L	$\alpha_1$
1362	68 Er	L	$\gamma_1$	1527	65 Tb	L	$\gamma_1$	1675	74 W	L	$l$
1367	71 Lu	L	$\beta_2$	1529	73 Ta	L	$\alpha_2$	1678	66 Dy	L	$\beta_3$
1368	67 Ho	L	$\gamma_2$	1531	29 Cu	K	$\alpha_3$	1679	70 Yb	L	$\alpha_2$
1370	72 Hf	L	$\beta_1$	1531	64 Gd	L	$\gamma_2$	1679	65 Tb	L	$\beta_2$
1371	66 Dy	L	$\gamma_4$	1531	65 Tb	L	$\gamma_9$	1685	65 Tb	L	$\beta_{14}$
1378	29 Cu	K	$\beta_2$	1537	29 Cu	K	$\alpha_1$	1699	66 Dy	L	$\beta_{13}$
1388	76 Os	L	$\alpha_1$	1541	29 Cu	K	$\alpha_2$	1705	63 Eu	L	$\gamma_5$
1389	29 Cu	K	$\beta_1$	1558	68 Er	L	$\beta_3$	1707	66 Dy	L	$\beta_1$
1398	76 Os	L	$\alpha_2$	1564	68 Er	L	$\beta_6$	1717	66 Dy	L	$\beta_4$
1398	71 Lu	L	$\beta_3$	1564	67 Ho	L	$\beta_2$	1720	64 Gd	L	$\beta_7$
1403	68 Er	L	$\gamma_5$	1566	72 Hf	L	$\alpha_1$	1723	62 Sm	L	$\gamma_1$
1413	70 Yb	L	$\beta_2$	1567	67 Ho	L	$\beta_{14}$	1724	73 Ta	L	$l$
1414	66 Dy	L	$\gamma_3$	1574	71 Lu	L	$\eta$	1728	64 Gd	L	$\beta_{10}$
1414	67 Ho	L	$\gamma_1$	1574	65 Tb	L	$\gamma_5$	1729	62 Sm	L	$\gamma_9$
1414	71 Lu	L	$\beta_0$	1576	68 Er	L	$\beta_{13}$	1738	65 Tb	L	$\beta_6$
1416	67 Ho	L	$\gamma_9$	1577	72 Hf	L	$\alpha_2$	1741	26 Fe	K	$\beta_2$
1418	74 W	L	$\eta$	1583	68 Er	L	$\beta_1$	1741	60 Nd	L	$\gamma_4$
1418	80 Hg	L	$l$	1588	63 Eu	L	$\gamma_3$	1742	64 Gd	L	$\beta_2$
1420	66 Dy	L	$\gamma_3$	1589	64 Gd	L	$\gamma_1$	1743	65 Tb	L	$\beta_3$
1421	71 Lu	L	$\beta_1$	1594	64 Gd	L	$\gamma_9$	1748	64 Gd	L	$\beta_{14}$
1424	65 Tb	L	$\gamma_4$	1594	63 Eu	L	$\gamma_2$	1753	26 Fe	K	$\beta_1$
1429	30 Zn	K	$\alpha_3$	1596	66 Dy	L	$\beta_7$	1755	68 Er	L	$\eta$
1432	30 Zn	K	$\alpha_1$	1596	68 Er	L	$\beta_4$	1756	26 Fe	K	$\beta'$
1436	30 Zn	K	$\alpha_2$	1603	62 Sm	L	$\gamma_4$	1766	65 Tb	L	$\beta_{13}$
1437	71 Lu	L	$\beta_4$	1605	27 Co	K	$\beta_2$	1773	65 Tb	L	$\beta_1$
1440	70 Yb	L	$\beta_3$	1616	71 Lu	L	$\alpha_1$	1775	62 Sm	L	$\gamma_5$
1457	79 Au	L	$l$	1616	67 Ho	L	$\beta_3$	1777	27 Co	K	$\alpha_2$
1459	67 Ho	L	$\gamma_5$	1617	27 Co	K	$\beta_1$	1780	68 Er	L	$\alpha_1$
1463	70 Yb	L	$\beta_6$	1619	67 Ho	L	$\beta_6$	1781	65 Tb	L	$\beta_4$
1466	73 Ta	L	$\eta$	1620	27 Co	K	$\beta'$	1781	63 Eu	L	$\beta_{14}$
1468	65 Tb	L	$\gamma_3$	1620	66 Dy	L	$\beta_2$	1784	63 Eu	L	$\beta_7$
1470	66 Dy	L	$\gamma_1$	1625	66 Dy	L	$\beta_{14}$	1785	27 Co	K	$\alpha_1$
1473	70 Yb	L	$\beta_1$	1626	71 Lu	L	$\alpha_2$	1788	63 Eu	L	$\beta_9$
1473	74 W	L	$\alpha_1$	1629	63 Eu	L	$\gamma_8$	1790	27 Co	K	$\alpha_2$

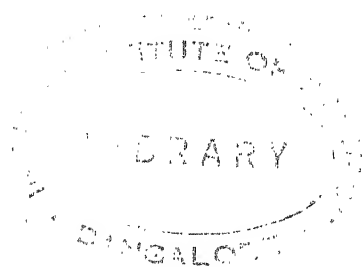
$\lambda \cdot 10^{11}$	Element.	Series.	Line.	$\lambda \cdot 10^{11}$	Element.	Series.	Line.	$\lambda \cdot 10^{11}$	Element.	Series.	Line.
1791	68 Er	L	$\alpha_2$	1962	59 Pr	L	$\gamma_9$	2186	59 Pr	L	$\beta_6$
1793	60 Nd	L	$\gamma_3$	1962	58 Ce	L	$\gamma_{10}$	2192	58 Ce	L	$\beta_{10}$
1796	63 Eu	L	$\beta_{10}$	1971	65 Tb	L	$\alpha_1$	2195	62 Sm	L	$\alpha_1$
1797	60 Nd	L	$\gamma_2$	1979	57 La	L	$\gamma_4$	2201	57 La	L	$\gamma_5$
1803	64 Gd	L	$\beta_6$	1982	65 Tb	L	$\alpha_2$	2204	58 Ce	L	$\beta_2$
1808	63 Eu	L	$\beta_2$	1987	62 Sm	L	$\beta_{13}$	2206	62 Sm	L	$\alpha_2$
1811	64 Gd	L	$\beta_3$	1994	62 Sm	L	$\beta_1$	2212	58 Ce	L	$\beta_{11}$
1815	59 Pr	L	$\gamma_4$	1996	62 Sm	L	$\beta_4$	2212	59 Pr	L	$\beta_3$
1822	67 Ho	L	$\eta$	2004	60 Nd	L	$\beta_7$	2214	62 Sm	L	$\eta$
1832	71 Lu	L	$l$	2012	60 Nd	L	$\beta_9$	2218	56 Ba	L	$\gamma_7$
1836	64 Gd	L	$\beta_{13}$	2015	68 Er	L	$l$	2227	55 Cs	L	$\gamma_3$
1841	69 Ho	L	$\alpha_1$	2016	59 Pr	L	$\gamma_5$	2229	65 Tb	L	$l$
1842	64 Gd	L	$\beta_1$	2019	58 Ce	L	$\gamma_8$	2232	55 Cs	L	$\gamma_2$
1849	64 Gd	L	$\beta_4$	2019	60 Nd	L	$\beta_{10}$	2237	56 Ba	L	$\gamma_1$
1852	67 Ho	L	$\alpha_2$	2029	58 Ce	L	$\gamma_7$	2237	55 Cs	L	$\gamma_{10}$
1852	62 Sm	L	$\beta_7$	2031	60 Nd	L	$\beta_2$	2248	92 U	M	$M_{15}P_1$
1858	62 Sm	L	$\beta_9$	2037	57 La	L	$\gamma_3$	2250	59 Pr	L	$\beta_4$
1859	60 Nd	L	$\gamma_7$	2039	60 Nd	L	$\beta_{14}$	2254	59 Pr	L	$\beta_1$
1866	62 Sm	L	$\beta_{10}$	2042	57 La	L	$\gamma_2$	2265	23 Va	K	$\beta_2$
1870	59 Pr	L	$\gamma_3$	2042	64 Gd	L	$\alpha_1$	2270	57 La	L	$\beta_7$
1871	63 Eu	L	$\beta_6$	2044	58 Ce	L	$\gamma_1$	2273	24 Cr	K	$\alpha_3$
1874	60 Nd	L	$\gamma_1$	2048	57 La	L	$\gamma_{10}$	2277	58 Ce	L	$\beta_6$
1875	59 Pr	L	$\gamma_3$	2051	58 Ce	L	$\gamma_9$	2277	57 La	L	$\beta_9$
1878	62 Sm	L	$\beta_2$	2053	64 Gd	L	$\alpha_2$	2280	23 Va	K	$\beta_1$
1880	60 Nd	L	$\gamma_9$	2067	24 Cr	K	$\beta_2$	2285	24 Cr	K	$\alpha_1$
1881	59 Pr	L	$\gamma_{10}$	2072	56 Ba	L	$\gamma_4$	2285	57 La	L	$\beta_{10}$
1883	63 Eu	L	$\beta_3$	2080	24 Cr	K	$\beta_1$	2285	23 Va	K	$\beta'$
1885	62 Sm	L	$\beta_{14}$	2082	67 Ho	L	$l$	2289	24 Cr	K	$\alpha_2$
1890	70 Yb	L	$l$	2086	24 Cr	K	$\beta'$	2298	57 La	L	$\beta_2$
1892	66 Dy	L	$\eta$	2087	59 Pr	L	$\beta_7$	2299	92 U	M	$M_{15}O_3$
1893	25 Mn	K	$\beta_2$	2088	25 Mn	K	$\alpha_3$	2302	56 Ba	L	$\gamma_5$
1895	58 Ce	L	$\gamma_4$	2096	59 Pr	L	$\beta_9$	2306	58 Ce	L	$\beta_3$
1905	66 Dy	L	$\alpha_1$	2097	25 Mn	K	$\alpha_1$	2307	64 Gd	L	$l$
1906	25 Mn	K	$\beta_1$	2099	60 Nd	L	$\beta_6$	2343	55 Cs	L	$\gamma_1$
1909	63 Eu	L	$\beta_{13}$	2103	59 Pr	L	$\beta_{10}$	2344	58 Ce	L	$\beta_4$
1911	25 Mn	K	$\beta'$	2106	58 Ce	L	$\gamma_5$	2351	58 Ce	L	$\beta_1$
1916	66 Dy	L	$\alpha_2$	2115	59 Pr	L	$\beta_2$	2365	60 Nd	L	$\alpha_1$
1916	63 Eu	L	$\beta_1$	2116	63 Eu	L	$\alpha_1$	2371	56 Ba	L	$\beta_9$
1922	63 Eu	L	$\beta_4$	2122	59 Pr	L	$\beta_{14}$	2374	57 La	L	$\beta_6$
1923	26 Fe	K	$\alpha_3$	2122	60 Nd	L	$\beta_3$	2376	56 Ba	L	$\beta_7$
1931	60 Nd	L	$\gamma_5$	2127	63 Eu	L	$\alpha_2$	2376	60 Nd	L	$\alpha_2$
1932	59 Pr	L	$\gamma_8$	2130	56 Ba	L	$\gamma_3$	2382	56 Ba	L	$\beta_{11}$
1932	26 Fe	L	$\alpha_1$	2134	56 Ba	L	$\gamma_2$	2390	63 Eu	L	$l$
1937	26 Fe	K	$\alpha_2$	2137	57 La	L	$\gamma_1$	2399	56 Ba	L	$\beta_2$
1942	62 Sm	L	$\beta_6$	2140	56 Ba	L	$\gamma_{10}$	2404	60 Nd	L	$\eta$
1942	59 Pr	L	$\gamma_7$	2154	66 Dy	L	$l$	2405	57 La	L	$\beta_3$
1951	58 Ce	L	$\gamma_3$	2162	60 Nd	L	$\beta_1$	2411	55 Cs	L	$\gamma_5$
1956	58 Ce	L	$\gamma_2$	2169	55 Cs	L	$\gamma_4$	2437	90 Th	M	$M_{15}O_3$
1957	59 Pr	L	$\gamma_1$	2176	58 Ce	L	$\beta_7$	2439	92 U	M	$M_{14}O_2$
1958	62 Sm	L	$\beta_3$	2184	58 Ce	L	$\beta_9$	2444	57 La	L	$\beta_4$

$\lambda, 10^{11}$	Element.	Series.	Line.	$\lambda, 10^{11}$	Element.	Series.	Line.	$\lambda, 10^{11}$	Element.	Series.	Line.
2453	57 La	L	$\beta_1$	2815	92 U	M	$M_4N_4$	3143	50 Sn	L	$\beta_{11}$
2458	59 Pr	L	$\alpha_1$	2827	50 Sn	L	$\gamma_2$	3145	51 Sb	L	$\beta_3$
2468	59 Pr	L	$\alpha_2$	2845	51 Sb	L	$\gamma_1$	3149	50 Sn	L	$\beta_7$
2473	55 Cs	L	$\beta_9$	2857	56 Ba	L	$\eta$	3151	53 I	L	$\alpha_2$
2477	62 Sm	L	$l$	2867	53 I	L	$\beta_3$	3155	49 In	L	$\gamma_1$
2477	56 Ba	L	$\beta_6$	2876	52 Te	L	$\beta_2$	3168	50 Sn	L	$\beta_2$
2480	55 Cs	L	$\beta_7$	2886	55 Cs	L	$\alpha_1$	3184	51 Sb	L	$\beta_4$
2483	55 Cs	L	$\beta_{11}$	2896	55 Cs	L	$\alpha_2$	3218	51 Sb	L	$\beta_1$
2485	23 Va	K	$\alpha_3$	2906	53 I	L	$\beta_4$	3242	49 In	L	$\gamma_5$
2494	22 Ti	K	$\beta_2$	2909	92 U	M	$M_5N_6$	3260	49 In	L	$\beta_9$
2498	23 Va	K	$\alpha_1$	2917	90 Th	M	$M_5N_5$	3262	50 Sn	L	$\beta_6$
2502	23 Va	K	$\alpha_2$	2919	49 In	L	$\gamma_4$	3266	49 In	L	$\beta_{10}$
2506	52 Te	L	$\gamma_4$	2926	51 Sb	L	$\gamma_5$	3276	90 Th	M	$M_3O_5$
2506	55 Cs	L	$\beta_2$	2927	92 U	M	$M_3O_1$	3282	52 Te	L	$\alpha_1$
2507	59 Pr	L	$\eta$	2931	53 I	L	$\beta_1$	3291	52 Te	L	$\alpha_2$
2509	22 Ti	K	$\beta_1$	2964	52 Te	L	$\beta_6$	3296	49 In	L	$\beta_{12}$
2511	56 Ba	L	$\beta_3$	2966	51 Sb	L	$\beta_9$	3299	50 Sn	L	$\beta_3$
2515	22 Ti	K	$\beta'$	2969	50 Sn	L	$\gamma_7$	3300	47 Ag	L	$\gamma_2$
2550	56 Ba	L	$\beta_4$	2973	51 Sb	L	$\beta_{10}$	3302	48 Cd	L	$\gamma_7$
2556	58 Ce	L	$\alpha_1$	2974	49 In	L	$\gamma_2$	3304	49 In	L	$\beta_{11}$
2562	56 Ba	L	$\beta_1$	2983	55 Cs	L	$\eta$	3317	49 In	L	$\beta_7$
2565	52 Te	L	$\gamma_2$	2986	51 Sb	L	$\beta_{12}$	3321	92 U	M	$M_4N_7$
2565	58 Ce	L	$\alpha_2$	2993	51 Sb	L	$\beta_{11}$	3328	48 Cd	L	$\gamma_1$
2577	53 I	L	$\gamma_1$	2995	50 Sn	L	$\gamma_1$	3330	20 Ca	K	$\alpha_4$
2588	55 Cs	L	$\beta_6$	2999	90 Th	M	$M_4N_4$	3331	49 In	L	$\beta_2$
2612	90 Th	M	$M_4O_2$	3000	57 La	L	$l$	3332	20 Ca	K	$\alpha_3$
2615	58 Ce	L	$\eta$	3001	52 Te	L	$\beta_3$	3336	50 Sn	L	$\beta_4$
2623	55 Cs	L	$\beta_3$	3006	21 Sc	K	$\alpha_3$	3349	20 Ca	K	$\alpha''$
2634	51 Sb	L	$\gamma_4$	3017	51 Sb	L	$\beta_2$	3352	20 Ca	K	$\alpha_1$
2660	57 La	L	$\alpha_1$	3023	21 Sc	K	$\alpha''$	3355	20 Ca	K	$\alpha_2$
2661	55 Cs	L	$\beta_4$	3025	21 Sc	K	$\alpha_1$	3378	50 Sn	L	$\beta_1$
2669	57 La	L	$\alpha_2$	3028	21 Sc	K	$\alpha_2$	3418	48 Cd	L	$\gamma_5$
2670	60 Nd	L	$l$	3040	52 Te	L	$\beta_4$	3428	49 In	L	$\beta_6$
2678	55 Cs	L	$\beta_1$	3067	20 Ca	K	$\beta_2$	3432	51 Sb	L	$\alpha_1$
2689	51 Sb	L	$\gamma_2$	3070	52 Te	L	$\beta_1$	3435	19 K	K	$\beta_2$
2706	52 Te	L	$\gamma_1$	3077	50 Sn	L	$\gamma_5$	3441	51 Sb	L	$\alpha_2$
2727	22 Ti	K	$\alpha_3$	3080	20 Ca	K	$\beta''$	3443	19 K	K	$\beta''$
2734	57 La	L	$\eta$	3083	20 Ca	K	$\beta_1$	3447	19 K	K	$\beta_1$
2743	22 Ti	K	$\alpha_1$	3091	20 Ca	K	$\beta'$	3459	92 U	M	$\gamma'$
2746	53 I	L	$\beta_2$	3107	92 U	M	$M_3O_5$	3462	49 In	L	$\beta_3$
2747	22 Ti	K	$\alpha_2$	3108	51 Sb	L	$\beta_6$	3468	48 Cd	L	$\beta_{12}$
2750	92 U	M	$M_5N_5$	3108	50 Sn	L	$\beta_9$	3472	92 U	M	$M_3N_3$
2756	21 Sc	K	$\beta_2$	3109	90 Th	M	$M_3O_1$	3478	48 Cd	L	$\beta_{11}$
2770	56 Ba	L	$\alpha_1$	3114	50 Sn	L	$\beta_{10}$	3480	47 Ag	L	$\gamma_7$
2771	50 Sn	L	$\gamma_4$	3125	49 In	L	$\gamma_7$	3481	46 Pd	L	$\gamma_2$
2774	21 Sc	K	$\beta_1$	3127	90 Th	M	$M_5N_6$	3499	49 In	L	$\beta_4$
2778	59 Pr	L	$l$	3129	56 Ba	L	$l$	3506	48 Cd	L	$\beta_2$
2779	56 Ba	L	$\alpha_2$	3132	48 Cd	L	$\gamma_2$	3514	92 U	M	$M_1P_1$
2783	52 Te	L	$\gamma_5$	3135	50 Sn	L	$\beta_{12}$	3515	47 Ag	L	$\gamma_1$
2799	21 Sc	K	$\beta'$	3142	53 I	L	$\alpha_1$	3530	90 Th	M	$M_4N_7$

$\lambda \cdot 10^{11}$	Element.	Series.	Line.	$\lambda \cdot 10^{11}$	Element.	Series.	Line.	$\lambda \cdot 10^{11}$	Element.	Series.	Line.
3548	49 In	L	$\beta_1$	3897	45 Rh	L	$\gamma_7$	4410	47 Ag	L	$\eta$
3570	92 U	M	$M_2O_4$	3901	46 Pd	L	$\beta_2$	4433	74 W	M	$M_5O_3$
3592	50 Sn	L	$\alpha_1$	3901	92 U	M	$M_1N_1$	4471	48 Cd	L	$l$
3600	51 Sb	L	$\eta$	3913	92 U	M	$M_1N_2$	4476	44 Ru	L	$\beta_3$
3601	50 Sn	L	$\alpha_2$	3921	90 Th	M	$\beta'$	4497	83 Bi	M	$\gamma'$
3607	48 Cd	L	$\beta_6$	3925	90 Th	M	$\beta''$	4513	44 Ru	L	$\beta_4$
3607	47 Ag	L	$\gamma_5$	3927	47 Ag	L	$\beta_1$	4513	83 Bi	M	$M_3N_3$
3620	47 Ag	L	$\beta_9$	3931	90 Th	M	$M_2N_2$	4548	77 Ir	M	$M_5N_5$
3630	47 Ag	L	$\beta_{10}$	3932	81 Tl	M	$M_5N_5$	4569	90 Th	M	$M_3N_7$
3636	48 Cd	L	$\beta_3$	3933	48 Cd	L	$\alpha_3$	4572	45 Rh	L	$\alpha_3$
3645	90 Th	M	$\gamma'$	3936	45 Rh	L	$\gamma_1$	4588	45 Rh	L	$\alpha_1$
3654	47 Ag	L	$\beta_{12}$	3945	82 Pb	M	$M_4N_4$	4596	45 Rh	L	$\alpha_2$
3657	90 Th	M	$M_3N_3$	3948	48 Cd	L	$\alpha_1$	4611	44 Ru	L	$\beta_1$
3663	47 Ag	L	$\beta_{11}$	3956	48 Cd	L	$\alpha_2$	4639	41 Nb	L	$\gamma_2$
3672	83 Bi	M	$M_5N_5$	3976	49 In	L	$\eta$	4646	82 Pb	M	$M_4N_7$
3674	48 Cd	L	$\beta_4$	4007	46 Pd	L	$\beta_6$	4650	46 Pd	L	$\eta$
3676	46 Pd	L	$\gamma_7$	4026	46 Pd	L	$\beta_3$	4666	82 Pb	M	$M_3N_3$
3677	45 Rh	L	$\gamma_2$	4035	45 Rh	L	$\gamma_5$	4684	17 Cl	K	$\alpha_4$
3684	92 U	M	$\beta'$	4049	45 Rh	L	$\beta_{11}$	4688	17 Cl	K	$\alpha_3$
3694	47 Ag	L	$\beta_2$	4062	46 Pd	L	$\beta_4$	4698	47 Ag	L	$l$
3696	92 U	M	$\beta''$	4063	50 Sn	L	$l$	4703	17 Cl	K	$\alpha'$
3700	92 U	M	$\beta'''$	4073	45 Rh	L	$\beta_{12}$	4711	42 Mo	L	$\gamma_1$
3709	19 K	K	$\alpha_4$	4095	81 Tl	M	$M_4N_4$	4712	17 Cl	K	$\alpha''$
3709	92 U	M	$M_2N_2$	4097	90 Th	M	$\alpha'$	4718	17 Cl	K	$\alpha_1$
3710	52 Te	L	$l$	4122	45 Rh	L	$\beta_2$	4721	17 Cl	K	$\alpha_2$
3711	19 K	K	$\alpha_3$	4129	90 Th	M	$M_1N_1$	4768	77 Ir	M	$M_4N_4$
3716	46 Pd	L	$\gamma_1$	4132	47 Ag	L	$\alpha_3$	4779	76 Os	M	$M_5N_5$
3719	19 K	K	$\alpha'$	4137	46 Pd	L	$\beta_1$	4798	81 Tl	M	$\gamma'$
3730	19 K	K	$\alpha''$	4138	90 Th	M	$M_1N_2$	4806	81 Tl	M	$M_3N_3$
3730	48 Cd	L	$\beta_1$	4146	47 Ag	L	$\alpha_1$	4815	83 Bi	M	$M_2O_4$
3734	19 K	K	$\alpha_1$	4154	47 Ag	L	$\alpha_2$	4818	44 Ru	L	$\alpha_3$
3737	19 K	K	$\alpha_2$	4173	44 Ru	L	$\gamma_1$	4819	42 Mo	L	$\gamma_5$
3750	49 In	L	$\alpha_3$	4188	48 Cd	L	$\eta$	4836	44 Ru	L	$\alpha_1$
3753	90 Th	M	$M_1P_1$	4230	79 Au	M	$M_5N_5$	4842	42 Mo	L	$\beta_{12}$
3764	49 In	L	$\alpha_1$	4230	45 Rh	L	$\beta_6$	4844	44 Ru	L	$\alpha_2$
3772	49 In	L	$\alpha_2$	4241	45 Rh	L	$\beta_3$	4860	42 Mo	L	$\beta_{11}$
3782	50 Sn	L	$\eta$	4259	49 In	L	$l$	4875	83 Bi	M	$\beta''$
3789	82 Pb	M	$M_5N_5$	4277	44 Ru	L	$\gamma_5$	4894	83 Bi	M	$M_2N_2$
3792	90 Th	M	$M_2O_4$	4278	45 Rh	L	$\beta_4$	4909	42 Mo	L	$\beta_2$
3799	47 Ag	L	$\beta_6$	4326	92 U	M	$M_3N_7$	4911	45 Rh	L	$\eta$
3812	46 Pd	L	$\gamma_5$	4344	46 Pd	L	$\alpha_3$	4929	92 U	M	$M_1N_5$
3816	83 Bi	M	$M_4N_4$	4359	46 Pd	L	$\alpha_1$	4940	46 Pd	L	$l$
3824	47 Ag	L	$\beta_3$	4361	42 Mo	L	$\gamma_2$	4941	40 Zr	L	$\gamma_2$
3857	46 Pd	L	$\beta_{12}$	4362	44 Ru	L	$\beta_2$	4949	76 Os	M	$M_4N_4$
3861	47 Ag	L	$\beta_4$	4364	45 Rh	L	$\beta_1$	4994	82 Pb	M	$M_2O_4$
3868	46 Pd	L	$\beta_{11}$	4367	46 Pd	L	$\alpha_2$	5000	42 Mo	L	$\beta_3$
3880	51 Sb	L	$l$	4391	17 Cl	K	$\beta''$	5013	16 S	K	$\beta_2$
3884	83 Bi	M	$M_5N_6$	4395	17 Cl	K	$\beta_1$	5021	16 S	K	$\beta_1$
3885	92 U	M	$\alpha''$	4406	17 Cl	K	$\beta_3$	5024	41 Nb	L	$\gamma_1$
3888	44 Ru	L	$\gamma_2$	4407	78 Pt	M	$M_6N_6$	5036	42 Mo	L	$\beta_4$

$\lambda, 10^{11}$	Element.	Series.	Line.	$\lambda, 10^{11}$	Element.	Series.	Line.	$\lambda, 10^{11}$	Element.	Series.	Line.
5042	82 Pb	M	$\beta''$	5672	76 Os	M	$M_3N_3$	6593	40 Zr	L	$\eta$
5045	16 S	K	$\beta'$	5687	82 Pb	M	$M_3N_7$	6609	38 Sr	L	$\beta_1$
5047	16 S	K	$\beta_3$	5689	41 Nb	L	$a_3$	6663	77 Ir	M	$M_3N_7$
5065	82 Pb	M	$M_2N_2$	5694	40 Zr	L	$\beta_6$	6726	74 W	M	$\beta''$
5078	83 Bi	M	$a'$	5711	41 Nb	L	$a_1$	6727	82 Pb	M	$M_1N_5$
5107	83 Bi	M	$M_1N_1$	5717	41 Nb	L	$a_2$	6733	74 W	M	$M_2N_2$
5117	83 Bi	M	$M_1N_2$	5786	15 P	K	$\beta_1$	6739	37 Rb	L	$\gamma_5$
5131	79 Au	M	$M_3N_3$	5797	78 Pt	M	$\beta''$	6739	14 Si	K	$\beta_1$
5157	74 W	M	$M_5N_5$	5802	76 Os	M	$M_4N_7$	6744	14 Si	K	$\beta'$
5161	41 Nb	L	$\beta_{11}$	5812	79 Au	M	$a''$	6750	74 W	M	$M_2O_3$
5166	42 Mo	L	$\beta_1$	5820	78 Pt	M	$M_2N_2$	6770	37 Rb	L	$\beta_3$
5185	81 Tl	M	$M_2O_4$	5820	15 P	K	$\beta_3$	6780	71 Lu	M	$M_3N_3$
5207	45 Rh	L	$l$	5823	40 Zr	L	$\beta_1$	6793	14 Si	K	$\beta_3$
5210	81 Tl	M	$\beta''$	5831	79 Au	M	$M_1N_1$	6803	37 Rb	L	$\beta_4$
5225	41 Nb	L	$\beta_2$	5835	42 Mo	L	$\eta$	6818	38 Sr	L	$a_3$
5233	81 Tl	M	$M_2N_2$	5879	81 Tl	M	$M_3N_7$	6848	38 Sr	L	$a_1$
5242	82 Pb	M	$a'$	5968	39 Y	L	$\beta_3$	6882	76 Os	M	$M_3N_7$
5245	90 Th	M	$M_1N_5$	6002	39 Y	L	$\beta_4$	6898	40 Zr	L	$l$
5250	82 Pb	M	$a''$	6011	77 Ir	M	$\beta''$	6952	74 W	M	$a''$
5263	16 S	K	$a_5$	6026	78 Pt	M	$a''$	6963	74 W	M	$M_1N_1$
5273	82 Pb	M	$M_1N_1$	6027	40 Zr	L	$a_3$	6968	37 Rb	L	$\beta_6$
5296	41 Nb	L	$\beta_3$	6028	37 Rb	L	$\gamma_2$	7001	73 Ta	M	$M_2N_2$
5303	78 Pt	M	$M_3N_3$	6030	77 Ir	M	$M_2N_2$	7003	14 Si	K	$a_6$
5323	16 S	K	$a_4$	6041	78 Pt	M	$M_1N_1$	7014	14 Si	K	$a_5$
5329	16 S	K	$a_3$	6056	40 Zr	L	$a_1$	7054	14 Si	K	$a_4$
5331	41 Nb	L	$\beta_4$	6066	74 W	M	$\gamma'$	7060	37 Rb	L	$\beta_1$
5341	16 S	K	$a'$	6083	74 W	M	$M_3N_3$	7064	14 Si	K	$a_3$
5346	41 Nb	L	$\beta_6$	6095	15 P	K	$a_4$	7083	14 Si	K	$a'$
5361	16 S	K	$a_1$	6102	15 P	K	$a_3$	7109	14 Si	K	$a_1$
5364	16 S	K	$a_2$	6123	74 W	M	$M_3N_4$	7238	73 Ta	M	$M_1N_1$
5365	74 W	M	$M_4N_4$	6142	15 P	K	$a_1$	7273	37 Rb	L	$a_3$
5372	42 Mo	L	$a_3$	6195	41 Nb	L	$\eta$	7303	37 Rb	L	$a_1$
5373	40 Zr	L	$\gamma_1$	6198	39 Y	L	$\beta_1$	7349	74 W	M	$M_3N_7$
5394	42 Mo	L	$a_1$	6223	77 Ir	M	$a''$	7505	38 Sr	L	$\eta$
5400	42 Mo	L	$a_2$	6233	76 Os	M	$\beta''$	7560	71 Lu	M	$\beta''$
5427	81 Tl	M	$a''$	6250	77 Ir	M	$M_1N_1$	7582	71 Lu	M	$M_2N_2$
5439	80 Hg	M	$M_2N_2$	6256	76 Os	M	$M_2N_2$	7787	71 Lu	M	$a'$
5443	81 Tl	M	$M_1N_1$	6264	79 Au	M	$M_3N_7$	7803	71 Lu	M	$a''$
5480	41 Nb	L	$\beta_1$	6271	74 W	M	$M_4N_7$	7820	71 Lu	M	$M_1N_1$
5481	40 Zr	L	$\gamma_5$	6279	38 Sr	L	$\gamma_5$	7821	38 Sr	L	$l$
5484	77 Ir	M	$M_3N_3$	6301	73 Ta	M	$M_3N_3$	7852	70 Yb	M	$\beta'$
5525	83 Bi	M	$M_3N_7$	6350	38 Sr	L	$\beta_3$	7870	70 Yb	M	$\beta''$
5573	40 Zr	L	$\beta_2$	6386	38 Sr	L	$\beta_4$	7891	70 Yb	M	$M_2N_2$
5607	74 W	M	$M_3O_5$	6407	39 Y	L	$a_3$	7941	13 Al	K	$\beta_1$
5618	40 Zr	L	$\beta_3$	6435	39 Y	L	$a_1$	8011	70 Yb	M	$a''$
5619	79 Au	M	$M_2N_2$	6459	76 Os	M	$a''$	8012	77 Ir	M	$M_1N_5$
5629	38 Sr	L	$\gamma_2$	6481	76 Os	M	$M_1N_1$	8025	13 Al	K	$\beta_3$
5649	80 Hg	M	$M_1N_1$	6498	83 Bi	M	$M_1N_5$	8029	37 Rb	L	$\eta$
5652	76 Os	M	$\gamma'$	6503	38 Sr	L	$\beta_6$	8090	70 Yb	M	$a'$
5653	40 Zr	L	$\beta_4$	6509	41 Nb	L	$l$	8108	35 Br	L	$\beta_1$

$\lambda, 10^{11}$	Element.	Series.	Line.	$\lambda, 10^{11}$	Element.	Series.	Line.	$\lambda, 10^{11}$	Element.	Series.	Line.
8125	70 Yb	<i>M</i>	$M_1N_1$	9323	66 Dy	<i>M</i>	$M_2N_2$	11781	11 Na	<i>K</i>	$a_4$
8189	13 Al	<i>K</i>	$a_6$	9394	33 As	<i>L</i>	$\beta_1$	11802	11 Na	<i>K</i>	$a_3$
8206	13 Al	<i>K</i>	$a_5$	9397	90 Th	<i>N</i>	$N_7P_1$	11835	11 Na	<i>K</i>	$a'$
8253	13 Al	<i>K</i>	$a_4$	9509	66 Dy	<i>M</i>	$a$	11884	11 Na	<i>K</i>	$\beta_1$
8265	13 Al	<i>K</i>	$a_3$	9535	12 Mg	<i>K</i>	$\beta_1$	11951	30 Zn	<i>L</i>	$\beta_1$
8286	13 Al	<i>K</i>	$a'$	9617	33 As	<i>L</i>	$a_3$	11990	30 Zn	<i>L</i>	$\beta_1$
8319	13 Al	<i>K</i>	$a_1$	9619	92 U	<i>N</i>	$N_7O_3$	12250	30 Zn	<i>L</i>	$a_1$
8326	35 Br	<i>L</i>	$a_3$	9647	12 Mg	<i>K</i>	$\beta_3$	12250	92 U	<i>N</i>	$N_5P_3$
8357	35 Br	<i>L</i>	$a_1$	9650	33 As	<i>L</i>	$a_1$	12874	92 U	<i>N</i>	$N_5O_1$
8549	74 W	<i>M</i>	$M_2N_5$	9712	12 Mg	<i>K</i>	$a_6$	13100	29 Cu	<i>L</i>	$\beta_1$
8573	68 Er	<i>M</i>	$M_2N_2$	9730	12 Mg	<i>K</i>	$a_5$	13149	90 Th	<i>N</i>	$N_5P_3$
8691	92 U	<i>N</i>	$N_7P_1$	9786	12 Mg	<i>K</i>	$a_4$	13208	83 Bi	<i>N</i>	$N_7P_1$
8717	34 Se	<i>L</i>	$\beta_1$	9799	12 Mg	<i>K</i>	$a_3$	13390	29 Cu	<i>L</i>	$a_1$
8783	68 Er	<i>M</i>	$M_1N_1$	9827	12 Mg	<i>K</i>	$a'$	13805	90 Th	<i>N</i>	$N_5O_1$
8919	67 Ho	<i>M</i>	$\beta''$	9868	12 Mg	<i>K</i>	$a_1$	14330	28 Ni	<i>L</i>	$\beta$
8939	34 Se	<i>L</i>	$a_3$	10030	90 Th	<i>N</i>	$N_7O_3$	14650	28 Ni	<i>L</i>	$a$
8943	67 Ho	<i>M</i>	$M_2N_2$	10385	92 U	<i>N</i>	$N_6O_2$	15800	27 Co	<i>L</i>	$\beta$
8948	74 W	<i>M</i>	$M_2N_6$	10413	32 Ge	<i>L</i>	$a_1$	16070	27 Co	<i>L</i>	$a$
8971	34 Se	<i>L</i>	$a_1$	11046	90 Th	<i>N</i>	$N_6O_2$	17330	26 Fe	<i>L</i>	$\beta$
9150	67 Ho	<i>M</i>	$M_1N_1$	11591	11 Na	<i>K</i>	$\beta_1$	17660	26 Fe	<i>L</i>	$a$





## BIBLIOGRAPHY.

### Before 1916.

- BARKLA, C. G., and G. H. MARTYN : The Photographic Effect of X-rays and X-ray Spectra. *Phil. Mag.* (6) 25, p. 296. 1913.
- BARKLA, C. G., and G. H. MARTYN : Interference of Röntgen Radiation. *Proc. Phys. Soc.* 25, p. 206. 1913.
- BARNES, J. : The High-Frequency Spectrum of Tungsten. *Phil. Mag.* (6) 30, p. 368. 1915.
- BRAGG, W. H. : The Reflexion of X-rays by Crystals. II. *Proc. Roy. Soc.* 89 A, p. 246. 1914.
- BRAGG, W. H. : The Influence of the Constituents of the Crystal on the Form of the Spectrum in the X-ray Spectrometer. *Proc. Roy. Soc.* 89 A, p. 430. 1914.
- BRAGG, W. H. : The X-ray Spectra given by Crystals of Sulphur and Quartz. *Proc. Roy. Soc.* 89 A, p. 575. 1914.
- BRAGG, W. H., and W. L. BRAGG : The Reflexion of X-rays by Crystals. *Proc. Roy. Soc.* 88 A, p. 428. 1913.
- DE BROGLIE, M. : Sur une nouveau procédé permettant d'obtenir la photographie des spectres de raies des rayons Röntgen. *Comptes Rendus*, 157, p. 924. 1913.
- DE BROGLIE, M. : Über eine Methode, die Spektre der Röntgenstrahlen zu photographieren. *Verhandl. d. dtsh. physik. Ges.* 15, p. 1348. 1913.
- DE BROGLIE, M. : Sur l'obtention des spectres des rayons de Röntgen par simple passage des rayons incidents au travers de feuilles minces. *Comptes Rendus*, 158, p. 333. 1914.
- DE BROGLIE, M. : Sur la spectroscopie des rayons secondaires émis hors des tubes à rayons de Röntgen, et les spectres d'absorption. *Comptes Rendus*, 158, p. 1493. 1914.
- DE BROGLIE, M. : Sur la spectrographie des rayons de Röntgen. *Journ. de physique* (5) 4, p. 101. 1914.
- DE BROGLIE, M. : Sur les spectres des rayons de Röntgen, rayons émis par des anticathodes de cuivre, de fer, d'or. *Comptes Rendus*, 158, pp. 623, 907. 1914.
- DE BROGLIE, M. : Sur l'analyse spectrale directe par les rayons secondaires des rayons de Röntgen. *Comptes Rendus*, 158, p. 1785. 1914.
- DE BROGLIE, M. : Sur les spectres des rayons X secondaires homogènes. *Comptes Rendus*, 160, p. 798. 1915.
- DE BROGLIE, M., and F. A. LINDEMANN : Einige Bemerkungen über Röntgenstrahlenspektren. *Verhandl. d. dtsh. physik. Ges.* 16, p. 100. 1914.
- DE BROGLIE, M., and F. A. LINDEMANN : Observations fluoroscopiques par vision direct des spectres des rayons de Röntgen. *Comptes Rendus*, 158, p. 180. 1914.
- DE BROGLIE, M., and F. A. LINDEMANN : Sur un nouveau procédé permettant d'obtenir très rapidement les spectres des rayons de Röntgen. *Comptes Rendus*, 158, p. 944. 1914.

- DE BROGLIE, M., and F. A. LINDEMANN: Sur les spectres des rayons de Röntgen obtenus au moyen de lames de mica. *Journ. de physique*, (5) 4, p. 265. 1914.
- CABRERA, B.: The Spectrum of X-rays. *Nature*, 96, p. 144. 1915.
- FRIEDRICH, W.: Eine neue Interferenzerscheinung bei Röntgenstrahlen. *Physikal. Zeitschr.* 14, p. 317. 1913.
- GLAGOLEW, M.: Sur le spectre des rayons X secondaires homogènes. *Comptes Rendus*, 160, p. 709. 1915.
- GLOCKER, R.: Experimenteller Beitrag zur Interferenz der Röntgenstrahlen II. *Physikal. Zeitschr.* 15, p. 401. 1914.
- HERWEG, J.: Über das Spektrum der Röntgenstrahlen. *Verhandl. d. dtsh. physik. Ges.* 15, p. 555. 1913.
- HERWEG, J.: Über das Spektrum der Röntgenstrahlen. Zweite Mitteilung. Ein Spektrograph für Röntgenstrahlen; die Linien des Platins und Wolframs. *Verhandl. d. dtsh. physik. Ges.* 16, p. 73. 1914.
- HUPKA, E.: Über den Durchgang von Röntgenstrahlen durch Metalle. *Physikal. Zeitschr.* 14, p. 623. 1913.
- JAUNCEY, G. E. M.: X-ray Spectra. *Nature*, 93, p. 214. 1914.
- KEENE, H. B.: On the Transmission of X-Rays through Metals. *Phil. Mag.* (6) 26, p. 712. 1913. *Physikal. Zeitschr.* 14, p. 903. 1913.
- KNIPPING, P.: Durchgang von Röntgenstrahlen durch Metalle. Bemerkung zur Veröffentlichung des Herrn Hupka. *Physikal. Zeitschr.* 14, p. 996. 1913.
- MALMER, IVAR: The High-Frequency Spectra of the Elements. *Phil. Mag.* (6) 28, p. 787. 1914.
- MALMER, IVAR: Untersuchungen über die Hochfrequenz-Spektren der Elemente. Diss. Lund, 1915.
- MOSELEY, H. G. J.: The High-Frequency Spectra of the Elements. *Phil. Mag.* (6) 26, p. 1024. 1913.
- MOSELEY, H. G. J.: The High-Frequency Spectra of the Elements. Part II. *Phil. Mag.* (6) 27, p. 703. 1914.
- MOSELEY, H. G. J. and C. G. DARWIN: The Reflexion of the X-rays. *Phil. Mag.* (6) 26, p. 210. 1913.
- NISHIKAWA, S., and S. ONO: Transmission of X-rays through Fibrous, Lamellar and Granular Substances. *Proc. of Tokyo Math.-Phys. Soc.* (2) 7, p. 131. 1913.
- NISHIKAWA, S.: On the Spectra of X-Rays Obtained by Means of Lamellar or Fibrous Substances. *Proc. of Tokyo Math.-Phys. Soc.* (2) 7, p. 296. 1914.
- RAWLINSON, F. W.: A Note on the X-Ray Spectrum of Nickel. *Phil. Mag.* (6) 28, p. 274. 1914.
- ROHMANN, H.: Ein Röntgenspektroskop. *Physikal. Zeitschr.* 15, p. 510. 1914.
- ROHMANN, H.: Die Röntgenspektren einiger Metalle. *Physikal. Zeitschr.* 15, p. 715. 1914.
- RUTHERFORD and E. N. DA C. ANDRADE: The Wave-length of the Soft  $\gamma$ -Rays from Radium B. *Phil. Mag.* (6) 27, p. 854. 1914.
- RUTHERFORD and ANDRADE: The Spectrum of the Penetrating  $\gamma$ -Rays from RaB and RaC. *Phil. Mag.* 28, p. 263. 1914.
- RUTHERFORD, E., and J. BARNES: Efficiency of Production of X-rays from a Coolidge Tube. *Phil. Mag.* (6) 30, p. 361. 1915.
- RUTHERFORD, E., J. BARNES and H. RICHARDSON: Maximum Frequency of the X-rays from a Coolidge Tube for Different Voltages. *Phil. Mag.* (6) 30, p. 339. 1915.
- RUTHERFORD, E., and H. RICHARDSON: Analysis of the  $\gamma$ -Rays of the Thorium and Actinium Products. *Phil. Mag.* 26, p. 937. 1913. (Uses the absorption method; gives a conspectus of the various radiations.)
- SIEGBAHN, MANNE: Undersökningar öfver Röntgenstrålspektra. *Arkiv för Mat., Astr. och Fysik*, 10, N:o 1. 1914.
- SIEGBAHN, M.: Ein neues Röntgenröhr für spektroskopische Zwecke. *Verhandl. d. dtsh. physik. Ges.* 17, p. 469. 1915.

- WAGNER, E. : Experimenteller Beitrag zur Interferenz der Röntgenstrahlen, nach Versuchen gemeinsam mit R. Glocker. *Physikal. Zeitschr.* 14, p. 1232. 1913.
- WAGNER, E. : Das Röntgenspektrum des Platins. *Physikal. Zeitschr.* 16, p. 30. 1915.
- WAGNER, E. : Spektraluntersuchungen an Röntgenstrahlen. I. *Ann. d. Physik* (4) 46, p. 868. 1915.
- 1916.
- BARKLA, C. G. : On the X-rays and the Theory of Radiation. *Proc. Roy. Soc.* (A) 92, p. 501. 1916.
- BARKLA, C. G. : Note on Experiments to detect Refraction of X-rays. *Phil. Mag.* (6) 31, p. 257. 1916.
- BARKLA, C. G., and J. G. DUNLOP : Note on the Scattering of X-rays and Atomic Structure. *Phil. Mag.* (6) 31, p. 222. 1916.
- BROGLIE, M. DE : Sur les radiations extrêmement pénétrants appartenant à la série K du tungstène et sur les spectres des rayons X des métaux lourds. *Comptes Rendus*, 162, p. 596. 1916.
- BROGLIE, M. DE : Sur la bande d'absorption K des éléments pour les rayons X suivie du brom au bismuth et l'émission d'un tube Coolidge vers les très courtes longueurs d'onde. *Comptes Rendus*, 163, p. 87. 1916.
- BROGLIE, M. DE : Sur un système de bandes d'absorption correspondant aux rayons L des spectres de rayons X. *Comptes Rendus*, 163, p. 352. 1916. *Journ. de physique*, 1916, p. 161.
- CERMAK, P. : Über Röntgenspektren, die an gekrümmten Krystallflächen erzeugt werden. *Physikal. Zeitschr.* 17, pp. 405 and 556. 1916.
- COMPTON, A. H. : A Recording X-ray Spectrometer and the High Frequency Spectrum of Tungsten. *Phys. Rev.* 7, p. 646. 1916.
- COMPTON, A. H. : The X-ray Spectrum of Tungsten. *Phys. Rev.* 7, p. 498. 1916.
- FRIMAN, E. : Untersuchungen über die Hochfrequenzspektren (L-Reihe) der Elemente. Diss. Lund. 1916.
- FRIMAN, E. : On the High-frequency Spectra (L series) of the elements Lutecium to Zinc. *Phil. Mag.* (6) 32, p. 497. 1916.
- GLOCKER, R. : Über die Absorption der Röntgenstrahlung durch die Kristalle von der Reihe der Elemente der L-Reihe. *Physikal. Zeitschr.* 17, p. 488. 1916.
- GOUY, J. : Sur la catoptrique des rayons X et son application à un spectrographe à foyers réels. *Ann. de Phys.* (9) 5, p. 241. 1916.
- GORTON, W. S. : The X-ray Spectrum of Tungsten. *Phys. Rev.* 7, p. 203. 1916.
- HULL, A. W., and M. RICE : The Law of Absorption of X-rays at High Frequencies. *Phys. Rev.* (2) 8, p. 326. 1916.
- HULL, A. W., and M. RICE : The High-Frequency Spectrum of Tungsten. *Journ. of Franklin Inst.* 182, p. 403. 1916.
- KOSSEL, W. : Bemerkungen zum Seriencharakter der Röntgenspektren. *Verhandl. d. dtsh. physik. Gesellsch.* pp. 339 and 396. 1916.
- LEDoux-LEBARD, R., et A. DAUVILLIER : La série K des rayons X et l'excitation des rayons X au point de vue de la théorie des spectres. *Comptes Rendus*, 163, p. 754. 1916.
- MILLER, C. D. : The Absorption Coefficients of Soft X-rays. *Phys. Rev.* (2) 8, p. 329. 1916.
- SCHOTTKY, W. : Bemerkungen zu den Gesetzen von Kossel und Glocker über Absorption und Emission von Röntgenstrahlung. *Physikal. Zeitschr.* 17, p. 581. 1916.
- SEEMAN, H. : Röntgenspektroskopische Methoden ohne Spalt. *Ann. de Phys.* (4) 49, p. 470. 1916.
- SEEMAN, H. : Zur Optik der Reflexion von Röntgenstrahlen an Krystallspaltflächen. I. *Ann. de Phys.* (4) 51, p. 391. 1916.

- SIEGBAHN, M.: Über das primäre Hochfrequenzspektrum des Jods und des Tellurs. *Verhandl. d. dtsh. physik. Ges.* 18, p. 39. 1916.
- SIEGBAHN, M.: Über eine neue Serie (I-Reihe) in den Hochfrequenzspektren der Elemente. *Verhandl. d. dtsh. physik. Ges.* 18, p. 150. 1916.
- SIEGBAHN, M.: Sur l'existence d'un nouveau groupe de lignes (série M) dans les spectres de haute fréquence. *Comptes Rendus*, 162, p. 787. 1916.
- SIEGBAHN, M.: Über eine weitere Reihe (M-Reihe) in den Hochfrequenzspektren der Elemente. *Verhandl. d. dtsh. physik. Ges.* 18, p. 278. 1916.
- SIEGBAHN, M., und E. FRIMAN: Über die Hochfrequenzspektren der Elemente Gold bis Uran. *Physikal. Zeitschr.* 17, p. 17. 1916.
- SIEGBAHN, M., und E. FRIMAN: Über die Hochfrequenzspektren der Elemente As bis Rh. *Ann. d. Physik.* (4) 49, p. 611. 1916.
- SIEGBAHN, M., und E. FRIMAN: Über die Hochfrequenzspektren (L-Reihe) der Elemente Tantal bis Wismut. *Ann. d. Physik.* 1916.
- SIEGBAHN, M., und E. FRIMAN: Über die Hochfrequenzspektren (L-Reihe) der Elemente Polonium, Radium, Thor und Uran. *Physikal. Zeitschr.* 17, p. 61. 1916.
- SIEGBAHN, M., und E. FRIMAN: Über einen Vakuum-Spektrographen zur Aufnahme von Hochfrequenzspektren und eine mit demselben durchgeführte vorläufige Untersuchung. *Physikal. Zeitschr.* 17, p. 176. 1916.
- SIEGBAHN, M., und W. STENSTRÖM: Über die Hochfrequenzspektren (K-Reihe) der Elemente Cr bis Ge. *Physikal. Zeitschr.* 17, p. 48. 1916.
- SIEGBAHN, M., und E. FRIMAN: On the High-Frequency Spectra of the Elements Au to U. *Phil. Mag.* 31, p. 403. 1916.
- SIEGBAHN, M., und W. STENSTRÖM: Die Röntgenspektren der Elemente Na bis Cr. *Physikal. Zeitschr.* 17, p. 318. 1916.
- SWINNE, R.: Zum Ursprung der  $\gamma$ -Strahlenspektren und Röntgenstrahlenserien. *Physikal. Zeitschr.* 17, p. 481. 1916.
- WAGNER, E.: Scatteringmessungen an Röntgenstrahlen. II. *Ber. d. k. Bayr. Akad. Mat.* 1916.
- WAGNER, E.: Über vergleichende Raumgittermessungen an Steinsalz und Sylvin mittels homogener Röntgenstrahlen und über deren exakte Wellenlängenbestimmung. *Ann. d. Physik.* 1, 49, p. 625. 1916.
- WEBSTER, D. L.: The Emission Quanta of Characteristic X-rays. *Proc. Nat. Acad. Sc. (U.S.A.)* 2, p. 90. 1916.
- WEBSTER, D. L.: Experiments on the Emission Quanta of Characteristic X-rays. *Phys. Rev.* (2) 7, pp. 403, 599. 1916.
- WEBSTER, D. L., and H. CLARK: A Test for X-ray Refraction made with Monochromatic Rays. *Phys. Rev.* (2) 8, p. 528. 1916.
- ZOBEL, O. J.: A Note on the Spectrum of Röntgen Rays. *Phys. Rev.* 7, p. 580. 1916.

## 1917.

- BARKLA, C. G., and M. P. WHITE: Notes on the Absorption and Scattering of X-rays and the Characteristic Radiations of J-series. *Phil. Mag.* (6) 34, p. 270. 1917.
- BLAKE and W. DUANE: The Absorption Bands of some of the Elements. *Phys. Rev.* 10, p. 1. 1917.
- BRAININ, C. I.: An Experimental Investigation of the Total Emission of X-rays from Certain Metals. *Phys. Rev.* 10, p. 461. 1917.
- BRENTANO, J.: Recherches spectrales sur les rayons X. *Arch. sc. phys. et nat.* 44, p. 469. 1917.
- BRENTANO, J.: Monochromateur pour rayons X. *Ibid.* 44, p. 66. 1917.
- COMPTON, A. H.: The Reflexion Coefficient of Monochromatic X-rays from Rock-salt and Calcite. *Phys. Rev.* 10, p. 95. 1917.
- COMPTON, A. H.: The Intensity of X-ray Reflexion and the Distribution of the Electrons in Atoms. *Phys. Rev.* 9, p. 29. 1917.

- DADOURIAN, H. M. : On the Production of Soft X-rays by Slow-moving Electrons. *Phys. Rev.* 9, p. 563. 1917.
- GLOCKER, R. : Die Messmethoden der Röntgenstrahlen. *Physikal. Zeitschr.* 18, pp. 302, 330. 1917.
- ISHIWARA, J. : Relations between the Spectra of X-rays. *Nature*, 99, p. 424. 1917.
- KAYE, G. W. C. : The Composition of the X-rays from Various Metals. *Proc. Roy. Soc. (A)* 93, p. 427. 1917.
- KOSSEL W. : Zum Ursprung der  $\gamma$ -Strahlenspektren und Röntgenstrahlenserien. *Physikal. Zeitschr.* 18, p. 240. 1917.
- LANG, M. : Untersuchung über die Absorption harter Röntgenstrahlen in Gasen. *Ann. d. Physik.* (4) 53, pp. 279, 337. 1917.
- LEDoux-LEBARD, R., et A. DAUVILLIER : Contribution à l'étude des séries L des éléments de poids atomique élevé. *Comptes Rendus*, 164, p. 687. 1917.
- LILLENFELD, J. E. : Einige Messungen an Röntgenstrahlen. *Fortschr. a. d. Geb. d. Röntgenstr.* 25, p. 77. 1917.
- MÜLLER, A. : Notiz, betr. die Emission sekundärer Röntgenstrahlen. *Verhandl. d. physik. Ges.* 19, p. 48. 1917.
- MÜLLER, A. : Tube à rayons X pour recherches de laboratoire. *Arch. sc. phys. et nat.* 44, pp. 89, 220. 1917.
- RAUSCH VON TRAUBENBERG, H. : Eine Röntgenröhre für physikalische Zwecke. *Physikal. Zeitschr.* 18, p. 241. 1917.
- RUTHERFORD, E. : Penetrating Power of the X-radiation from a Coolidge Tube. *Phil. Mag.* 34, p. 153. 1917.
- SEEMANN, H. : Zur Optik der Reflexion der Röntgenstrahlen an Krystallstrukturflächen. II. *Ann. d. Physik.* (4) 53, p. 461. 1917.
- SEEMANN, H. : Die Vermeidung der Verbreiterung der Röntgenspektallinien infolge der Tiefe der wirksamen Schicht. *Physikal. Zeitschr.* 18, p. 212. 1917.
- SIEGBAHN, M. : Sur les spectres de haute fréquence. *Comptes Rendus*, 165, p. 59. 1917.
- SIEGBAHN, M., und W. STENSTRÖM : Über die Röntgenspektren der isotopischen Elemente. *Physikal. Zeitschr.* 18, p. 547. 1917.
- UHLER, H. S. : On Moseley's Law for X-ray Spectra. *Phys. Rev.* 9, p. 562. 1917.
- UHLER, H. S. : Critical Examination of the Law of X-ray Line Spectra. *Phys. Rev.* 9, p. 325. 1917.
- UHLER, H. S., and C. D. COOKSEY : The K-Series of the X-ray Spectrum of Gallium. *Phys. Rev.* 10, p. 645. 1917.
- WAGNER, E. : Über Röntgenspektroskopie. *Physikal. Zeitschr.* 18, pp. 405, 432, 461, 488. 1917.
- WEBSTER, D. L. : X-ray Emissivity as a Function of Cathode Potential. *Phys. Rev.* 9, p. 220. 1917.
- WEBSTER, D. L., and H. CLARK : Intensities of X-rays of the L-Series as a Function of Voltage. *Phys. Rev.* 9, p. 571. 1917.
- VEGARD, L. : Über die Erklärung der Röntgenspektren. *Verhandl. d. physik. Ges.* 19, p. 328. 1917.
- VEGARD, L. : Der Atombau auf Grundlage der Röntgenspektren. *Verhandl. d. physik. Ges.* 19, p. 344. 1917.
- WEEKS, P. T. : A Determination of the Efficiency of Production of X-rays. *Phys. Rev.* 10, p. 564. 1917.

## 1918.

- COMPTON, A. H. : Note on the Grating Space of Calcite and the X-ray Spectrum of Gallium. *Phys. Rev.* 11, p. 430. 1918.
- DAVIS, B. : Characteristic X-ray Emission as a Function of the Applied Voltage. *Phys. Rev.* 11, p. 433. 1918.
- DERSCHEM, E. : Wave-lengths of the Tungsten X-ray Spectrum. *Phys. Rev.* 11, p. 461. 1918.

- DUANE, W., and KANG-FU-HU: On the Critical Absorption and Characteristic Emission X-ray Frequencies. *Phys. Rev.* 11, p. 489. 1918.
- DUANE, W., and KANG-FU-HU: On the Relation between the K-Series and the Atomic Numbers of the Chemical Elements. *Phys. Rev.* 11, p. 488. 1918.
- DUANE, W., and T. SHIMIZU: The Relation between the General X-radiation and the Atomic Number of the Target. *Phys. Rev.* 11, p. 491. 1918.
- GLOCKER, R.: Absorptionsgesetze für Röntgenstrahlen. *Physikal. Zeitschr.* 19, p. 66. 1918.
- LILIENTFELD, J. E., und H. SEEMANN: Photographische Aufnahme des Pt- und Ir-K-Spektrums. *Physikal. Zeitschr.* 19, p. 269. 1918.
- RICHARDSON, O. W.: The Photoelectric Action of X-rays. *Proc. Roy. Soc. (A)* 94, p. 269, 1918.
- STENSTRÖM, W.: Experimentelle Untersuchungen der Röntgenspektren, M-Reihe. *Ann. d. Physik.* (4) 57, p. 347. 1918.
- ULREY, C. T.: An Experimental Investigation of the Energy in the Continuous X-ray Spectrum of Certain Elements. *Phys. Rev.* 11, p. 401. 1918.
- VEGARD, L.: The X-ray Spectra and the Constitution of the Atom. *Phil. Mag.* 35, p. 293. 1918.

## 1919.

- BROGLIE, M. DE: Sur le spectre de rayons X du tungstène. *Comptes Rendus.* 169, p. 962. 1919.
- BROGLIE, M. DE: Sur le spectre d'absorption L du radium. *Comptes Rendus.* 168, p. 854. 1919.
- BROGLIE, M. DE: Sur les spectres des rayons X des éléments. *Comptes Rendus.* 169, p. 134. 1919. *Journ. de Phys.* 31. 1919.
- BRUNETTI, R.: La legge di eccitazione dei raggi X caratteristici primari. *Nuovo Cim.* 18, p. 266. 1919.
- COMPTON, A. H.: The Law of Absorption of High Frequency Radiation. *Phys. Rev.* 13, p. 296. 1919.
- DADOURIAN, H. M.: Soft X-rays. *Phys. Rev.* 14, p. 234. 1919.
- DESSAUER, F., und E. BACK: Über Röntgenstrahlung mit sehr hohen Spannungen. *Verhandl. d. deutsch. phys. Gesellsch.* 1919.
- DAVIS, B.: Note on a Method of Measuring the Decrease of Velocities in Thin Films by Means of Characteristic X-rays. *Phys. Rev.* 14, p. 539. 1919.
- DUANE, W., and KANG-FU-HU: On the Critical Absorption and Characteristic Emission X-ray Frequencies. *Phys. Rev.* 14, p. 369. 1919.
- DUANE, W., and KANG-FU-HU: On the X-ray Absorption Frequencies characteristic of the Chemical Elements. *Phys. Rev.* 14, pp. 516, 522. 1919.
- DUANE, W., and T. SHIMIZU: On the X-ray Absorption Wave-lengths of the Lead-Isotopes. *Proc. Nat. Acad. Sc. (U.S.A.)* 5, p. 198. 1919.
- DUANE, W., and T. SHIMIZU: On the Spectrum of X-rays from an Aluminium Target. *Phys. Rev.* 14, p. 389. 1919.
- DUANE, W., and T. SHIMIZU: Are the Frequencies in the K Series of X-rays the highest Frequencies characteristic of Chemical Elements? *Phys. Rev.* 13, p. 289. 1919.
- DUANE, W., and T. SHIMIZU: On the Relation between the K Series and the L Series of X-rays. *Phys. Rev.* 14, p. 67. 1919.
- DUANE, W., and T. SHIMIZU: The Relation between the Intensity of General X-radiation and the Atomic Number of the Anticathode. *Phys. Rev.* 14, p. 525. 1919.
- FRICKE, H.: Röntgenstrahlens Betydning for den kvantitative kemiske Analyse. (The significance of Röntgen rays in quantitative chemical analysis.) *Fys. Tidsskr.* 18, p. 80. 1919-1920.
- FRIEDRICH, W., und H. SEEMAN: Eine neue Röntgenspektroskopische Methode. *Physikal. Zeitschr.* 20, p. 55. 1919.
- GLOCKER, R.: Eine neue Messmethode zur Bestimmung der Zusammensetzung von Röntgenstrahlungen. *Fortschr. a. d. phys. Wiss.* 26, p. 363. 1919.

- LEDoux-LEBARD, R., et A. DAUVILLIER: Sur la structure spectrale des rayons J. *Comptes Rendus*, 168, p. 608. 1919.
- LILIENTFELD, J. E.: Die Hochvakuumröntgenröhren. *Jahrb. d. Rad.* 16, p. 105. 1919.
- MÜLLER, A.: Recherches sur les spectres des rayons X. *Arch. sc. phys. et nat.* 1, p. 127. 1919.
- OVERN, O. B.: The L Series in the Tungsten X-ray Spectrum. *Phys. Rev.* 14, p. 137. 1919.
- SANFORD, T.: Formula for the Wave-lengths of M Radiation. *Phys. Rev.* 14, p. 275. 1919.
- SANFORD, T.: Some Nuclear Charges calculated for L Radiation. *Phys. Rev.* 14, p. 177. 1919.
- SEEMAN, H.: Vollständige Spektraldiagramme von Krystallen. *Physikal. Zeitschr.* 20, p. 169. 1919.
- SEEMAN, H.: Über die Ökonomie der röntgenspektroskopischen Methoden. *Physikal. Zeitschr.* 20, p. 51. 1919.
- SIEGBAHN, M.: Über das Röntgenspektrum von Wolfram. *Physikal. Zeitschr.* 20, p. 533. 1919.
- SIEGBAHN, M.: Precision Measurements in the X-ray Spectra. *Phil. Mag.* (6) 37, p. 601; 38, p. 639; 38, 647. 1919.
- SIEGBAHN, M.: Präzisionsmessungen. 1. Mitteilung. *Ann. d. Physik*, 5, . . . . .
- SIEGBAHN, M., und E. Jönsson: Über die Absorptionsgrenzfrequenzen der Röntgenstrahlen bei den schweren Elementen, besonders bei den seltenen Erden. *Physikal. Zeitschr.* 20, p. 251. 1919.
- SMEKAL, A.: Zur Theorie der Röntgenspektren. *Wien. Anz.* 126. 1919.
- SMEKAL, A.: Bohrsche Theorie der Röntgenlinienspektren. *Verhandl. d. dtsch. physik. Ges.* . . . . .
- STENSTRÖM, W.: Experimentelle Untersuchungen der Röntgenspektren. *Diss.* Lund, 1919.
- WAGNER, E.: Bericht über das kontinuierliche Röntgenspektren. *Jahrbuch der Radioakt.* 16, p. 190. 1919.
- WEBSTER, D. L.: The Origin of the General Radiation Spectrum of X-rays. *Phys. Rev.* 13, p. 303. 1919.
- WOOTEN, B. A.: Energy of the Characteristic X-ray Emission from Molybdenum and Palladium as a Function of Applied Voltage. *Phys. Rev.* 13, p. 71. 1919.
- VEGARD, L.: On the X-ray Spectra and the Constitution of the Atom. II. *Phil. Mag.* 37, p. 237. 1919.
- VEGARD, L.: Über die Röntgenstrahlung und die Konstitution der Atome I, II. *Physikal. Zeitschr.* 20, . . . . . 1919.

## 1920.

- AURÉN, T. E.: The Absorption of X-rays. *Medd. Nobel Inst.* 4, No. 3. 1920.
- AURÉN, T. E.: Scattering and Absorption of Hard X-rays in the Lightest Elements. *Medd. Nobel Inst.* 4, No. 5. 1920.
- BEHNKEN, H.: Ein Beitrag zur Kenntnis des kontinuierlichen Röntgenspektrums. *Zeitschr. f. Phys.* 3, p. 48. 1920.
- BERGENGREN, J.: Über die Röntgenabsorption des Phosphors. *Zeitschr. f. Phys.* 3, p. 247. 1920.
- BERGENGREN, J.: Sur les spectres d'absorption du phosphore pour les rayons X. *Comptes Rendus*, 171, p. 624. 1920.
- BIRGE: The Mathematical Structure of X-ray Spectra. *Phys. Rev.* 16, p. 371. 1920.
- BRILLOUIN, L.: Le spectre continu des rayons X. *Comptes Rendus*, 170, p. 274. 1920.
- BROGLIE, M. DE, and DAUVILLIER: Sur la structure fine des discontinuités d'absorption dans les spectres des rayons X. *Comptes Rendus*, 171, 626-627. 1920.

- BROGLIE, LOUIS DE : Sur l'absorption des rayons de Röntgen par la matière. *Comptes Rendus*, 171, pp. 1137-1139. 1920.
- BROGLIE, M. DE : Sur la structure fine des spectres de rayons X. *Comptes Rendus*, 170, pp. 1245, 1344. 1920.
- BROGLIE, LOUIS DE : Sur le calcul de fréquences limites d'absorption K et L des éléments lourds. *Comptes Rendus*, 170, p. 585. 1920.
- BROGLIE, M. DE : Sur les bandes K d'absorption des terres rares pour les rayons X. *Comptes Rendus*, 170, p. 725. 1920.
- BROGLIE, M. DE : Sur les propriétés des écrans renforceurs vis-à-vis des spectres de rayons X et sur un dédoublement de la ligne bêta du spectre K du tungstène. *Comptes Rendus*, 170, p. 1053. 1920.
- BULAYAUD, F. : La loi de masse de l'absorption des rayons Röntgen. *Ann. de Phys.* (9) 13, p. 161. 1920.
- COOKSEY, C. D. : A New Design of Precision X-ray Spectrometer. *Phys. Rev.* 16, p. 305. 1920.
- COOKSEY, C. D., and D. COOKSEY : The High Frequency Spectra of Lead Isotopes. *Phys. Rev.* 16, pp. 327-336. 1920.
- DADOURIAN, H. M. : Soft X-rays, A Note of Interpretation. *Phys. Rev.* 16, pp. 481-485. 1922.
- DAUVILLIER, A. : Recherches spectrométriques sur les rayons X. *Ann. d. Phys.* (9) 13, p. 49. 1920.
- DAVIS, B. : Intensity of Emission of X-rays and their Reflexion from Crystals. *Bull. Nat. Res. Council.* 1, pp. 409-427. 1920.
- DESSAUER, FR., und FR. VIERHELLER : Versuche über Zerstreung von Röntgenstrahlen. 86. Naturf.-Vers. Bad Nauheim. 1920. *Physikal. Zeitschr.* 21, pp. 571-572. 1920.
- DUANE, W., and PATTERSON : On the Absorption of X-rays by Chemical Elements of High Atomic Numbers. *Phys. Rev.* 15, pp. 546-547. 1920.
- DUANE, W., and R. A. PATTERSON : On the X-ray Spectrum of Tungsten. *Phys. Rev.* (2) 15, p. 328 ; 16, pp. 526-539. 1920.
- DUANE, W., and R. A. PATTERSON : Characteristic Absorption of X-rays : L Series. *Proc. Nat. Acad. Sc. (U.S.A.)* (6), p. 509. 1920.
- DUANE, W., and R. A. PATTERSON : On the Relative Positions and Intensities of Lines in X-ray Spectra. *Proc. Nat. Acad. Sc. (U.S.A.)* (6), p. 518. 1920.
- DUANE, W., and W. STENSTROM : On the K Series of X-rays. *Phys. Rev.* (2) 15, pp. 328-330. 1920.
- DUANE, FRICKE and STENSTRÖM : The Absorption of X-rays by Chemical Elements of High Atomic Numbers. *Proc. Nat. Acad. Sc. (U.S.A.)* 6, pp. 607-612. 1920.
- EWALD, P. P. : Abweichungen vom Bragg'schen Reflexionsgesetz der Röntgenstrahlen. 86. Naturf.-Vers. Bad Nauheim, 1920. *Physikal. Zeitschr.* 21, pp. 617-619. 1920.
- EWALD, P. P. : Zum Reflexionsgesetz der Röntgenstrahlen. *Zeitschr. f. Phys.* 2, p. 332. 1920.
- FRANKE : Über die Möglichkeit einer exakten Messung des Vordringens von Röntgenstrahlen an Röntgenfolien. *Fortschr. a. d. Geb. d. Röntgenstr.* 27, p. 1. 1920.
- FRICKE, H. : The K Characteristic Absorption Frequencies for the Chem. Elements Mg, Fe, Cr. *Phys. Rev.* 16, p. 202. 1920.
- HADDING, ASSAR : Eine neue Röntgenröhre für Debyesche Aufnahmen. *Zeitschr. f. Phys.* 3, pp. 369-371. 1920.
- HERRMANN : Zerstreung von Röntgenstrahlen. *Physikal. Zeitschr.* 21, pp. 534-541. 1920.
- HERTZ, G. : Über Absorptionslinien im Röntgenspectrum. *Physikal. Zeitschr.* 21, pp. 630-632. 1920.
- HERTZ, G. : Über die Absorptionsgrenzen in der L-Serie. *Zeitschr. f. Phys.* 3, p. 19. 1920.
- HJALMAR, F. : Präzisionsmessungen in der L-Reihe der R-Spektren. *Elemente W bis Cu. Zeitschr. f. Phys.* 3, pp. 262-286. 1920.



- HJALMAR, E.: Präzisionsbestimmungen in der K-Reihe der Röntgenspektren, Elemente Cu bis Na. *Zeitschr. f. Phys.* 1, p. 439. 1920.
- HOYT, F. C.: The Intensities of X-rays of the L Series III. Critical Potential of the Platinum and Tungsten Lines. *Proc. Nat. Acad. Sc. (U.S.A.)* 6, p. 639. 1920.
- HOLWECK: Recherches expérimentales sur les rayons X de grande longueur d'onde. *Comptes Rendus*, 171, pp. 849-852. 1920.
- KARCHER: Wave-length Measurements in the M Series of some High Frequency Spectra. *Phys. Rev.* 5, p. 285. 1920.
- KNIPPING, P.: Zur Frage der Brechung der Röntgenstrahlen. *Zeitschr. f. Phys.* 1, p. 40. 1920.
- KOSSEL, W.: Zum Bau der Röntgenspektren. *Zeitschr. f. Phys.* 1, p. 119. 1920.
- KOSSEL, W.: Über die Ausbildung der Röntgenserien mit wachsender Ordnungszahl. *Zeitschr. f. Phys.* 2, p. 470. 1920.
- KRÖNCKE, H.: Ein rechnerisches Verfahren zur Ermittlung des Spektrums der Röntgenstrahlen. *Physikal. Zeitschr.* 21, p. 220. 1920.
- LAIRD, ELIZABETH R.: Note on Article by H. M. Dadourian on "Soft X-rays." *Phys. Rev.* 15, pp. 293-296. 1920.
- LAIRD, Elizabeth R., and V. P. BARTON: Soft X-rays produced by Cathode Rays of from 200 to 600 volts Velocities. *Phys. Rev. (2)* 15, pp. 297-308. 1920.
- LILLENFELD, J. E., und F. ROTHER: Untersuchungen über die sichtbare blaugraue Brennfleckstrahlung an der ... *Zeitschr.* 21, p. 360. 1920.
- MILLIKAN, R. A.: The Extension of the Ultra-violet Spectrum. *Astrophys. Journ.* 52, pp. 47-64. 1920.
- RICE, C. W.: Energy Content of Characteristic Radiations. *Phys. Rev.* 15, pp. 232-237. 1920.
- RICHTMYER, F. K., and K. GRANT: The Mass-Abs. Coeff. of Water, Aluminium, Copper and Molybdenum for X-rays of Short Wave-length. *Phys. Rev.* 15, pp. 547-549. 1920.
- SIEGBAHN, M., und K. A. WINGÄRDH: Eine Methode für Intensitätsmessungen bei Röntgenstrahlen nebst einigen vorläufigen Absorptionsbestimmungen. *Physikal. Zeitschr.* 21, p. 83. 1920.
- SIEGBAHN, M.: Methoden und Resultate der Röntgenspektroskopie. *Verhandl. d. dtsh. physik. Ges.* (3) 1, pp. 74-75. 1920.
- SMEKAL: Über die Absorptionskante der L-Serie. *Zeitschr. f. Phys.* 3, pp. 243-246. 1920.
- SMEKAL, A.: Über die Erklärung der ... und die Konstitution der Atome. *Physikal. Zeitschr.* 21, pp. ... 1920.
- SMEKAL, A.: Zur Theorie der Röntgenspektren. (Zur Frage der Elektronenanordnung im Atom.) 2. Mitteilung. *S.-A. Wien. Ber.* 129 (2 A), pp. 635-660. 1920.
- SMEKAL, A.: Die Feinstruktur der Röntgenspektren. *Verhandl. d. dtsh. physik. Ges.* 1, p. 58. 1920.
- SOMMERFELD, A.: Bemerkungen zur Feinstruktur der Röntgenspektren. *Zeitschr. f. Phys.* 1, p. 135. 1920.
- STENSSON, N.: Über die Dubletten der K-Reihe der Röntgenspektren. *Zeitschr. f. Phys.* 3, p. 60. 1920.
- VEGARD, L.: Die Verbreiterung von Spektrallinien im Röntgengebiet. *Physikal. Zeitschr.* 21, p. 6. 1920.
- VOLTZ, F., und F. ZACHER: Die Entwicklungsgeschichte der modernen Röntgenröhren. *Fortschr. a. d. Geb. d. Röntgenstr.* 27, p. 83. 1920.
- WAGNER, E.: Über die Grundlagen der Röntgenspektroskopie. *Die Naturwissenschaften* 8, p. 973. 1920.
- WAGNER, E.: Atombau und Röntgenspektren. *Zeitschr. f. Elektrochemie.* 26, p. 260. 1920.

- WAGNER, E.: Über Spektraluntersuchungen an Röntgenstrahlen. *Physikal. Zeitschr.* 21, pp. 621-625. 1920.
- WEBSTER: Critical Potentials of the L Series of Platinum. *Phys. Rev.* 15, p. 238. 1920.
- WEBSTER, D. L.: The Intensities of X-rays of the L Series. II. The Critical Potentials of the Platinum Lines. *Proc. Nat. Acad. Sc. (U.S.A.)* 6, p. 26. 1920.
- WHIDDINGTON, R.: Note on the X-ray Spectra of the Elements. *Phil. Mag.* (6) 39, pp. 694-696. 1920.
- WINTZ, H.: Messungen an Röntgenstrahlen. Diss. Erlangen. 1920.
- WOLFF, WALTER: Die Erzeugung von Röntgenstrahlen durch Kathodenstrahlen in Luft von gewöhnlicher Dichte. *Zeitschr. f. Phys.* 21, pp. 507-510. 1920.
- ZECHER, G.: Unters. am kontin. R-Spektrum der Glühkathodenröhre usw. *Ann. d. Physik*, 63, pp. 28-56. 1920.

## 1921.

- BEHNKEN, H.: Das kontinuierliche Röntgenspektrum. *Zeitschr. f. Phys.* 4, p. 241. 1921.
- BRAGG, W. L., R. W. JAMES and C. H. BOSANQUET: The Intensity of Reflexion of X-rays by Rock-Salt. *Phil. Mag.* 41, p. 309; 42, p. 1. 1921.
- BRAGG, JAMES, und BOSANQUET: Über die Streuung der Röntgenstrahlen durch die Atome eines Kristalls. *Zeitschr. f. Phys.* 8, pp. 77-84. 1922.
- BRAGG, W. H.: The Intensity of X-ray Reflexion by Diamond. *Nature*, 107, p. 477. 1921.
- BROGLIE, MAURICE DE: Sur les spectres corpusculaires des éléments. *Comptes Rendus*, 172, pp. 274-275. 1921.
- BROGLIE, M. DE: Sur les spectres corpusculaires. *Comptes Rendus*, 172, pp. 806-807. 1921.
- BROGLIE, LOUIS DE: Sur la théorie de l'absorption des rayons X par la matière et le principe de correspondance. *Comptes Rendus*, 173, pp. 1456-1458. 1921.
- BROGLIE, MAURICE et LOUIS DE: Sur le modèle d'atome de Bohr et les spectres corpusculaires. *Comptes Rendus*, 172, pp. 746-748. 1921.
- BROGLIE, MAURICE DE: Sur les spectres corpusculaires et leur utilisation pour l'étude des spectres de rayons X. *Comptes Rendus*, 173, pp. 1157-1160. 1921.
- BROGLIE, MAURICE DE: Les phénomènes photo-électriques pour les rayons X et les spectres corpusculaires des éléments. *Journ. de phys. et le Radium* (6) 2, pp. 265-287. 1921.
- COMPTON, A. H.: Secondary High-frequency Radiation. *Phys. Rev.* 18, pp. 96-97. 1921.
- COMPTON, A. H.: The Width of X-ray Spectrum Lines. *Phys. Rev.* 18, p. 322. 1921.
- COMPTON, A. H.: A Possible Origin of the Defect of the Combination Principle in X-rays. *Phys. Rev.* 18, pp. 336-338. 1921.
- COMPTON, A. H., and C. F. HAGENOW: The Polarisation of Secondary X-rays. *Phys. Rev.* 18, pp. 97-98. 1921.
- COSTER, D.: Zur Systematik der R-Spektren. *Zeitschr. f. Phys.* 6, pp. 185-203. 1921.
- COSTER, D.: On the Emission and Absorption Wave-lengths of the Characteristic radiation in the L Series. *Phys. Rev.* 18, pp. 218-220. 1921.
- COSTER, D.: Präzisionsmessungen in der L-Serie der schwereren Elemente. *Zeitschrift f. Phys.* 4, p. 178. 1921.
- COSTER, D.: Über das Kombinationsprinzip in den Röntgenspektren. *Zeitschr. f. Phys.* 5, p. 139. 1921.
- COSTER, D.: Le principe de combinaison et la loi de Stokes dans les séries de rayons X. *Comptes Rendus*, 172, p. 1176. 1921.
- COSTER, D.: Sur la structure fine des séries de rayons X. *Comptes Rendus*, 173, p. 77. 1921.

- CROWTHER, J. A. : "J."-Radiation. *Phil. Mag.* 42, pp. 719-728. 1921.
- DAUVILLIER, A. : Sur le fonctionnement du Tube Lilienfeld. *Comptes Rendus*, 172, p. 1033. 1921.
- DAUVILLIER, A. : Sur le principe de combinaison et les raies d'absorption dans les spectres de rayons X. *Comptes Rendus*, 173, p. 35. 1921.
- DAUVILLIER, A. : Sur la structure de la série L. *Comptes Rendus*, 172, p. 915. 1921.
- DAUVILLIER, A. : Sur les séries L de l'uranium et le principe de combinaison dans les spectres de rayons X. *Comptes Rendus*, 172, p. 1350. 1921.
- DAVIS, B., and W. M. STEMPER : The Reflexion of X-rays from Calcite. *Phys. Rev.* (2) 17, pp. 526-527. 1921.
- DAVIS, B., and W. M. STEMPER : An Experimental Study of the Reflexion of X-rays from Calcite. *Phys. Rev.* 17, p. 608. 1921.
- DERSCHEM, E., and C. T. DOZIER : The Concentration of Monochromatic X-rays by Crystal Reflexion. *Phys. Rev.* 17, p. 519. 1921.
- DERSCHEM, E. : An X-ray Spectrometer for the Determination of Absorption Coefficients. *Phys. Rev.* 18, p. 324. 1921.
- DOZIER, C. T. : An Explanation of X-ray Diffraction Patterns from Rolled Metals. *Phys. Rev.* (2) 17, p. 519. 1921.
- DUANE, W. : On the Calculation of the X-ray Absorption Frequencies of the Chemical Elements. *Proc. Nat. Acad. Sc. (U.S.A.)* 7, pp. 260-267, 267-273. 1921.
- DUANE, W. : Approx. Computations of X-ray Absorption-frequencies. *Phys. Rev.* (2) 17, pp. 431-433. 1921.
- DUANE, W., and H. FRICKE : On the Absorption of X-rays by Chromium, Manganese and Iron. *Phys. Rev.* 17, pp. 529-531. 1921.
- DUANE, PALMER and CHI-SUN-YEH : A Remeasurement of the Radiation Constant  $h$  by Means of X-rays. *Proc. Nat. Acad. Sc. (U.S.A.)* 7, pp. 237-242. 1921.
- DUANE, PALMER and CHI-SUN-YEH : A Remeasurement of the Radiation Constant  $h$  by Means of X-rays. *Phys. Rev.* 18, pp. 98-99. 1921.
- DUANE, W., and R. A. PATTERSON : On the Relative Position of Lines in X-ray Spectra. *Phys. Rev.* 17, p. 259. 1921.
- GILCHRIST, L. : The Width of X-ray Spectral Lines. *Phys. Rev.* 18, pp. 89-94. 1921.
- GLOCKER, R., und M. KAUFF : Die Berechnung des Absorptionsverlustes der Streustrahlung innerhalb des streuenden Körpers. *Phys. Zeitschr.* 22, pp. 200-209. 1921.
- GLOCKER, R., und W. TRAUB : Das photographische Schwärzungsgesetz der Röntgenstrahlen. *Phys. Zeitschr.* 22, p. 345. 1921.
- GOCHT, HERMANN : Die Röntgen-Literatur. IV. Teil. (1914-1917.) P. 6605. Stuttgart : Verlag F. Enke. 1921.
- GROTRIAN, W. : Das L-Dublett des Neon. *Zeitschr. f. Phys.* 8, pp. 116-125. 1921.
- HALBERSTRÄDTER und TUGENDREICH : Über die von der Rückseite der Antikathode ausgehende Röntgenstrahlung. *Fortschr. a. d. Geb. d. Röntgenstr.* 28, p. 64. 1921.
- HEWLETT, C. W. : The Absorption and Scattering Coefficient for Homogeneous X-rays in Several Elements of Low Atomic Weight. *Phys. Rev.* 17, p. 267. 1921.
- HEWLETT, C. W. : The Mass Absorption and Mass Scattering Coefficient for Homogeneous X-rays of Wave-length between 0.13 and 1.05 Angström Units in Water, Lithium, Carbon, Nitrogen, Aluminium, Oxygen and Iron. *Phys. Rev.* 17, p. 284. 1921.
- HJALMAR, E. : Precision Measurements in the X-ray Spectra. Part IV., K Series, the Element Cu-Na. *Phil. Mag.* 41, p. 675. 1921.
- HJALMAR, E. : Beiträge zur Kenntnis der Röntgenspektren. *Zeitschr. f. Phys.* 7, pp. 341-350. 1921.
- HOLWECK : Absorption des rayons X de grande longueur d'onde. Liaison entre les rayons X et les rayons gamma. *Comptes Rendus*, 172, pp. 439-442. 1921.

- HOLWECK : Potentiels critiques relatifs aux discontinuités K et L<sub>1</sub> d'absorption de l'aluminium. Nouv. determ. de la const.  $h$  de Planck. *Comptes Rendus*, 173, pp. 709-712. 1921.
- HOLWECK, M. : Recherches expérimentales sur la liaison entre les rayons X et la lumière. *Journ. chim. phys.* 19, pp. 261-263. 1921.
- HOYT, F. C. : Structure of the L Series of Tungsten and Platinum. *Phys. Rev.* 18, pp. 333-335. 1921.
- HUGHES, A. LL. : The characteristic K-Radiation from Boron. *Trans. Proc. Roy. Soc. Canada*, 15, pp. 1-6. 1921.
- HÜCKEL, E. : Zerstreuung von Röntgenstrahlen durch anisotrope Flüssigkeiten. *Physikal. Zeitschr.* 22, pp. 561-563. 1921.
- JAUNCEY : The Effect of Damping on the Width of X-ray Spectrum Lines. *Phys. Rev.* 18, p. 322. 1921.
- KIRKPATRICK, PAUL : Experiments on Polarisation of X-rays. *Phys. Rev.* 18, p. 323. 1921.
- KORN, A. : Eine mechanische Theorie der Serienspektren 3, Schwingungsdauer der Röntgenstrahlen und Atomgewicht. *Physikal. Zeitschr.* 22, p. 148. 1921.
- KURTH, E. H. : Soft X-rays of Characteristic Type. *Phys. Rev.* 18, pp. 99-100. 1921.
- KURTH, E. H. : Soft X-rays of Characteristic Type. *Phys. Rev.* 17, pp. 528-529. 1921.
- KURTH : The Extension of the X-ray Spectrum to the Ultra-violet. *Phys. Rev.* 18, pp. 461-476. 1921.
- KÜSTNER, HANS : Die Röntgenstrahlung im kontinuierlichen Röntgenspektrum. *Verhandl. d. dtsh. phys. Ges.* 56-57. 1921.
- KÜSTNER : Der entstellende Einfluss des Spektrometerkrystals auf das kontinuierliche R-Spektrum. *Zeitschr. f. Phys.* 7, pp. 97-110. 1921.
- LINDH, AXEL E. : Zur Kenntnis des Röntgenabsorptionsspektrums von Chlor. *Zeitschr. f. Phys.* 6, p. 303-310. 1921.
- LINDH, A. E. : Sur les spectres d'absorption du chlore pour les rayons X. *Comptes Rendus hebdom. des séances de l'acad. des sciences*, 172, p. 1175. 1921.
- MARCH, A. : Die Röntgenstrahlung im kontinuierlichen Röntgenspektrum. *Ann. de Physik*, (4) 56, pp. 1-10. 1921.
- MARCH, A. : Die Röntgen-Bremsstrahlung. *Physikal. Zeitschr.* 22, pp. 209-213. 1921.
- MARCH, A. : Die Röntgenstrahlung im kontinuierlichen Röntgenspektrum. *Physikal. Zeitschr.* 22, pp. 214-215. 1921.
- MILLIKAN, BOWEN and SAWYER : The Vacuum Spark Spectra in the Extreme Ultra-violet of Carbon, Iron and Nickel. *Astrophys. Journ.* 53, pp. 150-160. 1921.
- MOHLER, F. L., and P. D. FOOTE : Characteristic Low Voltage X-radiation from Arcs in Metallic Vapours. *Phys. Rev.* 18, pp. 94-95. 1921.
- MOHLER, F. L., and P. D. FOOTE : Soft X-rays from Arcs in Vapours. *Journ. Opt. Soc. Amer.* 5, pp. 328-333. 1921.
- MÜLLER, ALEX. : On an X-ray Bulb with a Liquid Mercury Anticathode and on Wave-length Measurements of the L Spectrum of Mercury. *Phil. Mag.* (6) 42, pp. 419-427. 1921.
- OVERN, OSWALD, B. : An Absolute Scale of X-ray Wave-length. *Phys. Rev.* 18, pp. 350-355. 1921.
- PEALING, H. : The Reflexion of the X-ray Spectrum of Palladium from Fluorspar. *Nature*, 107, p. 477. 1921.
- PLIMPTON, S. J. : On the Scattering of Rays in X-ray Diffraction. *Phil. Mag.* 42, pp. 302-304. 1921.
- RATNER, S. : Polarisation Phenomena in an X-ray Bulb. *Nature*, 107, pp. 522-523. 1921.
- REBOUL : Sur un nouveau rayonnement de courte longueur d'onde. *Comptes Rendus*, 173, pp. 1162-1165. 1921.

- RICHTMYER, F. K. : The Laws of Absorption of X-rays. *Phys. Rev.* (2) 18, pp. 13-30. 1921.
- RICHTMYER, F. K. : The Evidence regarding the so-called "J" Radiation. *Phys. Rev.* (2) 17, pp. 433-434. 1921.
- RICHTMYER, F. K. : Mass Absorption Coefficient as a Function of Wave-length above and below the K X-ray Limit of the Absorber. *Phys. Rev.* 17, p. 264. 1921.
- RICHARDSON, O. W., and C. B. BAZZONI : The Excitation of Soft Characteristic X-rays. *Phil. Mag.* 42, pp. 1015-1019. 1921.
- ROSS, P. A. : Prelim. Measurements of the Critical Potentials of the M Lines in the X-ray Spectrum of Lead. *Phys. Rev.* 18, p. 336. 1921.
- SAWYER, R. A. : The Vacuum Hot-spark Spectrum of Zinc in the Extreme Ultra-violet Region. *Astrophys. Journ.* 52, pp. 286-300. 1921.
- SEEMAN, H. : Ein Präzisions-Röntgenspektrograph. *Physikal. Zeitschr.* 22, pp. 580-581. 1921.
- SIEGBAHN, M. : Nouvelles mesures de précision dans le spectre de rayons X. *Comptes Rendus*, 173, pp. 1350-1352. 1921.
- SIEGBAHN, M. : Bericht über die letzte Entwicklung der Röntgenspektroskopie. *Jahrb. d. Radioakt.* 18, pp. 240-292. 1921.
- SIEGBAHN, M., A. E. LINDH und N. STENSSON : Über ein Verfahren der Spektralanalyse mittels Röntgenstrahlen. *Zeitschr. f. Phys.* 4, p. 61. 1921.
- SIMONS, LEWIS : The Beta Ray Emission from Thin Films of the Elements exposed to Röntgen Rays. *Phil. Mag.* 41, p. 120. 1921.
- SMEKAL, A. : Bemerkungen zu der Arbeit des Herrn D. Costers zur Systematik der Röntgenspektren. *Zeitschr. f. Phys.* 7, pp. 410-412. 1921.
- SMEKAL, A. : Antwort auf Herrn L. Vegard. *Physikal. Zeitschr.* 22, pp. 401-402. 1921.
- SMEKAL, A. : Über die Feinstruktur der Röntgenspektren. *Physikal. Zeitschr.* 22, pp. 559-561. 1921.
- SMEKAL, A. : Zur Feinstruktur der Röntgenserien. (Vorläufige Mitteilung.) *Wiener Ber.* 130 (2 A), pp. 25-30. 1921.
- SMEKAL, A. : Zur Feinstruktur der Röntgenspektren. *Zeitschr. f. Phys.* 4, p. 26; 5, pp. 91, 121. 1921.
- SOMMERFELD, A. : Bemerkungen zur Feinstruktur der Röntgenspektren 2. *Zeitschr. f. Phys.* 5, p. 1. 1921.
- SOMMERFELD, A., und G. WENTZEL : Über reguläre und irreguläre Dubletts. *Zeitschr. f. Phys.* 7, pp. 86-92. 1921.
- STEMPEL, W. M. : Reflexion of X-rays from Crystals. *Phys. Rev.* 17, p. 521. 1921.
- VEGARD, L. : Über die Erklärung der Röntgenspektren und die Konstitution der Atome. *Physikal. Zeitschr.* 22, p. 271. 1921.
- VOGEL, W. : Anordnung, den Seemanschen Röntgenspektrometer zu Präzisionswellenlängenmessungen zu benutzen. *Zeitschr. f. Phys.* 4, p. 1. 1921.
- WEBER, A. : Neuerungen am Seemanschen Röntgenspektrometer zwecks Präzisionsmessungen. *Zeitschr. f. Phys.* 4, p. 1. 1921.
- WEBSTER, D. L. : The High Freq. Limits of X-ray Spectra at Different Angles from the Cathode Stream. *Phys. Rev.* 18, p. 155. 1921.
- WEBSTER, D. L. : Some X-ray Isochromats. *Phys. Rev.* 18, pp. 321-322. 1921.
- WENTZEL, G. : Zur Systematik der Röntgenspektren. *Zeitschr. f. Phys.* 6, pp. 84-99. 1921.
- WENTZEL, GREGOR : Klassifizierung der O- und P-Niveaus mittels des Auswahlprinzips für die Übergänge. *Zeitschr. f. Phys.* 8, pp. 85-88. 1921.
- WENTZEL, G. : Funkenlinien im Röntgenspektrum. *Ann. d. Phys.* 66, pp. 437-462. 1921.
- WHIDDINGTON, R. : Note on the Velocity of X-ray Electrons. *Proc. Cam. Phil. Soc.* 20, pp. 442-444. 1921.
- WILLIAMS, W. E., and B. L. WORSNOP : Absorption of X-rays. *Nature*, 108, pp. 306-307. 1921.

- YOSHIDA, USABURO : On a Mica X-ray Spectrometer. *Mem. Coll. Sci. Kyoto Imp. Univ.* 4, pp. 343-347. 1921.
- YOSHIDA, U., and S. TANAKA : The Tungsten X-ray Spectrum with a Mica Spectrometer. *Mem. Coll. Sci. Kyoto Imp. Univ.* 5, pp. 173-178. 1921.

## 1922.

- AURÉN, T. E. : Absorption of X-rays in Crystals. *Medd. Vetenskapsakad. Nobelinst* 4, No. 10. 1922.
- BACKHURST, IVOR : Variation of the Intensity of Reflected X-radiation with the Temperature of the Crystal. *Proc. Roy. Soc. (A)* 102, pp. 340-352. 1922.
- BOHR, N., und D. COSTER : Periodisches und periodisches System der Elemente *Zeitschr. f. Phys.* 12, pp. . . . .
- BRAGG, W. L., and R. W. JAMES : The Intensity of X-ray Reflexion. *Nature*, 110, p. 148. 1922.
- BROGLIE, M. DE : Sur les spectres corpusculaires des éléments. *Comptes Rendus*, 174, pp. 939-941. 1922.
- BROGLIE, M. DE, et A. DAUVILLIER : Sur un nouveau phénomène d'absorption observé dans le domaine des rayons X. *Comptes Rendus*, 174, pp. 1546-1548. 1922.
- BROGLIE, L. DE : Rayons X et équilibre thermodynamique. *Journ. de Phys. et le Radium* (6) 3, pp. 33-45. 1922.
- BURBRIDGE, P. W. : The Absorption of the K X-rays of Silver in Gases and Gaseous Mixtures. *Phil. Mag.* 43, pp. 381-389. 1922.
- BURBRIDGE, P. W. : Note on the Absorption of Narrow X-ray Beams. *Phil. Mag.* 43, pp. 389-392. 1922.
- COMPTON, A. H. : The Width of X-ray Spectrum Lines. *Phys. Rev.* 19, pp. 68-72. 1922.
- COMPTON, A. H. : The Spectrum of Secondary X-rays. *Phys. Rev.* 19, pp. 267-268. 1922.
- COMPTON, A. H. : Total Reflexion of X-rays from Glass and Silver. *Phys. Rev.* (2) 20, p. 84. 1922.
- COMPTON, A. H., and FREEMAN : The Intensity of X-ray Reflexion from Powdered Crystals. *Nature*, 110, p. 38. 1922.
- CORK, J. M. : Characteristic X-ray Absorption in the L Series for Elements N 62 to N 77. *Phys. Rev.* 20, p. 81. 1922.
- COSTER, D. : On the Spectra of X-rays and the Theory of Atomic Structure. *Phil. Mag.* 44, pp. 546-573. 1922.
- COSTER, D. : On the Principle of Combination and Stokes' Law in the X-ray Series. *Phys. Rev.* 19, pp. 20-23. 1922.
- COSTER, D. : On the Spectra of X-rays and the Theory of Atomic Structure. *Phil. Mag.* 43, pp. 1070-1107. 1922.
- COSTER, D. : Sur la série L du spectra des rayons X. *Comptes Rendus*, 174, pp. 378-379. 1922.
- DARBORD, R. : Vers la détermination directe de la longueur d'onde des rayons X. *Journ. de phys. et le radium*, 3, pp. 212-217. 1922.
- DARBORD, R. : Sur la réflexion des rayons X par les cristaux. *Journ. de phys. et le radium*, 3, pp. 218-220. 1922.
- DARWIN, C. G. : The Reflexion of X-rays from Imperfect Crystals. *Phil. Mag.* 43, pp. 800-829. 1922.
- DAUVILLIER, A., et L. DE BROGLIE : Remarques sur le travail de E. Hjalmar concernant la série M des éléments. *Comptes Rendus*, 175, pp. 1198-1201. 1922.
- DAUVILLIER, A. : Sur la complexité de la série K des éléments légers et son interprétation théorique. *Comptes Rendus*, 174, pp. 443-445. 1922.
- DAUVILLIER, A. : Sur les séries L du lutécium et de l'ytterbium et sur l'identification du celtium avec l'élément de nombre 72. *Comptes Rendus*, 174, pp. 1347-1349. 1922.

- DAVIS, B., and H. M. TERRILL: The Refraction of X-rays in Calcite. *Proc. Nat. Acad. Sc. (U.S.A.)* 8, pp. 357-361. 1922.
- DAVIS, B., and W. M. STEMPEL: Reflection of X-rays from Rock-salt. *Phys. Rev.* 19, pp. 504-511. 1922.
- DOLEJSEK, V.: Sur les lignes K  $\alpha$  des éléments légers. *Comptes Rendus*, 174, pp. 441-443. 1922.
- DOLEJSEK, V.: Über die N-Serie der Röntgenspektren. *Zeitschr. f. Phys.* 10, pp. 129-236. 1922.
- DUANE, A. R. and W.: The Scattering of X-rays at Small Angles. *Phys. Rev.* 20, pp. 86-87. 1922.
- DUANE, W., and K. C. MAZUMDER: Absorption of Short X-rays by Aluminium and Copper. *Proc. Nat. Acad. Sc. (U.S.A.)* 8, pp. 45-49. 1922.
- DUANE, W., and K. C. MAZUMDER: On the Spectra of X-rays of Short Wave-length. *Phys. Rev.* 19, pp. 536-537. 1922.
- DUANE, W., and R. A. PATTERSON: Note on X-ray Spectra. *Phys. Rev.* 19, pp. 542-543. 1922.
- DUANE, W., and R. A. PATTERSON: Note on X-ray Spectra. *Proc. Nat. Acad. Sc. (U.S.A.)* 8, pp. 85-90. 1922.
- FRITZ, O.: Zur Wirkung der Verstärkungsschirme bei Röntgenspektrogrammen. *Fortschr. a. d. Geb. d. Röntgenstr.* 29, pp. 717-720. 1922.
- GERLACH, W.: Das K  $\alpha$ -Dublett, nebst einer Neubestimmung der Gitterkonstanten einiger Krystalle. *Physikal. Zeitschr.* 23, pp. 114-120. 1922.
- GRAY, J. A.: Energy Relations between X- and  $\beta$ -rays. *Phys. Rev.* 19, pp. 430-431. 1922.
- GROTRIAN, W.: Über das L-Dublett des Neon. *Verhandl. d. deutsch. physik. Ges.* (3) 3, p. 41. 1922.
- HEWLETT, C. W.: An Experimental Study of the Scattering of Approx. Homog. X-rays, etc. *Phys. Rev.* 20, pp. 688-708. 1922.
- HEWLETT, C. W.: Measurements of the Amount of Scattered Homogeneous X-rays of Wave-length 0.718 Å pr. gram of Carbon. *Phys. Rev.* 19, pp. 265-267. 1922.
- HJALMAR, E.: Recherches sur la série M des Rayons X. *Comptes Rendus*, 175, pp. 878-880. 1922.
- HOLTSMARK, J.: Über die charakteristische Röntgenstrahlung von Kohle und Bor. *Physikal. Zeitschr.* 23, pp. 252-255. 1922.
- HOLWECK, M. F.: Recherches expérimentales sur les rayons X de grande longueur d'onde. *Ann. de Phys.* 17, pp. 5-53. 1922.
- HOPFIELD, J. J.: Spectra of Hydrogen, Nitrogen and Oxygen in the Extreme Ultra-violet. *Phys. Rev.* 20, pp. 573-588. 1922.
- HUGHES, A. LI.: Charact. X-rays from Boron and Carbon. *Phil. Mag.* 43, pp. 145-161. 1922.
- JAECKEL, G.: Eine neue Anwendung des Röntgenspektrographen. *Zeitschr. f. Phys.* 9, pp. 300-301. 1922.
- JAUNCEY, G. E. M.: The Effect of Damping on the Width of X-ray Spectrum Lines. *Phys. Rev.* 19, pp. 64-67. 1922.
- JAUNCEY, G. E. M.: Secondary X-rays from Crystals. *Phys. Rev.* 19, pp. 435-436. 1922.
- JAUNCEY, G. E. M.: Effect of Temperature on the X-rays scattered by Crystals. *Phys. Rev.* (2), 20, p. 82. 1922.
- JAUNCEY, G. E. M.: The Scattering of X-rays by Crystals. *Phys. Rev.* 20, pp. 405-420. 1922.
- JAUNCEY, G. E. M.: The Effect of Temperature on the Scattering of X-rays by Crystals. *Phys. Rev.* 20, pp. 421-423. 1922.
- KIRKPATRICK, P.: Energy Distribution in Continuous X-ray Spectra. *Phys. Rev.* 20, p. 197. 1922.
- KNIPPING, PAUL: Zehn Jahre Röntgenspektroskopie. *Die Naturwissenschaften*, 10, pp. 366-369. 1922.

- KÜSTNER, F.: Scharfe Spektrallinien bei kurzer Expositionszeit der Debye-Scherrer Methode. *Physikal. Zeitschr.* 23, pp. 257-262. 1922.
- KULENKAMPFF, H.: Über das kontinuierliche Röntgenspektrum. *Ann. d. Phys.* 69, pp. 548-596. 1922.
- LAPP, C. J.: On the Effect of Short Electromagnetic Waves on a Beam of Electrons. *Phys. Rev.* (2) 20, pp. 104-105. 1922.
- LILIENTHAL, J. E.: Die Entladung der Kathode bei der autoelektronischen Entladung. *Physikal. Zeitschr.* 23, pp. 506-511. 1922.
- LINDH, A. E.: Röntgenabsorptionsspektren och kemisk valens. *Fysisk. Tidskr.* 20, pp. 132-133. 1922.
- LINDH, A. E.: Sur le spectre d'absorption de soufre pour les rayons X. *Comptes Rendus*, 175, pp. 25-27. 1922.
- LINDSAY, G. A.: Sur les limites d'absorption L des éléments Ba-Sb. *Comptes Rendus*, 175, pp. 150-151. 1922.
- MARCH: Die Abhängigkeit der Röntgen-Bremsstrahlung von der Emissionsrichtung. *Physikal. Zeitschr.* 23, pp. 84-86. 1922.
- MOHLER, F. L., and P. D. FOOTE: X-ray limits beyond the range of spectroscopic measurements. *Phys. Rev.* 20, pp. 82-83. 1922.
- MOHLER, F. L., and P. D. FOOTE: Characteristic Soft X-rays from Arcs in Gases and Vapours. *Scient. Pap. Bur. of Stand.* 17, pp. 471-496. 1922.
- ODENCRANTZ, A.: Om det kontinuerliga röntgenspektret och dess fotografiska verkningar. *Fysisk. Tidskr.* 20, pp. 125-126. 1922.
- RATNER, S.: Polarization Phenomena in X-ray Bulbs. *Phil. Mag.* 43, pp. 193-204. 1922.
- RICHTMYER, F. K.: "J"-Radiation: A Summary. *Phys. Rev.* 19, p. 418. 1922.
- ROGERS, J. S.: High Frequency Spectra K Series of Platinum. *Proc. Roy. Soc. Victoria*, 34, pp. 196-206. 1922.
- ROSSELAND, S.: Om Intensiteten av karakteristiske Röntgenstråler. *Fysisk. Tidskr.* 20, pp. 124-125. 1922.
- SEEMAN, H.: Präzisions-Röntgenspektrograph. *Zeitschr. f. tech. Phys.* 3, pp. 57-59; *Elektrotechn. Zeitschr.* 43, p. 220. 1922.
- SHEARER, G.: The Emission of Electrons by X-rays. *Phil. Mag.* 44, pp. 793-808. 1922.
- SIEGBAHN, M.: Erhöhung der Messgenauigkeit innerhalb der Röntgenspektren I. *Zeitschr. f. Phys.* 9, pp. 68-80. 1922.
- SIEGBAHN, M., and V. DOLEJSEK: Erhöhung der Messgenauigkeit innerhalb der Röntgenspektren II. *Zeitschr. f. Phys.* 10, pp. 1-11. 1922.
- STATT, W.: Eine experimentelle Bestimmung des wahren Absorptionskoeffizienten von harten Röntgenstrahlen. *Zeitschr. f. Phys.* 11, pp. 304-325. 1922.
- STAUNIG: Erfahrungen über die Verwendbarkeit des Röntgenspektrometers von March, Staunig und Fritz. *Münch. med. Wochenschr.* 69, pp. 933-934. 1922.
- STINTZING, H.: Röntgenspektroskopie für das Gebiet der Ultraviolett und Röntgenstrahlung. *Zeitschr. f. Phys.* 11, pp. 467-472. 1922.
- STUHLMAN, O.: The Extension of the X-ray into the Ultra-violet Spectrum. *Science*, 56, p. 344. 1922.
- TAYLOR, E. G.: Absorption Coefficients for Homogeneous X-rays. *Phys. Rev.* 20, pp. 709-714. 1922.
- WAGNER, E., and H. KULENKAMPFF: Die Intensität der Reflexion von Röntgenstrahlen verschiedener Wellenlänge an Kalkspat und Steinsalz. *Ann. d. Physik* (4) 68, pp. 369-413. 1922.
- WENTZEL, GREGOR: Bericht über neuere Ergebnisse der Röntgenspektroskopie. *Naturwissenschaften* 10, pp. 369-381. 1922.
- WENTZEL, G.: Röntgenspektren und chemische Valenz. *Naturwissenschaften*, 10, pp. 464-468. 1922.
- WHIDDINGTON, R.: X-ray Electrons. *Phil. Mag.* 43, pp. 1116-1126. 1922.
- WINGÅRDH, K. A.: Untersuchungen über die Absorption der Röntgenstrahlen I. *Zeitschr. f. Phys.* 11, pp. 1-11. 1922.
- DE WISNIEWSKI, F.: Essai de théorie de l'influence du champ magnétique sur l'émission des rayons X. *Arch. sc. phys. et mat.* 4, pp. 120-128. 1922.



1923.

- AUGER, P., et A. DAUVILLIER : Sur l'existence de nouvelles lignes, dont un doublet de Sommerfeld, exclues par le principe de selection, dans la série L des éléments lourds. *Comptes Rendus*, 176, pp. 1297-1298. 1923.
- BARKLA, C. G., and RHODA SALE : Notes on X-ray Scattering and on J-radiations. *Phil. Mag.* 45, pp. 737-750. 1923.
- BECKER, J. A. : Magnetic  $\beta$ -ray Analysis of Soft X-rays. *Phys. Rev.* 22, p. 524. 1923.
- BOTHE, W. : Über eine neue Sekundärstrahlung der Röntgenstrahlen. *Zeitschr. f. Phys.* 16, pp. 319-320. 1923.
- BOTHE, W. : Über eine neue Sekundärstrahlung der Röntgenstrahlen. *Zeitschr. f. Phys.* 20, pp. 237-255. 1923.
- BRENTANO, J. : A New Method of Crystal Powder Analysis by X-rays. *Nature*, 112, pp. 652-653. 1923.
- BROGLIE, M. DE, et J. CABRERA : Étude des rayons X au moyen de leur effet photo-électrique. *Journ. de physique et le radium*, 6, pp. 224-225. 1923.
- BROGLIE, M. DE, et E. FRIEDEL : La diffraction des rayons X par les corps smectiques. *Comptes Rendus*, 176, pp. 738-740. 1923.
- CABRERA, J. : Über die Grenzen der Absorption der K-Serie bei einigen Elementen. *Anales soc. espanola Fis. Quim.* 21, pp. 245-252. 1923.
- CABRERA, J. : On the absorption limits of the K series for certain elements. *Comptes Rendus*, 176, pp. 740-741. 1923.
- CERMAK, P. Die Röntgenstrahlen. (Verlag : J. A. Barth.) 1923.
- CLARK, G. L., and W. DUANE : The Abnormal Reflexion of X-rays by Crystals. *Science*, 58, pp. 400-402. 1923.
- CLARK, G. L., and W. DUANE : A New Method of Crystal Analysis and the Reflexion of Characteristic X-rays. *Journ. Opt. Soc. Amer.* 7, pp. 455-482. 1923.
- CLARK, G. L., and W. DUANE : On the Abnormal Reflexion of X-rays by Crystals. *Proc. Nat. Acad. Sc. (U.S.A.)* 9, pp. 131-135. 1923.
- CLARK, G. L., and W. DUANE : The Reflexion by a Crystal of X-rays characteristic of Chemical Elements in it. *Proc. Nat. Acad. Sc. (U.S.A.)* 9, pp. 126-130. 1923.
- COMPTON, A. H. : Wave-length Measurements of Scattered X-rays. *Phys. Rev.* 21, p. 715. 1923.
- COMPTON, A. H. : A Quantum Theory of the Scattering of X-rays by Light Elements. *Phys. Rev.* 21, p. 207. 1923.
- COMPTON, A. H. : Absorption Measurements of the Change of Wave-length accompanying the Scattering of X-rays. *Phil. Mag.* 46, pp. 956-963. 1923.
- COMPTON, A. H. : The Spectrum of Scattered X-rays. *Phys. Rev.* 22, pp. 409-413. 1923.
- CORK, J. M. : Characteristic L-absorption of X-rays for Elements of Atomic Numbers 62 to 77. *Phys. Rev. (2)* 21, pp. 326-333. 1923.
- COSTER, NISHINA und WERNER : Über die Absorptionsspektren in der L-Serie der Elemente. *Zeitschr. f. Phys.* 18, pp. 207-211. 1923.
- COSTER, D. : Qualitative und quantitative chemische Analyse mittels Röntgenstrahlen. *Zeitschr. f. Elektrochemie*, 29, pp. 344-348. 1923.
- COSTER, D. : On the X-ray Spectra of Hafnium and Thulium. *Phil. Mag.* 46, pp. 956-963. 1923.
- DAUVILLIER, A. : Recherches sur les rayons X de haute fréquence dans le groupe des terres rares. *Comptes Rendus*, 176, pp. 1381-1383. 1923.
- DAVIS and TERRELL : A Determination of the Coefficient of Reflexion of X-rays for Calcite and Rock-salt. *Phil. Mag.* 45, pp. 463-470. 1923.
- DEBYE, P. : Zerstreuung von Röntgenstrahlen und Quantentheorie. *Phys. Zeitschr.* 24, pp. 161-166. 1923.

- DUANE, W., and G. L. CLARK : On the Abnormal Reflexion of X-rays by Crystals. *Phys. Rev.* 21, pp. 379-380. 1923.
- FOWLER, A. : *Proc. Roy. Soc. A* 103, p. 413. 1923.
- GLOCKER : Die Verwendung der Röntgenstrahlen zur qualitativen chemischen Analyse. *Fortschritte auf d. Geb. d. Röntgenstr.* 31, pp. 90-92. 1923.
- GOTTHARDT, P. P., und A. WERTHEIMER : Über Wellenlängenmessungen an Therapieröntgenröhren. *Münch. Med. Wochenschr.* 70, p. 459. 1923.
- GREEN, J. B. : Note on Relativistic Röntgen  $\alpha$ -doublets and the Screening constant ; a correction. *Phys. Rev.* 22, p. 546. 1923.
- GREEN, J. B. : Note on Relativistic Röntgen L-doublets and the "Screening Constant." *Phys. Rev.* 21, pp. 397-401. 1923.
- GÜNTHER, P., und I. STRANSKI : Ein Röntgenspektrograph für chemischanalytische Zwecke. *Zeitschr. f. Physikal. Chemie.* 106, p. 433. 1923.
- HENNINGS, A. E. : The Appearance of "Ghosts" in the White Spectrum reflected from Calcite. *Phys. Rev.* 22, p. 524. 1923.
- HJALMAR, E. : Röntgenspektroskopische Messungen. Beitrag zur Kenntnis der Röntgenspektren. *Zeitschr. f. Phys.* 15, p. 65. 1923. *Diss. Lund.*
- HOLMSMARK, J. : Über die charakteristische Röntgenstrahlung der ersten Elemente. *Phys. Zeitschr.* 24, pp. 225-230. 1923.
- HOLWECK, F. : Propriétés optiques des rayons X mous.—Diffraction : Reflexion. *Journ. de phys. et le radium*, 4, pp. 211-212. 1923.
- JAUNCEY, G. E. M., and H. L. MAY : The Scattering of X-rays from Crystal at Small Angles. *Phys. Rev.* 21, pp. 206-207. 1923.
- KAROLUS, A. : Über das kontinuierliche Röntgenspektrum bei verschiedenen Spannungen. *Ann. d. Phys.* (4), 1923.
- KETTMAN, G. : Über die Intensität des kontinuierlichen Röntgenspektrums bei höheren Spannungen. *Zeitschr. f. Phys.* 18, pp. 1-10. 1923.
- KIRKPATRICK, P. : Continuous Spectral Energy Distribution within the X-ray Tube. *Phys. Rev.* 22, p. 37. 1923.
- KIRKPATRICK, P. : An Experimental Check of the Optical Theory of X-ray Reflexion. *Phys. Rev.* 22, p. 414. 1923.
- KIRKPATRICK, P. : Polarisation of X-rays as a Function of Wave-length. *Phys. Rev.* 22, pp. 226-232. 1923.
- KOSSEL, W. : Über die Ergiebigkeit der Röntgenfluoreszenz und die Frage des Intensitätsvergleichs an Röntgenstrahlen verschiedener Wellenlängen. *Zeitschr. f. Phys.* 19, pp. 333-346. 1923.
- KRAMERS, H. A. : On the theory of X-ray Absorption and the Continuous X-ray Spectrum. *Phil. Mag.* 46, p. 836. 1923.
- LANDÉ, A. : Zur Theorie der Röntgenspektren. *Zeitschr. f. Phys.* 16, p. 391. 1923.
- LEDUR, R. : Sur la dispersion dans les spectres photoélectriques des rayons X. *Comptes Rendus*, 176, pp. 383-385. 1923.
- LEFAPE, A., and A. DAUVILLIER : Sur la structure fine des limites d'absorption de haute fréquence ; Limites L du Xénon. *Comptes Rendus*, 177, p. 34. 1923.
- LINDH, A. E. : Experimentelle Untersuchungen über die K-Röntgenabsorptionsspektren der Elemente Chlor, Brom, Iod. *Diss. Lund.* 1923.
- MARCH, A. : Zur Arbeit H. Kulenkampfs.—Über das kontinuierliche Röntgenspektrum. *Ann. d. Phys.* 71, pp. 603-606. 1923.
- MAUGUIN, CH. : Réflexion des rayons de Röntgen sur certains plans réticulaires remarquables de la calcite. *Comptes Rendus*, 176, pp. 1331-1334. 1923.
- MCLENNAN, J. C., and M. L. CLARK : On the Excitation of Characteristic X-rays from light elements. *Proc. Roy. Soc. (A)* 102, pp. 389-410. 1923.
- MIE, G. : Echte optische Resonanz bei Röntgenstrahlen. *Zeitschr. f. Phys.* 18, pp. 105-108. 1923.

- MILLIKAN, R. A., and I. S. BOWEN: Extreme Ultra-violet Spectra. *Phys. Rev.* 22, p. 523. 1923.
- MILLIKAN, R. A., and I. S. BOWEN: Extreme Ultra-violet Spectra. *Phys. Rev.* 23, pp. 1-34. 1923.
- MÜLLER, ALEX.: The X-ray Investigation of Fatty Acids. *Journ. Chem. Soc.* 123, pp. 2043-2047. 1923.
- MÜLLER, A., and G. SHEARER: Further X-ray Measurements of Long-chain Compounds and a Note on their Interpretation. *Journ. Chem. Soc.* 123, pp. 3156-3164. 1923.
- NAGAOKA, H., and Y. SUGIURA: Vacuum Arc for obtaining Spectra extending from Visible Light to Soft X-rays. *Astrophys. Journ.* 57, pp. 86-91. 1923.
- OLSON, DERSHEM and STORCH: X-ray Absorption Coefficients of Carbon, Hydrogen and Oxygen. *Phys. Rev.* 21, pp. 30-37. 1923.
- PASCHEN, F.: Die Funkenspektren des Aluminium I. *Ann. d. Phys.* 71, p. 142. 1923.
- RAMAN, C. V.: The Scattering of X-rays in Liquids. *Nature*, 111, p. 185. 1923.
- RICHTMYER, F. K., and F. W. WARBURTON: The Absorption of X-rays by Iron, Cobalt, Nickel and Copper. *Phys. Rev.* 22, p. 539. 1923.
- RICHTMYER, F. K.: Absorption of Short X-rays by Water and Carbon. *Phys. Rev.* 21, p. 478. 1923.
- RICHTMYER, F. K., and F. W. WARBURTON: X-ray Absorption Coefficients of Cobalt and Nickel. *Phys. Rev.* 21, p. 721. 1923.
- ROGERS, J. S.: L Series of Tungsten and Platinum. *Proc. Cambr. Phil. Soc.* 21, pp. 430-433. 1923.
- ROLLEFSON, G. H.: Very Soft X-rays—the M Series for Iron. *Science (N.S.)* 57, pp. 562-563. 1923.
- ROSS, P. A.: The Wave-length and Intensity of Scattered X-rays. *Phys. Rev.* 22, p. 524. 1923.
- ROSS, P. A.: Change in Wave-length by Scattering. *Proc. Nat. Acad. Sc. (U.S.A.)* 9, pp. 246-248. 1923.
- ROSS, P. A.: Critical Potentials of the Thorium M Series Lines. *Phys. Rev.* 22, pp. 221-225. 1923.
- ROSS, P. A.: Crystal Reflexion and Change of Wave-length. *Phys. Rev.* 23, pp. 290. 1923.
- ROSSELAND, S.: On the Theory of Ionization by Swiftly-moving Electrified Particles and the Production of Characteristic X-rays. *Phil. Mag.* 45, 65-83. 1923.
- SCHLECHTER, E.: Einfluss der Entwicklungsweise und Wirkung des Verstärkungsschirmes auf die photographische Platte bei Röntgenstrahlen. *Phys. Zeitschr.* 24, pp. 29-35. 1923.
- SHEARER, G.: An X-ray Investigation of Certain Organic Esters and Other Long-chain Compounds. *Journ. Chem. Soc.* 123, pp. 3152-3156. 1923.
- SIEGBAHN, M.: Röntgenstrålnarnas totalreflexion. *Tysisk. Tidskr.* 21, pp. 170-171. 1923.
- SIEGBAHN, M., und A. ZAČEK: Über die relative Intensität der K-Linien in Röntgenspektren. *Ann. d. Phys.* 71, pp. 187-198. 1923.
- UNNEWEHR, E. C.: An Experimental Investigation of the Energy of the Characteristic K-radiation from Certain Metals. *Phys. Rev.* 22, p. 529. 1923.
- WALTER, B.: Über die Reflexion der charakteristischen Röntgenstrahlen der chemischen Elemente eines Kristalles durch diesen. *Zeitschr. f. Phys.* 20, pp. 257-271. 1923.
- WEBSTER, D. L., and A. E. HENNINGS: X-ray Isocromats of Molybdenum. *Phys. Rev.* 21, pp. 312-325. 1923.
- WENTZEL, G.: Neue numerische Untersuchung der Röntgenspektraltermen. *Zeitschr. f. Phys.* 16, pp. 46-53. 1923.
- WILSON, C. T. R.: Investigations on X-rays and  $\beta$ -rays by the Cloud Method. Part 1.—X-rays. *Proc. Roy. Soc. (A)* 104, pp. 1-27. 1923.
- WINGÅRDH, K. A.: Experimentelle Untersuchungen über die Schwächung der Röntgenstrahlen. *Diss. Lund.* 1923.

WOLFERS, F. : La déviation des rayons X à la surface des corps et les effets produits par une fente. *Comptes Rendus*, 177, pp. 32-34. 1923.

WYCKOFF, R. W. G. : On the Existence of an Anomalous Reflexion of X-rays in Laue Photographs of Crystals. *Sill. Journ.* 6, pp. 277-287. 1923.

## 1924.

ALLEN, S. J. M. : The Absorption Coefficients of Homogeneous X-rays between Wave-lengths 0.1 Å and 0.71 Å. *Phys. Rev.* 24, p. 1. 1924.

ALLISON, S. K., and W. DUANE : The Reflexion of Characteristic Bromine X-radiation by a Crystal of Potassium Bromide. *Phys. Rev.* 23, p. 761. 1924.

BARKLA, C. G., and A. E. M. M. DALLAS : Notes on Corpuscular Radiation excited by X-rays. *Phil. Mag.* (6) 47, pp. 1-23. 1924.

BOHR, N. : The Spectra of the Lighter Elements. *Nature*, 113, pp. 223-224. 1924.

BOYCE, J. C. : Soft X-rays from Heavy Elements, Tantalum to Gold. *Phys. Rev.* 23, pp. 575-579. 1924.

BUBB, FRANK W. : Direction of Ejection of Photo-electrons by Polarized X-rays. *Phys. Rev.* 23, pp. 137-143. 1924.

BÄCKLIN, E. : Notiz über die Erregung der sogenannten Funkenlinien in der K-Reihe. *Zeitschr. f. Phys.* 27, p. 30. 1924.

CARRANA, N. : Sulla riflessione totale dei raggi X. *Il Nuovo Cimento*, pp. 107-114. 1924.

✓ CHU, C. T. : N and O X-rays from Tungsten. *Phys. Rev.* 23, p. 551. 1924.

CLARK, G. L., and W. DUANE : Further Experiments upon the Reflexion by a Crystal of its Characteristic X-radiation. *Proc. Nat. Acad. (U.S.A.)* 10, pp. 48-53. 1924.

CLARK, G. L., and W. DUANE : Evidence as to the Mechanism of Characteristic Radiation. *Phys. Rev.* 23, p. 761. 1924.

CLARK, STIFLER and DUANE : Scattering Experiments with Molybdenum primary X-rays and Secondary Radiators of Elements with Atomic Number 6 to 17. *Phys. Rev.* 23, p. 551. 1924.

COLLINS, E. H. : The Temperature Effect on the Regular Reflexion of X-rays by Aluminium Foil. *Phys. Rev.* 23, p. 105. 1924.

COMPTON, A. H., and J. C. HUBBARD : The Recoil of Electrons from Scattered X-rays. *Phys. Rev.* 23, pp. 439-449. 1924.

COSTER, D. : Über die Absorptionsspektren im Röntgengebiet. *Zeitschr. f. Phys.* 25, pp. 83-98. 1924.

CROFUTT, C. B. : The K and L Absorption and Emission Spectra of Tungsten. *Phys. Rev.* 24, p. 9. 1924.

DAVIS, B., and R. v. NARDROFF : Refraction of X-rays in Pyrites. *Proc. Nat. Acad. Sc. (U.S.A.)* 10, pp. 60-63. 1924.

DAVIS, B., and R. v. NARDROFF : Refraction of X-rays in Pyrites. *Phys. Rev.* 23, p. 291. 1924.

DUANE, W., and G. L. CLARK : The Character of Tertiary Rays at Different Angles from the Primary Rays. *Phys. Rev.* 23, p. 551. 1924.

FOWLER, A. : The Spectra of the Lighter Elements. *Nature*, 113, pp. 219-223. 1924.

FRIEDRICH, W., and M. BENDER : Über gestreute Röntgenstrahlung. *Ann. d. Phys.* 73, pp. 505-553. 1924.

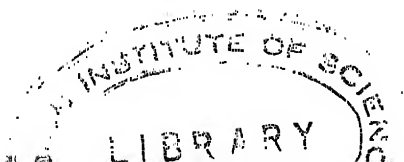
GRAY, J. A. : The Scattering of X-rays. *Phys. Rev.* 23, p. 289. 1924.

HATLEY, C. C., and B. DAVIS : The Refraction of X-rays in Calcite. *Phys. Rev.* 23, p. 290. 1924.

HIRATA, H. : Constitution of the X-ray Spectra belonging to the L Series of the Elements. *Proc. Roy. Soc.* 105 A, pp. 40-59. 1924.

HULBURT, E. O. : On the Theory of the Refraction of X-rays. *Phys. Rev.* 23, p. 106. 1924.

- MACINNES, D. A., and T. SHEDLOVSKY : The Intensities of Reflection of the Characteristic Rays of Palladium from Fluorite. *Phys. Rev.* 23, p. 290. 1924.
- JAUNCEY, G. E. M., and H. L. MAY : The Intensity of the X-rays Scattered from Rock-salt. *Phys. Rev.* 23, pp. 128-136. 1924.
- LANDÉ, A. : Das Wesen der relativistischen Röntgendoublets. *Zeitschr. f. Phys.* 24, pp. 88-97. 1924.
- LANDÉ, A. : Die Absoluten Intervalle der optischen Doublets und Triplets. *Zeitschr. f. Phys.* 25, p. 46. 1924.
- LINDH, A. E. : Über die K  $\gamma$ -Strahlung der Elemente Kalium und Calcium. *Arkiv. f. Mat.* 17. 1924.
- LINDH, A. E., und OSVALD LUNDQUIST : Die Struktur der  $K\beta_1$ -Linie des Schwefels. *Arkiv. f. Matem. Astr. o. Fys.* 18, pp. 3-11. 1924.
- LUKIRSKY, P. T. : On Soft X-rays from Carbon. *Phil. Mag.* (6) 47, pp. 466-470. 1924.
- MILLIKAN, R. A. : The Spectra of the Lighter Elements. *Nature*, 113, pp. 218-219. 1924.
- MILLIKAN, R. A., and I. S. BOWEN : Extreme Ultra-violet spectra. *Phys. Rev.* 23, pp. 1-34. 1924.
- NARDROFF, R. v. : The Refraction of X-rays in Iron Pyrites. *Phys. Rev.* 24, p. 143. 1924.
- RICHTMYER, F. K. : The Relative Number of K and L Electrons expelled by X-rays. *Phys. Rev.* 23, p. 292. 1924.
- RICHTMYER, F. K., and R. C. SPENCER : The Width of the K Absorption Discontinuity in Silver. *Phys. Rev.* 23, p. 760. 1924.
- RICHTMYER, F. K., and R. C. SPENCER : The Structure of the  $K_{\alpha}$  Lines of Molybdenum. *Phys. Rev.* 23, p. 550. 1924.
- ROLLEFSON, G. K. : Spectral Series in the Soft X-ray Region. *Phys. Rev.* 23, pp. 35-45. 1924.
- ROSS, P. A. : An X-ray Spectrograph for Scattered Radiation. *Phys. Rev.* 23, p. 662. 1924.
- SAWYER, R. A. : New Members in the Series Spectrum of Trebly Ionized Silicon. *Phys. Rev.* 23, p. 108. 1924.
- SCHOTT, G. A. : On the Scattering of X-rays by Hydrogen. *Phys. Rev.* 23, pp. 119-127. 1924.
- SEITZ, W. : Über die Asymmetrie der Elektronenemission an sehr dünnen Metallschichten unter der Einwirkung von Röntgenstrahlen. *Ann. d. Phys.* 73, pp. 182-189. 1924.
- SIEGBAHN, M., und R. THOREUS : Eine Erweiterung des Röntgenspektroskopischen Gebietes. *Ark. f. Mat. Astr. Fys.* 18, No. 24, 1924.
- SPONSLER, O. L. : X-ray Reflection from very Thin Crystals. *Phys. Rev.* 23, p. 662. 1924.
- TANDBERG, J. : Über das L-Röntgenabsorptionsspektrum des Jods. *Arkiv. for Matem., Astr. o. Fys.* 18, No. 14, pp. 1 and 2. 1924.
- THOREUS, ROBERT : Die M-Reihe von Wolfram. *Zeitschr. f. Phys.* 26, p. 396. 1924.
- WALTER, B. : Röntgenabsorptionen an Spaltaufnahmen mit Röntgenstrahlen. *Verhandl. d. ...* 10. 1924.
- WARBURTON, F. W., and F. K. RICHTMYER : X-ray Absorption Coefficients in the Neighbourhood of K-limits. *Phys. Rev.* 23, p. 292. 1924.
- WENTZEL, G. : Funkenlinien im Röntgenspektrum (Nachträge). *Ann. d. Phys.* 73, pp. 647-650. 1924.
- WILLS, A. P. : On the Change of Wave-lengths in X-ray Scattering. *Phys. Rev.* 23, p. 551. 1924.



## NAME INDEX.

- Auger, 179.  
Ayres, 10.  
Back, 104.  
Bäcklin, 194.  
Barkla, 2, 4, 8, 9, 10, 12,  
18, 30, 38, 86, 88, 90,  
91, 125, 131, 205.  
Bassler, 8.  
Bazzoni, 237, 238.  
Beatty, 92, 213.  
Becker, 229, 236.  
Behnken, 208, 219, 226.  
Bergengren, 135, 142, 148.  
Bergen-Davis, 27, 28, 226.  
Bestelmeyer, 229.  
Blake, 74, 210, 211.  
Bohr, 112, 150, 151, 152,  
156, 164, 166, 167, 174,  
180, 191, 195, 196, 200,  
201, 226, 244.  
Bosanquet, 220.  
Bowen, 244.  
Boyce, 242.  
Bragg, W. H. and W. L.,  
15, 16, 17, 18, 19, 20,  
21, 22, 23, 24, 25, 26,  
27, 28, 67, 72, 73, 83,  
84, 86, 90, 92, 97, 113,  
131, 204, 205, 209, 210,  
220.  
Brainin, 48.  
Broglie, de, 20, 38, 52, 53,  
86, 87, 98, 113, 131,  
132, 133, 135, 138, 230,  
231, 232.  
Cabrera, 138.  
Carter, 213, 216.  
Chi-Sun Yeh, 211.  
Clark, 94, 96, 109, 237,  
238.  
Compton, 29, 72, 90.  
Cooksey, 60, 84, 104.  
Coolidge, *passim*.  
Coster, 91, 112, 115, 126,  
133, 139, 172, 174, 177,  
181, 182, 191, 193, 196,  
200, 244.  
Crofutt, 98, 114, 115.  
Darwin, 23.  
Dauvillier, 5, 79, 172, 179,  
193.  
Davies, 239.  
Davis, 27, 28, 95, 220.  
Debye, 170, 195.  
Dershem, 114.  
Dessauer, 104.  
Dolejssek, 85, 88, 104, 106,  
130, 190.  
Dorn, 228, 229.  
Duane, 74, 88, 97, 98, 111,  
138, 139, 154, 163, 175,  
206, 209, 210, 211, 214,  
217, 229.  
Einstein, 30, 75, 77, 96,  
153, 206, 209, 222, 223,  
224, 229, 236, 243.  
Ellis, 234.  
Ewald, 23, 24.  
Foote, 238, 239.  
Fowler, 188, 190.  
Fricke, 135, 138, 193.  
Friedrich, 13, 14, 15.  
Friman, 51, 53, 88, 104,  
192.  
Gaede, 80.  
Grotrian, 188, 239.  
Hadding, 36, 70.  
Haga, 13.  
Ham, 9.  
Hatley, 27.  
Hennings, 227.  
Hertz, 135, 139, 162, 163,  
170, 171, 193.  
Hevesy, 91.  
Hewlett, 5, 88.  
Heydweiller, 79.  
Hjalmar, 22, 27, 44, 67,  
85, 88, 98, 99, 106, 115,  
126, 130, 172, 181, 190,  
192, 243.  
Holtsmark, 237, 238.  
Holweck, 81.  
Horton, 239.  
Hoyt, 96, 109, 111.  
Hughes, 237, 238.  
Hull, 5, 78, 80, 206, 208,  
218.  
Hunt, 206, 209, 229.  
Innes, 229.  
James, 220.  
Jancke, 236.  
Jönsson, 5.  
Kang-Fuh-Hu, 230.  
Karcher, 71, 125.  
Kaye, 35, 61, 215, 216,  
218.  
Kettmann, 95.  
Kirkpatrick, 225, 226.  
Kohlrausch, 33.  
Kossel, 151, 152, 189,  
244.  
Knipping, 13, 14, 15, 16.  
Kramers, 226, 227.  
Kroo, 170, 195.  
Kulenkampff, 216, 219,  
220, 225, 226.  
Kurth, 237, 242.  
Ladenburg, 212.  
Landé, 188, 189.  
Langmuir, 42, 43, 80, 82.  
Larsson, 85, 194.  
Laub, 229.  
Laue, von, 2, 4, 13, 14, 15,  
16, 23, 48.  
Leide, 104, 168.  
Lilienfeld, 37, 46, 49.  
Lindh, 99, 134, 135, 138,  
143, 145, 148, 241.  
Lindsay, 139, 163.  
Lundquist, 29, 99.  
McLennan, 237, 238.  
Malmer, 88, 104.  
March, 226.  
Meitner, 235.  
Michelson, 243.  
Miller, 48.  
Millikan, 209, 243, 244,  
245.  
Mohler, 238, 239.

- PRINTED IN GREAT BRITAIN BY ROBERT MACLEHOSE AND CO. LTD.  
THE UNIVERSITY PRESS, GLASGOW.